Coordinated Complexes with Functional Chelating Ligands having Nitrogen and/or Oxygen Donor Atoms

Submitted in

fulfillment of the requirements for the degree of

Doctor of Philosophy

by

Tanuja Kumari

ID: 2012RCY9525

Under the Supervision of

Prof. (Dr.) Jyoti Joshi

DEPARTMENT OF CHEMISTRY

MALAVIYA NATIONAL INSTITUTE OF TECHNOLOGY JAIPUR

August, 2019

DECLARATION

I, **Tanuja Kumari**, declare that this thesis titled, **"Coordinated Complexes with Functional Chelating Ligands Having Nitrogen and/or Oxygen Donor Atoms"** and the works presented in it are my own. I confirm that:

- This work was done wholly or mainly while in candidature for a research degree at MNIT.
- Where any part of this thesis has previously been submitted for a degree or any other qualification at this university or any other institution, this has been clearly stated.
- Where I have consulted the published work of others, this is always clearly attributed.
- Where I have quoted from the work of others, the source is always given. With the exception of such quotations, this thesis is entirely my own work.
- I have acknowledged all main sources of help.
- Where the thesis is based on work done by myself, jointly with others, I have made clear exactly what was done by others and what I have contributed myself.

Date: Tanuja Kumari

Place: (ID 2012RCY9525)

CERTIFICATE

This is to certify that the work reported in this thesis entitled **"Coordinated Complexes with Functional Chelating Ligands Having Nitrogen and/or Oxygen Donor Atoms"** has been carried out by Ms. Tanuja Kumari and submitted to the Malaviya National Institute of Technology Jaipur, for the award of **Doctor of Philosophy** in chemistry is a bona fide record of research work carried out by her under my supervision and guidance. The thesis work, in my opinion, has reached the requisite standard fulfilling the requirement for the degree of **Doctor of Philosophy**. The thesis embodies the original work done by her and to the best of my knowledge and belief, this work has not been carried out earlier.

Date:

Place:

(Dr. Jyoti Joshi)
Professor
Department of Chemistry
MNIT, Jaipur
Jaipur-302017
India

ACKNOWLEDGEMENT

(Tanuja Kumari)

ABSTRACT

Coordination complexes of nitrogen and oxygen functionalized ligands have great importance in the field of biological and environmental chemistry. These are known to be potentially useful as catalysts in biomedical applications and a variety of other applications.

In view of the wide range of applications associated with the complexes of N-O donor ligands and based on our interest to develop new metal complexes with N-O donor ligands and explore their applications, work presented in this thesis entitled "**Coordinated Complexes with Functional Chelating Ligands having Nitrogen and/or Oxygen Donor atoms"** contains six chapters including one review, four series of new metal complexes synthesized and one chapter comprising of biological evaluation of synthesized complexes.

The work embodied in the thesis has been divided into six chapters.

Chapter 1st is devoted to the basic idea on chemistry, coordination compounds, type of ligands and brief review on N-O donor chelating ligands and their metal complexes including their applications in different areas. Amongst various N-O donor ligands 8-Hydroxyqinoline molecule is one of the most revered N-O donor bidentate chelating ligand which is known to form simple mononuclear complexes as well as polynuclear complexes. In this chapter a number of applications such as electron carriers in organic light-emitting diodes (OLEDs), fluorescent chemosensors, pharmacological and pharmaceutical fields, etc. of 8-Hydroxyquinoline and its derivatives have been reviewed along with the aim of the work.

Chapter 2nd is focused on the chemistry of cobalt complexes with N-O donor chelating ligand and their role in the development of coordination chemistry. Further in this chapter we report the synthesis and characterization of nine new cobalt complexes: [dichlorobis (8-methoxyquinoline)cobalt(II)](1), [dichloro(8Pyridin-2-ylmethoxy quinoline)Co(II)](2), [dichloro{1,3-bis(quinolin-8-yloxy)propane}Co(II)](3), [bis (8-methoxyquinoline)Co(II) pentafluorophenolate](4),[(8-pyridine-2-ylmethoxyquinoline)Co(II)pentafluorophenolate] (5), [(1, 3 bisquinoxy-8-yloxy propane)Co(II)pentafluorophenolate] (6), [bis(8-

methoxyquinoline)Co(II)heptaflurobutyrate] (7), [(8-pyridine-2-ylmethoxy quinoline) Co(II) pentafluorophenoxide] (8) and [(1,3-bisquinoxy-8-yloxy propane) Co(II) heptafluorobutyrate] (9) with 8-hydroxylquinoline derived bidentate, tridentate and tetradentate neutral chelating ligands.

Chapter 3rd begins with brief introduction of palladium complexes of heterocyclic ligands, their biological applications, nanotechnology and PdO nanoparticles. Further in this chapter we report synthesis and characterization of four Pd(II) complexes: dichlorobis(8-methoxyquinoline) Pd(II) [(MOQ)$_2$PdCl$_2$], dichloro(8-Pyridin-2-ylmethoxyquinoline) Pd(II) [(PMOQ)PdCl$_2$], dichloro{1,3-bis(quinolin-8-yloxy)propane}Pd(II) [(BQOP)PdCl$_2$] and dichloro{1,6-bis(quinolin-8-yloxy)hexane}Pd(II) [(BQOH) PdCl$_2$]. One of the synthesized Pd derivatives [(PMOQ) PdCl$_2$] has been used as precursor for the synthesis of palladium oxide nanostructure using sol–gel method resulting in the formation of Pd@PdO core shell.

Chapter 4th starts with brief introduction of TiO$_2$ nanoparticles and various techniques used in the synthesis of nanoparticles highlighting the advantages of sol-gel route over other techniques. Further we report here, the synthesis and characterization of two Ti(IV) complexes [{acac}$_2$Ti{OPr^i}{ONC$_9$H$_6$}] [1] and [{acac}$_2$Ti{ONC$_9$H$_6$}$_2$] [2] by 8-hydroxyquinoline modification of titanium(IV)bis(acetylacetonate) diisopropoxide. Further [Ti{OPr^i}$_4$] and complexes (1) and (2) were used as precursors for the formation of nano sized TiO$_2$ nanoparticles using low temperature aqueous sol-gel method in organic medium resulting in the formation of nano-sized anatase titania.

Chapter 5th starts with description of ionic compounds comprising of organic-inorganic framework and their applications. Ionic compounds comprising of organic cations in combination with inorganic anions bearing typically diffused charges which have low melting points are often termed as ionic liquids (ILs). Considering potential applications of ionic liquids in this chapter we report synthesis, structural characterization of six novel 8-Hydroxyquinolenium based cyclic geminal dicationic ionic compounds.

Chapter 6th deals with the antibacterial, antifungal and antioxidant studies of compounds synthesized in chapters 2-5.

All the synthesized complexes, described in chapters 2-5 were successfully synthesized in good yield and were fully characterized on the basis of their detailed spectral studies such as IR, ^{1}H NMR, ^{13}C NMR, UV-Visible spectroscopy and Mass spectrometry. Geometry of some of the complexes was confirmed by the single crystal X-ray analysis.

Conclusion

In view of the medicinal and various other applications of the N-O donor ligands derived from 8-Hydroxyquinoline and their metal complexes, designing of novel metal complexes has always been the area of interest for inorganic chemists. The present work is an effort in the direction of the development and study of some new coordinated complexes of cobalt, palladium and titanium with N-O donor chelating ligands derived from 8-Hydroxyquinoline.

LIST OF CONTENT

LIST OF FIGURE

LIST OF TABLES

1.1 Introduction

Chemistry involves study of compounds formed of atoms, elements and molecules, i.e. composition, properties, behavior, structure as well as their transformations during a reaction [1, 2]. Chemistry deals with areas such as how atoms and molecules interact by forming chemical bonds resulting in chemically new compounds. It is a very broad subject and for the sake of simplicity it is broadly divided into following five branches:
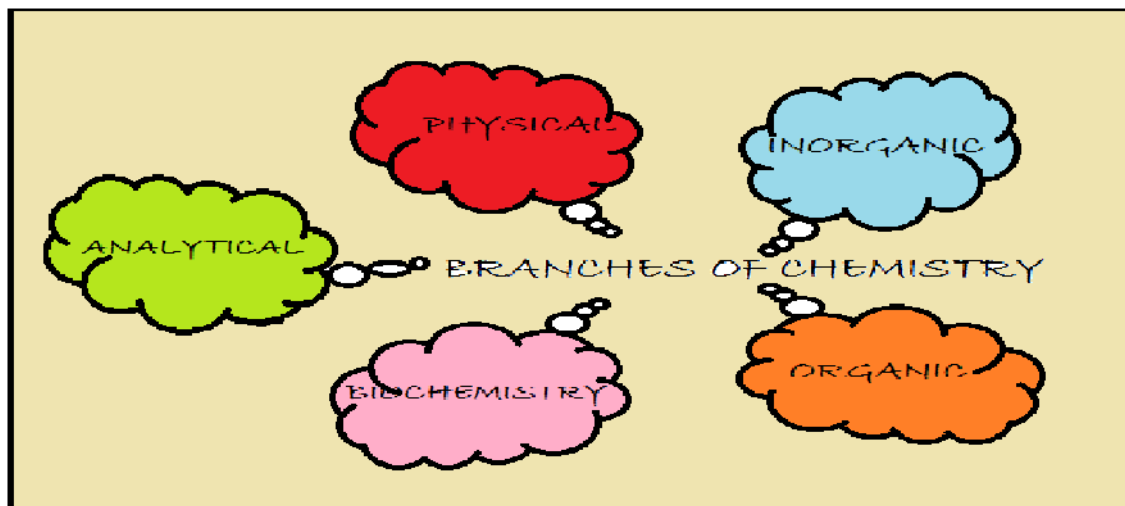
Figure 1.1 Branches of chemistry

(i)   **Analytical chemistry**

It is the branch of chemistry that governs study of the techniques and methods engaged in formulating the quality, quantity and types of various elements present in a given substance.

(ii)   **Physical chemistry**

This branch of chemistry deals with the principles and laws governing the combination of atoms and molecules in chemical reactions and study of physical properties of matter.

(iii)   **Organic chemistry**

Organic chemistry deals with the study of the composition, structure, reactions, synthesis and properties of the carbon-containing compounds, primarily hydrocarbons and their derivatives.

(iv)   **Biochemistry**

This branch of chemistry deals with the study of the chemical reactions and compounds involved in living organism i.e. plants and animals cell.

(v)   **Inorganic chemistry**

Inorganic chemistry governs the properties and nature of inorganic compounds usually comprising of non-living organisms that consists of minerals, metals, non-metals, and organometallic compounds.

Historically, inorganic chemistry is the oldest branch of chemistry. Classical inorganic chemistry was primarily concerned with the preparation and studies of the properties of all the elements and their compounds. Main branches of inorganic chemistry include:

a)   **Coordination Chemistry:** This branch of chemistry deals with study of compounds comprising of a metal centre surrounded by ligands which could be molecules or ions. Ligands bound to the metal centre via coordinate bonds, where both the electrons involved in bond formation are provided by the same atom of the ligand.

b)   Organometallic chemistry: Organometallic chemistry involves the study of synthesis, structure and reactivity of complexes containing metal-carbon bonds.

c)   Bioinorganic chemistry: It is the field of inorganic chemistry which studies the role of metals in biology. Bioinorganic chemistry examines both naturally occuring phenomena for instance the actions of metalloproteins as well as artificially introduced metals, including non-essential metals in toxicology and medicine.

d)   Solid state chemistry: It governs the study of the formation, characteristics and structure of the materials in solid phase.

e)   Nuclear chemistry: It is the branch of inorganic chemistry which deals with study of radioactivity, nuclear processes and properties.

Coordination Chemistry is the most active and advanced investigation area in inorganic Chemistry. It has gained great interest among researchers offering fruitful results and hence became exceptionally striking area of research. The study of

coordination chemistry may be said to have originated in 1704 with the discovery of Prussian blue by Diesbach, a colour maker. After this one might site the investigation of the products of oxidation of ammonical cobalt solution of Tassaert (1799). In the years that followed, Cleve, Wolcott Gibbs, Blomstrand and Fermy did a large amount of effort towards the study of complexes [3].

By 1870, a great deal of information on the complexes had been gathered and it was Prof. Jorgenson who for the first time methodized this field to a great extent by the designing and characterization of several coordination complexes [4].

Coordinated metal complexes were first explored, at the time of Alfred Werner, in nineteenth century, who is regarded as the father of coordination chemistry since he started with his work to recognize coordination complexes and their properties [5]. Subsequently, the inorganic chemistry witnessed an immense outpouring of coordination complexes bearing distinctive structural features as well as miscellaneous applications. Afterwards, amongst various research areas of the inorganic chemistry, coordination chemistry dominated due to rapid growth of research work in this area [6-8].

Coordination compounds are comprised of a central metal atom or ion surrounded by ligands. A ligand is an ion or a molecule that is capable of donating one or more lone pair of electrons to the empty orbital of central metal atom. When a ligand can donate more than one electron pair to the central metal ion through more than one donor atoms, such ligands are termed as polydentate ligands or chelating ligands and the resulting complexes are said to be metal chelates. A coordination complex is referred as a binary system if there is only one type of ligand and central metal atom present in it. While, if there are more than one type of ligands are present then these complexes are known as mixed ligand complexes, which can be further termed as ternary or quaternary systems depending on the stoichiometry of the metal and ligands [9].

The nature of the coordination complexes primarily relies on the central metal atom as well as donor atoms of the ligand and the structure resulting due to the interaction of ligand with the metal [10]. The broad applications of coordination complexes in biological, chemical and industrial fields have lead scientists to carry

out research in this field [11, 12].

Transition metals constitute largest class of coordination complexes owing to their capability of forming a broad range of coordination complexes. There have been reported several coordination compounds of different transition metals as central metal having various geometries like tetrahedral, square-planar, square-pyramidal and octahedral [13-17].

Incredible growth of coordination chemistry has been witnessed in several fields ranging from purely academic synthesis to large-scale industrial production. Various modern spectral techniques such as ^{1}HNMR, Mass, IR, UV-Vis, X-ray, ESR etc. and thermal techniques like TGA, DTA, DTG and DSC have been extensively used for elucidating the structures of coordination complexes [18-25].

1.2 Ligands and their types

Ligand is an atom, ion or molecule which can bind with central metal atom by the donation of lone pair of electron to form a coordination complex. Ligands can be classified on several bases, on the basis of denticity ligands may be classified as:

(a) Monodentate Ligands

The term 'monodentate' meant 'one tooth,' and is referred to the ligands which can bind to the central metal atom through only one atom. Chemically, monodentate ligands are Lewis bases which can donate a lone pair of electron to a Lewis acid i.e central metal atom. These ligands can be both ions and neutral molecules. e g. H_2O, NH_3, Cl^-, NO_2, CN^- etc.

(b) Bidentate Ligands

Bidentate ligands are Lewis bases that donate two pairs of electrons to central metal atom. These ligands are also termed as chelating ligands because they can grip a metal atom from two sites.

Acetylacetonate ion   ethane-1,2-diamine   oxalate   1,10-phenanthroline
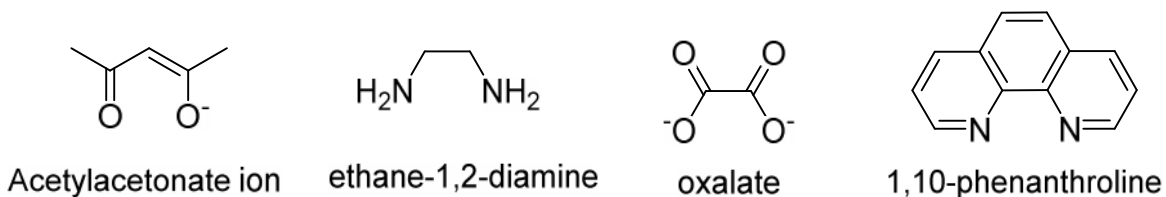
Figure 1.2 Bidentate ligands

(c) Tridentate ligands

A tridentate ligand has three atoms that can function as donor atoms in a coordination compound. Ligands having three donor groups may act as a tridentate ligand when all donor groups involve in bond formation, while if only two donor group participate in bond formation it act as bidentate ligand.
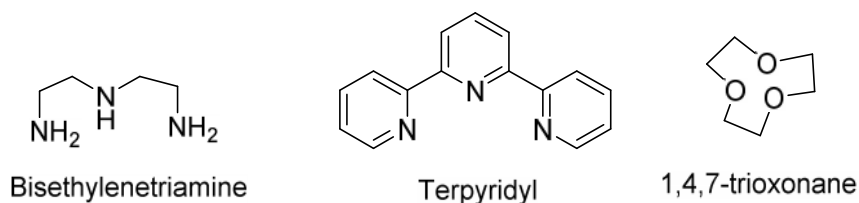
Figure 1.3 Tridentate ligands

(d) Tetradentate ligands

Tetradentate ligands are ligands that bind with four donor atoms to a central atom to form a coordination complex. Tetradentate ligands are common in nature in the form of chlorophyll which has a core ligand called chlorin, and hemoglobin with a core ligand called porphyrin. They add much of the colour seen in plants and humans. Phthalocyanine is an artificial macrocyclic tetradentate ligand and its complexes with metal (Fe, Co, Cu, Ru, Mn, Cr, Al, and Zn) used in catalysis and to make blue and green pigments [26].
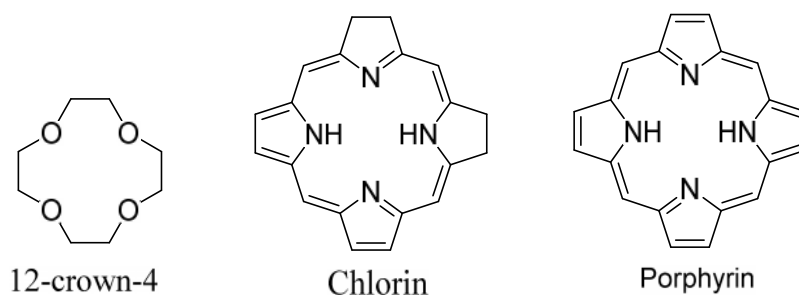
Figure 1.4 Tetradentate ligands

1.2.1 Homo donor and Hetero donor ligands

On the basis of types of donor atoms, bidentate or polydentate ligands are classified into two categories.

(i)   **Homo donor ligands:** In these ligands, all donor atoms coordinated to the metal are same (one type of donor atoms). e g. non-functional homodonor, with N-donors include ethylene diammine (en) (N-N), azines (N-N), diketones (O-O), porphyrines (N-N) etc.

ethane-1,2-diamine   1,2-di(propan-2-ylidene) hydrazine   biacetyl   ethanebis(thioic) O,O-acid
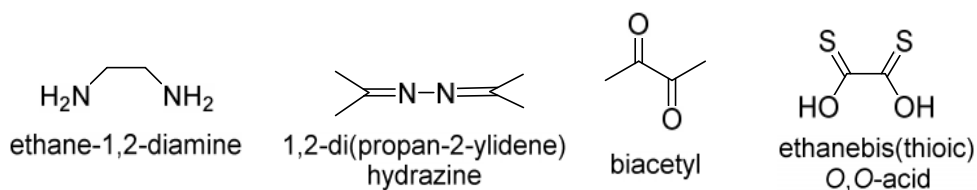
Figure 1.5 Homodonor ligands

(ii)   **Hetero donor ligands:** These ligands contain more than one type of donor atoms. For example, oximes (N-O), -ketoammines (N-O), semicarbazones (N-O), thiosemicarbazone (N-S) etc. In a way simple approach these types of ligands can be classified as, hetero N-O donor, O-S donor, N-S donor, N-O-S donor, N-X or N-O-X or N-S-X (X=P,As,Se etc.)

Aldoxime   Ketoxime   Acetonecarbazide   Thiosemicarbazide
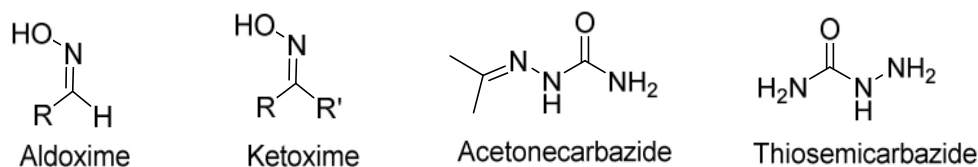
Figure 1.6 Heterodonor ligands

Hetero donor ligands, generally termed as mixed donor ligands play very important role in coordination chemistry. The general mode of coordination of bidentate, tridentate and tetradentate ligand system is shown in Figure 1.7, where different donor atoms forming coordinate bonds with the central metal atom M are represented by A, B, C, and D.
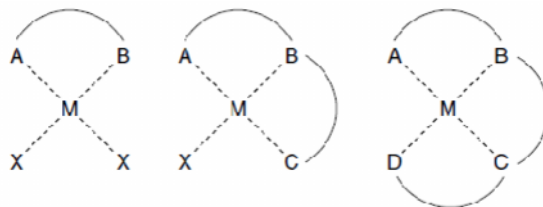
Figure 1.7 Type of the mixed donor ligands

The metal-donor atom bond lengths in a mixed donor ligand complex are different which leads to distorted geometries of the complex. Amino acids represemt most common example of a conventional mixed donor ligand, having N and O donor atoms; these donor groups behave differently than those present in individual solo N-donor in diamine or O-donor in dicarboxylate molecules. Conversely, different chelate groups with N or O atom donor atoms such as an amine or pyridine group, or a carboxylate or alcohol group in which donor atoms are common these are termed as mixed donor ligands. Such molecules are considered as mixed donor ligands because of the presence of in equivalent chemical and structural environment [27].
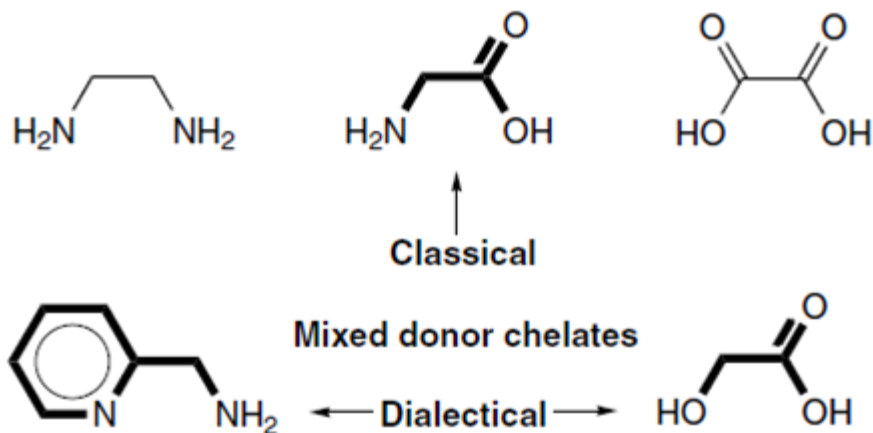
Figure 1.8 Classical and dialectical mixed donor ligands

Increase in number of donor atoms in a ligand increases the number of ways in which ligands may be arranged around central metal atom in the complex i.e. ligand topologies increases. Various possible topologies of a tetradentate A3B type ligand having three donor sites (A) and a single donor group (B) compared to a single donor

group (A4) is shown in Figure 1.9. For ligand system A4 there are total six possible topologies which are prolonged to fifteen for the ligand system A3B. Further for an A2B2 type system possible topology options increases. Although all the topological options shown may not be possible, but it is clearly evident that in case of mixed donor ligands the diversity of ligand is enhanced.
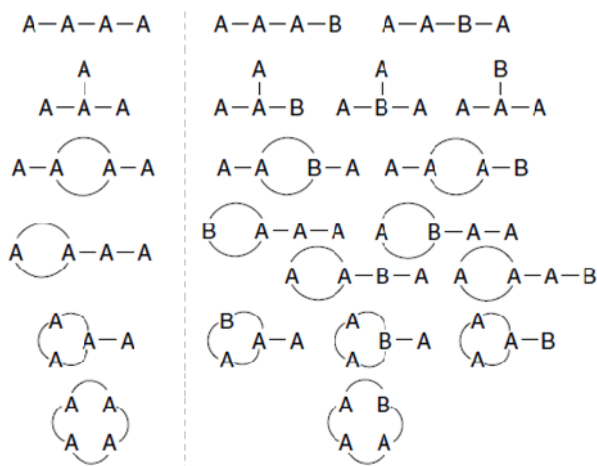
Figure 1.9 Ligand topologies for mixed donor system (A_3B) and simple system (A_4)

Due to diverse possible structural features hetero donor ligands offer challenge to the chemists working in this area. Besides, donor atoms of explicitly diverse nature, like a N-donor or an O-donor group affects significantly the selectivity of metal ions, stability and other features of the complexes [28].

Polydentate ligands impart extra stability to the complexes as compared to monodentate ligand complexes; this extra stability is attributed to the chelate effect, which reveals that the increase in stability of a complex resulting due to replaced polydentate ligand that is linked to central metal atom by chelate rings. Chelating ligands are the molecules which have minimum two donor groups capable of forming ring with metal ion. Such ring structures are termed as chelate ring [29] and the resulting coordination compounds are known as metal chelates.

Chelating ligands are often categorized depending on the number of donor groups present, which is known as denticity of the ligand. Chelating ligands bearing two donor groups are the simplest and termed as bidentate, ligands having three donor groups are called tridentate. If more than three donor groups are present such ligands are called

polydentate. Bidentate, tridentate, tetradentate, pentadentate and hexadentate chelating agents are the most common in coordination chemistry however, chelating ligands with higher denticity have also been reported. In polydentate ligand metal complexes it is not essential that all donor groups necessarily participate in forming metal chelate [8]. The most common donor groups have oxygen, sulphur, nitrogen, or phosphorus atom, referred as the donor atom and the metal ion is the acceptor group. The bidentate ligands are most extensively studied category of chelating agents [30]. Chelating ligands of higher denticity have also been studied selectively [31] and a few such as the amino carboxylic acids like EDTA have been explored extensively [32-33].

Chelating ligands possessing mixed donor groups interests the researchers working in the field of coordination chemistry because of their versatile structural features. Further, if the donor groups present in hetero donor chelating ligands have different binding ability, it affects their selectivity of metal ions, stability of the complex as well as other properties of the coordination compound formed [34].

Table 1.1 Common types of donor groups and ambivalent donors

Donor Atom	Donor Group	Example
N	Amine	$-NH_2$, $-NHR$, $-NR_2$
	Heterocyclic N-donor	Pyridine, imidazole
	Imine	$HN=CR-$, $-N=CR-$
	Amido	$-N^--CO^-$
O	Alcohol	$HO-C-$
	Carboxylate	$-COO-$
	Ether	$C-O-C$
	Carbonyl	$>C=O$
S	Thiol	$-SH$
	Thioether	$C-S-C$
	Thioacid	CSS^-
P	Phosphine	$-PH_3$, $-PRH_2$, $-PR_2H$, $-PR_3$
Ambivalent donors	Thioacid (O or S)	$HO-C(=S)-$
	Amide (N or O)	$-NH-CO-$
	Thiophosphate (O or S)	$-PSO_3$, $-S=O$

Although hetero donor ligands possessing two dissimilar donor groups corresponds to the simplest class of hetero donor ligands still their binding ability and structural range is vast. All the possible arrangements of prospective hetero donor groups have been studied practically. Class of hetero donor groups including the most commonly involved four donor atoms are listed in Table 1.1. In the selection of donor atom metal ions play vital role in case of both ambidentate ligands and polydentate ligands [35].

1.3   Types of Hetero Donor ligands

A number of donor atoms belonging to the main group elements of the periodic table constitute several classes of hetero donor ligands. However, the most common donor atoms are nitrogen (N) and oxygen (O) atoms. Sulphur (S) and phosphorus (P) and heavier elements like As, Se, and Te atoms are comparatively less common donors. Some of the commonly used classes of hetero donor ligands are described here.

1.3.1   N-S Donor Ligands

N-S donor ligands represent mixed hard-soft donor class of ligands. A number of N-S donor ligands that can bind with central metal atom forming chelate ring sizes ranging from three to six have been reported. Some of the important types of N-S donor chelating ligands are shown in Figure 1.10 (1-9). Aminothiol represents one of the well known class of N-S donor ligands, 2-aminoethanethiol (**1**) is the simplest aminothiol derivative, this ligand usually offers simple ML_2 (M = Ni, Cu, Pd) type metal chelates, however polymeric complexes in which the S act as bridging atom have also been reported [36].

Another class of N-S donor ligands aminothioethers (2) and aminothiols derived from S-valine are used as catalysts for asymmetric addition of diethyl zinc (Et_2Zn) to aromatic aldehydes [37].

The aminothioacid (**3**) and its various N-alkylated analogues constitute an N-S donor ligand, and forms six-membered chelate rings with metals like Rh(III) [38]. The typical imine-thiol derivative (4) usually form simple ML2 type compounds with metals Ni(II) and Pd(II) [39].

Dithiol derivative (5) containing two identical branches represents tridentate (N-S-S) donor ligands set that forms two five-membered chelate with metals [40]. Ligands (6) and their analogue with varied number of methylenes in both arms have reported to form simple mononuclear complexes containing five or six-membered chelate rings with Cu (II) metal ion [41]**.**
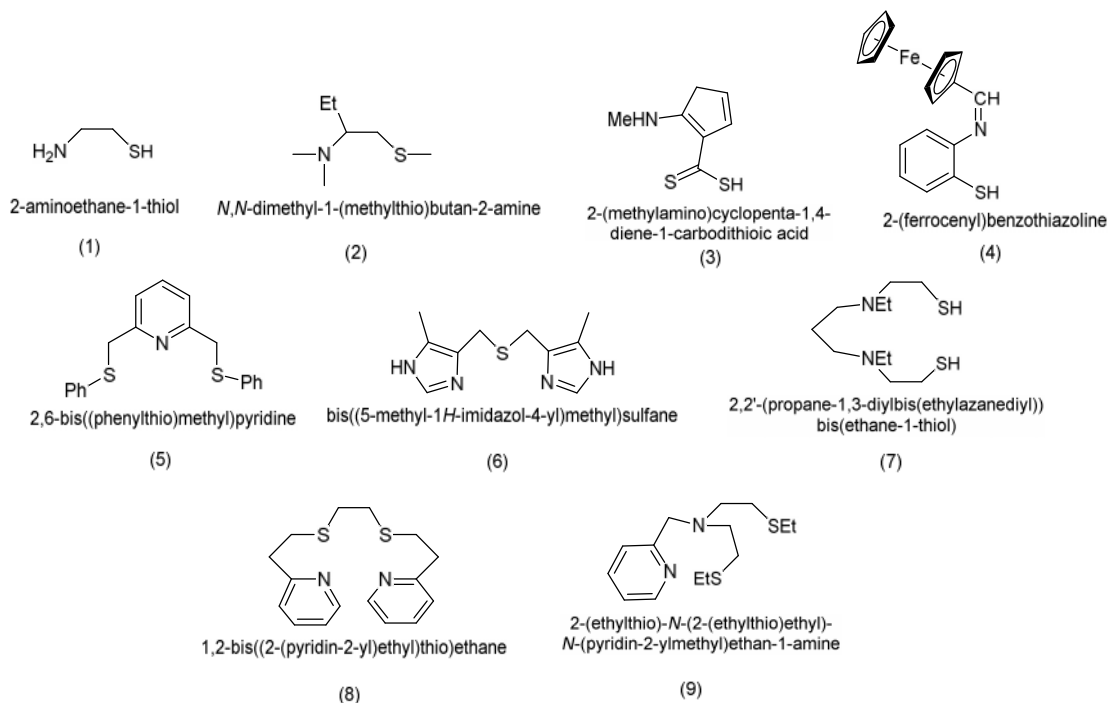
Figure 1.10 Bidentate, tridentate and tetradentate N-S donor ligands

Tetradentate N-S donor linear ligands with an (N-N-S-S) donor set generally consists of terminal S donor atoms as thiols or thioether groups, example of the thiols is (7), that gives hexanuclear cluster compounds with Fe (III) [42]. The molecule (8) represent class of a simple thioether (N-N-S-S) donor set ligand type, which primarily gives mononuclear complexes with Ni(II). The diaquanickel(II) complex of this ligand has shown to acts as a nickel metalloprotein active site model [43]. Another interesting tetradentate (N-N-S-S) donor ligand (**9**) readily forms complex with Cu that act like a model compound for copper proteins [44].

1.3.2 O-S Donor Ligands

O-S donor chelating ligands have known to show significant antimicrobial activity and play a key role in the coordination of metals at the active sites of numerous metallo

biomolecules [45]. Chelating ligands having only O-S donor atoms are relatively few. Some important O-S donor ligands are shown in figure 1.11 (1-8). Simple O-S donor ligands are derivatives of hydroxy-thiols (2), thioethers and thioether-carboxylates (2), these ligands reported to form metal complexes in a fashion similar to corresponding amine derivatives. Thioacetic acids and their ether derivatives form five-membered chelate rings. 2-mercaptoethanol usually forms monomeric of five-membered chelate ring complexes, however their polymeric complexes have also been reported where bridging through both O and S atoms occur [46].
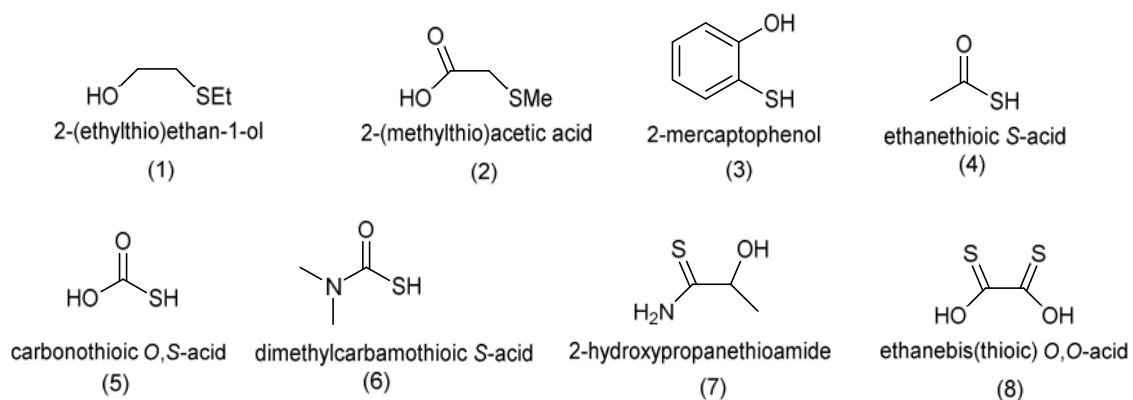
Figure 1.11 Bidentate O-S donor ligands

Compound 2-mercaptophenol (3) in its dianionic form represents another simple category of O-S donor chelate and forms stable complexes with metals [47]. Molecules like thioacetate (4), monothiocarbonate (5) and monothiocarbamates (6) are the examples of chelates containing mixed hard and soft O-S donor ligand group which form four-membered chelate rings [48]. N-hydroxythiohydroxamic acid (7), a derivative of thiohydroxamic acids is a well known O-S donor ligand having vast range of biological and analytical applications [49]. It is an ambidentate ligand that can either form five-membered O-S rings or four membered N-S rings. Dithiooxamide derivatives exemplified by dithiooxalate (8) represent another example of ambidentate ligands which is able to coordinate with metals through S-S or via hetero donor atoms O-S [50]. Dithiooxalate (8) molecule however predominantly behaves as an O-S donor bidentate ligand with various metal ions such as Cu(II) Ag(I) and In(III) [51].

1.3.3 N-P Donor Ligands

The N-P donor ligands have been widely used in the synthesis of stable transition metal complexes having very low or very high oxidation states. Simple chelating ligands containing soft P donor atom in combination with other common donors are well known [52]. Some of the important N-P donor ligands have shown in figure 1.12 (1-5). Bulky and inert aminophosphine derived ligands (**1**) have been extensively employed in the synthesis of organometallic compounds [53]. Another N-P donor ligand comprising of iminophosphine moiety (2) have been reported to form Ni(II) complexes [54]. The 2-(diphenylphosphanyl)pyridine ligand (**3**) form four-membered chelate ring with cobalt in tetrahedral arrangement [55]. The P-N donor aminophosphine ligand (**4**) have reported to show 4, 5, and 6-coordination geometries with bivalent metal atoms [56]. Tridentate (P-N-N) donor ligand (5) act as very good chelating ligand for Pt group metals, it has been reported to form unusual Cu(I) complex $[Cu_2(CH_3CN)_2 (L)_2]^{2+}$ (L=5) where ligand (5) form chelate with one metal via both N donor atoms and coordinate with other metal atom through P donor atom [57].
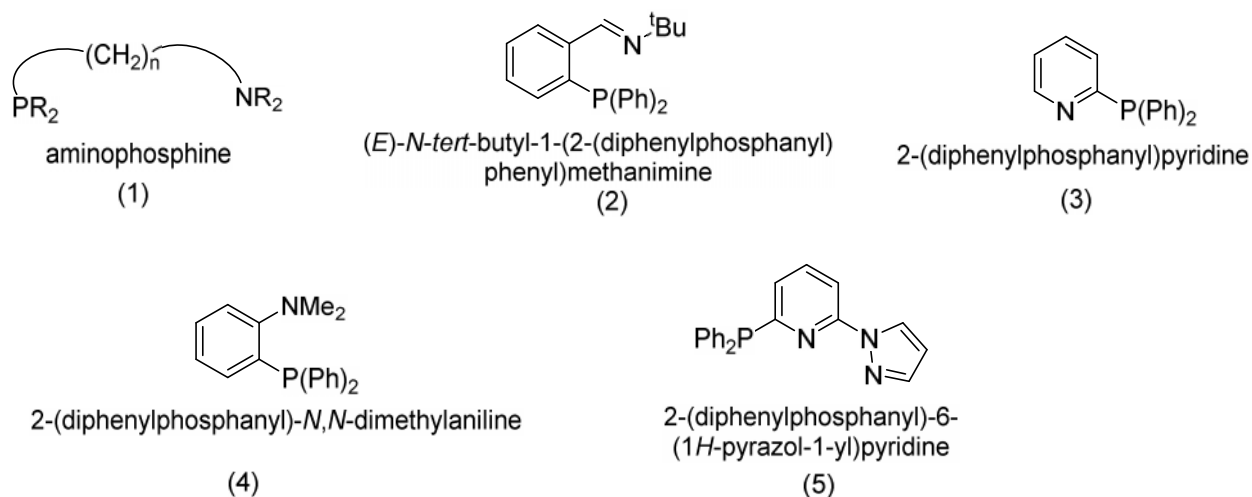
Figure 1.12 N-P donor ligands

1.3.4 O- P Donor Ligands

Some typical examples of O-P donor ligands are given in figure 1.13 (1-4). Most of the O-P donor ligands like (1) and (2) have known to form strong coordination

complexes with platinum and palladium metals. The (P-P-O-O) donor tetradentate ligand (3) has been reported to form complexes with Pt metal via only three (P-P-O) donor atoms. The tridentate (P-P-O) donor ligand (4) readily forms complex with Pd(II) which is soluble in water and act as potential catalyst in hydroformylation of alkenes [58].

2-(dimethylphosphanyl)phenol

(1)

(Z)-2-(di-*tert*-butylphosphanyl)-
1-phenylethen-1-ol

(2)

(oxybis(ethane-2,1-diyl))bis
(diphenylphosphane)

(3)

sodium 4,5-bis(diphenylphosphanyl)-7,9,9-
trimethyl-9*H*-xanthene-2-sulfonate

(4)
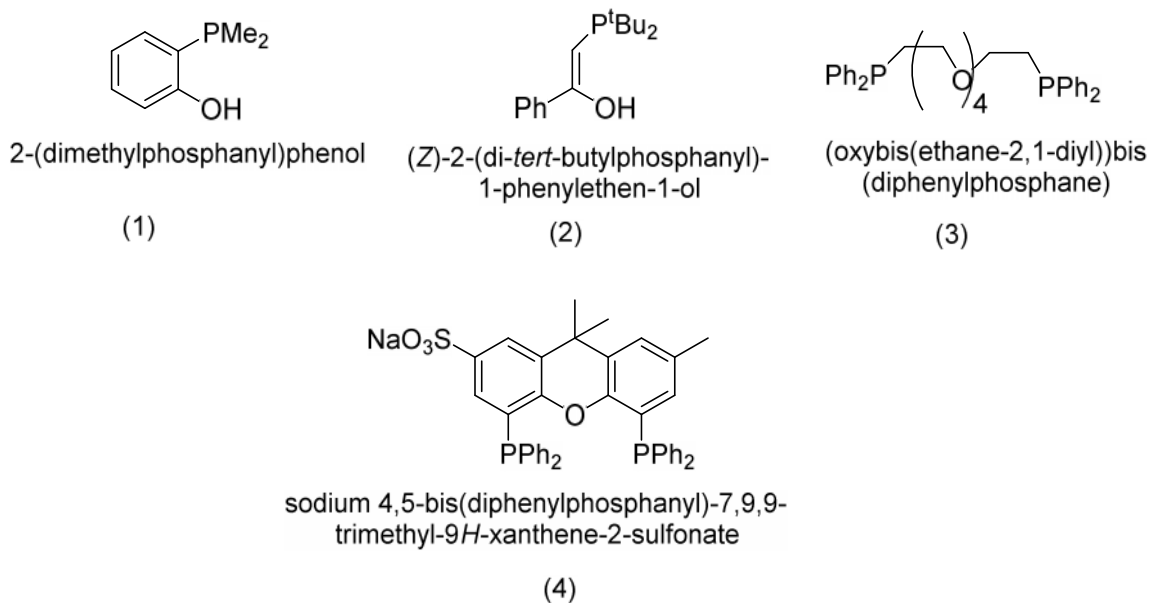
Figure 1.13 O-P Donor Ligands

1.3.5   N-O Donor Ligands

N-O donor ligands constitute largest class of the hetero donor ligands and have been extensively used in the synthesis of coordinated complexes with various metal atoms. Metal complexes of nitrogen and oxygen functionalized ligands have great importance in the field of biological and environmental chemistry [59, 60]. A large number of nitrogen and oxygen donor ligands and their metal complexes are also of significant interest and attention due to their significant biological activity [61, 62]. These are known to be potentially useful as catalysts [63, 64], in biomedical applications [65-70] and a variety of other applications. These derivatives are also known to show anti-tumor and cytotoxic activities [71].

There are a number of bidentate, tridentate, tetradentate and polydentate N-O donor ligands have been designed and further used in the synthesis of variety of metal

complexes of diverse applications. Some of the important bidentate, tridentate and tetradentate N-O donor chelating ligands and their complexes have been reviewed.

1.3.5.1 Bidentate N-O donor ligands

Most common and widely studied class of bidentate N-O donor ligands are Amino acids and their derivatives (Figure 1.15) these ligands have gained interest due to their potential application as catalysts and bioactive complexes. Glycine (1) and 2-aminoethanol (2) are the simplest members of -amino acids and -amino alcohols respectively, which results in the formation of five membered chelate rings while their analogues -amino acid derivatives, 3-aminopropane (3) and 3-aminopropanol (**4**) can form chelate rings of six member with metal atoms [72].

Amino acids mostly chelate with the carboxylate, but in some cases coordination of acid groups have come into sight. Few metal complexes of amino alcohol have been reported in which both deprotonated and protonated hydroxy groups coexist [73].
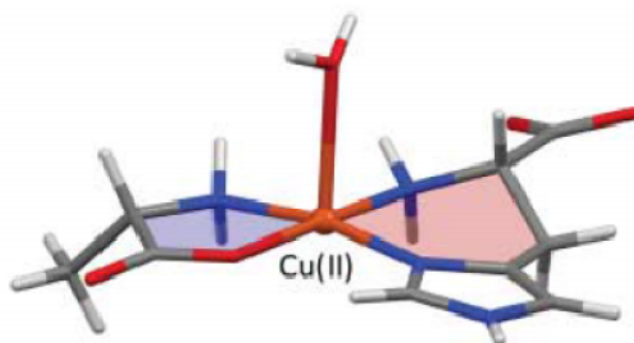
Figure 1.14 L-Alanine, L-Histidine - Cu(II) complex containing both five membered and six membered chelate

Characteristic feature of small bidentate N-O donor ligands viz. oxime, N-oxide and N -hydroxides is of being able to form small chelate rings, including rare three-membered chelate rings. N-Hydroxides (7) and their N-alkylated derivatives can also form chelate ring of three members that is highly unstable due to ring strain. Oximes act as ambidentate ligands which can coordinate to metal ion either through both O atoms or via O and N donor atoms; however they predominantly coordinate through nitrogen atom.

Amidoximes molecules (8) are established N-O donor ligands, and have been used as metal chelating reagent in analytical studies. Malonamide oximes, represented by the simplest molecule of this class nitrosomalonodiamide (9) that is known to coordinate with Fe (II) [74] are well known N-O donor bidentate ligands. The oximes of acetylacetone have been reported to coordinate with several metal ions in +2 and +3 oxidation states. One of the simplest cyanoxime molecules (10), is capable of acting as N-O donor bidentate ligand but its binding ability have not been explored much.
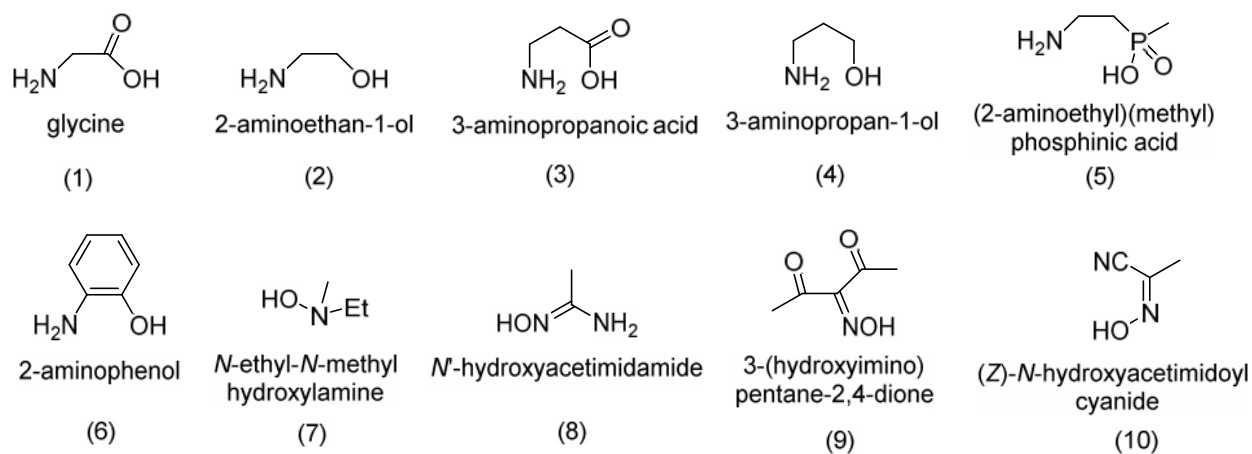
Figure 1.15 Bidentate N-O Donor ligands

There are some examples of N-O ligands reported that posses four donor atom sets, but act as bidentate ligand while binding to different metal ions instead of tetradentate. These ligands bind to two different metal ions forming two bidentate chelate rings, these category of ligands are usually termed as bis chelating ligands. One examples of such types of ligands shown in fig 1.16 is 2, 5-di(3H-pyrazol-2-yl)benzene-1,4-diol, that binds with two metals Ru and Os forming two compartments [75].
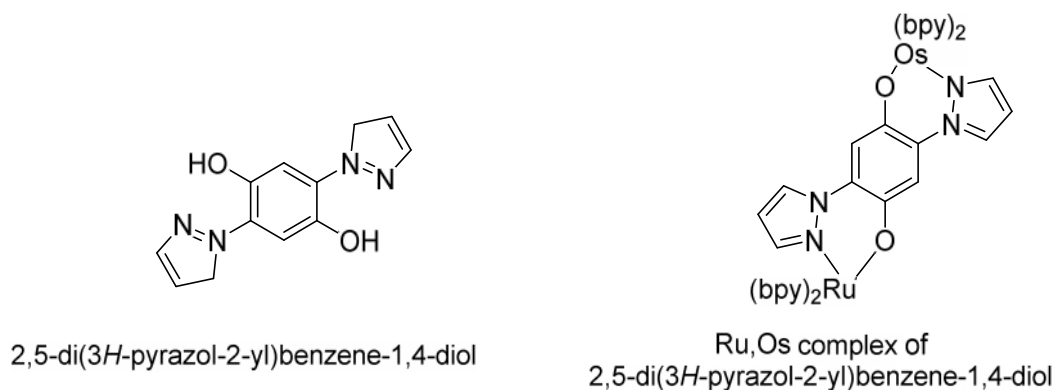
Figure 1.16 Bis chelating ligand 2, 5-di(3H-pyrazol-2-yl)benzene-1,4-diol and its metal complex

Another ligand of this category nitronyl nitroxide shown in figure 1.15 (a) is paramagnetic in nature, and forms linear polymeric complexes with Mn(II) through N-O atoms in reverse paths. Some of these complexes have shown to exhibit weak ferromagnetism [76].

(a)   (b)
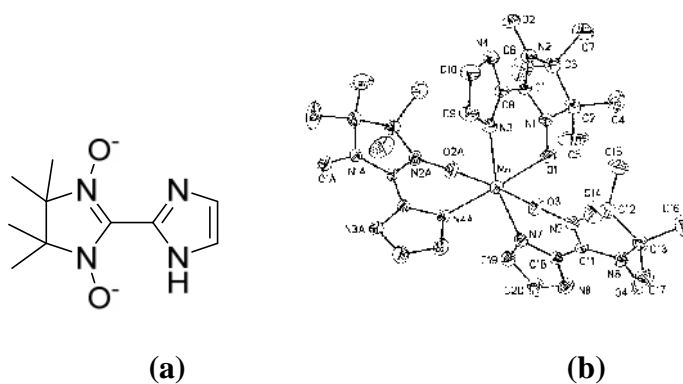
Figure 1.17 (a) Bis chelating nitronyl nitroxide ligand (b) ORTEP structure of Mn (II) nitronyl nitroxide complex

1.3.5.2 Tridentate N-O donor ligands

Some typical tridentate N-O donor ligands (1-12) with (N-N-N), (N-N-O) and (N-O-O) donor atoms are shown in figure 1.19. There are many examples of ligands having N-N-N or O-O-O donor sets which are dialectical hetero donors. Pyridine derivative (**1**) is an example of such type of ligands where the three N-N-N set of donor atoms, one from

pyridine group in centre and two belonging to imidazole groups attached to the pyridine are regarded as mixed donor ligand [77]. Fe(II) complex of this ligand showed a considerable shift of ($\sim$0.5V) in the redox potential upon deprotonation of the imidazole groups, whereas substitution on the imidazole ring brought changes in the magnetic properties of its Cu(II) complex [78]. Compound (2) represents other (N-N-N) donor dialectical ligands and with metal ions it coordinates through imidazolate resulting in oligomeric complexes.

Compounds (3) and (4) are typical (N-O-O) donor tridentate ligands originated from a central aromatic component. The $TiCl_2$ complex of the ligand (3) acts as catalyst in olefin polymerization [79]. In spite of forming 1:1 complexes with metals, ligand (4) forms M_2L_2 type of complexes (M = Co, Ni, Cu) [4]. 1, 2-Pyrazole derivative (5) acts as excellent (N-N-O) donor ligand with early tran\]ition metals and forms two six-membered metal chelate [80]. Potentially chiral (N-N-O) donor ligand (6), contains two types of N donor which forms ML_2 type complexes with metal ions Cu(II) and Co(III) having slightly distorted octahedral geometry [81]. The diethanol (7), dipropanol amines (8) and the extensively studied ligand 2, 6-pyridinedicarboxylic acid (9) exemplifies the (N-N-O) donors which consist of two equal side chains attached to a central aliphatic or aromatic amine group [82].
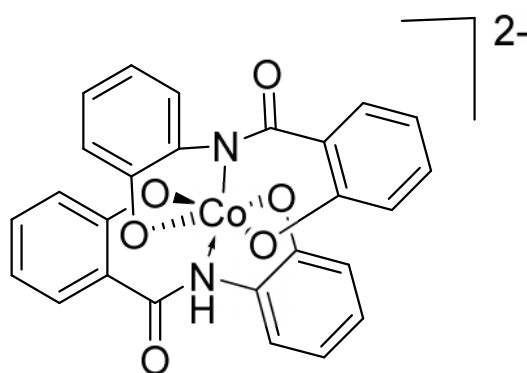
Figure 1.18 Co(IV) complex with (O-N-O) donor tridentate ligand

Another ligand of this category having side chains of different length is amidodiol (10), which forms stable Co(IV) complex [83].Compound (11) behaves as a tridentate chelating logand and mostly forms binuclear complex with Cu(II) and other transition

metals. Methyl sulfoxide substituted amino acid derivatives (12) are unusual tridentate chelating ligands having ambidentate characteristic and it may bind through (N-O-O) or (N-O-S) donor sets [84].

(1*Z*,1'*E*)-1,1'-(2-hydroxy-1,3-phenylene)bis(ethan-1-one) dioxime

4

1,1'-(oxybis(ethane-2,1-diyl))bis(3,5-dimethyl-1*H*-pyrazole)

5

(2*R*)-2-((pyridin-2-ylmethyl)amino)cyclohexan-1-ol

6

2,2'-azanediylbis(ethan-1-ol)

7

3,3'-azanediylbis(propan-1-ol)

8

pyridine-2,6-dicarboxylic acid

9

2-hydroxy-*N*-(2-hydroxyphenyl)benzamide

10

*N*¹,*N*²-bis(3-(methylamino)propyl)oxalamide

11

(methylsulfinyl)alanine

12
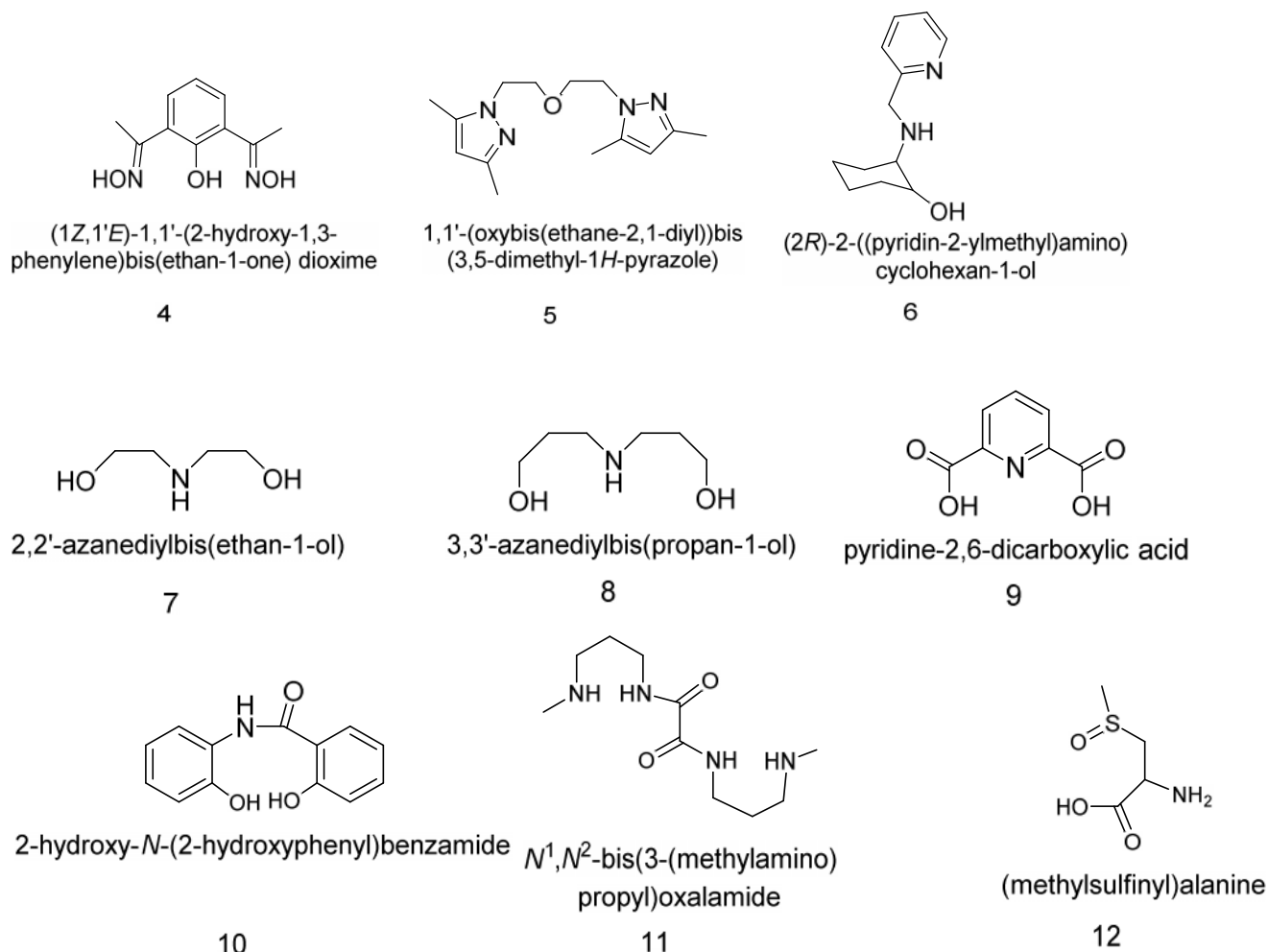
Figure 1.19 Tridentate N-O donor ligands

1.3.5.3 Tetradentate N-O donor ligands

There are several tetradentate N-O donor chelating ligands and their complexes with various metals have been reported in literature. Some examples of the tetradentate N-O donor moieties are shown in Figures 1.26. Linear ligand systems such as molecule (1) with (N-O-O-O) donor atoms are comprised of simple molecules, and they favorably binds with metal ions having small size and high charge density [85]. Branched tripodal ligand systems like (2) and (3) comprise of Nitrogen as central atom and O-donors as

branched chains, these ligands tend to form trigonal bipyramidal complexes. Example of this type of complex with Ti(IV) is shown below [86].
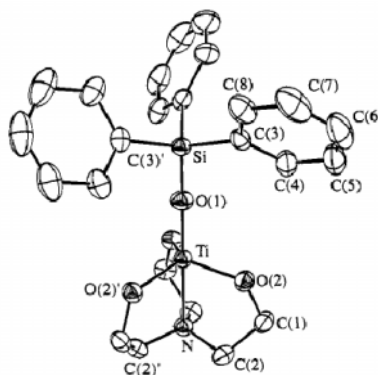
Figure1.20 ORTEP diagram of pentacoordinated Ti(IV) complex with triethanolamine

Tetradentate (N-O-O-N) donor ligand systems containing amino groups attached with oxo ethers (4) and their analogues having varied chain sizes are extensively studied, these ligands are primarily used as precursors in the synthesis of macrocycles [87,88].
Four-stranded aminoalcohol derivative (5) have unusual topology and it tends to coordinate majorly with first-row transition metal ions [89]. The diacetate derivative of a diaza heterocycle (6), acts as tetradentate N-O donor ligand [90]. Extensively studied compound (7) represents a huge category of ligands, which may coordinate with two separate metal ions, one in an (N-N-O-O) environment and the other in an (O-O-O-O) cavity [91]. 1, 2-pyrazole-3,5-dicarboxylic acid (8) represents another class of (N-N-O-O) tetradentate donor ligand that coordinate with two different metal atoms in a binuclear bis-chelate fashion [92].

The copper complex of the diaminodiol derivative (9) acts as a model for *galactose oxidase* [93], structurally similar diamidodiol derivative (10) have shown tendency to coordinates with high-valent Os and Ru. Formation of hetero metal mixed ligand complexes of (9) and (10) [Cu{L}M(bipy)2] (M= Co, Ni, Zn) have been also reported [94].
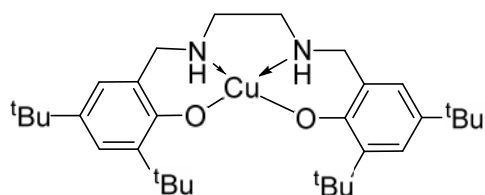
Figure 1.21 Model galactose oxidase Cu (II) complex of ligand (9)

Several diamine-diacid ligands such as (11) have been synthesized from -amino acids by a metal-directed route [95]. Amide analogue of this ligand (12) mostly forms simple mononuclear metal complexes, but it is also reported to behave as bridging ligand [96].

Vanadyl complexes which act as halogen peroxidase models have been reported with the tripodal (N-N-O-O) and (N-N-N-O) donor ligands derived from iminodiacetic acid. These ligands exemplify class of ligands which are electronically similar to potential donors to vanadium(IV) in other biological systems [97].

(N-N-N-O) and (N-N-O-O) donor tetradentate ligands of aminoalcohol are known to form mononuclear complex with Cu(II) which have trigonal bipyramidal geometry [98] and Fe(III) complex having square-pyramidal arrangement which act as model catalyst for catechol-1,2-dioxidase [99].
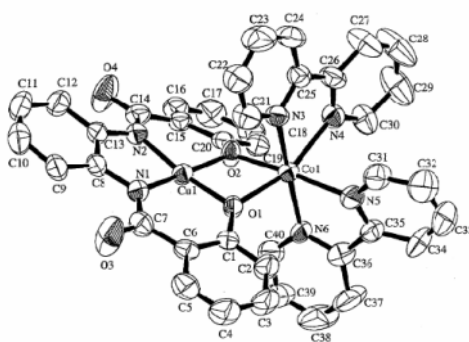
Figure 1.22 ORTEP diagram of hetero metal complex [Cu {L}Co(bipy)2]
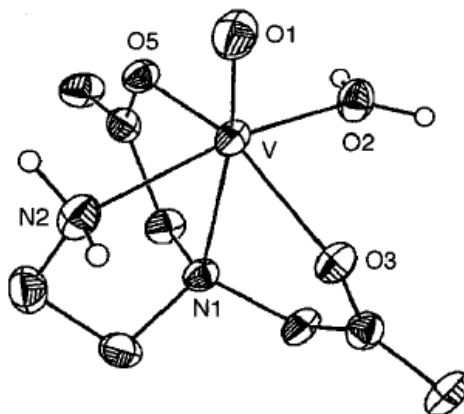
Figure 1.23 ORTEP diagram of V(IV) complex of N-(2-hydroxyethyl)iminodiacetic acid

N,N-Bis(2-pyridylmethyl)-N-(2-hydroxybenzyl) amine

(a)   (b)
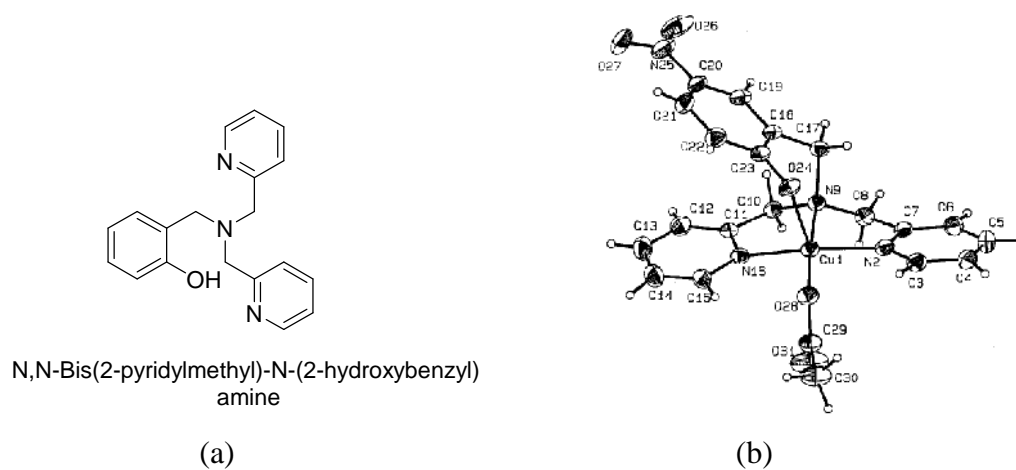
Figure 1.24 (a) 2-(bis(pyrid-2-ylmethyl)aminomethyl)-4-nitrophenol (Hbpnp) (b) ORTEP drawing of [Cu(bpnp)(CH$_3$COO)]

The sterically crowded ligand 2, 4-bis[(R) -2-hydroxy-2-methylbutyramido] -2,4-dimethylpentan-3-one (HMBA-DMP) forms an exceptional rare square-planar Co(III) complex, shown in figure 1.25 which act as good catalyst in epoxidation of styrene [100].

(a) (b)

Figure 1.25 (a) (-)2,4-bis[(R) -2-hydroxy-2-methylbutyramido] -2,4-dimethylpentan-3-one (HMBA-DMP) (b) ORTEP structure of Co(III)- (HMBA-DMP) complex

2-(2-(2-aminoethoxy)ethoxy)ethan-1-ol

(1)

2,2',2''-nitrilotris(ethan-1-ol)

(2)

2,2'-((3-hydroxypropyl)azanediyl)bis(ethan-1-ol)

(3)

2,2'-(propane-1,3-diylbis(oxy))bis(ethan-1-amine)

(4)

((1R,4S)-5,6-bis(aminomethyl)bicyclo[2.2.1]heptane-2,3-diyl)dimethanol

(5)

2,2'-(1,5-diazocane-1,5-diyl)diacetic acid

(6)

6,6'-(propane-1,3-diylbis(azanediyl))bis(2-hydroxyheptan-4-one)

1*H*-pyrazole-3,5-dicarboxylic acid

(8)

6,6'-((ethane-1,2-diylbis(azanediyl))bis(methylene))bis(2,4-di-*tert*-butylphenol)

(9)

Figure 1.26 Tetradentate N-O donor ligands

1.3.5.4 N-O donor ligands derived from Nitrogen Heterocycles

Ligands derived from nitrogen heterocycles constitute an important class of N-O donor chelating ligands. A common potential bidentate N-N donor molecule derived from nitrogen heterocycles is exemplified by (1). This molecule is capable of forming chelate as well as may act as bridging ligand forming multinuclear complexes [101]. Bidentate N-O donor ligands in which the aromatic N donor group is present for example pyridine, imidazole, pyrazine, pyrimidine etc. are common. Pyridines and its derivatives constitute broad category of this type of ligands. The 2-hydroxypyridine derivative is also known to form stable four-membered N-O or N-S chelates [102, 103].

Another such category of N-O donor bidentate ligand, 2-pyridinecarboxylic acid (2) has been reported to form several five-membered chelate rings complexes [104]. Pyridine N-oxides derivatives (3) that act as N-O donor bidentat ligand generally form six-membered chelate rings. The molecule pyridine-2-sulfonic acid (4), a sulfonate analogue of picolinic acid, interestingly known to acts as an N-O chelating ligand with Ag(I) forming polymeric complex. Pyrazole and imidazole are other important heterocyclic rings constituting category of mixed donor ligands.

There are several ligands containing pyrazine ring have been reported, for example pyrazine-2-carboxylic acid (5) that works as N-O bidentate ligand with transition metals forming five-membered chelate rings [105].
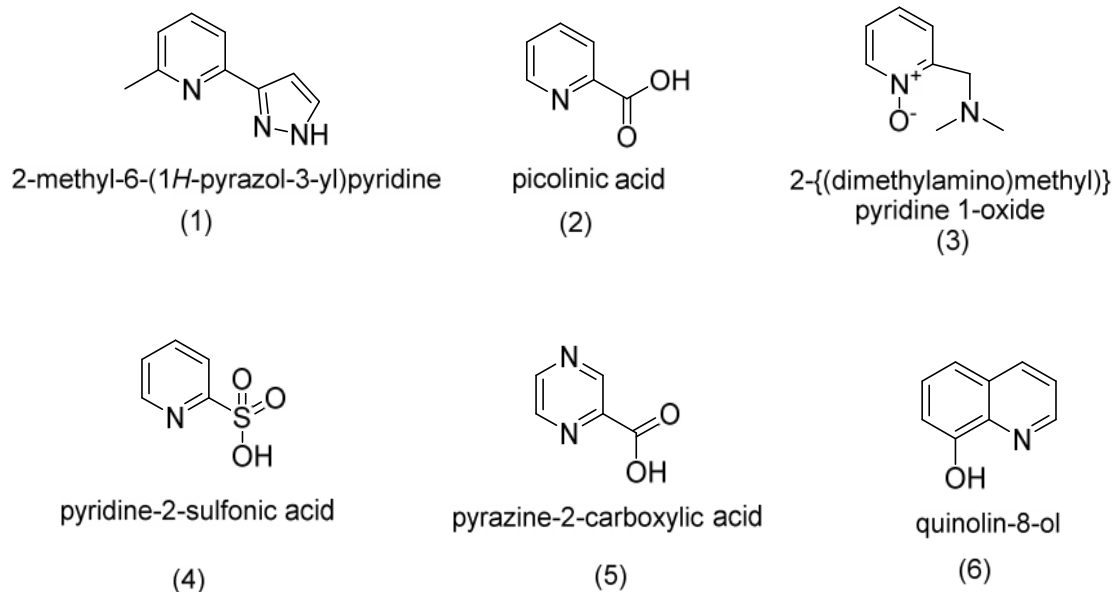
Figure 1.27 Bidentate chelates containing N-heterocycles

1.4 8-Hydroxyquinoline as potential N-O donor ligand

Quinoline derivatives, suitably substituted at the 8-position formulate brilliant N-O donor chelating ligands and were extensively used in analytical studies. The 8-hydroxyqinoline (6) molecule is one of the most revered N-O donor bidentate chelating ligands derived from quinoline that is known to form mostly simple mononuclear complexes and sometimes forms polynuclear complexes for instance a tetranuclear complex with Mn(III) [106].

8-Hydroxquinoline (8-HQ) is the most versatile and trendy organic compound. It is a colorless crystalline organic compound which structurally consists of a phenol group attached to a pyridine ring. There are a number of applications such as electron carriers in organic light-emitting diodes (OLEDs), fluorescent chemosensors, pharmacological and pharmaceutical fields, etc. where 8-Hydroxyquinoline and its derivatives have been used [107].

In the field of medicine, 8-hydroxyquinoline and its derivatives have been used as antibacterial, fungicidal, insecticides, neuroprotective, and also anti-HIV agents. Besides these medicinal applications, owing to their excellent binding ability for variety of metal ions, 8-hydroxyquinoline and its derivatives have established numerous applicabilty in

sensing metal ions such as Zn^{2+} and Al^{3+} which are of biological and environmental importance [108]. 8-hydroxyquinoline and its derived ligands have been widely used for analytical and separation techniques. Some of these ligands act as exceptionally good agent for quantitative determination of analytes and therefore have been used for various metal extractions [109].

8- hydroxyquinoline molecule shows weak fluorescence due to the intermolecular proton transfer of the excited state proton of the hydroxyl group to the low lying nitrogen atom of the pyridine ring. Upon chelation of 8-hydroxyquinoline with metals ions fluorescence emission greatly increases. This increase in the emission can be attributed to the increased rigidity in the 8-hydroxyquinoline molecule after chelation [110].

1.4.1 Synthetic methods for the preparation of 8-hydroxyquinoline and its derivatives

There are three most convenient synthetic routes are available for the synthesis of 8-hydroxyquinoline and its derivatives. Skraup or Friedlander methods involve synthesis of 8-hydroxyquinoline and its derivatives via construction of the heterocyclic ring [111]. In the Skraup method, substituted aromatic amines are reacted with , -unsaturated aldehydes and in the Friedlander reaction derivatives of 8-hydroxyquinoline are synthesized by reacting substituted o-aminobenzaldehyde/ o-aminoacetophenone with suitable carbonyl compounds (Scheme-1.1).

3-amino-[1,1'-biphenyl]-4-ol   acrylaldehyde   5-phenylquinolin-8-ol
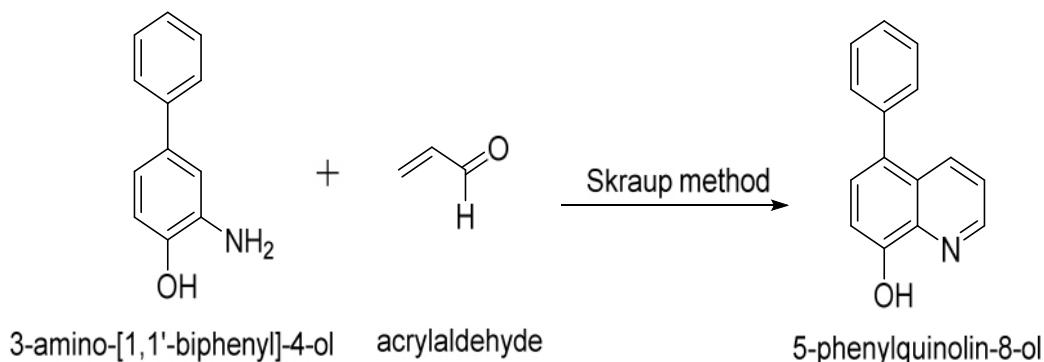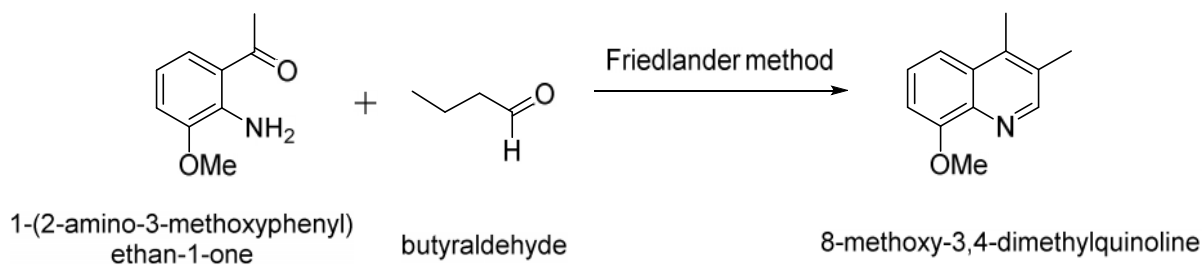
Scheme 1.1: Preparation of 8-hydroxyquinoline by Skraup and Friedlander methods

Another synthetic route for synthesis of 8-hydroxyquinoline involves introduction of –OH group to the quinoline moiety. It can be achieved either by diazotization reaction of amine substituted quinoline or by reacting 8-sulphonic acid with alkali (Scheme-1.2) [112].

Scheme 1.2: Preparation of 8-hydroxyquinoline by diazotization and alkali fusion methods

Suzuki cross-coupling reaction is the most versatile and widely used method for the synthesis of 8-hydroxyquinoline. In this reaction a new substitution at position 5 or 7 or both of the 8-hydroxyquinoline moiety can be commenced (Scheme-1.3) [113, 114].

Scheme 1.3: Preparation of 8-hydroxyquinoline by Suzuki coupling reaction

1.4.2 Structural aspects of 8-hydroxyquinoline

8-hydroxyquinoline (8-HQ) consists of two ring systems of quinoline having substituted -OH group at 8th position (Figure-1.26). Due to the presence of phenol ring 8-hydroxyquinoline has characteristic phenolic properties such as, it gives violet color with ferric chloride, involve in Reimer-Tiemann and Bucherer reactions, undergoes coupling with diazonium salts and its acetate ester easily undertake Fries rearrangement in presence of Lewis acids resulting in its acetyl derivative [115].

Figure1.28 Structure of 8-hydroxyquinoline and quinoline

8-hydroxyquinolines are present in the form of an equilibrium mixture of the hydroxyl-form and the N-protonated zwitterionic form like other hydroxyquinolines.

Figure 1.29 Zwitterionic form of 8-hydroxyquinoline

Due to the existence of -OH group within the vicinity of the aromatic nitrogen, 8-hydroxyquinoline work as excellent bidentate N-O donor chelating ligand and forms

chelats with a number of metal ions like Mg^{2+}, Cu^{2+}, Bi^{2+}, Al^{3+}, Mn^{2+}, Fe^{3+}, Ni^{3+} and Zn^{2+} [116]. 8-hydroxyquinoline forms chelate with metal ions in the ionic form removing its hydroxyl hydrogen and coordinated through oxygen and nitrogen donor atoms. Pyridine derivatives are frequently used as building blocks in the designing of suitable ligands [117]. In the monoionic form 8-hydroxyquinolinate consists of one N-donor atom of bipyridine and an O-donor atom belonging to phenolate and hence possesses the propertieas of both bipyridine as a neutral ligand as well as doubly charged catecholate ligands.

Therefore tetravalent metals react with two 8-HQ molecules and hexavalent metal complexes involve three 8-HQ molecules.
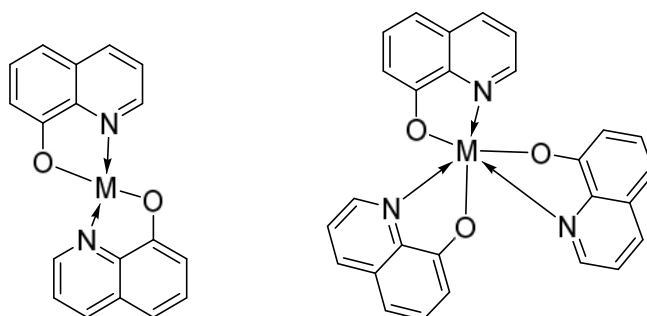
Figure 1.30 Four and six covalent metal complexes of 8-hydroxyquinoline

In the begining 8-hydroxyquinoline ligand was mainly used for quantitative analysis and separation techniques. But in recent time 8-hydroxyquinoline has been extensively used towards the synthesis of luminescent coordination complexes which are used for sensors, light emitting devices [118] and diagnostics [119]. 5-chloro-8-hydroxy-7-iodoquinoline (Clioquinol) is commercially available on highly effective antisepticum [120]. This compound is a potent chelator for Cu(II) and Zn(II) and restrains the asparagine and ubiquitination hydroxylation of the hypoxia-inducible factor-1 (HIF-1) [121].

1.4.3 Applications of 8-hydroxyquinoline and its derivatives

A brief study of the metal complexes of 8-hydroxyquinoline and its derivatives applicable in several fields outlined here.

1.4.3.1 8-hydroxyquinoline derivatives in organic light emitting diodes (OLEDS)

In 1987 a 3:1 complex (Alq3) of 8-hydroxyquinoline with Al(III) reported by Tang and Van Slyke for the very first time [122]. From the time of its invention Alq3 has been the most widely explored substance used in transport of electron and in organic light emitting appliances. Invention of this complex opened an entirely new research area towards development of organic electroluminescence devices. There have been several light emitting materials and devices with enhanced performance designed till date. So far a variety of derivatives of Alq3 and their conductance and optical properties were widely investigated [123-125]. The structures of some important electroluminescent 8-hydroxyquinoline Al(III) metal complexes are shown in Fig.1.31.
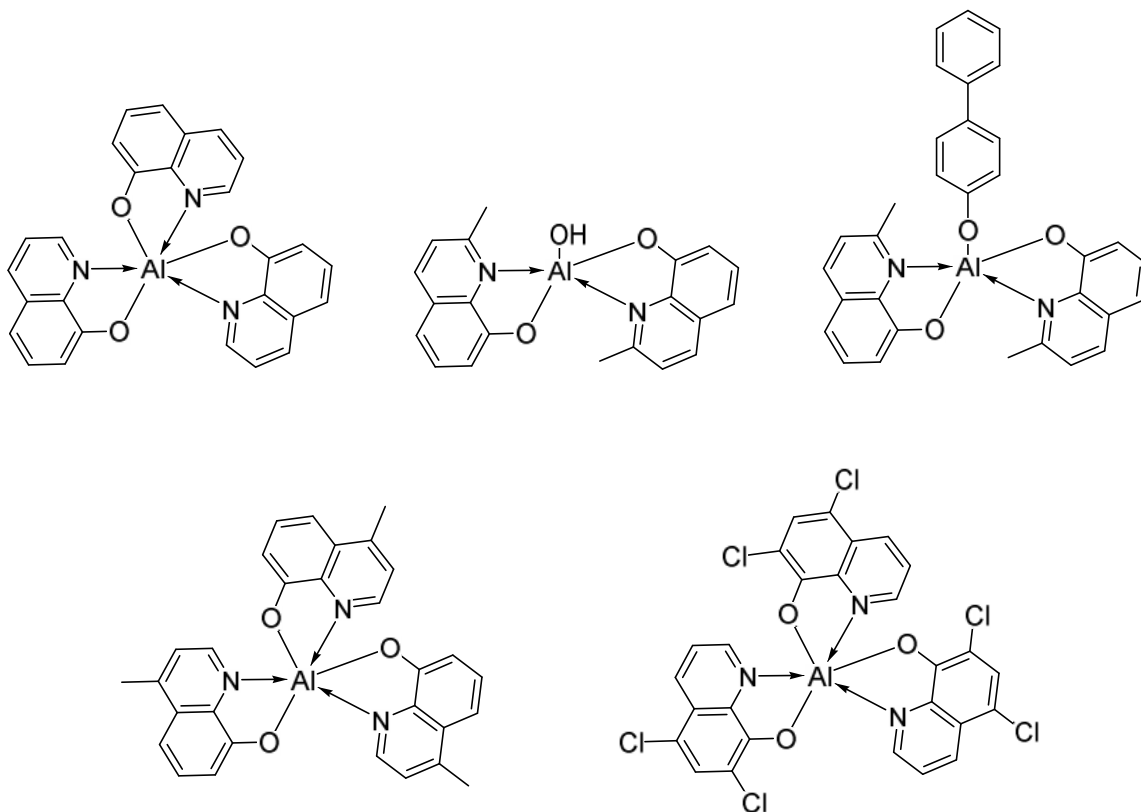
Figure 1.31 Al complexes of 8-Hq derivatives displaying light emitting property

Other than Aluminium complexes, organo boron quinolate complexes have also been reported to display high photoluminescence [126].This discovery opened up possibility to explore novel organo boron derived complexes exhibiting enhanced

luminescence properties. Kappaun et. al. in 2006 designed a stable polymeric 5,7-disubstituted organoboron quinolinolate complex having tunable photoluminescence [127].

$X= C_6F_5, H, Cl, C_6H_4OMe$
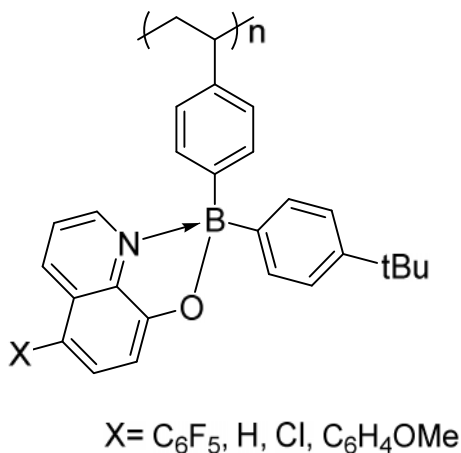
Figure 1.32 Organoboron quinolinolates

Further Beryllium complexes with 8-hydroxyquinoline exhibiting light emitting properties were reported by Sano group in 2000 [128]. Some of the examples are:

bis(quinolinate)Be(II)   bis(5,7-dimethylquinolinate)Be(II)
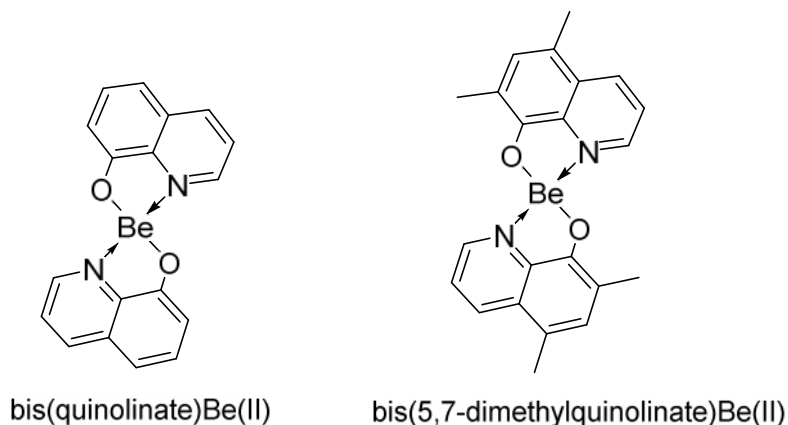
Figure 1.33 Be complexes of 8-Hq derivatives displaying light emitting property

A lithium complex with 8-hydroxyquinoline showing good electron injecting properties was reported by Hua Wang et. al.[129] Amit et. al. reported synthesise of white light emitting devices with lithium complex of 8-hydroxyquinoline which efficiency was improved by coating DCM dye between the emissive layers [130].
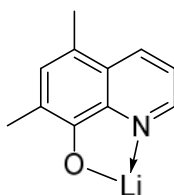
Figure 1.34 Li complexes of 8-HQ derivatives displaying light emitting property

Green luminance at 520 nm showing Mg complex of 8-hydroxyquinoline, magnesium-bis(5-chloro,8-hydrxyquinoine) was reported by Anita et. al. [131]. Jeng Keun Park et. al synthesized Sn complexes with 8-hydroxyquinoline, 2-(2-hydroxyphenyl)benzoxazole (HPB) and diphenyl [132].
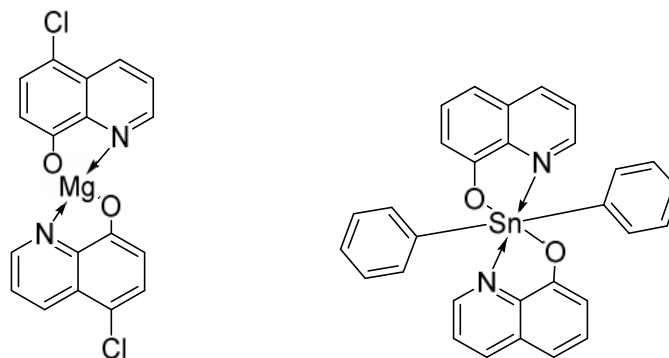
Figure 1.35 Sn & Mg complexes of 8-HQ derivatives displaying light emitting property

Zinc complexes with 8-hydroxyquinoline have been used in OLEDs for the first time in 2000 [133]. Further green light emitting zinc complexes with 8-hydroxyquinoline ligand, bis(2- methylquinolin-8-olato)-bis[(acetato)-(methanol)zinc(II)] was reported [134].
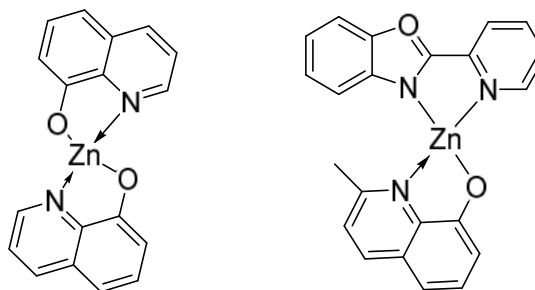
Figure 1.36 Zn(II) complexes of 8-Hq showing light emitting property

1.4.3.2 Complexes of 8-hydroxyquinoline derivatives used in chemosensors applications

Molecules which upon bonding with an analyte exhibit significant indication of the bond formation are regarded as chemosensors. As a consequence of excellent ability of 8-hydroxyquinoline molecule to form stable chelate ring with various metal ions, it has been widely used as fluorescent chemosensor for detection of several metal ions of biological and environmental interest [135].

There are a number of bidentate 8-hydroxyquinoline derivatives have been designed and studied for their complexation and sensitization properties for group 13 elements and lanthanides. Since very long 8-hydroxyquinoline has been known as an efficient sensitizer for europium metal and it forms Eu (8-HQ)$_3$ complex [136].

The 8-hydroxyquinoline benzoates substituted at 2 and 7 positions have been investigated as fluorescent chemosensors for transition metal ions such as Cu^{2+} and Hg^{2+} [137], apart from these various derivatives with substituted at the C-5 position have also been reported [138].

Recently, highly sensitive and selective fluorescent chemosensors (methleneimino-1-phenyl-2, 3-′-hydroxyquinolin-5′ and 4-(8 dimethyl-5-pyzole) for Al^{3+} ion synthesized by Schiff-base condensation reaction of 4-aminoantipryrine and 8-hydroxyquinoline-5-carbaldehyde have been investigated [139].
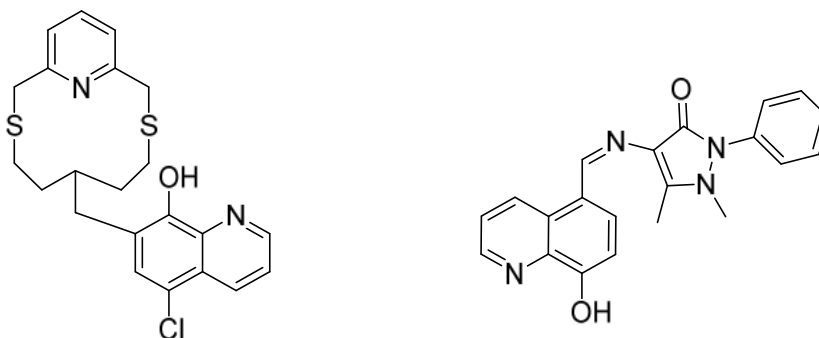
Figure 1.37 Fluorescent chemosensor methleneimino-1-phenyl-2,3′-hydroxyquinolin-5′& 4-(8 dimethyl-5-pyzole)

The pH based study of photoluminescence properties suggested that this ligand could serve as an excellent chelator in weakly acidic aqueous medium for highly toxic aluminium ions. Literature reports that monopodal bidentate 8-hydroxyquinoline and its

derivatives bind with variety of metal ions. Even though the synthesis, electronic absorption and redox properties of Ru(II) complexes of various 8-hydroxyquinoline derivatives have been reported long time before [140], yet binding capacity of bidentate 8-hydroxyquinoline for Ru(II) has not received much attention [141].
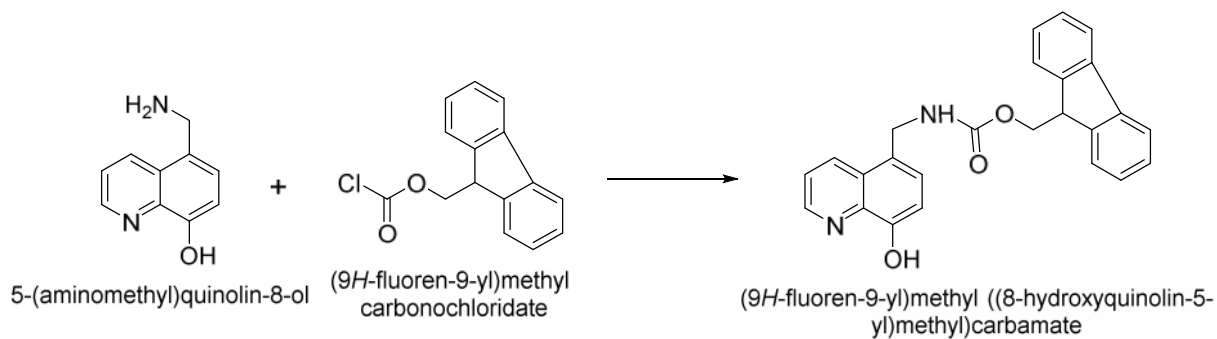
Scheme 1.4: Synthesis of C-5 substituted *8*-hydroxyquinoline derivatives
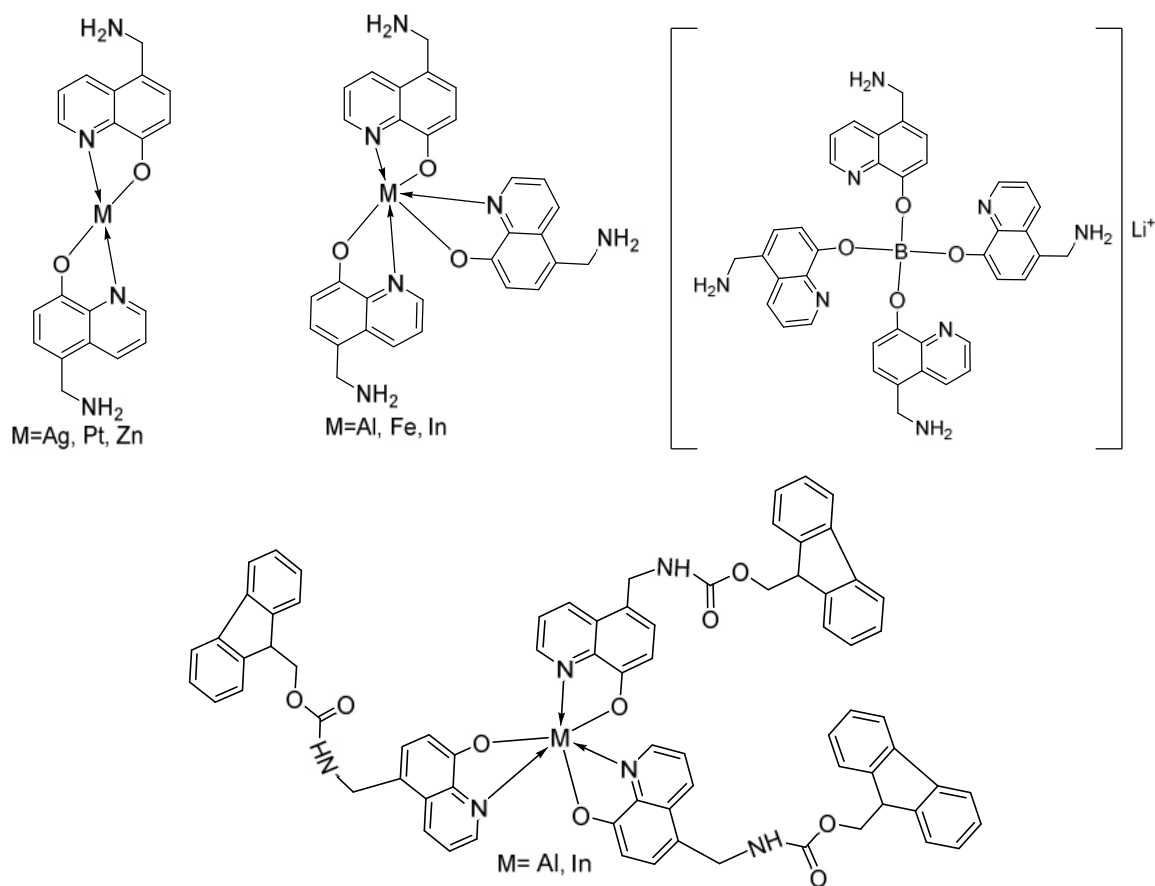
Figure 1.38 8-Hq derivatives as bidentate chelaters

Lately, tridentate (N-N-O) donor ligands derived from 8-HQ were reported. These ligands were synthesized by incorporating 8-HQ unit to the polypyridine ligand unit using Friedlander condensation method [142]. 2-(pyridin-2-yl)-8- hydroxyquinoline shown in Figure 1.37 represents the parent component of this category of new tridentate ligand series and have been extensively used in chelation [143]. These class of tridentate ligands have been reported to form interesting complexes with several metal ions specifically with Ru(II) metal ions.

2-(pyridin-2-yl)quinolin-8-ol   bis {2-(pyridin-2-yl)quinolinate}Ru(II)
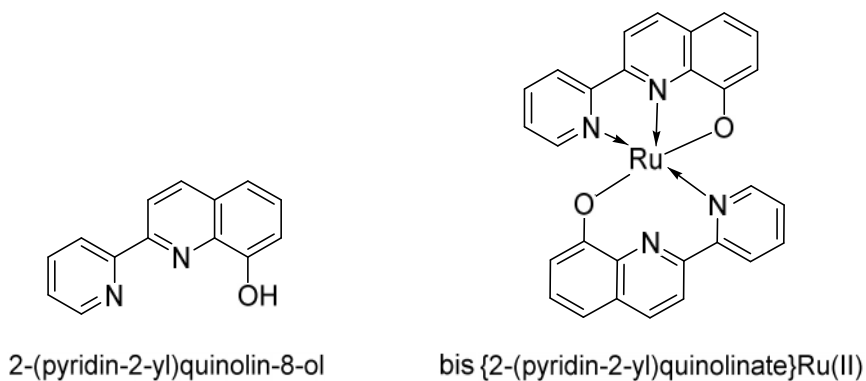
Figure 1.39 Ruthenium complex of tridentate derivative of 8-Hq

Chelating properties of the ligands, bis(oxine) comprising of two units linked with various spacer group or linkages has been broadly investigated [144]. Various ligands of this caltegory were designed by linking two 8-HQ molecules with the methylene (-CH$_2$-), sulfonyl (-SO$_2$-), dimethylene sulfide (-CH$_2$-S-CH$_2$-) and ether (-CH$_2$-O-CH$_2$-) groups [145,146]. Further synthesis and characterization of polymeric coordination complexes with the bis(oxine) ligand designed by bridging two 8-HQ units with -H$_2$C-O-Ph-O-CH$_2$ (Ph = 1,3 phenylene) and -H$_2$CO-Ph-C(CH$_3$)$_2$-Ph -OCH$_2$ were reported [147].

Recently, chelating ability of bis 8-HQ derived ligands were enhanced by the introduction of N,N'-diethyl-1,3-propane diammine as a bridge between two 8-HQ subunits. Synthesis of polymeric coordination complexes of this ligand with Cu(II), Ni(II), Co(II), Zn(II) and Mn(II) metal ions were reported [148].

The chemosensor based on two 8-methylene-dianiline through imine hydroxyquinoline chromophores connected with 4, 4 linkage has been reported [149]. The complexation and photophysical properties of this ligand with group 13 metal ions Al^{3+} , Ga^{3+} and In^{3+} have been investigated using fluorescent emission spectroscopy and UV-vis spectroscopy

and reported the formation of helicate type structure. Two chelators of this category derived from 8-hydroxy quinoline and 1,5-bis(2-aminophenoxy)-3-oxopentane have been investigated for both bivalent metal ions Cu^{2+}, Zn^{2+} and trivalent metal ions Sm^{2+} and Eu^{2+} [150].
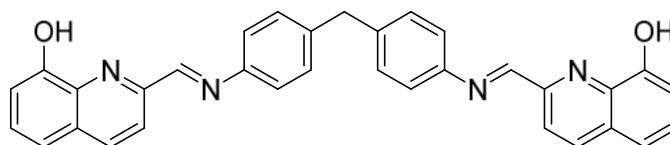
2,2'-methylenebis(4,1-phenylene)bis(azanylylidene) bis(methanylylidene)bis(quinolin-8-ol)
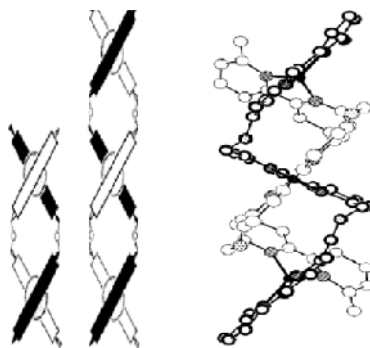
Figure 1.40 Chemosensor bis(oxime) ligand and its helical polymeric complex with Al^{3+}

Furthermore, coordination complexes of lanthanide metals with chelating 8-HQ derived ligands have attracted numerous investigations due to their appealing luminescence emission properties in NIR region [151]. These lanthanide complexes of 8-hydroxyquinolinate based ligands act as excellent candidates owing to their high stability, low cytotoxicity, remarkable luminescence quantum yield in water as well as their capability to interact with proteins for the designing of NIR-emitting luminescent materials for biomedical applications [152].

1.4.3.3 Applications of 8-HQ derivatives in pharmaceuticals

8-HQ and its numerous derivatives have been found to be applicable in agricultural and medicinal fields due to their distinctive chemical properties. There are a number of compounds comprising of 8-HQ which have shown to exhibit compelling pharmacological activities against a number of bacteria, fungi and insects. In addition,

some of the other 8-HQ derivatives have known to show antitumor and antioxidant activities too.

1.4.3.3.1 Antiviral activity of 8-Hydroxyquinoline derivatives

In order to show antiviral activity RNA-dependent-DNA polymerase inhibition is essential and for this ability to bind with nucleic acid is a vital factor. 8-hydroxyquinoline showed approximately 50 times higher antiviral activity among the various investigated metal-chelating compounds. It has been reported that the nucleic acid binding ability for the complexes of Cu(II) with 8-hydroxyquinoline and its analogues were considerably greater than their particular free ligand. This activity was observed to be enhanced notably upon addition of equimolar concentration of Copper [153].

Albert et al reported that the ratio of free ligand and their metal complex has shown significant effect on their antimicrobial activities, activity was prominently exhibited only when the ratio was 1:1. Further it was concluded that the increase in the quantity of ligands decrease the activity, this phenomenon is known as concentration quenching [154].

5-chloro-7-iodoquinolin-8-ol   bis(5-chloro-7-iodoquinolate-8-ol) Cu(II)
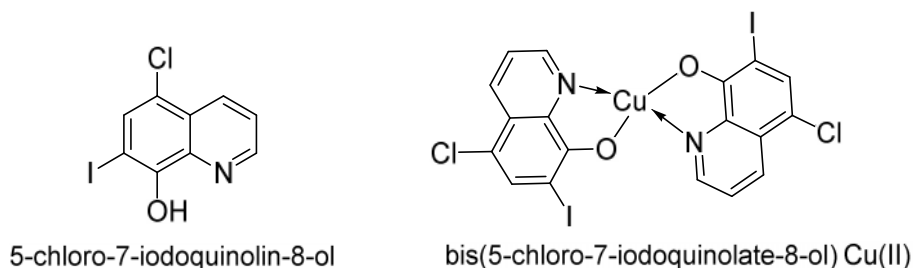
Figure 1.41 8-HQ derivative and its Cu(II) complex showing antiviral activity

The antiviral activity of 8-HQ and its derivatives can be attributed to its binding ability with viral nucleic acid while the other possible mechanism for exhibiting antiviral activity proposes that they bind to Zn present in enzymes, thus resulting in the deactivation of viral enzymes [155,156]. The Cu complex of 8-HQ is reportedly much more than that of the Zn complex [157], further the investigation demonstrating RNA-dependent-DNA polymerase inhibition and inactivation of herpes simplex and Rous sarcoma virus

using 8HQ-Cu(II) complex with equal potential as compared to free 8-hydroxyquinoline ligand supported this mechanism [158].

1.4.3.3.2 Fungicidal and Insecticidal Properties of 8-HQ Derivatives

8-hydroxyquinoline and its derived molecules act as potential metal chelator with lipophilic nature. Copper complex of   8-hydroxyquinoline $Cu(8Hq)_2$, has been extensively used as fungicide in several countries in order to prevent the symptom of diseases like scab, black spot and brown patch found in several fruits and vegetables [159]. Significant antifungal activity have been reported to shown by 8-hydroxyquinoline substituted at 2, 3, 4, 5, 6, and 7 positions by chloro or bromo groups against Aspergillus oryzae, Aspergillus niger, Trichoderma viride, Trichophyton mentagrophytes and Myrothecium verrucaria. Among the various tested derivatives of 8-HQ, the 5, 7-dibromo and 5, 7-dichloro derivatives have shown the highest fungicidal activity [160].
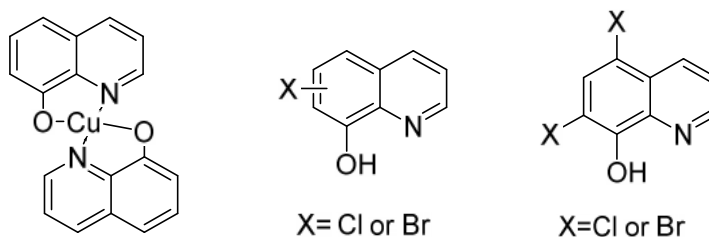
Figure 1.42 8-hydroxyquinoline derivatives bearing fungicidal activity

8-HQ   derivative   8-hydroxy-2-methylquinoline   have   shown   to   have   high insecticidal effects against Sogatella furcifera, Nilaparva talugens and Laodelphax striatellus   suggesting that these derivatives may serve as new potential agents for prevention and controlling the damages   by various category of bugs found in paddy cultivating areas [161]. The substituted 8-HQ derivatives; 5-bromo-7-sulfonic acids, 7-bromo-5-sulfonic acids and 7-chloro derivatives showed much higher antifungal activity than that of simple 8-HQ [162].
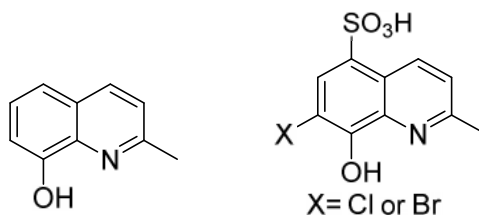
Figure 1.43 8-hydroxyquinoline derivatives showing insecticidal activity

1.4.3.3.3 Antibacterial activities of 8-hydroxyquinoline Derivatives

8-hydroxyquinoline and its derivatives have been used as antibacterial agents since long time. Several antibacterial drugs derived from them have been used in medicinal field as chemotherapeutics before 120 years. Bivalent metal complexes of 8-hydroxyquinoline have been extensively used as antimicrobial agent. [163]. The proposed mechanism suggest that due to high lipophilicity 8-HQ pierce membranes of bacterial cell and arrive at its target site, where it possibly binds with metal present in bacterial enzymes. It is assumed that the metal-8-hydroxyquinoline complex break into a 1:1 ratio of 8HQ free ligand and 8-hydroxyquinoline - metal charged complex [164]. The charged metal- 8-hydroxyquinoline complex hinders the sites on bacterial enzymes for metal-binding via bond formation; this resulted into the antimicrobial effect [165]. According to this mechanism of action the lipophilicity (logP) of the compound is considered to be an important factor in order to show antimicrobial activity. Additionally, the dissociated 8-hydroxyquinoline ligand has very strong chelating ability and it can bind with metallic prosthetic groups of microbial enzymes thus resulting in the inhibition of enzymatic activity [166].

Lately, 8-hydroxyquinoline- uracil metal complexes were known to exhibit potential antimicrobial activity (Figure 1.44). These complexes were shown to inhibit growth of many Gram-positive and Gram-negative bacteria strains for example *Candida albicans, S. aureus*, and *Enterococcus faecalis* including resistant pathogens [167].
4-[(8-hydroxyquinolin-5-yl)methyl]aminobenzenesulfonamide (HQMABS), shown in Figure 1.45, is a derivative of 8-hydroxyquinoline that act as chelating ligand for various metals [168]. HQMABS has been reported to exhibit effective antimicrobial activity against Gram-positive bacteria in comparison to their individual parent compounds

sulfanilamide and 8-hydroxyquinoline. This study reveals that there is a synergistic effect of 8-HQ and sulfanilamide which assists the diffusion of HQMABS into the site of action in bacterial cell membranes. Consequently, the mode of action for HQMABS exhibiting antimicrobial effects is similar to that of 8-HQ [169]. On the contrary, metal complexes of HQMABS show weak to moderate activity as compared to their respective free ligand, HQMABS.
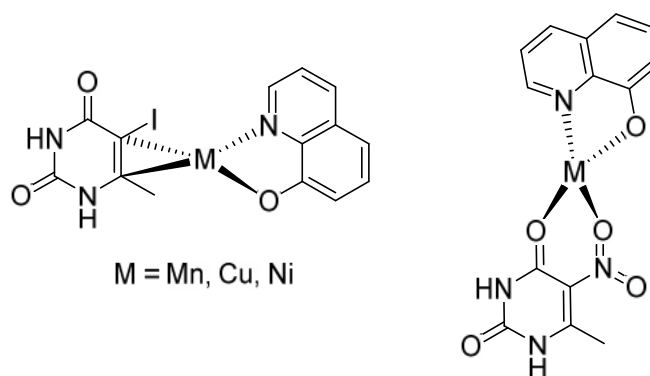
Figure 1.44 Mixed ligand complexes of 8-hydroxyquinoline bearing antibacterial activity

The antimicrobial activity of 8-HQ derived complexes depends on the several factors such as the environment of the ligands, lipophilicity and concentration of the compound, character of metal ions, coordination sites and geometry of the complex [168].
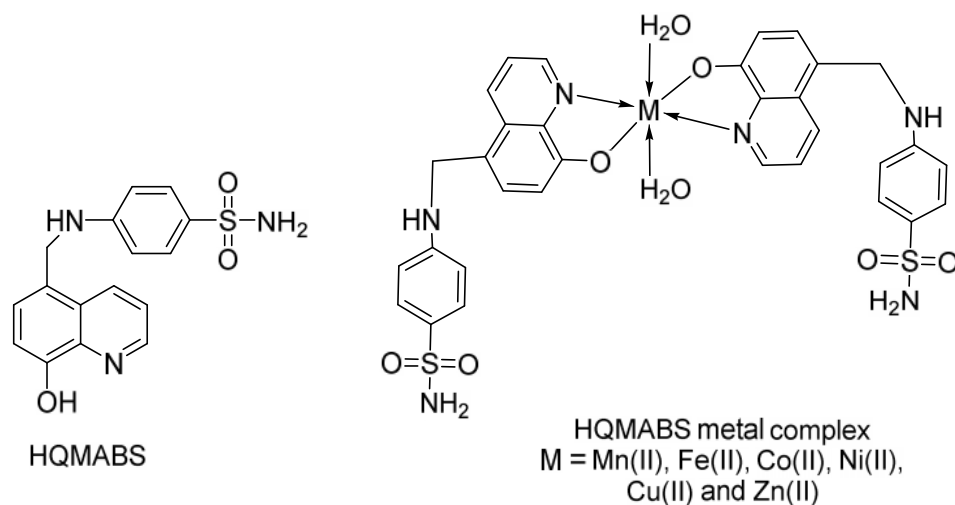
Figure 1.45 8-Hydroxyquimoline metal complexes showing antibacterial activity

Some of the newly designed derivatives of 8-HQ were reported to show greater antimicrobial activity. [170]. A derivative 5-alkoxymethyl-8-quinolinol (a) (Figure-1.46) shows higher activity against bacterial strains and fungal strains than that of simple 8-HQ, however shows moderate activity as compared to standard drugs [171].

7-Morpholinomethyl-8-hydroxyquinoline (b) (Figure-1.46) is an additional 8-HQ derivative which is known to show potent antimicrobial activity. It was observed to display higher activity against Gram positive bacteria than Gram negative bacteria. Effectiveness of this compound was correlated with its chelation ability with iron. 7-Morpholinomethyl-8-hydroxyquinoline (b) forms a chelate with Fe in of 2: 1 ratio and this complex displayed higher antibacterial activity than free ligand (b) [172].

Another 8-HQ derivative 5-nitro-7-((4-phenylpiperazine-1-yl-)methyl)quinolin-8-ol (c) (Figure-1.46) has been used to hinder type III secretion (T3S) in the Gram-negative pathogen *Yersinia pseudo tuberculosis*. This molecule (c) targets both the extracellular bacterium *Chlamydia trachomatis* and the intracellular pathogen *Y. pseudo tuberculosis* in cell-based infection models [173].

5-(*sec*-butoxymethyl)quinolin-8-ol   7-(morpholinomethyl)quinolin-8-ol   5-nitro-7-((4-phenylpiperazin-1-yl) methyl)quinolin-8-ol

(a)   (b)   (c)
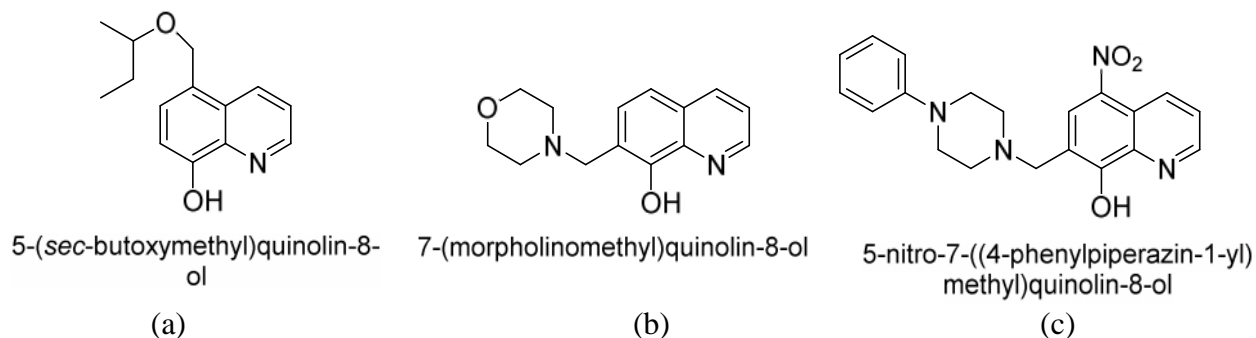
Figure 1.46 8-Hydroxyquinoline derivatives bearing antibacterial activity

1.4.3.3.4 Anti HIV and Antitumor Activities of 8-HQ Derivatives

Gallium complex of 8-hydroxyquinoline, Tris (8-quinolinolato) Ga(III) have been reported to show potential inhibition against growth of carcinoma cells (A549) which causes lung cancer in human 10 times higher than that of $GaCl_3$ [174]. In the course of antitumor treatment, chelation of Iron with cancer cells was proved to be very effective. Incidentally, an efficient new generation iron chelator quilamines (b) was designed by

incorporating 8-HQ moiety with a linear polyamine system. These newly designed derivatives of 8-HQ were confirmed to exhibit potent antitumor activity in the micromolar range while, cytotoxicity was observed at higher concentrations as much as 100 μM [175].

Another derivative of 8-HQ, 8-quinolinyl- -D-glucopyranoside (c), was reportedly cleaved -glucosidase *in vitro*. In the presence of Cu(II) ions it is reported to display antiproliferative activity against various tumor cell lines [176]. Poly hydroxylatedstyryl quinolines derivatives (SQLs) represented by the compound (d), are known to check HIV-1 replication in vitro at very low concentrations and hence can act as potent HIV-1 integrase (IN) inhibitors [177].

tris(8-quinolinol)Ga(III)
(a)

amino methyl derivative of quinolin-8-ol
(b)

(2*R*,3*R*,5*S*)-2-(hydroxymethyl)-6-(quinolin-8-yloxy)
tetrahydro-2*H*-pyran-3,4,5-triol
(c)

(*E*)-2-(3,5-dibromo-4-hydroxystyryl)
-8-hydroxyquinoline-7-carboxylic acid
(d)
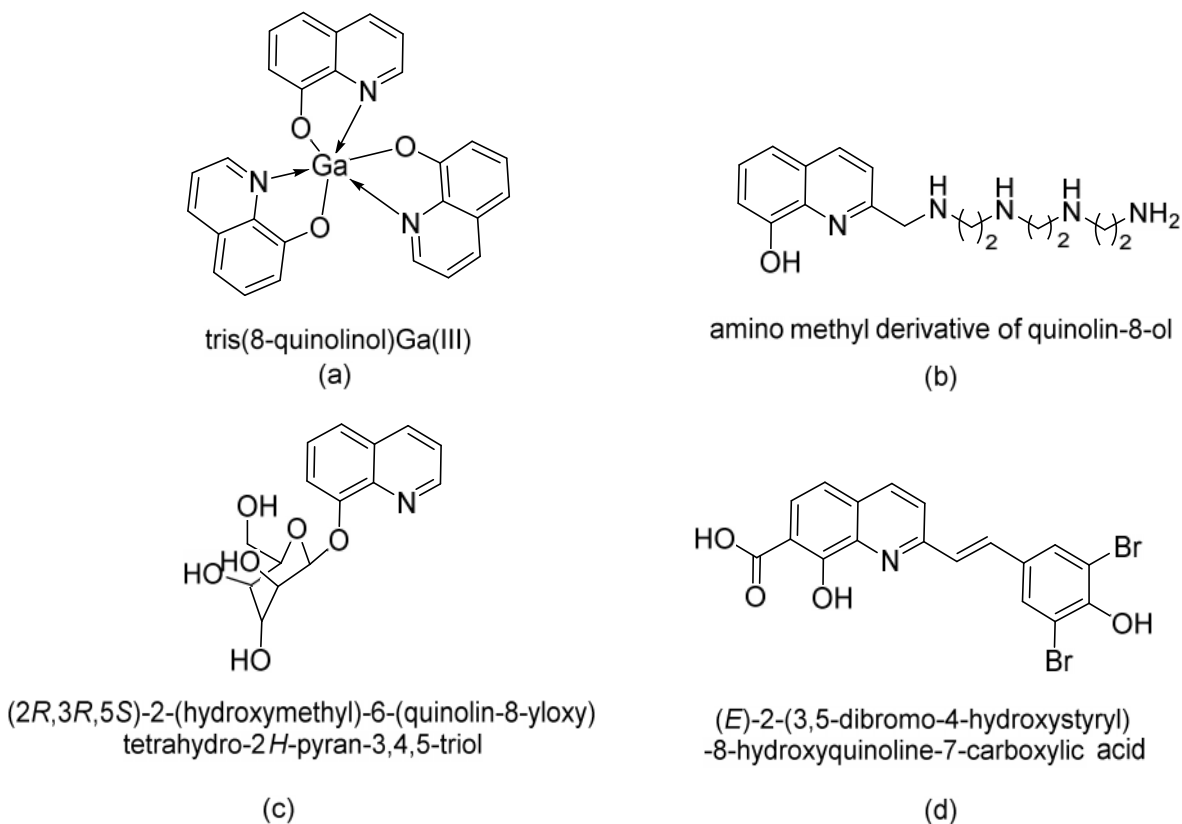
Figure 1.47 8-hydroxyquinoline derivatives acting as Antitumour agent

1.4.3.3.5 8-Hydroxyquinoline derivatives as Anti-Neuro degenerative Agents

Actual reasons causing neuro degenerative diseases like Alzeheimer's, Huntington's, Prion's and Parkinson's is yet difficult to find however, for their

complications and progress life style, trace metals and radicals are usually said to be responsible. One of the most lethal neurodegenerative is Alzheimer's disease which mostly affects the old persons, mainly causes behavioural abnormalities and memory loss. The majority of the therapeutic approaches for treating Alzheimer's disease function by targeting a small amyloidogenic peptide known as amyloid- peptide, which gets accumulated in the brain affected by Alzheimer's disease [178]. These therapies comprise inhibition of amyloid- formation, anti amyloid- immunotherapy and treatment promoting clearance of amyloid- peptide. However, these therapeutics have eventually been unsuccessful in slowing down the development of Alzheimer's disease.

Another approach for Alzheimer's disease therapy include targeting the interaction among amyloid- and the metal ions by means of chelating compounds that can bind with iron, zinc, and copper metals that are responsible for stabilization and accumulation of amyloid- in the brain [179].

Compound clioquinol (5-chloro-7-iodo-8-hydroxyquinoline) shown in figure-1.48 (a) was the earliest reported 8-hydroxyquinoline derivative which was tested in vivo due to its high chelating ability for Zn^{2+} and Cu^{2+} metals as well as its permeability to the blood-brain barricade [180].

Use of clioquinol compound in transgenic mice having Alzheimer disease signs has reported to decrease 49% amyloid- deposition in brain resulting in improvement of the disease. However, further expansion of using clioquinol as a efficient drug for treatment of Alzheimer's disease could not be progressed since, in the process of large scale production of clioquinol little amount of diiodo-8- hydroxyquinoline which is a known carcinogen, contamination occurred [181].

| (a) | (b) | (c) |
| Clioquinol | M30 dihydrochloride | PBT2 |
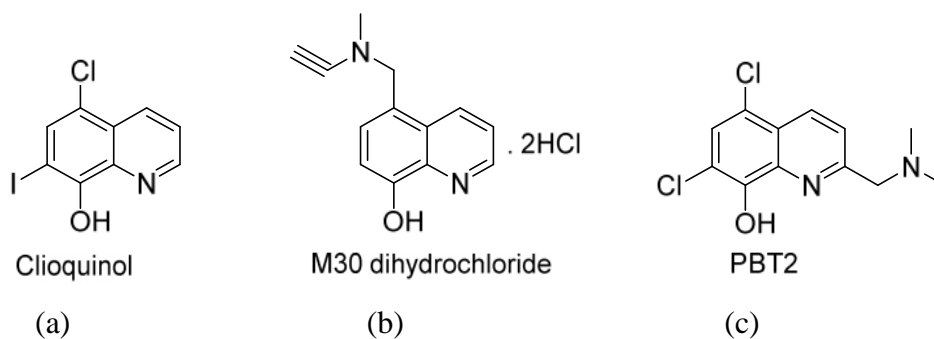
Figure 1.48 8- hydroxyquinoline derivatives showing Anti-Neuro degenerative property

Further,   a   novel   8-HQ   derivative,   5,   7-Dichloro-2-[(dimethylamino)methyl]quinolin-8-ol (PBT2) have been designed and used as a therapeutic drug for treatment of Alzheimer's disease as a succesor of clioquinol [182]. Recently,   molecule   5-[(ethynyl(methyl)aminomethyl)quinolin-8-ol]   (M30 dihydrochloride) have shown significant activity against Alzheimer's disease [183].

1.4.3.4 8-Hydroxyquinoline based quaternary cationic surfactant

Synthesis of quaternary cationic surfactants derived from 8-hydroxyquinoline (Figure 1.49) have been reported by the reaction of 8-HQ with alkyl halides containing long chain [184]. These quaternary cationic salts having both hydrophilic and lipophilic nature permitted their interaction with the bacterial phospholipid bilayer membrane [185]. This interaction may affect either the cell membrane or may cause toxicity to the membrane and hence resulting in bacterial cell death [186].

Both the size and electronic charge distribution on polar heads as well as the length of non polar hydrocarbon chain affects the activity shown by these 8-hydroxyquinolium salt derivatives [184]. It has been observed that from C-12 to C-14 carbon atoms activity increases while for the system having C-16 carbon atoms activity decreases surprisingly [184]. This study proposed that long chain hydrocarbons of suitable length and cationic charge may support the killing of bacteria through membrane.
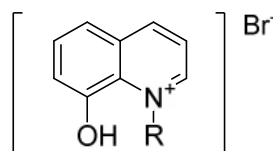
R = n-dodecyl, n-tetradecyl and n-hexadecyl

Figure 1.49 Quarternary salt of 8-Hydroxyquinoline

1.5 Polydentate (N-O) donor neutral ligand Systems derived from 8-Hydroxyquinoline

Most of the N-O donor ligands comprised of 8-hydroxyquinoline coordinate with metals in monoanionic fashion while, relatively fewer research have been conducted towards the synthesis of neutral ligand system derived from 8-hydroxyquinoline. O-alkylated

quinolinates are one of the most studied neutral ligands of this category. Quinolinate substituted tripodal ligands have been used for the chelation of several metal ions selectively since 1970s. Ether linked derivatives of quinoline such as compound (a) shown in figure 1.47, were used for the detection of alkaline group metal ions and structures of these complexes formed have been thoroughly studied by V¨ogtle and Weber [187].

8,8'-((oxybis(alkane-2,1-diyl))bis(oxy))diquinoline
n=0-6

(a)
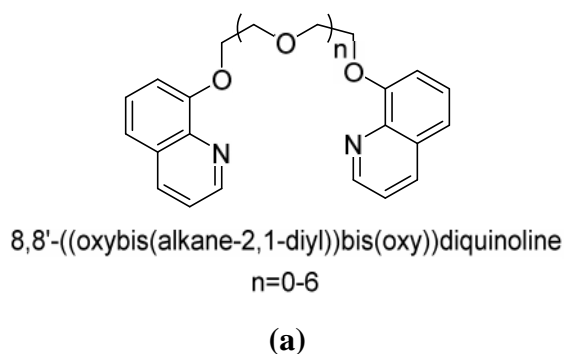
Figure 1.50 O-alkylated 8-Hq derivative

In recent times such types of ligands have experienced a new start. Polymeric Ag(I) complexes of ligands **(b)** and **(c)** have been reported in which both the ligands link two tetracoordinated metal centers having highly distorted geometry and additionally bind with each other. This results in the formation of unique trinuclear cyclic Ag(I) complex $[\{Ag(\mathbf{b})\}_3]^{3+}$ where three ligands draping helically the triangular framework of silver metal ions (Scheme 1.5). These types of structures are regarded as circular helicates [188]. Ligand **(c)** forms a one dimensional polymeric complex $[\{Ag(\mathbf{c})\}n]^{n+}$ having alternate configuration at the metal centre [189].

(b) $[Ag(b)_3]^{3+}$
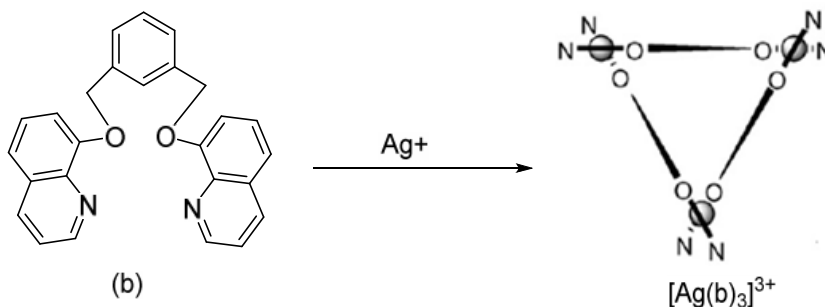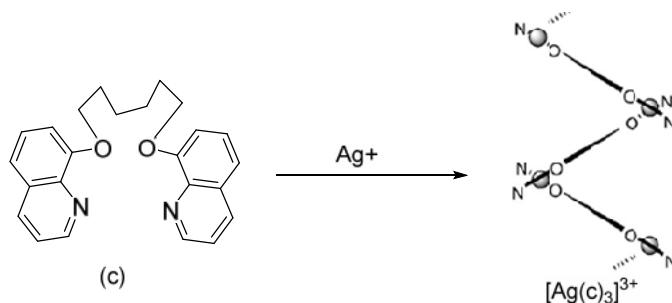
Scheme 1.5: Synthetic route for Linear polymeric complex of Ag with neutral 8-hydroxyquinoline derived ligand

Other than above mentioned ether linked two quinolinate ligands, tripodal(d)   and tetrapodal (e)   ligands containing three and four quinolinate moieties respectively have also been reported and their chelating ability with several metal cations like Ag^+,$Cu^{2+,}$ Ni^{2+}, Co^{2+}, Zn^{2+}, and Cd^{2+} were investigated using fluorescence measurement techniques [190].
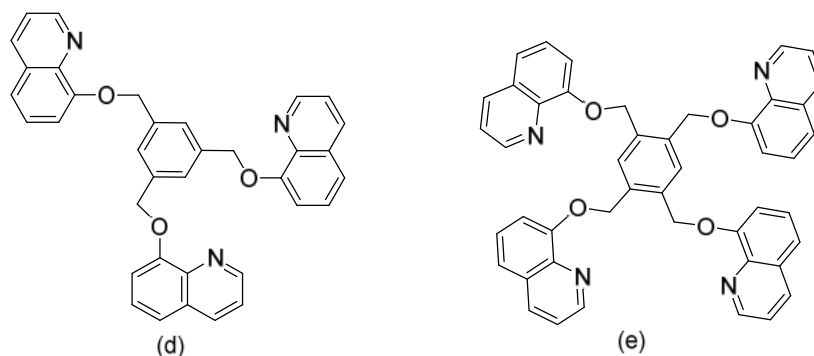
Figure 1.51 Ether bridged neutral ligand derived from 8-hydroxyquinoline

Mandhary et. al. reported Ag(I), Cu(II) and Ni(II) complexes of neutral tetradentate ligand 1,3-bis(quinoloxy)propane derived from 8-HQ where, with Ag(I) and Cu(II) this ligand acted as N-N donor bidentate ligand while with Ni(II) it behaved as N-O-O-N donor tetradentate ligand [188].

(a)   (b)   (c)
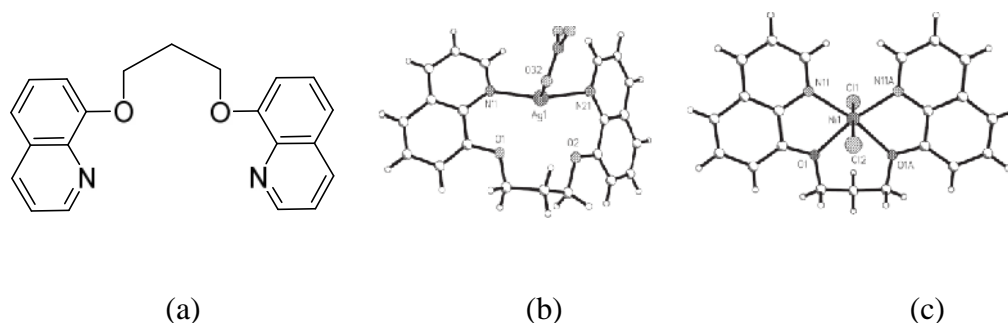
Figure 1.52 (a) 1,3-bis(quinoloxy)propane (b) ORTEP view of Ag(I) complex (c) ORTEP view of Ni(II) complex

Further, Muna et. al. reported a potential neutral tridentate N-O-N donor ligand 8-(2-pyridylmethoxy)quinoline and its Pd(II), Ni(II) and Cu(II) complexes. This ligand works as a flexible ligand and can either act as bidentate or tridentate, depending on the metal. With Pd(II) it acts as N-N donor bidentate ligand forming eight membered chelate ring while with pentacoordinate Cu(II) and octahedral Ni(II) behaves as N-O-N donor tridentate ligand and forms two five membered fused chelate rings [191].

quinolin-8-ol   2-(chloromethyl)pyridine   8-(pyridin-2-ylmethoxy)quinoline
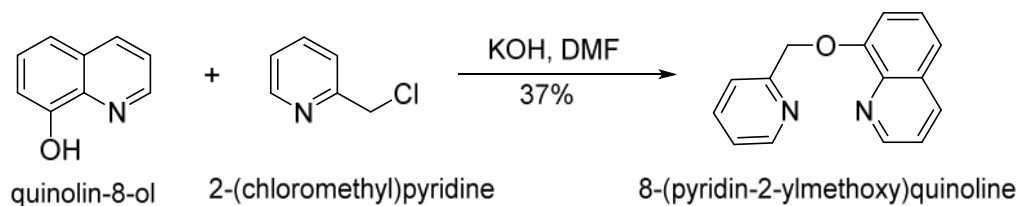
Scheme 1.6 Synthetic route for ligand (2-pyridylmethoxy)quinoline
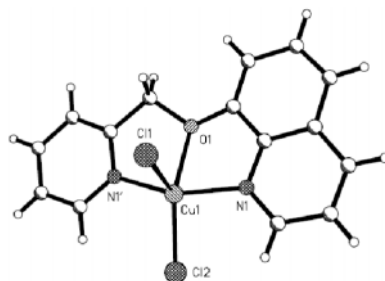
Figure 1.53 Perspective view of pentacoordinated Cu(II) complex of -(2-pyridylmethoxy)quinoline

Even though there have been enormous research work carried out towards synthesis of N-O donor ligands derived from 8-hydroxyquinoline and their metal complexes, in the field of coordination chemistry yet there are lots of scope remaining specially in the direction of synthesis of neutral N-O donor ligand systems derived from 8-hydroxyquinoline and their metal complexes as well as exploring their applications in various fields.

Keeping all these aspects in mind and considering potential of 8-hydroxyquinoline based N-O donor ligand metal complexes, in the present work novel metal complexes of N-O donor chelating ligands were synthesized and screened for various applications like antibacterial, antifungal and antioxidant properties. Some of the complexes synthesized were further used for the synthesis of metal nano particles using sol-gel technique.

1.6 Aims and objectives

The major objectives of the current study are:

(i)   Synthesis of bidentate, tridentate and tetradentate neutral N-O donor chelating ligands derived from 8-hydroxyquinoline. The complexes incorporating 8-hydroxyquinoline derivatives are known to exhibit photocatalytic activity.

(ii)   Synthesis of coordinated complexes with the above ligands using metals Co, Pd & Ti.

(iii)   In the present investigation (1) synthesis of some new complexes in which neutral 8-hydroxyquinoline ligand incorporated have been accomplished. (2) The synthesis of some ionic complexes with neutral ligands derived from 8-HQ have been reported and the complexes were prepared using metal such as Co, Pd and Ti.

(iv)   Characterization of the synthesized ligands and their metal complexes and their structure elucidation by using spectral techniques like FTIR, NMR, UV, Mass and single crystal X-ray.

(v)   To explore the applicability of complexes towards biological studies such as antifungal, antibacterial and antioxidant activity.

(vi)   To synthesize metal oxide nano particles of Ti and Pd from 8-hydroxyquinoline substituted ligands by using sol-gel technique.

1.7 Future scope

Present work consists of several future aspects some of which are:

(i)   Various other derivatives of 8-Hydroxyquinoline will be synthesized and screened for their anti neuro degenerative diseases, anti HIV antitumor agents and anti carcinogenic activity.

(ii)   The 8-hydroxyquinoline derivatives used in the present investigation are promising precursor for the synthesis of diverse nano structures. Further investigation in this area needs to be explored.

(iii) Synthesis of some new N-O donor chelating ligands with flexible coordination ability.

(iv)   Synthesis of metal complexes using different metals of various valencies.

(v)   Growth of single crystal of the remaining complexes and elucidation of their structure by single crystal X-ray.

(vi)   To explore the luminescence properties of the synthesized ligands and metal complexes.

1.8 References

[1]   G. B. Kauffman, J. Chem. Educ. 67 (2) (1990) A54-A55.

[2]   J. J. Lagowski, Chemistry: foundations and applications, New York USA, c2004) 4 v

[3]   H.M. Goff, Synth. React. Inorg. Met.-org. Chem. 12 (1982) 329-330.

[4]   F.A. Cottan, J. Chem. Soc., Dalton Trans. (2000) 1961-1968.

[5]   D.H. Busch, Chem. Rev. 93 (1993) 847-860.

[6]   Z. Stasicka, J.J. Ziołkowski, Coord. Chem. Rev. 249 (2005) 2133-2143.

[7]   M. J. M Campbell, Coord. Chem. Rev. 15 (**1975**) 279-283.

[8]   G. B. Kauffman, S. M. Jørgensen, J. Chem. Educ. 36 (1959) 521; A. J. Ihde, W. F. Kieffer, Eds.; J. Chem. Educ. (1965) 185-191.

[9]   A. Warner, Z. Anorg. Allg. Chem. 3 (1983) 267-330.

[10] A. D. Garnovskii, E. V. Sennikova, B. I. Kharisov, Open J. Inorg. Chem. 3 (2009) 1- 20.

[11] Jr. J. C. Bailar, "The Early Development of the Coordination Theory," In The Chemistry of the Coordination Compounds; Jr., J. C. Bailar, Ed., Reinhold Publishing Corp.: New York, 1956.

[12] D.F. Shriver, P.W. Atkins, Inorganic Chemistry, University Press: Oxford, 1999.

[13] Yu. D. Tretyakov, Yu.D. Martynenko, A.N. Grigoriev, A.Yu. Tsivadze, Inorganic Chemistry, Khimiya: Moscow, 2001.

[14] M.S. El-Ezaby, M. Rashad, N.M. Moussa, Polyhedron 2(4) (1983) 245-256.

[15] R. S. Nyholm, Proc. Chem. Soc. (1961) 273.

[16] R. J. Sanderson, "Chemical Periodicity", East-West Press, Pvt. Ltd., New Delhi (1969).

[17] S. Kumar, D.N. Dhar, P.N. Saxena, J. Sci. Ind. Res. 68 (2009) 181–187.

[18] C.K. Prier, D.A. Rankic, D.W.C. MacMillan, Chem. Rev. 113 (2013) 5322-5363.

[19] H. Furukawa, K.E. Cordova, M. O'Keeffe, O.M. Yaghi, *Science* 341 (2013) 974- 988.

[20] B. A. Schaefer, G. W. Margulieux, B. L. Small, P. J. Chirik, Organometallics 34 (7) (2015) 1307-1320.

[21]   H.F. Abd El-Halim, G.G. Mohamed, Appl. Organometal Chem. 32 (2017)

e4176 (1-12)

[22]   M. B. Davies, Coord. Chem. Rev. 124 (1993) 107-181.

[23]   M. G. Gardiner, C.C. Ho, Coord. Chem. Rev. 375 (2018) 373-388.

[24]   I. M. Grigorieva, T. V. Serebryanskaya, Y.V. Grigoriev, A. S. Lyakhov, L. S. Ivashkevich, A.S. Bogomyakov, L.G. Lavrenova, S.V. Voitekhovich, O.A. Ivashkevich, Polyhedron 151 (2018) 74-81.

[25]   Y. Li, X. Zhou, Z. L. Chen, H. H. Zou, F.P. Liang, Polyhedron, 119 (2016) 505-511

[26]   P.P. Netalkar, S.P. Netalkar, V.K. Revankar, Polyhedron 100 (2015) 215-222.

[27]   H.A.O. Hill, P. Day, "Physical Methods in Advanced Inorganic Chemistry", Interscience, New York (1968).

[28]   B. N. Figgis, J. Lewis, "Progress in Inorganic Chemistry", Interscience, New York (1964).

[29]   I. S. Grifith, J. Chem. Phys. 41 (1964) 576-577.

[30]   P.O. Lumme, H. Knuuttila, Polyhedron, 14 (1995) 1553-1563.

[31]   J. R. Allan, G.M. Baillie, J.G. Bonner, D.L. Gerrard, S. Hoey, Thermochimica Acta (1989) 283-288.

[32]   S.S. Kandil, F.I. Abdel-Hay, R.M. Issa, J. Therm. Anal. Calorim. 63 (2001) 173-180.

[33]   J. W. Huang, J. Chen, W. R. Berti, S. D. Cunningham, Environ. Sci. Technol. 31(1997) 800-805

[34]   W. Keim, F.H. Kowaldt, R. Goddard, C. Krüger, Angew. Chem. Int. Ed 17 (1978) 466-467.

[35]   W. Levason, S.D. Orchard, G. Reid, Coord. Chem. Rev. 225 (2002) 159-199.

[36]   T. Konno, J. Hidaka, and K.I. Okamoto, Bull. Chem. Soc. Jpn. 68 (1995) 1343-1353.

[37]   H. D. Stackel, E. Immerz-Winkler, H. Poschenrieder, A. Windt, W. Weigand, N. Drescher, R. Wuensch, Helv. Chim. Acta 86 (2003) 2471-2480.

[38]   I. Nagasawa, T. Kawamoto, H. Kuma, Y. Kushi, Bull.Chem. Soc. Jpn. 71 (1998) 1337-1342.

[39] I. Nagasawa, T. Kawamoto, H. Kuma, and Y. Kushi, Bull. Chem. Soc. Jpn., 71 (1998) 1337-1342.

[40] R. H. Holm, Chem. Rev. 87 (1987) 1401-1449.

[41] F. Mani, Coord. Chem. Rev. 120 (1992) 325-359.

[42] F. Osterloh, W. Saak, S. Pohl, M. Kroeckel, C. Meier, A. X. Trautwein, Inorg. Chem. 37 (1998) 3581-3587.

[43] C. Kimblin, T. Hascall, G. Parkin, Inorg. Chem. 36 (25) (1997) 5680-5681.

[44] G. Papini, S. Alidori, J.S. Lewis, D.E. Reichert, M. Pellei, G.G. Lobbia, G.B. Biddlecombe, C. J. Anderson, C. Santini, Dalton Trans. (2009) 177-184.

[45] J. M. Vila, M. T. Pereira, C. Rodriguez, J. J. Jesus, J. M. Origueira, A. Fernandez, M. L. Torres, Recent Res. Dev. Organomet. Chem. 4 (2001) 1.

[46] H. F. D. Brabander, L.C.V. Poucke, Z. Eeckhaut, Inorganica Chimica Acta 6 (1972) 459- 462.

[47] J. C. Shi, T. B. Wen, Y. Zheng, S. J. Zhong, D. X. Wu, Q. T. Liu, B. S. Kang, B. M. Wu, T. C. W. Mak, Polyhedron 16 (1997) 369-375.

[48] G. Rajput, V. Singh, K. Singh, Santosh, L.B.Prasad, G. B. Drew, Michael N. Singh, Eur. J. Inorg. Chem. (2012) 3885–3891.

[49] M. Alimi, A. Allam, M. Selkti, A. Tomas, P. Roussel, E. Galardon, I. Artaud, Inorg. Chem. 51 (2012) 9350-9356.

[50] R. S. Vagg, 'Comprehensive Coordination Chemistry', eds. G. Wilkinson, R. D. Gillard, and J. A. McCleverty, Pergamon, Oxford, 2 (1987) 793.

[51] W. Dietzsch, P. Strauch, E. Hoyer, Coord. Chem. Rev. 121 (1992) 43-130.

[52] G. Sánchez, J.L. Serrano, C.M. López, J. Garcıa, J. Pérez, G. López, Inorganica Chimica Acta, 306 (2000) 168-173.

[53] A. Bader and E. Lindner, Coord. Chem. Rev. 108 (1991) 27-110.

[54] H. Tafazolian, J.A.R. Schmidt, Chem. Eur. J. 23 (2017) 1507-1511.

[55] J. L. Roustan, N. Ansari, F.R. Ahmed, Inorg. Chim. Acta 129 (1987) L11– L12.

[56] Gopalakrishnan, Appl. Organomet. Chem. 23 (2009) 291-318.

[57] S. M. Kuang, Z. Z. Zhang, Q.G.Wang, T.C.W. Mak, J. Chem. Soc., Dalton Trans., (1998) 1115-1119.

[58] M. S. Goedheijt, J.N.H. Reek, P.C.J. Kamer, P.W.N.M. van Leeuwen, J. Chem. Soc., Chem. Commun., 1998, 2431-2432.

[59] Ng. Pb. Duu-Hol, Ng. D. Xuong, Ng H. Ham, F. Binon, R. Roger, J. Chem. Sot., (1951) 1358.

[60] T. S. Ma, M. Tlcn, Antlbtoticr and Chemotherapy 3 (1959) 491.

[61] J. S. Valentine, Chem. Rev. 73 (1993) 235-245.

[62] M.C.C. Barahona, M.N. Cordovilla, J.M. Genov, et al., Dalton Trans. 42 (2013) 14576-14582.

[63] J. Witt, A. Pöthig, F.E. Kühn, W. Baratta, Organometallics 32 (2013) 4042-4045.

[64] A.R. Hajipour, F. Rafiee, Tetrahedron Lett. 53 (2012) 4661- 4664.

[65] H. Nie, G. Zhou, Q. Wang, W. Chen, S. Zhang, Tetrahedron: Asymmetry 24 (2013)1567-1571.

[66] S. R. Rave, F. E. Negrete, R. A. Toscano, S. H. Ortega, D. M. Morales, J. M. Grévy, J. Organomet. Chem. 749 (2014) 287-295.

[67] A. Chartoire, M. Lesieur, A.M.Z. Slawin, S.P. Nolan, C.S.J. Cazin, Organometallics, 30 (2011) 4432-4436.

[68] M.G. Burgess, M. N. Zafar, S.T. Horner, G.R. Clark, L. James Wright, Dalton Trans. (2014) 17006-17016.

[69] A. Colette, B. Yuoh, M.O. Agwara, D.M. Yufanyi, M.A. Conde, R. Jagan, K.O. Eyong, Int. J. Inorg. Chem. (2015) 9-12.

[70] L. Kuckova, K. Jomov, A. Svorcova, M. Valko, P. Seg la, J. Moncol, J. Kozísek, Molecules 20 (2015) 2115-2137.

[71] C.M.X. Jose, C.L.V. Emilio, da G. N.-M. Maria, S.de B.V. Glauce, Neurosci. Med. 3(01) (2012) 107-123.

[72] D. L. Ma, V. P. Y. Ma, D. S. H. Chan, K. H. Leung, H. Z. He, C.H. Leung, Coord. Chem. Rev. 256 (2012) 3087-3113.

[73] J.A. Bertrand, P.G. Eller, Prog. Inorg. Chem. 21 (1976) 29-53.

[74] A. Chakravorty, Coord. Chem. Rev. 13 (1974) 1-46.

[75] T.E. Keyes, R.J. Forster, P.M. Jayaweera, C.G. Coates, J.J. McGarvey, J.G. Vos, Inorg. Chem. 37 (1998) 5925-5932.

[76] K. Fegy, D. Luneau, E. Belorizky, M. Novak, J.L. Tholence, C. Paulsen, T. Ohms, P. Rey, Inorg. Chem. 37 (1998) 4524-4532.

[77] M.O. Savchuk, O.O. Litsis, K.O. Znovjyak, T.Y. Sliva, N.G. Kobylinskaya, S.V. Shishkina, V.V. Dyakonenko, V.M. Amirkhanov, Polyhedron 133 (2017) 162-168.

[78] N. K. Solanki, E.J.L. McInnes, F.E. Mabbs, S. Radojevic, M. McPartlin, N. Feeder, J. E. Davies, M.A. Halcrow, Angew. Chem., Int. Ed. Engl. 37 (1998) 2221-2223.

[79] D. Black, A.J. Blake, K.P. Dancey, A. Harrison, M.M. Partlin, S. Parsons, P.A. Tasker, G. Whittaker, M. Schroder, J. Chem. Soc. Dalton Trans. (1998) 3953-3960.

[80] C. Kutal, Coord. Chem. Rev. 99 (1990) 213-252.

[81] M. J. Robertson, G.A. Lawrance, M. Maeder, P. Turner, Aust. J. Chem. 57 (2004) 483-490.

[82] S. Khan, S. A. A. Nami, K. S. Siddiqi, E. Husain, I. Naseem, Spectrochim. Acta A Mol. Biomol. Spectrosc. 72 (2009) 421-428.

[83] M. Koikawa, M. Gotoh, H. Okawa, S. Kida, T. Kohzuma, J. Chem. Soc. Dalton Trans. 0 (1989) 1613-1616.

[84] T.P. Tang, J.A. Ellman, J. Org. Chem. 67 (2002) 7819-7832.

[85] S. I. Kirin, C. M. Happel, S. Hrubanova, T. Weyhermuller, C. Klein, N. Metzler- Nolte, Dalton Trans. 21 (2004) 1201-1207.

[86] W. M. P. B. Menge, J.G. Verkade, Inorg. Chem. 30 (1991) 4628-4631.

[87] R.D. Hancock, A.E. Martell, Chem. Rev. 89 (1989) 1875-1880.

[88] K.E. Krakowiak, J.S. Bradshaw, D.J. Zameska-Krakowiak, Chem. Rev. 89 (1989) 929-972.

[89] P. Adao, Maxim L. Kuznetsov, S. Barroso, A.M. Martins, F. Avecilla, J.C. Pessoa, Inorg. Chem. 51 (2012) 11430-11449.

[90] X. H. Bu, M. Du, L. Zhang, D.Z. Liao, J. K. Tang, R. H. Zhang, M. Shionoya, Dalton Trans. 0 (2001) 593-598.

[91] J. G. H. Du Preez, T.I.A. Gerber, O. Knoesen, J. Coord. Chem. 16 (1987) 285- 291.

[92]   S. Budagumpi, G. S. Kurdekar, G.S. Hegde, N.H. Bevinahalli, V.K. Revankar, J. Coord. Chem. 63(8) (2010) 1430-1439.

[93]   E. Saint-Aman, S. Menage, J.L. Pierre, E. Defrancq, G. Gellon, New J. Chem. 22 (1998) 393-394.

[94]   Y. Sunatsuki, T. Matsuo, M. Nakamura, F. Kai, N. Matsumoto, J. P. Tuchagues, Bull. Chem. Soc. Jpn. 71 (1998) 2611-2619.

[95]   P. Comba, T. W. Hambley, G. A. Lawrance, L. L. Martin, P. Renold, K. Varnagy, J. Chem. Soc., Dalton Trans. (1991) 277-283.

[96]   R. Ruiz, A. Aukauloo, Y. Journaux, I. Fernandez, J.R. Pedro, A.L. Rosello, B. Cervera, I. Castro, M.C. Munoz, Chem. Commun. (1998) 989-990.

[97]   B.J. Hamstra, G.J. Colpas, V. Pecoraro, Inorg. Chem. 37 (1998) 949-955.

[98]   M. Vaidyanathan, R. Viswanathan, M. Palaniandavar, T. Balasubramanian, P. Prabhaharan, T.P. Muthiah, Inorg. Chem., 37 (1998) 6418-6427.

[99]   F. Li, M. Wang, P. Li, T. Zhang, L. Sun, Inorg. Chem. 46 (2007) 9364-9371.

[100]   J.D. Koola, J.K. Kochi, J. Org. Chem. 52 (1987) 4545-4553.

[101]   H. Y. Ding, H. J. Cheng, F. Wang, D. Xian Liu, H. Xi Li, Y.Y. Fang, W. Zhao, J. P. Lang, Journal of Organometallic Chemistry 741 (2013) 1–6.

[102]   E. S. Raper, Coord. Chem. Rev. 165 (1997) 475.

[103]   E. S. Raper, Coord. Chem. Rev. 153 (1996) 199.

[104]   K. A. Jorgensen, Chem. Rev. 89 (1989) 438.

[105]   T. Premkumar, S. Govindarajan, J Therm Anal Calorim 79 (2005)115.

[106]   E. Bouwman, M. A. Bolcar, E. Libby, J. Huffman, K. Folting, G. Christou, Inorg. Chem. 31(1992) 5185.

[107]   S. N. Al-Busafi, F. E. O. Suliman, Z. R. Al-Alawi, Research and Reviews: Journal of Chemistry 3 (2014)

[108]   B. R. Short, M. A. Vargas, J. C. Thomas, S. O'Hanlon, M. C. Enright, J Antimicrob Chemother. 57 (2006) 104–109.

[109]   M. Albrecht, M. Fiege, O. Osetska, Coord Chem Rev. 252 (2008) 812–824.

[110]   J. Kido, Y. Iizumi, Chem Lett. 26 (1997) 963-64.

[111]   R. H. F. Manske, M. Fulka, Organic Reactions 7 (1953) 59-98.

[112]   Y. Nakano, D. Imai, Synthesis 12 (1997) 1425

[113]   F. O. Suliman, S. N. Al-Busafi, M. Al-Risi, K. Al-Badi, Dyes and Pigments. 92 (2012) 1153-1159.

[114]   J. P. Heiskanen, O. E. O. Hormi, Tetrahedron. 65 (2009) 518-524.

[115]   A. Godard, Y. Robin, G. Queguiner, J Organometallic Chem.336 (1987)1-2.

[116]   A. R. Katritzky, J. M. Lagowski, Adv Heterocyclic Chem. 2 (1963) 27.

[117]   E. Shoji, J Polym Sci Part A. Polym Chem. 41 (2003) 3006.

[118]   L. M. Leung, W.Y. Lo, S. K. So, K. M. Lee, W. K. Choi, J Am Chem Soc 122 (2000) 5640-41.

[119]   S. F. Vanparia, T. S. Patel, N. A. Sojitra, Acta Chim Slov. 57 (2010) 600– 667.

[120]   H. Zheng, S. Gal, L. M. Weiner, J Neurochem. 95 (2005) 68–78.

[121]   D. Kaur, F. Yantiri, S. Rajagopalan, Neuron. 37 (2003) 899–909.

[122]   T. A. Hopkins, Chem. Mater. 8 (1996) 344-351.

[123]   R. Ballardini, G. Varani, M. T. Indelli, F. Scandola, Inorg Chem. 25(1986) 3858- 3865.

[124]   S. Wang, Coord Chem Rev. 215 (2001) 79-98.

[125]   G. Farruggia, J Am Chem Soc. 128 (2006) 344-350.

[126]   J. E. Douglass, J Org Chem 26 (1961) 1312-13.

[127]   S. Kappaun, S. Rentenberger, A. Pogantsch, E. Zojer, K. Mereiter, G. Trimmel, R. Saf, K. C. Moller, F. Stelzer, C. Slugovc, Chem Mater 18 (2006) 3539-47.

[128]   T. Sano, Y. Nishio, Y. Hamada, H. Takahashi, T. Usuki, K. Shibata, J Mater Chem 10 (2000) 157-61.

[129]   C. Schmitz, H. W. Schmidt, M. Thelakkat, Chem Mater 12 (2000) 3012- 3019.

[130]   H. Wang, B. Xu, X. Liu, H. Zhou, Y. Hao, H. Xu, L. Chen, Org Elect. 10 (2009) 918-924.

[131]   A. Sharma, D. Singh, J. K. Makrandi, M. N. Kamalasanan, R. Shrivastva, I. Singh, Mater Chem Phys. 108 (2008) 179-83.

[132]   J. K. Park, W. S. Kim, G. Otgondemberel, B. J. Lee, D. E. Kim, Y.S. Kwon, Coll Surfaces A: Physi Eng Aspects 321 (2008) 266-70.

[133]   F. Dumur, L. Beouch, M. A. Tehfe, E. Contal, M. Lepeltier, G. Wantz, B. Graff, F. Goubard, C. R. Mayer, J. Lalevée, D. Gigmes, Thin Solid Films 564 (2014) 351-60.

[134]   A. Sharma, D. Singh, J. K. Makrandi, M. N. Kamalasanan, R. Shrivastva, I. Singh, Mater Lett. 61 (2007) 4614-17.

[135]   R. Ballardini, G. Varani, M. T. Indelli, F. Scandola, Inorg. Chem. 25 (1986) 3858- 3865

[136]   A. G. Crosby, E. R. Whan, M. R Alire, J. Chem. Phys. 34 (1961) 743-748

[137]   H. Zhang, L. Han, A. K. Zachariasse, Y. Jiang, Org. Lett. 7 (2005) 4217-4220

[138]   L. Lihua, X. Bing, Tetrahedron 64 (2008) 10986-10995

[139]   X. Jiang, B. Wang, Z.Yang, Y. Liu, T. Li, Z. Liu, Inorg. Chem. Com. 14 (2011) 1224-1227.

[140]   B. M. Holligan, J. C. Jeffery, M. K. Norgett, E. Schatz, M. D. Ward, J. Chem. Soc. Dalton Trans. 23 (1992) 3345-3351.

[141]   M. E. Ojaimi, P. R. Thummel, Inorg. Chem. 50 (2011) 10966-1097.

[142]   D. L. Boger, J. H. Chen, J. Org. Chem.22 (1995) 7369–7371.

[143]   O. Sigouin, A. L. Beauchamp, Can. J. Chem. 83 (2005) 460-470.

[144]   R. D. Patel, H. S. Patel, S. R. Patel, Eur. Polym. J. 23 (1987) 229-232.

[145]   M. Garaleh, M. Lahcini, H. R. Kricheldorf, S. M. Weidner, Polym. Chem. 47 (2009) 170- 177.

[146]   Y. H. Tsai, C. H. Lin, C. C. Lin, B. T. Ko, Polym. Chem. 47 (2009) 4927-4936.

[147]   K. D. Patel, S. C. Pachani, Ulter. of Phys. Sciences 15 (2003) 195-200.

[148]   D. A. Patel, S. R. Patel, E. Journal of Chem. 7 (2010) 1023-1028.

[149]   C. Nuñez, J. F. Lodeiro, M. Dinis, M. Larguinho, L. J. Capelo, C. Lodeiro, Inorg. Chem. Commun. 14 (2011) 831–835.

[150]   L. J. Fernandez, C. Nunez, N. O. Faza, L. J. Capelo, C. Lodeiro, S. Seixas de Melo, J. S. C. López, 38 (2012) Inorg. Chim. Acta. 218–228.

[151]   G. Tallec, P. H. Fries, D. Imbert, M. Mazzanti, Dalton Trans. 39 (2010)
          9490-9492.

[152]   G. Tallec, P. H. Fries, D. Imbert, M. Mazzanti, Inorg. Chem. 50 (2011)
          7943-7945.

[153]   W. Rohde, P. Mikelens, J. Jackson, J. Blackman, J. Whitcher, W. Levinson,
          Antimicrob Agents Chemother. 2 (1976) 234–240.

[154]   A. Albert, M. I. Gibson, S. D. Rubbo, Br J Exp Pathol. 2 (1953) 119–130.

[155]   D. S. Auld, H. Kawaguchi, D. M. Livingston, B. L. Vallee. Proc Natl Acad
          Sci U S A. 5 (1974) 2091–2095.

[156]   P. Valenzuela, R. W. Morris, A. Faras, W. Levinson, W. J. Rutter. Biochem
          Biophys Res Commun. 3 (1973) 1036–1041.

[157]   A. Albert, Biochem J. 4 (1953) 646–654.

[158]   J. M. Tanzer, A. M. Slee, B. Kamay, E. Scheer, Antimicrob Agents
          Chemother. 6 (1978) 1044–1045.

[159]   H. Gershon, D. D. Clarke, M. Gershon, Monatsh Chem. 1 (1994) 51-59.

[160]   C. H. Lee, J. H. Jeon, S. G. Lee, H. S. Lee, J Korean Soc Appl Biol Chem. 4
          (2010) 464- 469.

[161]   H. Gershon, M. Gershon, D. D. Clarke, Mycopathologia. 4 (2002) 213-217.

[162]   C. M. Darby, C. F. Nathan, J Antimicrob Chemother. 7 (2010) 1424-1427.

[163]   Y. Anjaneyulu, R. P. Rao, R.Y. Swamy, A. Eknath, K. N. Rao, Proc Indian
          Acad Sci (Chem Sci) 2 (1982) 157–163.

[164]   A. Albert, M. I. Gibson, S. D. Rubbo, Br J Exp Pathol. 2 (1953) 119–130.

[165]   B. R. Short, M. A. Vargas, J. C. Thomas, S. O'Hanlon, M. C. Enright, J
          Antimicrob Chemother. 1 (2006) 104–109.

[166]   S. Srisung, T. Suksrichavalit, S. Prachayasittikul, S. Ruchirawat, V.
          Prachayasittikul Int J Pharmacol. 2 (2013) 170–175.

[167]   S. Srisung, T. Suksrichav, S. Prachayasi, S. Ruchirawat, V. Prachayasi, 9
          (2013) 170- 175.

[168]   S. F. Vanparia, T. S. Patel, N. A Sojitra, Acta Chim Slov. 3 (2010) 600–667.

[169]   S. F. Vanparia, T. S. Patel, N. A. Sojitra, C. L. Jagani, B. C. Dixit, P. S.
          Patel, R. B. Dixit, Acta chimica Slovenica 57 3 (2010) 660-7.

[170]   R. D. Benjamin, M. A. Short, J. C. Vargas, S. O. Thomas, C. E. Mark, J Antimicrob Chemother. 1 (2006) 104-109.

[171]   K. B. Patel, K. S. Nimavat Res J Pharm Biol Chem Sci. 3 (2012) 838-844.

[172]   A. Y. Shen, C. P. Chenb, S. A. Raffler, Life Sci. 9 (1999) 813-825.

[173]   P. A. Enquist, et al. Bioorg Med Chem Lett. 22 (2012) 3550-3553.

[174]   P. Collery, et al. Anticancer Res. 2A (2000) 955-958.

[175]   V. Oliveri, M. L. Giuffrida, G. Vecchio, C. Aiello, M. Viale, Dalton Trans. 15 2012) 4530-4535.

[176]   F. Zouhiri, et al. J. Med. Chem. 8 (2000) 1533-1540.

[177]   P. J. Crouch, S. M. Harding, A. R. White, J. Camakaris, C. L. Masters, Cell Biol. 40 (2008) 81-198.

[178]   A. I. Bush, Trends Neurosci 4 (2003) 207-214.

[179]   W. Orly, M. Silvia, B. A. Orit, Y. F. Merav, A. T. Yael, A. Tamar, B. H. Y. Moussa. Neurotherapeutics 6 (2009) 163-174.

[180]   R. A. Cherny, et al. J. Biol. Chem. 33 (1999) 23223-23228.

[181]   P. A. Adlard, Neuron 6 (2008) 43-55.

[182]   N. G. Faux, C. W. Ritchie, A. Gunn, J Alzheimers Dis. 2 (2010) 509–516.

[183]   Y. Pollak, D. Mehlovich, T. Amit, J. Neural Transm. 1 (2013) 37–48.

[184]   S. M. Ahmed, D. A. Ismail, J Surfact Deterg. 3(2008) 231–235.

[185]   A. Y. Shen, C. P. Chen, S. Roffler, Life Sci. 9 (1999) 813–825.

[186]   A. M. Badawi, M. A. Mohamed, M. Z. Mohamed, M. M. Khowdairy, J Cancer Res Ther. 3 (2007)198–206.

[187]   F. V¨ogtle, E. Weber, Angew. Chem. Int. Ed. 18 (1979) 753.

[188]   M. R. A. Al-Mandhary, P. J. Steel, Inorg. Chem. Commun. 5 (2002) 954.

[189]   Y.P. Cai, H.X. Zhang, A.W. Xu, C.Y. Su, C.L. Chen, H.Q. Liu, L. Zhang, B.S. Kang, Dalton Trans. (2001) 2429.

[190]   (a) P. Singh, S. Kumar, Tetrahedron 62 (2006) 6379; (b) P. Singh, S. Kumar, Tetrahedron Lett. 47 (2006) 109.

[191]   M. R. A. Al-Mandhary , P. J. Steel, Inorganica Chim. Acta. 351 (2003) 7 – 11.

2.1 Introduction

Metal complexes of nitrogen and oxygen functionalized ligands have great importance in the field of coordination chemistry [1, 2]. A large number of nitrogen and oxygen donor ligands and their metal complexes have shown potential biological activity and hence gained interest of researchers [3]. These are known to be potentially useful as catalysts, in biomedical applications and a variety of other applications. These derivatives are also known to show anti-tumour and cytotoxic activities [4].

The chemistry of cobalt metal complexes with O, N donor chelating ligand has played imperative part in the advancement of coordination chemistry. Cobalt is an essential element even though required in a very small amount (approx 1 mg) [5]. Mostly Cobalt is obtained from green vegetables and cereals [6], and is also a common supplement in vitamins [7]. Cobalt plays key role in vitamin B12, cobalamin [8], some of the enzymes have also been identified which have cobalt [9].

Cobalt shows various oxidation states ranging from +1 to +5. The most common oxidation states are +2 and +3 [10]. Complexes of cobalt exhibit variable coordination number, geometry, stability etc. From the literature it reveals that Co(II) is associated with different type of stereochemical configurations such as tetrahedral, octahedral and square planar [11,12]. Coordination complexes of Cobalt exhibit interesting redox and magnetic properties that make them suitable for a remarkable extent of applications in biology and medicine [13].

A large number of references in literature are available on the chemistry and the biological activities of transition metal complexes containing O, N donor atoms [10-13].
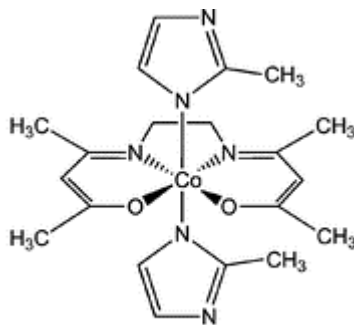
Figure 2.1: Doxovir

Even though cobalt complexes are versatile, they have not been explored well in the field of inorganic pharmaceuticals in comparison to other metals. So far, Doxovir is the only cobalt complex which has reached clinical trials. Doxovir is a Co(III) complex of Schiff base and is highly active against drug-resistant herpes simplex virus 1 [14].

In the recent years, a significant amount of research has been done towards study of bioactive cobalt complexes and their application in medicinal field [15, 16].

In order to explore role of Cobalt in medicinal field, small bioactive molecules which are of therapeutic use for example, non-steroidal anti-inflammatory drugs (NSAIDs) [17–19], antifungal agents [24, 25], antiprotozoal agents [22, 23], antibacterial agents [20,21] and antihelmintic agents [26], were interacted with cobalt complexes to get better or to change their therapeutic efficiency. Though mechanisms of action for most of these complexes have not been established so far however, complexation of cobalt moities is considered to alter the therapeutic ability of these bioactive ligands [26, 27, 28]. For instance, bioactive agents were attached with Co(III) complex, cobalamin (Vitamin B_{12}) which is found in nature for drug delivery. Further, this idea was extensively studied [28, 29]. Peptides, proteins and some other small molecules like Rh-based CO-releasing molecules [30] and cisplatin analogues [31] were joined to cobalamin in order to improve their stability, biocompatibility and their uptake..

Upon coordination of small bioactive molecules with binuclear cobalt cluster $Co_2(CO)_6$ through an alkyne bond activity of the resulting complex ([alkyne]-$Co_2(CO)_6$) gets modified. There have been a number of studies done for evaluating the result of [alkyne]-$Co_2(CO)_6$ on the antitumor potency of the nonsteroidal anti-inflammatory drug (NSAID) aspirin (Figure 2.2). Aspirin shows intermediate pro-apoptotic property via cyclooxygenase (COX) enzymes inhibition [27, 32]. When coordinated to [alkyne]-$Co_2(CO)_6$ activity of aspirin significantly increases towards inhibition of COX enzymes and the resultant cytotoxicity levels were analogous to cisplatin. Ott *et al.* and Rubner *et al.* systematically modified the alkyne bond, the bioactive agents and the $Co_2(CO)_6$ cluster and showed that apart from NSAID which direct the complex towards the COX enzymes, cobalt cluster was essential for the significant activity [33, 34].
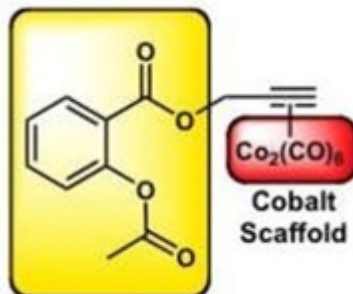
Figure 2.2 NSAID aspirin

8-Hydroxyquinoline is a prominent N, O donor chelating ligand extensively used in coordination chemistry. 8-Hydroxyquinoline (8-HQ) and its derivatives are excellent chelating agents because of their high ability towards coordination to various metal ions [35–37] consequently, have been broadly used for extraction of metal ions in industry and analytical field [38, 39]. Complexes of 8-HQ have been widely explored from both applied and theoretical point of view [40–42]; Cu(II), Co(II) and Zn(II) complexes were used in industrial applications because of their ability to protect wood and textiles from rot-producing fungi [43, 44]. Several 8-HQ complexes have been used as the emitting elements in electroluminescent devices [45–48]. Electroluminescent devices with Al(III), Zn(II) and Be(II) complexes of 8-HQ as emitters show high external quantum efficiency and brightness at less than 10V driving voltage.

The organic compounds coordinated with metals cause drastic change in the biological property of the ligand [49]. Therefore, keeping in mind broad biological applications of 8-hydroxyquinoline derivatives and cobalt complexes, herein, we herein report the synthesis and characterization of nine cobalt complexes (1-9) with 8-hydroxylquinoline derived bidentate, tridentate and tetradentate neutral chelating ligands and investigated their biological properties.

2.2   Experimental

2.2.1 General methods and materials

All reagents and solvents used were of analytical grade and purified by conventional methods prior to use. $CoCl_2.6H_2O$ and 8-hydroxyquinoline (99%) were procured from

Sigma-Aldrich and were used as received. HPLC grade DMSO-d_6 and CDCl$_3$ were used for NMR spectroscopic studies and ethanol, methanol were used for synthesis of ligands and metal complexes. IR spectra were recorded on a Perkin-Elmer Spectrum RXI spectrometer as dry KBr pellets. ^{1}H and ^{13}C NMR spectra were recorded with a JEOL FX 400 FTNMR spectrometer using SiMe$_4$ as an internal standard, at 399.78 MHz and 75.45 MHz frequencies, respectively. Absorption spectra of all the cobalt complexes were recorded on a Lamda25, PerkinElmer spectrophotometer 200 to 800 nm wavelength ranges. ESI mass spectra of some complexes were recorded using a Xevo G2-SQ TOF Waters, USA spectrometer in the electron spray mode using methanol solvent. The C, H, N analyses were performed on Thermo scientific Flash 2000.

2.2.2   Synthesis of ligands

2.2.2.1 Preparation of bidentate 8-methoxyquinoline ligand (MOQ)

8-methoxyquinoline (MOQ) was prepared as previously reported method by using 8-hydroxyquinoline [50]. A weighted amount of 8-hydroxyquinoline (3 mmol), methyl iodide (1 mmol) and potassium carbonate (10 mmol) were dissolved in anhydrous acetone (~20 ml). The reaction mixture was refluxed for 24 hrs and cooled at room temperature. Excess of the solvent was removed under reduced pressure to dryness. To this mixture water and dichloromethane (CH$_2$Cl$_2$) were added and the organic layer extracted 2 to 3 times. At last the organic layers of resulting mixture were combined, washed with brine, dried on Na$_2$SO$_4$, filtered and evaporated resulting in reddish brown colored oily product. This oily product was further purified by column chromatography. Synthetic and analytical data of ligand (MOQ) are summarized below:

Yield: 70%. ESI-MS: m/z, 160.0 [M+H]$^+$, 182.0 [M+Na]$^+$. ^{1}H NMR (CDCl$_3$, 400 MHz): : 4.08 (s, 3H), 7.17(m, 1H), 7.51 (m, 3H), 8.1 (m, 1H), 8.84 (m, 1H).
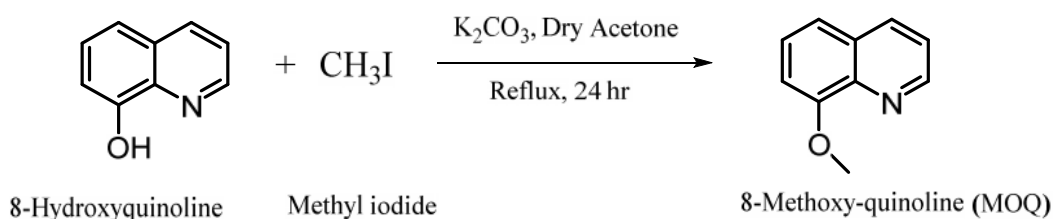
Scheme-2.1 Synthetic route of 8-Methoxyquinoline

2.2.2.2 Preparation of tridentate ligand 8-(Pyridin-2-ylmethoxy)-quinoline (PMOQ)

Tridentate 8-(Pyridin-2-ylmethoxy)-quinoline (PMOQ) ligand was synthesized by the earlier reported method [51] from the reaction of 8-hydroxyquinoline (1mmol), picolyl chloride (1mmol) and potassium hydroxide (2mmol) in DMF. The reaction contents were refluxed overnight and cooled it at room temperature. The final resulting oily product was obtained was purified by the procedure discussed for the purification of MOQ. Synthetic and analytical data of ligand are summarized below:

Yield: 37%. ^{1}H NMR (CDCl$_3$ 400 MHz) : 8.98, 1H; 8.61, 1H; 8.11, 1H; 7.64, 2H; 7.42, 1H; 7.36, 2H; 7.19, 1H; 7.05, 1H; 5.56, 2H.

8-Hydroxyquinoline   Picolyl chloride   8-(Pyridin-2-ylmethoxy)-quinoline (PMOQ)
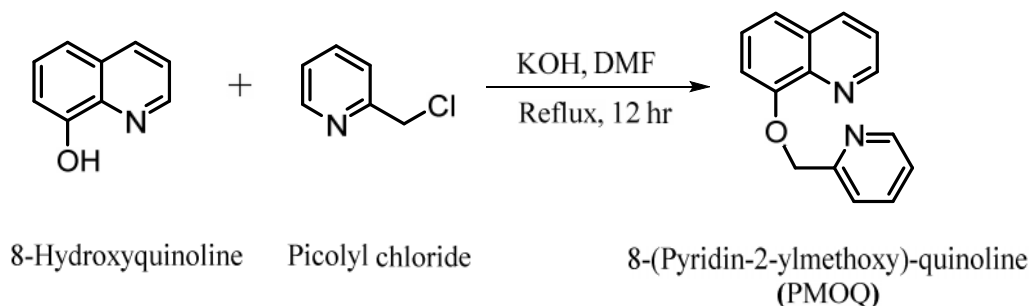
Scheme- 2.2 Synthetic route of 8-(Pyridin-2-ylmethoxy)-quinoline (PMOQ)

2.2.2.3 Preparation of tetradentate ligand 1, 3-Bis(8-quinoxy)propane (BQOP)

Tetracoordinating ligand 1,3-bis(8-quinoxy)propane (BQOP) was synthesized from 8-Hydroxyquinoline (2 mmol), 1,3-dibromopropane (1 mmol) and potassium carbonate (10 mmol) in anhydrous acetone. The reaction contents was refluxed with constant stirring for 12 hrs on a hot plate magnetic stirrer and then cooled at room temperature. The resulting white solid was filtered, recrystallized from ethyl acetate/pet ether mixture and characterized by proton NMR. The synthetic and analytical data of ligand are summarized below:

M. P.- 140 ^{o}C, Yield: 58%. ^{1}H NMR (CDCl$_3$ 400 MHz) : 8.918 dd 2H; 8.06 dd 2H; 7.35 m 6H, 7.135 dd 2H; 4.53 t 4H; 2.703 quintet, 2H.
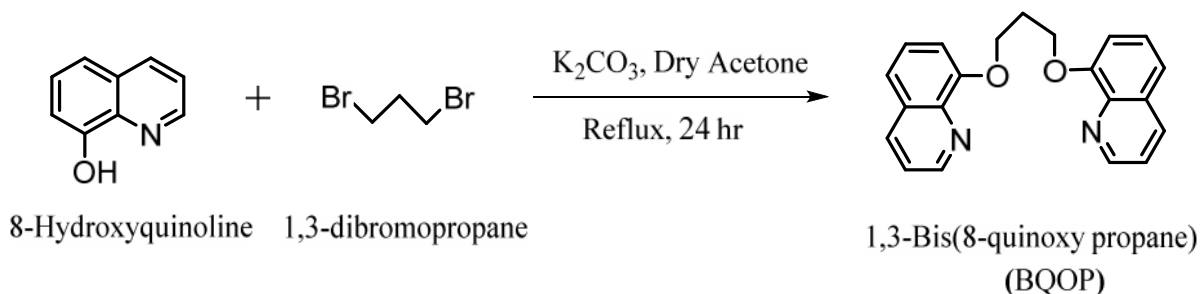
Scheme- 2.3 Synthetic route for 1, 3-bis(8-quinoxy)propane

2.2.2.4 Preparation of sodium salt of pentafluorophenol ($NaOC_6F_5$) and heptafluorobutyric acid (C_3F_7COONa)

Sodium salt of pentafluorophenol ($NaOC_6F_5$) was prepared by the reaction of pentafluorophenol with freshly prepared sodium methoxide using earlier reported method [52]. Similarly, sodium salt of heptafluorobutyric acid *(*C_3F_7COONa*)* was obtained by reacting heptafluorobutyric acid with sodium methoxide in anhydrous condition as reported in literature [53].

2.2.3 Synthesis of cobalt (II) complexes

2.2.3.1 Synthesis of [Dichloro bis (8-methoxyquinoline) cobalt (II)] [$Co(MOQ)_2Cl_2$] (1)

8-methoxy quinolin (MOQ) (0.213g, 1.3 mmol) was added to the methanolic solution of $CoCl_2.6H_2O$ (0.151g, 0.63 mmol in ~5 ml of methanol). This reaction mixture was stirred at room temperature for 48 hr on a magnetic stirrer. The excess of solvent was removed under reduced pressure; resulting blue colored solid washed with pet ether and recrystallized by slow evaporation of the methanolic solution of the complex to give transparent blue crystals.

[($C_{20}H_{18}Cl_2N_2O_2$) Co] (1): Yield: 74%, M.P.: 210^oC, decomposed; analyses (%) obs. (calc.): C: 53.57 (53.60), H: 4.01 (4.05), N: 6.21 (6.25); FT-IR (KBr, cm^{-1}): 2950 (C-H), 1262 (C=N), 1535 (C=Car,asym), 1463 (C=Car, sym), 1390 (C-N-alkyl chain), 1276(C-O-alkyl chain), 1110(C-Oar); ESI-MS (m/z):$[M-H]^+$ 446, $[CoCl_2(C_9H_6NO)(C_5H_5N)]^+$ 352, $[CoCl(C_9H_6NO)]^+$ 237, $[C_{10}H_9NO]^+$ 160. UV: max-600 nm.
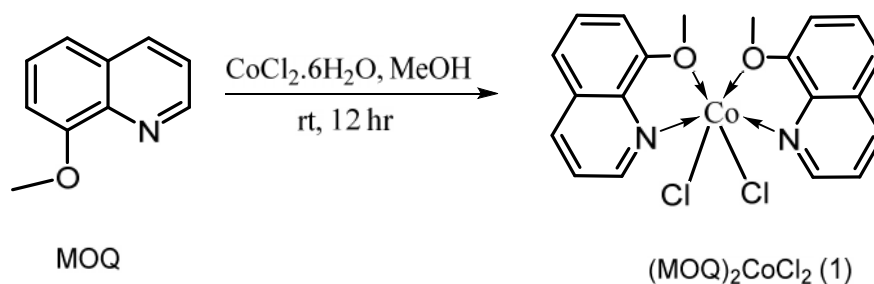
Scheme-2.4 Synthesis of [Dichloro bis (8-methoxyquinoline) cobalt (II)] complex

2.2.3.2 Synthesis of [Dichloro (8 Pyridin-2-ylmethoxy quinoline)Co(II)] [Co(PMOQ)Cl₂] (2)

Solution of 8-(Pyridin-2-ylmethoxy)-quinoline (PMOQ) (0.2g, 0.84 mmol in ~5 ml of methanol) was slowly added to a methanolic solution (~5 ml) of $CoCl_2$ (0.11g, 0.84 mmol) and the mixture was stirred at room temperature for 12 hr. The blue color precipitate obtained was filtered, washed with pet-ether and dried under vacuum. The product obtained was recrystallized by slow evaporation of its methanolic solution resulting in the formation of transparent blue crystals.

[(C₁₅H₁₂Cl₂N₂O)Co] (2): Yield 61%, M.P.: 270°C, decomposed; analyses (%) obs. (calc.): C: 49.20 (49.21), H: 3.30 (3.30), N: 7.61 (7.65); IR (KBr, , cm⁻¹): 2926 (C-H); 1273 (C=N); 1535 (C=Car, asym); 1463 (C=Car, sym); 1322 (C-O-alkyl chain); 1104(C-Oar). ESI-MS (m/z): [M-Cl]⁺ 331, [CoCl(C₁₄H₁₀N₂)]⁺ 299, [CoCl(C₉H₆NO)]⁺ 237, [(C₁₅H₁₂N₂O)]⁺ 237. UV: max-630 nm.
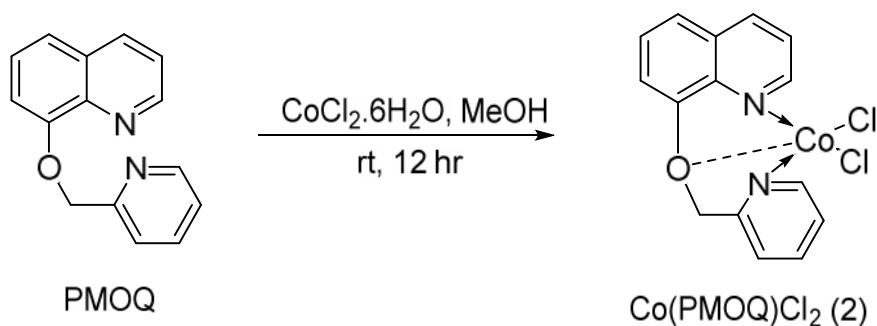
Scheme-2.5 Synthesis of [Dichloro (8 Pyridin-2-ylmethoxy quinoline) Co(II)] (2)

2.2.3.3 Synthesis of [dichloro{1,3-bis(quinolin-8-yloxy)propane}Co(II)] [(BQOP)CoCl$_2$] (3)

To a solution of CoCl$_2$.6H$_2$O (0.084 g, 0.3532 mmol) in methanol (~5 ml) was added a solution of 1, 3-bis(quinolin-8-yloxy)propane (BQOP) (0.2 g, 0.6060 mmol in ~5 ml methanol) and it was observed that the color of the reaction mixture instantaneously changed from light blue to dark purple. The solution was stirred continuously for 12 hr, and resulting purple colored solid obtained was filtered and dried. Good quality crystals of the product were obtained by slow evaporation of a methanolic solution of the complex, which were characterized by single crystal X-ray analysis.

[(C$_{21}$H$_{18}$Cl$_2$N$_2$O$_2$)Co] (3): Yield: 48%, M.P.: 230°C, decomposed; analyses (%) obs. (calc.): C: 54.78 (54.81), H: 3.96 (3.94), N: 6.05 (6.09); IR (KBr, , cm^{-1}): 2949 (C-H); 1262 (C=N); 1535 (C=Car,asym); 1463 (C=Car, sym); 1378 (C-O-alkyl chain); 1106 (C-Oar). ESI-MS (m/z):[M-CH]$^+$ 446, [CoCl(C$_9$H$_6$NO)(C$_9$H$_6$N)(C$_2$H$_5$)]$^+$ 392, [CoCl(C$_9$H$_7$N)(C$_9$H$_7$N)]$^+$ 352, [(C$_9$H$_6$NO)(C$_9$H$_6$NO)(CH$_2$)$_3$]$^+$ 331, [(C$_9$H$_6$NO)]$^+$ 160. UV: max-562 nm.
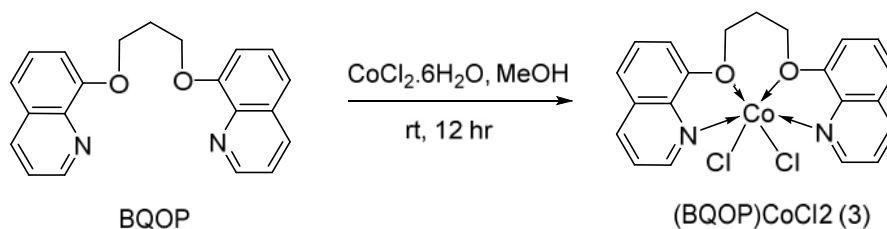
Scheme-2.6 Synthesis of [(BQOP) CoCl$_2$] (3)

2.2.4 Reactions of the quinoline Co(II) complexes

The reactions of the prepared complexes (1-3) with sodium salt of pentafluorophenol and heptafluorobutyric acid were conducted.

2.2.4.1 Reactions of Co(II) complexes with sodium pentafluorophenoxide

The general procedure for the reaction of cobalt complexes and sodium pentafluorophenoxide is outlined in the preparation of [bis (8-methoxyquinoline) Co(II) pentafluorophenoxide] (4). For all other reactions a similar procedure was employed.

2.2.4.1.1 Preparation of bis (8-methoxyquinoline)Co(II) pentafluorophenoxide (4)

Solid sodium pentafluoro phenoxide (NaOC$_6$F$_5$, 0.114 g, 5.5 mmol) was added to a dichloromethane solution of [dichloro bis (8-methoxy quinolin) Co(II)] complex (0.05g, 0.1 mmol) and the mixture was stirred at room temperature for 3 hr. The precipitated NaCl was filtered off and excess solvent was removed under reduced pressure to give a dark blue solid, which was purified by washing with minimum amount of cold dichloromethane and dried in air. The observed analytical and spectral data are given below

[(MOQ)$_2$Co(C$_6$F$_5$O)$_2$] (4): Yield 46%, M.P.: 246°C, decomposed; analyses (%) obs. (calc.): C: 51.61 (51.70), H: 2.42 (2.44), N: 3.71 (3.77); IR (KBr, Cm^{-1}): 2900(C-H); 1250 (C=N); 1130 (C-F); 1535 (C=Car,asym); 1463 (C=Car, sym); 1120(C-O-alkyl chain); 1107 (C-Oar). ESI-MS (m/z): [M-OC$_6$F$_5$]$^+$ 560, [C$_{10}$H$_9$NO]$^+$ 160, [OC$_6$F$_5$]$^+$ 182. UV: max-550 nm.
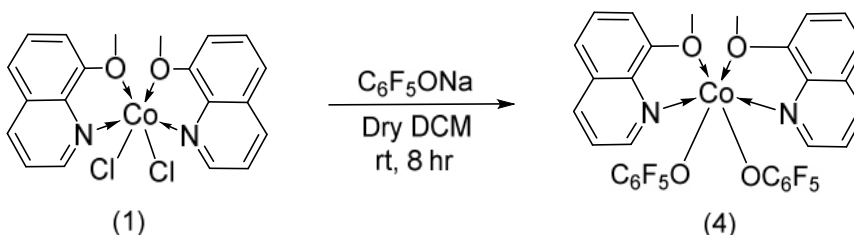
Scheme 2.7 Synthesis of [(MOQ)$_2$Co(C$_6$F$_5$O)$_2$]

2.2.4.1.2 Preparation of (8-pyridine-2-ylmethoxy quinoline)Co(II) pentafluorophenoxide (5)

The complex was prepared by the reaction of sodium pentafluoro phenoxide (NaOC$_6$F$_5$, 0.114 g, 5.5 mmol) and [dichloro bis (8-pyridine-2-ylmethoxy quinoline) Co(II)] (2) (0.036 g, 0.1 mmol) using similar procedure discussed in section 2.2.4.1.1. The observed analytical and spectral data are given below

[(PMOQ) Co (C$_6$F$_5$O)$_2$] (5): Yield 51%, M.P.: 190 ^{o}C, decomposed; analyses (%) obs. (calc.): C: 49.0 (49.04), H: 1.83 (1.83), N: 4.20 (4.24); IR (KBr, Cm^{-1}): 2926(C-H); 1250 (C=N); 1130 (C-F); 1535 (C=Car,asym); 1463 (C=Car, sym); 1120(C-O-alkyl chain);

1107 (C-Oar). ESI-MS (m/z): $[M-OC_6F_5]^+$ 479, $[Co(OC_6F_4)(C_9H_6NO.C_6H_4N)]^+$ 446, $[Co(O)(C_9H_6NO.C_6H_4N)]^+$ 298, $[C_9H_6NO.CH_2.C_6H_4N]^+$ 237 ,$[OC_6F_5]^+$ 182, $[C_{10}H_9NO]^+$ 160. UV: max-599, 557, 504 nm
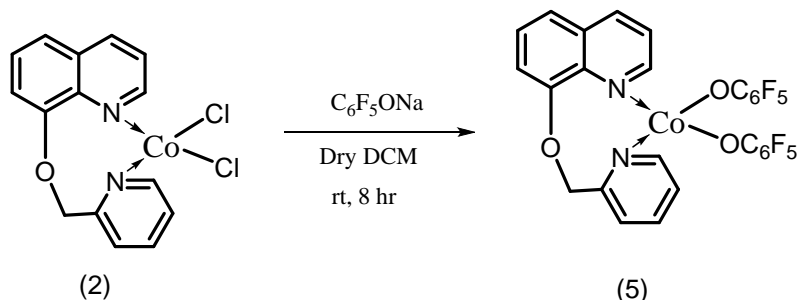
Scheme 2.8 Synthesis of $[(PMOQ) Co (C_6F_5O)_2]$

2.2.4.1.3 Preparation of (1,3 bisquinoxy-8-yloxy propane) Cobalt (II) phenoxide (6)

The complex was prepared by the reaction of sodium pentafluoro phenoxide ($NaOC_6F_5$, 0.114 g, 5.5 mmol) and [dichloro (1,3 bisquinoxy-8-yloxy propane) Cobalt (II)] (2) (0.045 g, 0.1 mmol) using similar procedure discussed in section 2.2.4.1.1.
The observed analytical and spectral data are given below

[(BQOP)Co(C$_6$F$_5$O)$_2$] (6): Yield 40%, M.P.: 247 ^{o}C, decomposed; analyses (%) obs. (calc.): C: 52.45 (52.47), H: 2.40 (2.40), N: 3.70 (3.71); IR (KBr, Cm^{-1}): 2900(C-H); 1250 (C=N); 1725 (C=O); 1535 (C=Car, asym); 1463 (C=Car, sym); 1120 (C-O-alkyl chain); 1107 (C-Oar). ESI-MS (m/z): $[M-OC_6F_5]^+$ 572, $[(C_9H_6NO)(C_9H_6NO)(CH_2)_3]^+$ 331, $[(C_9H_6NO)]^+$ 160. UV: max-601, 562, 505 nm
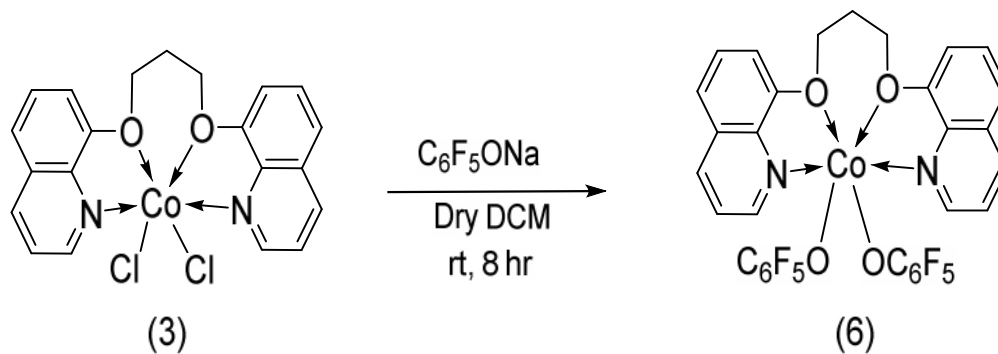
Scheme 2.9 Synthesis of $[(BQOP)Co(C_6F_5O)_2]$

2.2.4.2 Reactions of cobalt complexes with sodium heptaflurobutyrate

The general procedure for the reactions of the cobalt complexes with sodium heptaflurobutyrate is outlined in the preparation of [bis (8-methoxyquinoline) cobalt (II) heptaflurobutyrate]. Similar process was employed for all the reactions.

2.2.4.2.1 Preparation of bis (8-methoxyquinoline) cobalt (II) heptaflurobutyrate (7)

To a solution of complex [dichloro bis (8-methoxyquinoline) cobalt (II)] (**1**) (0.051 g, 0.11 mmol) in dichloromethane, solid sodium heptafluorobutyrate (0.132 g, 0.05 mmol) was added. This reaction mixture was stirred continuously for 3-4 hr at room temperature. Wine red colored solid obtained by filtration was washed with cold dichloromethane and dried in air.

The observed synthetic and analytical details are summarized below

[(MOQ)Co(C$_3$F$_7$COO)$_2$] (7): Yield 43%, M.P.: 225 $^{\circ}$C, decomposed; analyses (%) obs. (calc.): C: 41.81 (41.86), H: 2.25 (2.26), N: 3.44 (3.49); IR (KBr, Cm^{-1}): 2900(C-H); 1250 (C=N); 1725 (C=O); 1535 (C=Car, asym); 1463 (C=Car, sym); 1120 (C-O-alkyl chain); 1107 (C-Oar). ESI-MS (m/z): [M-OOCC$_3$F$_7$]$^{+}$ 590, [Co(OOCC$_3$F$_7$)(C$_{10}$H$_9$NO)]$^{+}$ 430, [OOCC$_3$F$_7$]$^{+}$ 212, [C$_{10}$H$_9$NO]$^{+}$ 160. UV: max-542 nm.
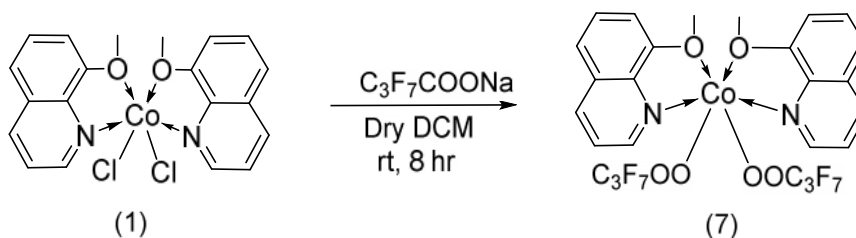
Scheme 2.10 Synthesis of [(MOQ)Co(C$_3$F$_7$COO)$_2$]

2.2.4.2.2 Preparation of (8-pyridine-2-ylmethoxy quinoline)Co(II) pentafluorophenoxide (8)

The complex was prepared by the reaction of sodium heptafluorobutyarate (0.132 g, 0.05 mmol) and [dichloro bis (8-pyridine-2-ylmethoxy quinoline) Co(II)] (2) (0.036 g, 0.1 mmol) using similar procedure discussed in section 2.2.4.2.1.

The observed analytical and spectral data are given below

[(PMOQ)Co(C$_3$F$_7$COO)$_2$] (8): Yield 37%, M.P.: 198 $^{\circ}$C, decomposed; analyses (%) obs. (calc.): C: 38.25 (38.30), H: 1.65 (1.68), N: 3.85 (3.88); IR (KBr, Cm^{-1}): 2900(C-H); 1250

(C=N); 1725 (C=O); 1535 (C=Car, asym); 1463 (C=Car, sym); 1120 (C-O-alkyl chain); 1107 (C-Oar). ESI-MS (m/z): $[M-OOCC_3F_7]^+$ 508, $[Co(OOCC_3F_7)(C_9H_6NO)(C_5H_4N)]^+$ 495, $[Co(O) (C_9H_6NO) (C_5H_4N)]^+$ 298, $[Co(C_9H_6NO)(C_3H_4N)]^+$ 258, $[OOCC_3F_7]^+$ 213, $[C_{10}H_9NO]^+$ 160. UV: max-599, 557, 504 nm
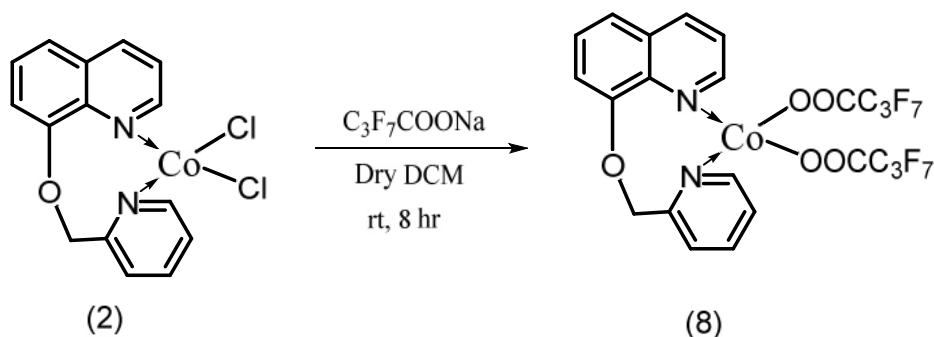
Scheme 2.11 Synthesis of $[(PMOQ)Co(C_3F_7COO)_2]$

2.2.4.2.3 Preparation of (1, 3 bisquinoxy-8-yloxy propane) Cobalt (II) heptafluorobutyrate (9)

The complex was prepared by the reaction of sodium heptafluorobutyrate (0.132 g, 0.05 mmol) and [dichloro (1,3 bisquinoxy-8-yloxy propane) Cobalt (II)] (3) (0.045 g, 0.1 mmol) using similar procedure discussed in section 2.2.4.2.1.

The observed analytical and spectral data are given below:

$[(BQOP)Co(C_3F_7COO)_2]$ (9): Yield 41%, M.P.: 220 ^{o}C, decomposed; analyses (%) obs. (calc.): C: 42.70 (42.72), H: 2.22 (2.23), N: 3.41 (3.44); IR (KBr, Cm^{-1}): 2900(C-H); 1250 (C=N); 1725 (C=O); 1535 (C=Car, asym); 1463 (C=Car, sym); 1120 (C-O-alkyl chain); 1107 (C-Oar). ESI-MS (m/z): $[Co(OOCC_3F_7) (C_9H_6NOCH_2)(O)]^+$ 446, $[Co(OOCC_3F_5)$ $(C_9H_6NOCH_2)]^+$ 391, $[Co(OOCC_3F_3)(C_9H_6NOCH_2)]^+$ 353, $[Co(C_9H_6N)]^+$ 186, $[Co(C_7H_8N)]^+$ 166, $[C_{10}H_9NO]^+$ 160, UV: max-560 nm.
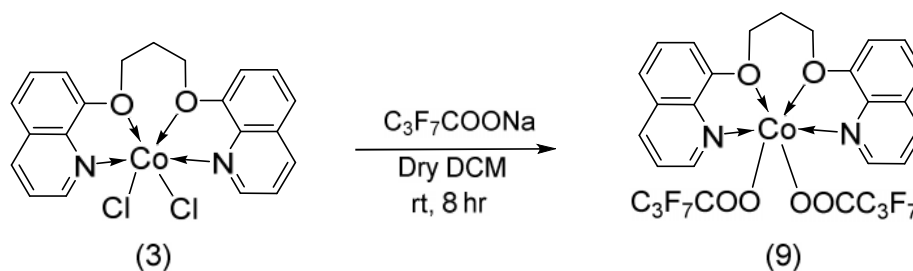
Scheme 2.11 Synthesis of [(BQOP)Co(C$_3$F$_7$COO)$_2$]

2.2.5 Crystal and molecular structures of [(PMOQ)CoCl$_2$] (2) and [(BQOP)CoCl$_2$] (3)

When complexes (**2**) and (**3**) were subjected to re-crystallization in methanol with slow evaporation, blue colored crystals of (**2**) and light purple colored crystals of (**3**) were obtained. The single crystal X-ray data for (**2**) and (**3**) were collected at 150 K on Bruker APEX-II CCD system equipped with a low-temperature attachment. Data were collected at 150(2) K using graphite-monochromated Mo Ka radiation (ka = 0.71073 Å). The strategy for the Data collection was evaluated by using the Bruker APEX2 software. The data were collected by the standard '□-□' scan techniques and were scaled and reduced using CRYSALISPRO RED software. The structures were solved by direct methods using SHELXS-97 and refined by full matrix least squares with SHELXL-2014, refining on F^2. The positions of all the atoms were obtained by direct methods. The positions of all the atoms were obtained by direct methods. All non-hydrogen atoms were refined anisotropically. The remaining hydrogen atoms were placed in geometrically constrained positions and refined with isotropic temperature factors, generally 1.2×9 Ueq of their parent atoms. All the H-bonding interactions, mean plane analyses, and molecular drawings were obtained using the program Ortep. Atomic coordinates, bond lengths and angles, and thermal parameters have been deposited at the Cambridge crystallographic data center. Symmetry transformations used to generate equivalent atoms: 'x, y, z '-x+1/2, y+1/2, -z+1/2' '-x, -y, -z' 'x-1/2, -y-1/2, z-1/2'. The crystal data and refinement are summarized in table 2.1.

Table 2.1 Crystal data and structure refinement for complex (2)

Complex	(PMOQ)CoCl$_2$
Empirical formula	C$_{15}$H$_{12}$Cl$_2$CoN$_2$O
Formula weight	365.09
Temperature	100 K
Wavelength	0.71073 A
Crystal system, space group	Monoclinic, P 2(1)/c
Unit cell dimensions	a = 13.271(7)Å = 90
	b = 8.674(4)Å = 115.788(6)
	c = 14.099(7)Å = 90
Volume	1461.3(13)Å^3
Z, Calculated density	4, 1.659 g cm^{-3}
Absorption coefficient	1.537 mm-1
F(000)	736
Crystal size	0.31 x 0.28 x 0.16 mm3
Theta range for data collection	2.84 to 28.94°
Limiting indices	-17<=h<=18, -11<=k<=11, -19<=l<=19
Reflections collected / unique	3800/1980 [R(int) = 0.1847]
Completeness to = 28.73	98.4%
Absorption correction	Multi-scan
Max. and min. transmission	0.6472 and 0.7910
Refinement method	Full-matrix least-squares on F2
Data / restraints / parameters	3800 / 0 / 190
Goodness-of-fit on F2	0.971

Final R indices [I>2 (I)]	R1 = 0.0549, wR2 = 0.1427
R indices (all data)	R1 = 0.1402, wR2 = 0.1848
Absolute structure parameter	0.83(4)
Largest diff. peak and hole	0.698 and -0.452e.Å-3

Table 2.2 Crystal data and structure refinement for complex (3)

Complex	**(BQOP)CoCl$_2$**
Empirical formula	C$_{21}$ H$_{18}$ Cl$_2$ Co N$_2$ O$_2$
Formula weight	460.20
Temperature	273 K
Wavelength	0.71073 A^o
Crystal system, space group	Monoclinic, C 2/m
Unit cell dimensions	a = 15.154(13)Å = 90
	14.650(14)Å = 118.20(2)
	10.076(9)Å = 90
Volume	1971(3)Å^3
Z, Calculated density	4, 1.551g cm^{-3}
Absorption coefficient	1.161 mm-1
F(000)	940.0
Crystal size	0.4 x 0.2 x 0.3 mm3
Theta range for data collection	2.063 to 26.589^o
Limiting indices	-18<=h<=18, -18<=k<=18, -12<=l<=12
Reflections collected / unique	21955/2131 [R(int) = 0.0373]

Completeness to = 28.73	98.4%
Absorption correction	Multi-scan
Max. and min. transmission	0.7454 and 0.5325
Refinement method	Full-matrix least-squares on F2
Data / restraints / parameters	3800 / 0 / 190
Goodness-of-fit on F2	0.971
Final R indices [I>2 (I)]	R1 = 0.0284, wR2 = 0.0790
R indices (all data)	R1 = 0.0331, wR2 = 0.0790
Absolute structure parameter	0.83(4)
Largest diff. peak and hole	0.698 and -0.452e.Å-3

2.3   Results and discussion

2.3.1   Synthesis and characterization

The preparation of some new cobalt (II) mixed chloro complexes from quinoline derivatives have been achieved. The quinoline derived ligands in the present studies include di, tri and tetradentate chelates. The X-ray crystal structures of the complexes have revealed interesting and diverse modes of coordination.

The reactions of the complexes with sodium salt of pentafluorophenol and heptafluorobutyric acid have also been carried out. In both cases products with chlorides replaced was obtained.

To confirm structure of the synthesized compounds and characterize the complexes various analytical and spectral techniques including microanalysis (CHN), IR, Mass, UV and single crystal X-ray analysis were performed. All these metal complexes are non-hygroscopic in nature, stable at room temperature. These metal complexes are insoluble in water and partially soluble in chloroform, dichloromethane, ethanol and methanol but completely soluble in DMSO.

2.3.2 Elemental analysis

The observed elemental (C, H, N) analytical data of all the complexes are consistent with their compositions. It appears from the formulation of the complexes that the ligand 1, 2 and 3 are serving as bidentate, tridentate and tetradentate ligands respectively in them. In order to authenticate the coordination mode of the ligands in these complexes, structure of the complexes (**2**) and (**3**) have been determined by X-ray crystallography.

2.3.3 Description of X-ray structure of complex (2)

The atom numbering schemes for this complex is given in Figure 2.1 with the relevant bond distances and angles collected in Table 2.2. The structure shows that the complex consists of a molecule of PMOQ coordinated to $CoCl_2$ unit in a distorted trigonal bipyrapidal environment. The ligand formally acts as an N, N'- bidentate ligand with the formation of eight membered chelate ring. However, the ligand contorts itself that brings the non-coordinated ether oxygen atom closer to the cobalt atom. The Co(1)-O(1) interatomic distance is 2.342 A^o which is significantly less than the Vander Waals radii, viz. 3.15 A^o [51, 53]. This interaction is shown as a dotted line in fig. 2.3. Similar interaction of this ligand has been reported with $PdCl_2$ [53].

The cobalt (II) chloride complex (2) crystallizes in the monoclinic space group p21/c and consists of ligand (PMOQ) chelating the $CoCl_2$ unit. Thus the ligand acts as (N- O- N') tridentate donor and forms two fused rings. The coordination environment around the Co atom is best described as distorted trigonal bipyramidal with a tetragonal component of structural index = 0.43[= (-)/60, where = 115.788^o & = 90°]. For perfectly tetragonal geometry is equal to zero while it becomes unity for perfectly trigonal bipyramidal geometry [51]. The ether O(1) and Cl(2) occupy axial positions while two nitrogens N(1), N(2) and Cl(1) occupy the equatorial positions. The bond distances in equatorial plane are not equal in length: Co(1)-N(1)= 2.094(3) A^o, Co(1)-N(2)= 2.074(4) A^o and Co(1)-Cl(2)= 2.2717(15) A^o. Also bond length for the axial atoms are not equal in length: Co(1)-O(1)= 2.342(3) A^o and Co(1)-Cl(2)= 2.2850(3) A^o. The axial angle Cl(2)-Co(1)-O(1) = 171.68(8) ^{o} deviates slightly from the ideal co-ordination angle of 180°. The equatorial bond angles [N(2)-Co(1)-Cl(1)] = 120.92^o, [N(1)-Co(1)-Cl(1)] = 119.35^o and

[N(2)-Co(1)-N(1)] = 105.26^o reveal distortion from the perfectly trigonal bipyramidal geometry.

Table 2.3 Important bond length and angles of complex [(PMOQ)CoCl$_2$] (2)

Bond lengths			
Co(1)-N(2)	2.074 (4)	C(4)-C(5)	1.412(6)
Co(1)-N(1)	2.094 (3)	C(4)-C(6)	1.407(6)
Co(1)-Cl(1)	2.2717(15)	C(1)-C(2)	1.399(6)
Co(1)- Cl(2)	2.2850 (15)	C(4)-C(3)	1.414(6)
Co(1)-O(1)	2.342 (3)	C(10)-H(10)	0.9300
O(1)-C(9)	1.387(5)	C(2)-H(2)	0.9300
O(1)-C(15)	1.450(5)	C(5)-C(4)	1.433(5)
C(14)-C(13)	1.383(5)	C(6)-C(7)	1.361(6)
C(14)-C(15)	1.494(5)	C(7)-C(8)	1.403(6)
C(13)-H(13)	0.9300	C(15)-H(15A)	0.9700
C(1)-C(2)	1.399(6)	C(15)-H(15B)	0.9700
C(4)-C(6)	1.407(6)	C(12)-C(11)	0.9300
Bond Angles			
N(2)-Co(1)-N(1)	105.26(13)	C(8)-C(9)-C(5)	120.7(4)
N(2)-Co(1)-Cl(1)	121.92(10)	O(1)-C(9)-C(5)	114.5(3)
N(1)-Co(1)-Cl(1)	119.35 (10)	N(2)-C(1)-C(2)	122.0(4)
N(2)-Co(1)-Cl(2)	100.70(9)	C(6)- C(4)- C(5)	118.3(4)
N(1)-Co(1)-Cl(2)	102.45(10)	C(6)- C(4)- C(3)	123.4(4)
C(11)-Co(1)-Cl(2)	103.62(5)	C(5)- C(4)- C(3)	118.3(4)
N(2)-Co(1)-O(1)	73.61(11)	N(1)- C(10)- C(11)	122.0(4)
N(1)-Co(1)-O(1)	73.80(11)	N(1)- C(10)- H(10)	119.0
Cl(1)-Co(1)-O(1)	84.63(8)	C(11)- C(10)-H(10)	119.0
Cl(2)-Co(1)-O(1)	171.68(8)	C(3)- C(2) C(1)	120.8(4)
C(9)-O(1)-C(15)	117.9(3)	C(3)- C(2) –H(2)	119.6

C(9)-O(1)-Co(1)	106.1(2)	C(1)- C(2) –H(2)	119.6
C(15)-O(1)-Co(1)	106.1(2)	C(7)- C(6)- C4	120.1(4)
C(14)-N(1)-C(10)	118.2(3)	C(7) –C(6)- H(6)	119.9
C(14)-N(1)-Co(1)	119.9(3)	C(4) -C(6) -H(6)	119.9
C(10)-N(1)-Co(1)	121.9(3)	N(2)- C(5)- C(9)	118.6(4)
N(1)-C(14)-C(13)	122.2(4)	N(2)- C(5)- C(4)	121.6(4)
N(1)-C(14)-C(15)	116.0(3)	C(9)- C(5)- C(4)	119.8(4)
C(13)-C(14)-C(15)	121.7(4)	C(6) –C(7) –C(8)	121.6(4)
C(1)-N(2)-C(5)	118.5(4)	C(6)- C(7)- H(7)	119.2
C(1)-N(2)-Co(1)	121.9(3)	C(8)- C(7)- H(7)	119.2
C(5)-N(2)-Co(1)	119.6(3)	C(2)- C(3)- C(4)	118.9(4)
C(12)-C(13)-C(14)	119.2(4)	C(2)- C(3)- H(3)	120.6
C(12)-C(13)-H(13)	120.4	C(4)- C(3)- H(3)	120.6
C(14)-C(13)-H(13)	120.4	O(1)- C(15) –C(14)	110.2(3)
C(8)-C(9)-O(1)	124.6(4)	O(1)- C(15)- H(15A)	109.6
C(14)- C(15)- H(15A)	109.6	C(9)- C(8)- C(7)	119.4(4)
O(1)- C(15)- H(15B)	109.6	C(9)- C(8)- H(8)	120.3
C(14)- C(15)- H(15B)	109.6	C(7)- C(8)- H(8)	120.3
H(15A)- C(15)- H(15B)	108.1	C(12)- C(11)- C(10)	118.8(4)
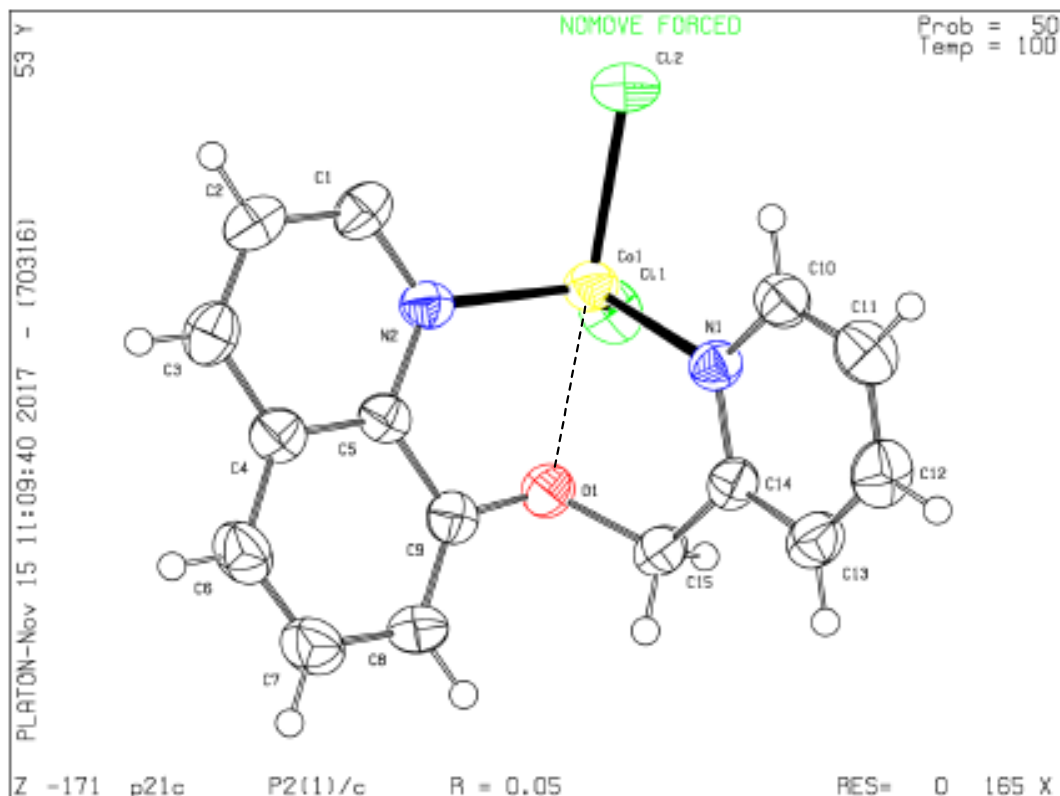
Figure 2.3 Perspective view of the structure of the cobalt complex [(PMOQ) CoCl₂] (2)

2.3.4 Description of X-ray structure of complex (3)

Figure 2.2 shows atom numbering scheme and perspective view of the X-ray structure of the complex 3, which crystallizes in the monoclinic space group C 2/m with a crystallographic mirror plane passing through the central methylene carbon and the CoCl2 unit. The ligand acts as N,O,O',N'-tetradentate forming two five membered and one six membered chelate ring. The coordination geometry of the complex shows most likely octahedral coordination of the cobalt atom. The basal plane is described by two N atoms of quinoline at distances [Co(1)-N(1)=2.0931A°] and [Co(1-N(1a)= 2.0931(2) A°] and two ether bridged O atoms at distances of [Co(1)-O(1)= 2.1859 A°] and [Co(1)-O(1)= 2.1859 A°]. The apical positions are occupied by two Cl atoms at distances [Co(1)-Cl(1)= 2.3914(18) A°] and [Co(1)-Cl(2)= 2.4451 (18) A°]. The distortion from octahedral

geometry is evident from deviation in bond angles viz. bond angles [N(1)-Co(1)-N(1)= 116.13(10)°], [N(1)-Co(1)-O(1a)= 76.76 (8)°] instead of ideal 90°. Largest deviation from optimal octahedral coordination is in the N-Co-N angle [116.13(10)°], which is increased by the adjacent three fused chelate rings and in order to avoid steric interactions between the quinoline rings[15]. Bond angles [O(1)-Co(1)-O(1a)= 90.03(10)°], [N(1)-Co(1)-Cl(1)= 92.75(5)°], [N(1a)-Co(1)-Cl(1)= 116.13(10)°] are close to ideal 90°. Trans axial bond angles of the complex [N(1)-Co(1)-O(1)= 166.29(5)°], [Cl(1)-Co(1)-Cl(2)= 175.38(2)°] diverge from perfect angle 180° showing slight distortion from octahedral geometry.

Table 2.4 Important bond length and angles of complex [(BQOP)CoCl$_2$] (3)

Bond lengths			
Co(1)-N(1)	2.093(2)	C(7)-C(6)	1.497(3)
Co(1)-N(1a)	2.093(2)	C(7)-H(8B)	1.00(3)
Co(1)-O(1)	2.1859(18)	C(7)-H(8A)	0.95(3)
Co(1)-O(1)	2.1859(18)	C(6)-H(4B)	0.98(2)
Co(1)-Cl(1)	2.3914(18)	C(6)-H(4A)	0.88(3)
Co(1)-Cl(2)	2.4451(19)	C(5)-C(4)	1.341(4)
O(1)-C(10)	1.368(3)	C(5)-H(5)	0.98(3)
O(1)-C(6)	1.456(2)	C(4)-H(6)	1.02(3)
N(1)-C(9)	1.328(2)	C(3)-C(2)	1.417(4)
N(1)-C(11)	1.362(2)	C(3)-H(2)	0.90(3)
C(11)-C(8)	1.415(3)	C(2)-C(1)	1.345(5)
C(11)-C(10)	1.430(3)	C(2)-H(3)	0.95(3)
C(10)-C(3)	1.369(3)	C(1)-H(1)	0.99(3)
C(9)-C(4)	1.400(3)	C(8)-C(5)	1.419(4)
C(9)-H(7)	0.98(2)	C(7)-C(6)	1.497(3)
C(8)-C(1)	1.410(4)		
Bond Angles			
N1 Co1 N1	116.13(10)	C4 C9 H7	117.0(12)

N1 Co1 O1	166.29(5)	C1 C8 C11	118.6(2)
N1 Co1 O1	76.76(8)	C1 C8 C5	123.7(2)
N1 Co1 O1	76.77(8)	C11 C8 C5	117.67(19)
N1 Co1 O1	166.29(5)	C6 C7 C6	118.7(3)
O1 Co1 O1	90.03(10)	C6 C7 H8B	110.3(7)
N1 Co1 Cl1	92.75(5)	C6 C7 H8B	110.3(7)
N1 Co1 Cl1	92.75(5)	C6 C7 H8A	105.7(9)
O1 Co1 Cl1	91.16(6)	C6 C7 H8A	105.7(9)
O1 Co1 Cl1	91.16(6)	H8B C7 H8A	105(3)
N1 Co1 Cl2	89.69(5)	O1 C6 C7	109.60(18)
N1 Co1 Cl2	89.69(5)	O1 C6 H4B	108.1(13)
O1 Co1 Cl2	85.58(6)	C7 C6 H4B	111.2(14)
O1 Co1 Cl2	85.58(6)	O1 C6 H4A	108.0(17)
Cl1 Co1 Cl2	175.38(2)	C7 C6 H4A	108.7(17)
C10 O1 C6	119.24(15)	H4B C6 H4A	111(2)
C10 O1 Co1	113.36(12)	C4 C5 C8	120.01(19)
C6 O1 Co1	124.71(14)	C4 C5 H5	117.2(14)
C9 N1 C11	118.24(16)	C8 C5 H5	122.7(14)
C9 N1 Co1	126.75(12)	C5 C4 C9	119.0(2)
C11 N1 Co1	114.85(13)	C5 C4 H6	122.5(16)
N1 C11 C8	121.41(18)	C9 C4 H6	118.5(17)
N1 C11 C10	118.79(16)	C10 C3 C2	119.5(3)
C8 C11 C10	119.80(17)	C10 C3 H2	118.5(19)
O1 C10 C3	125.8(2)	C2 C3 H2	121.8(19)
O1 C10 C11	114.57(15)	C1 C2 C3	121.8(2)
C3 C10 C11	119.6(2)	C1 C2 H3	122.2(17)
N1 C9 C4	123.65(19)	C3 C2 H3	116.0(17)
N1 C9 H7	119.3(12)	C2 C1 C8	120.6(2)

Datablock: datam - ellipsoid plot
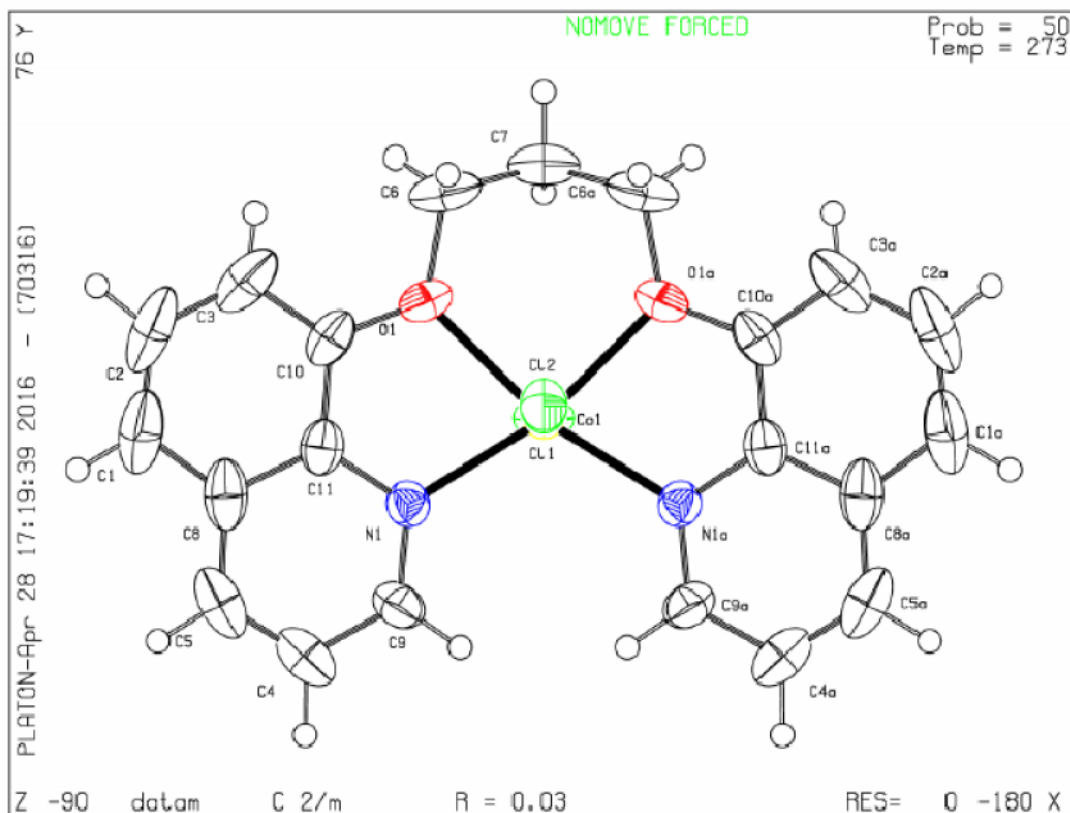
Figure 2.4 Perspective view of the structure of the cobalt complex [(BQOP)CoCl$_2$] (3)

2.3.5 Spectral Characterizations

2.3.5.1 IR spectroscopy

Infrared spectroscopy is a well known technique which is used to characterize the complexation of the transition metal ions by the organic ligands. The polydentete ligands normally coordinate with metal ions through nitrogen of the pyridine ring and oxygen of the carbonyl group [18, 19]. The IR spectra of some representative complexes are shown in Fig. 2.3-2.5. Infrared spectra of the ligands and their complexes have been assigned and described in the experimental section as shown in figures.

The IR spectra of 8-methoxyquinoline ligand containing Co(II) complexes displays characteristic bands with the significant shifts due to complex formation. The band

observed at lower frequencies as compared to free ligand (1581-1604 cm^{-1}) due to (C=N) stretching vibrations showing coordination of nitrogen of the pyridine rings to the cobalt metal. This observation is further supported by the new bands appeared in the region (471–450 cm^{-1}) assigned to v(Co–N) in the above-mentioned complexes [46, 47]. Shifting of bands than free ligand (1104-1107) cm^{-1} for C-O of phenoxy ring at slightly higher wave number in complexes indicating the coordination of the phenolic oxygen atom to the cobalt ion [8]. Further strong bands appeared near 498 cm^{-1} is attributed to v(Co-O) vibrations and supports the coordination of metal to oxygen in complexes. The other bands displayed near 3045-3050, 1107-1110 cm^{-1} are attributed to v(CH$_2$) and v(C-O) vibrations of alkoxy group. In the IR spectra of complexes (**4**) and (**5**) bands observed at 1130 cm^{-1} are assigned to the v(C-F) stretching vibration –C$_6$F$_5$ as well as CF$_3$ groups.

In the IR spectral data of the 8-(Pyridin-2-ylmethoxy)-quinoline derived cobalt complexes (**2**), (**6**) and (**7**) also displayed in experimental section. In the spectrum, the appearance of (C=N) stretching vibration at 1640–1665 cm^{-1} is shifted to the lower-frequency region (1568–1616 cm^{-1}) in the corresponding cobalt(II) complexes, and suggest the involvement of the nitrogen atom to the cobalt. The complexes also exhibits band at 1104-1107 cm^{-1} which assigned to the v(C-O) of O-CH$_2$ group which attached to the two pyridine rings. This band shows a slight shift to lower or higher wave number by 6–51 cm-1 suggesting the coordination of the oxigen atoms to the cobalt metal ion in a tridentate fashion [13, 20]. The new bands appeared in the region (420–429 cm^{-1}) and 575 cm^{-1} assigned to v(Co–N) and (Co-O) vibrations, respectively, also support the coordination of N and O to the metal atom in complexes (**2**), (**6**) and (**7**). The study and comparison of infrared spectra of ligand and its metal complexes imply that in the cobalt complexes (**2**), (**6**) and (**7**), ligand is coordinated to the metal atom by three sites and suggesting that ligand is acts as a tridentate ligand.

The characteristic bands of the complexes (**3**), (**8**) and (**9**) appeared at 1560-1580 cm^{-1} and 1265-70 cm^{-1} are due to the azomethene nitrogen (C=N) of pyridine ring and (C-O) of the phenolic ring. In the free ligand these bands shifted to slightly higher frequency (5-7 cm^{-1}) compare to complexes indicating the coordination of N and O atom to metal ion. This fact was further support by appearance of new absorption band in the region (420–429 cm^{-1}) and 575 cm^{-1} assigned to v(Co–N) and (Co-O) vibrations in all these

above mentioned complexes. The observed shifts in band positions in the above discussion are a clearly indicate that all the ligands are coordinated to the respective metal centers and formed chelating complexes.

2.3.5.2 Mass spectroscopy

The ESI-mass spectral studies of some of the representative cobalt complexes, (1)-(9) suggest monomeric nature for these derivatives. The characteristic signals for the fragmentation of these compounds are summarized in experimental sections. On the basis of the fragmentation pattern of the complexes (1-3) are clearly indicating the loss of chlorine atom, which is present outside the coordination sphere and showed peaks, attributed to the molecular ion m/z at 413 [M^+ - Cl], 331 [M^+ - Cl] and 543 [M^+-Cl]. The parent organic ligands peaks are appeared in the mass spectra of all the complexes at 160, 237 and 330 amu also confirmed the complex formation. This data is in good agreement with the proposed molecular formula for these complexes. Although, it is difficult to rationalize the fragmentation pathways without an appropriate MS technique, yet appearance of some molecular ion peaks at higher m/e value than the molecular ion in the ESI mass spectra could be due to reassociation of the molecular fragments [15, 43–45].

2.3.5.3 UV-visible spectra

The UV–vis absorption spectra of all the above free ligands (MOQ, PMOQ and BPOP) and their cobalt complexes (1-9) were recorded in methanol solution against ligands blank in the wavelength range 200–800 nm (Fig. 2.6- 2.7). The UV spectra of free ligand as shown in fig. 2.7 indicate the absorbance at 305 nm. It supported by literature and related to the – * transitions of the pyridine and benzene rings.

In the cobalt complexes of ligand MOQ (1), (4) and (5), the broad absorption band observed at 590-540 nm which can be attributed to the n– * transition. This band was not appeared in free ligand UV spectra, which can be ascribed to the binding of these coordination centers to the central metal ions. These types of band are also observed in the previously reported cobalt complexes and confirmed the complexation of cobalt metal to ligand.

In the absorption spectra of the 8-(Pyridin-2-ylmethoxy)-quinoline derived cobalt complexes (2), (6) and (7) are shown in fig.2.7. The UV spectra of the free ligand and its cobalt complexes showed that, the appearance of absorption at 260 and 309 nm in ultraviolet for free ligand disappear in corresponding cobalt(II) complexes and suggest the involvement of the ligand to the cobalt metal. The bands appeared at 260 and 309 nm in free ligand are also due to the – * and n- * transitions of the benzene and pyridine rings, respectively. Similar to the above complexes, The cobalt complexes (**2**), (**6**) and (**7**) also showed a similar broad and weak absorption bands in the UV range of 501–607 nm was due to n– * transition and these band are also disappear in the free ligand. Upon complexation, the bands undergo a bathochromic shift as compared to ligand.

The UV spectra of the another complexes of cobalt derived from 1,3-bis(quinolin-8-yloxy) propane ligand (3), (8) and (9) against ligand were also recorded in methanol at 200-800 nm region at room temperature and shown in figure 8. The UV spectral data of the ligand and its cobalt complexes are also presented in experimental section. The aromatic band of the ligand observed at 238 was due to the – * transition of benzene and pyridine ring. Another intense band appeared at 308 nm was observed to the n– * transition of the non-bonding electrons present on the nitrogen of the C=N group in the pyridine ring of ligand. As similar to the above complexes, the complexes (**3**), (**8**) and (**9**) also exhibit broad and weak bands in the UV range 498-617 nm which are not observed for ligands.

All the complexes of the cobalt(II) (**1-9**) show broad and less intense shoulders at ca 565–660 nm, which are assigned to *d-d* transition of the cobalt ions. The former band is probably due to the $^4A_2$-$^4T_1$ (P) for Co(II) transition of tetrahedral geometry. The above results of UV-vis spectra are also supported by single crystal results and confirmed the coordination of N and O to the metal atom.
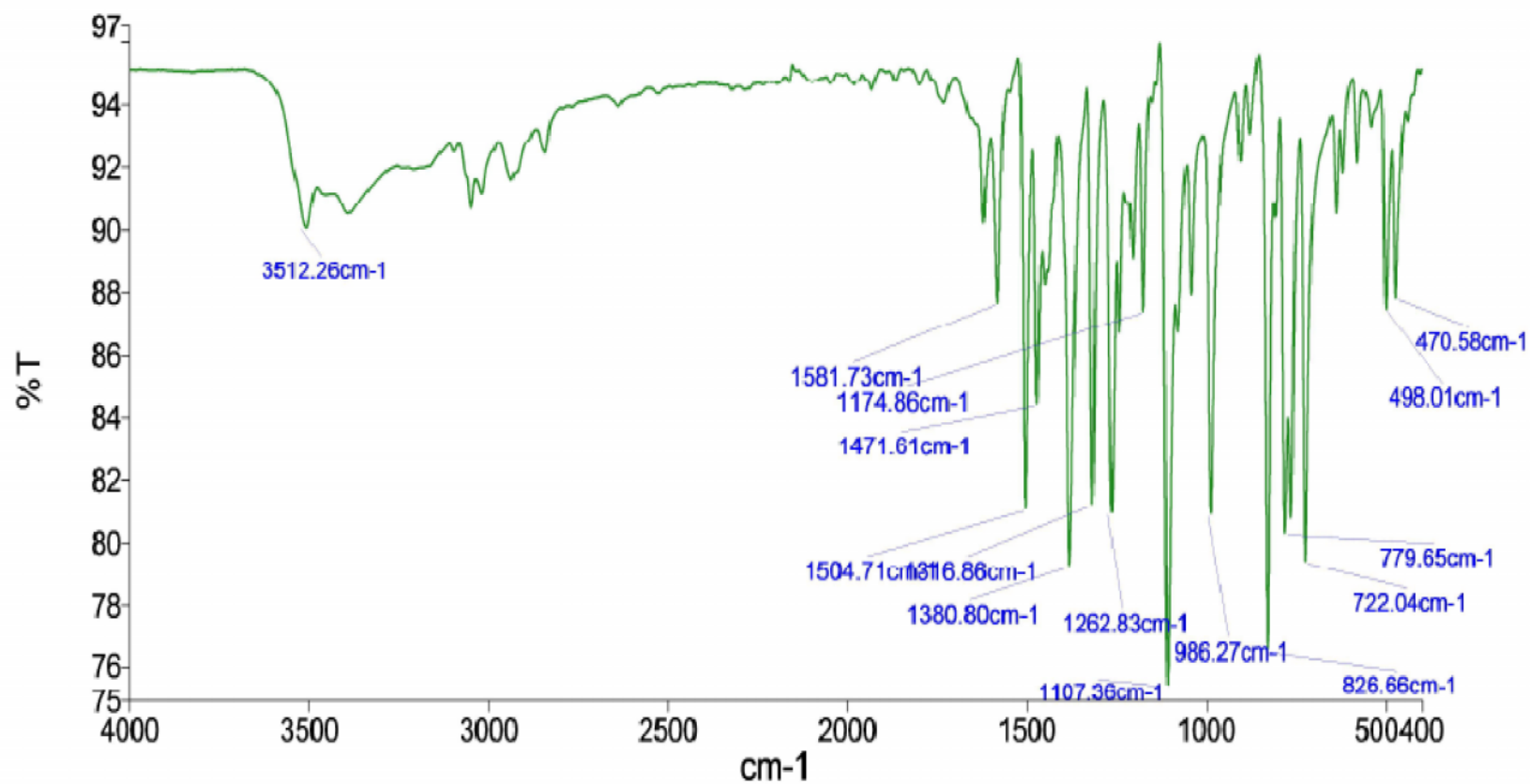
Figure 2.5 FTIR of complex (1)
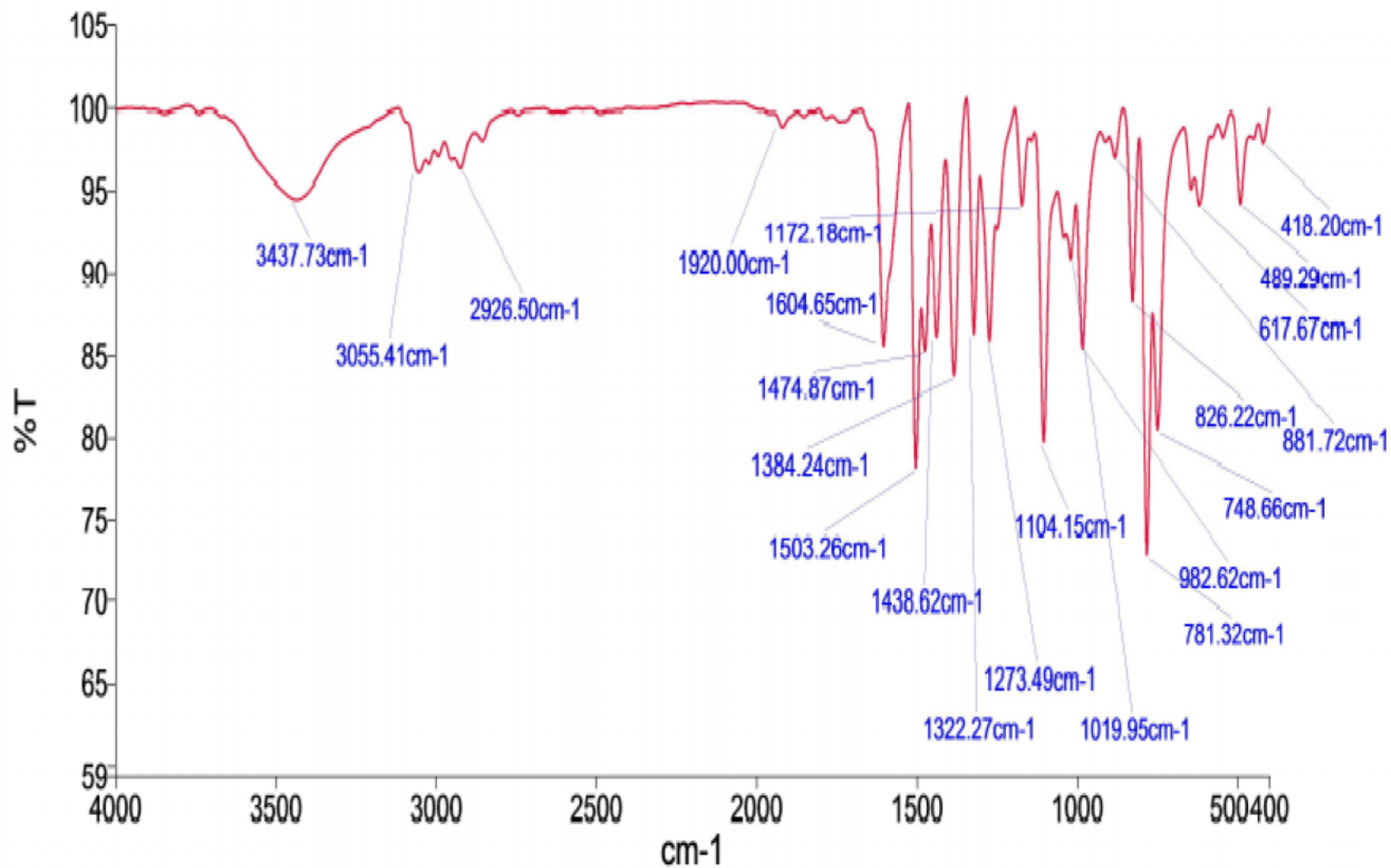
Figure 2.6 FTIR of complex (2)
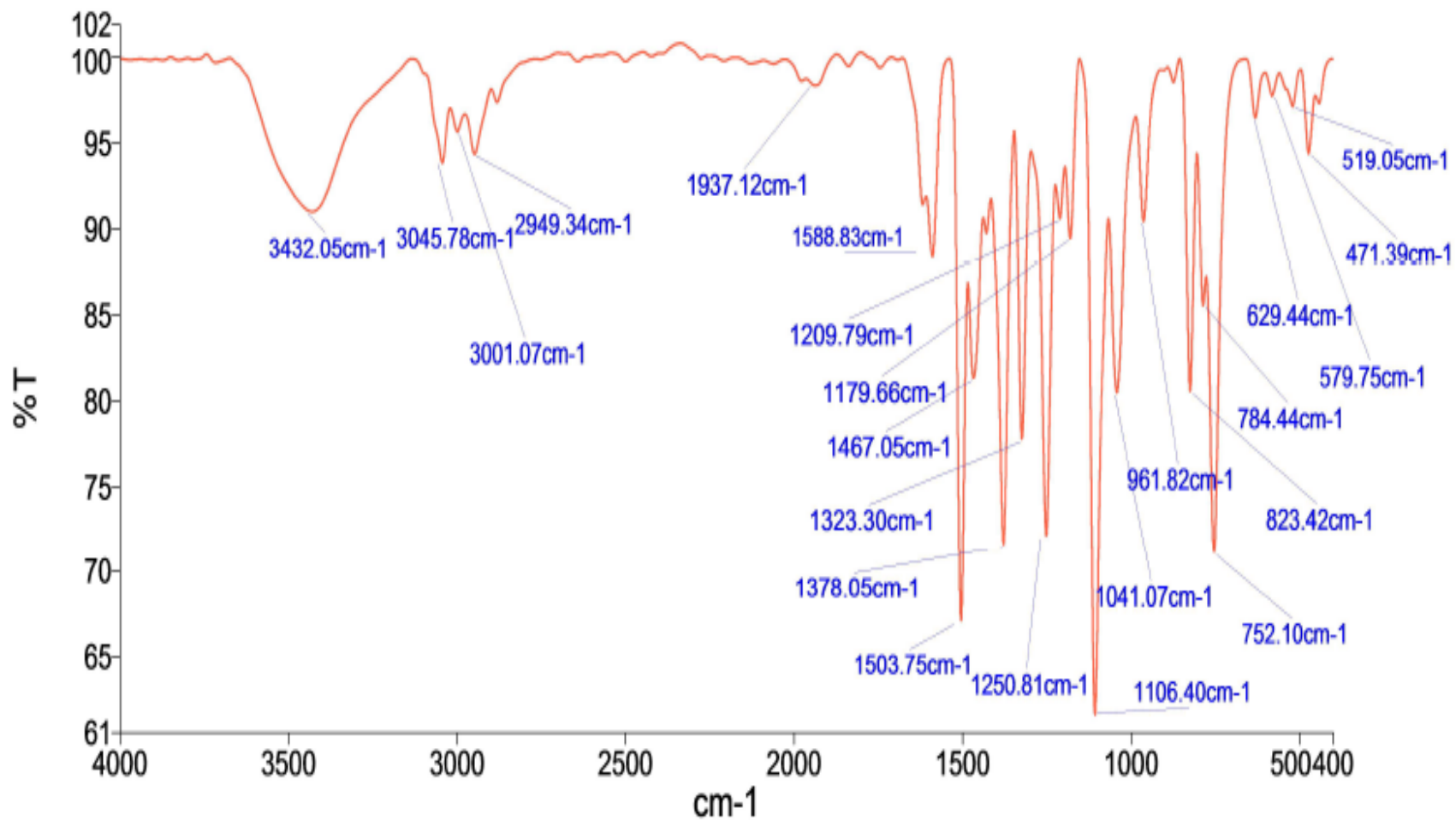
Figure 2.7 FTIR of complex (3)
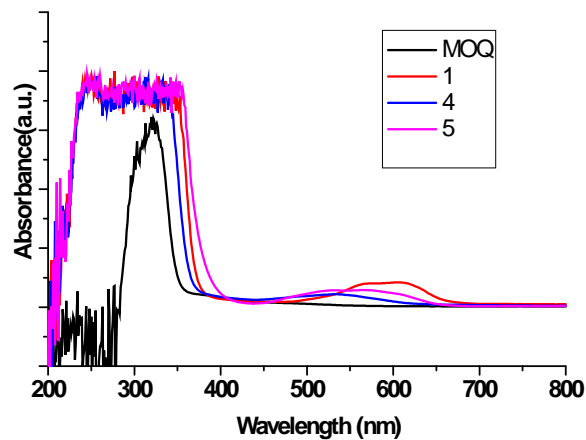
Figure 2.8 Absorption spectra of ligand (MOQ) and its complexes (1, 4 &5) (against ligands)
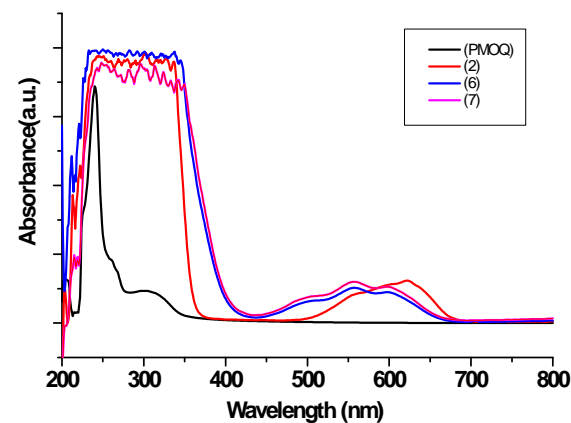
Figure 2.9 Absorption spectra of ligand (PMOQ) and its complexes (2, 6 &7) (against ligands)
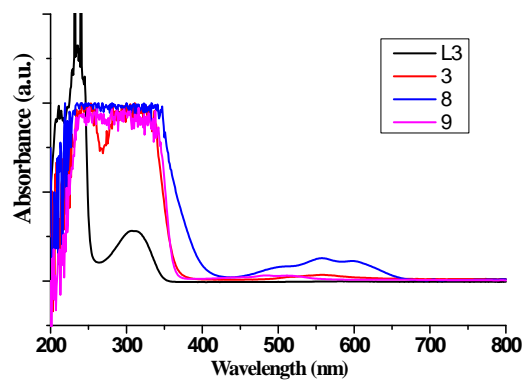
Figure 2.10 Absorption spectra of ligand (BQOP) and its complexes (3, 8 & 9) (against ligands)
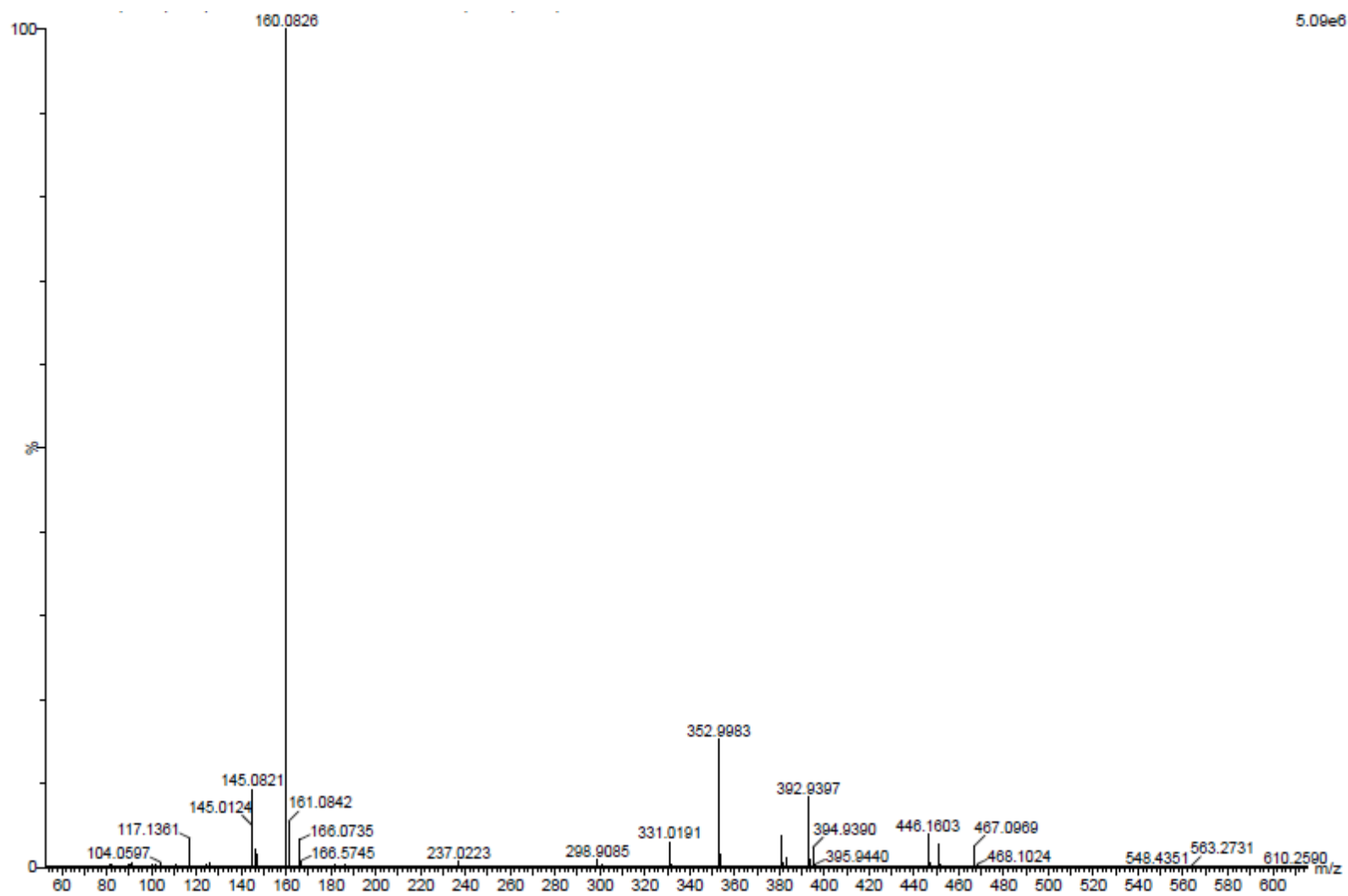
Figure 2.11 ESI mass spectra of complex (1)
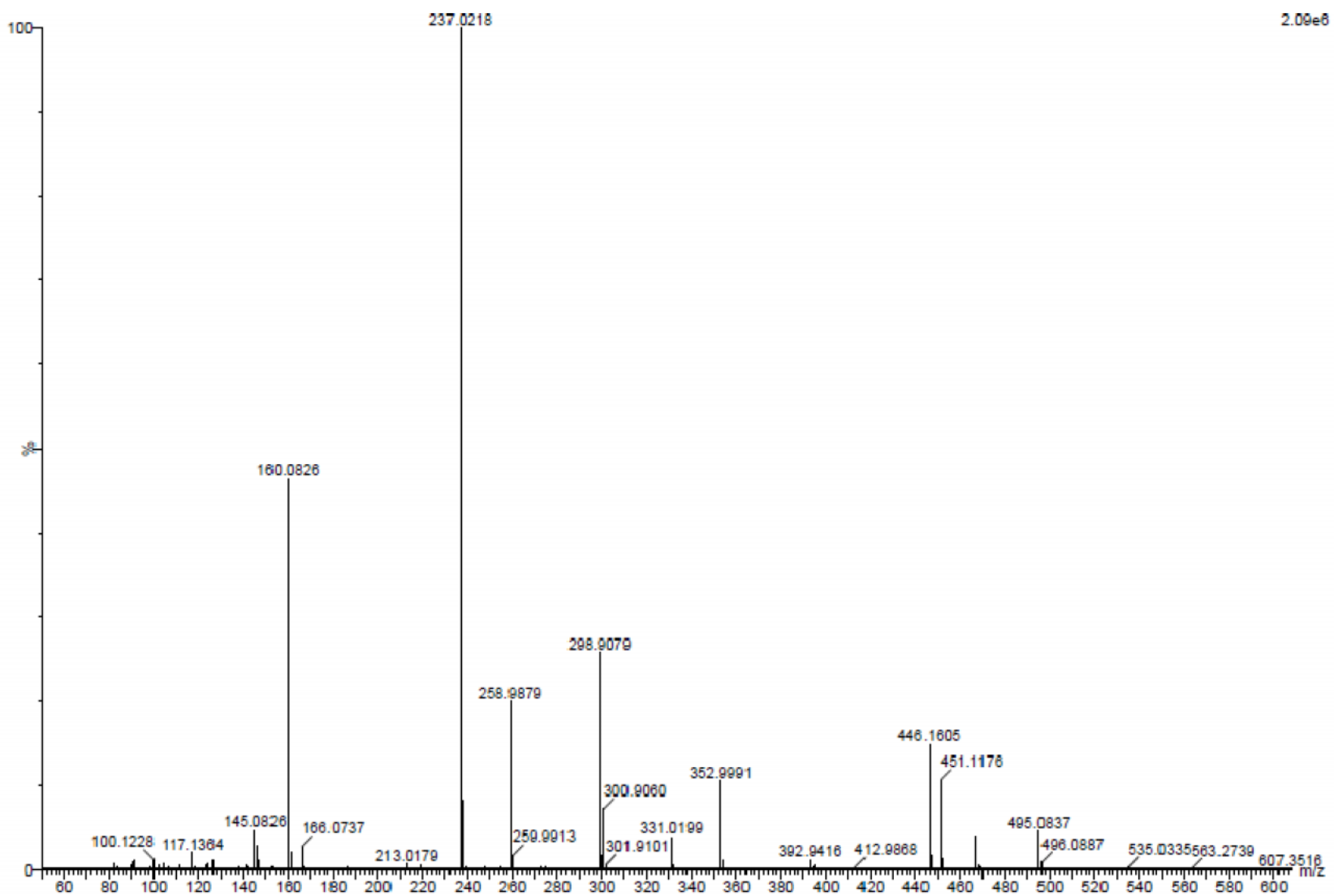
Figure 2.12 ESI mass spectra of complex (2)
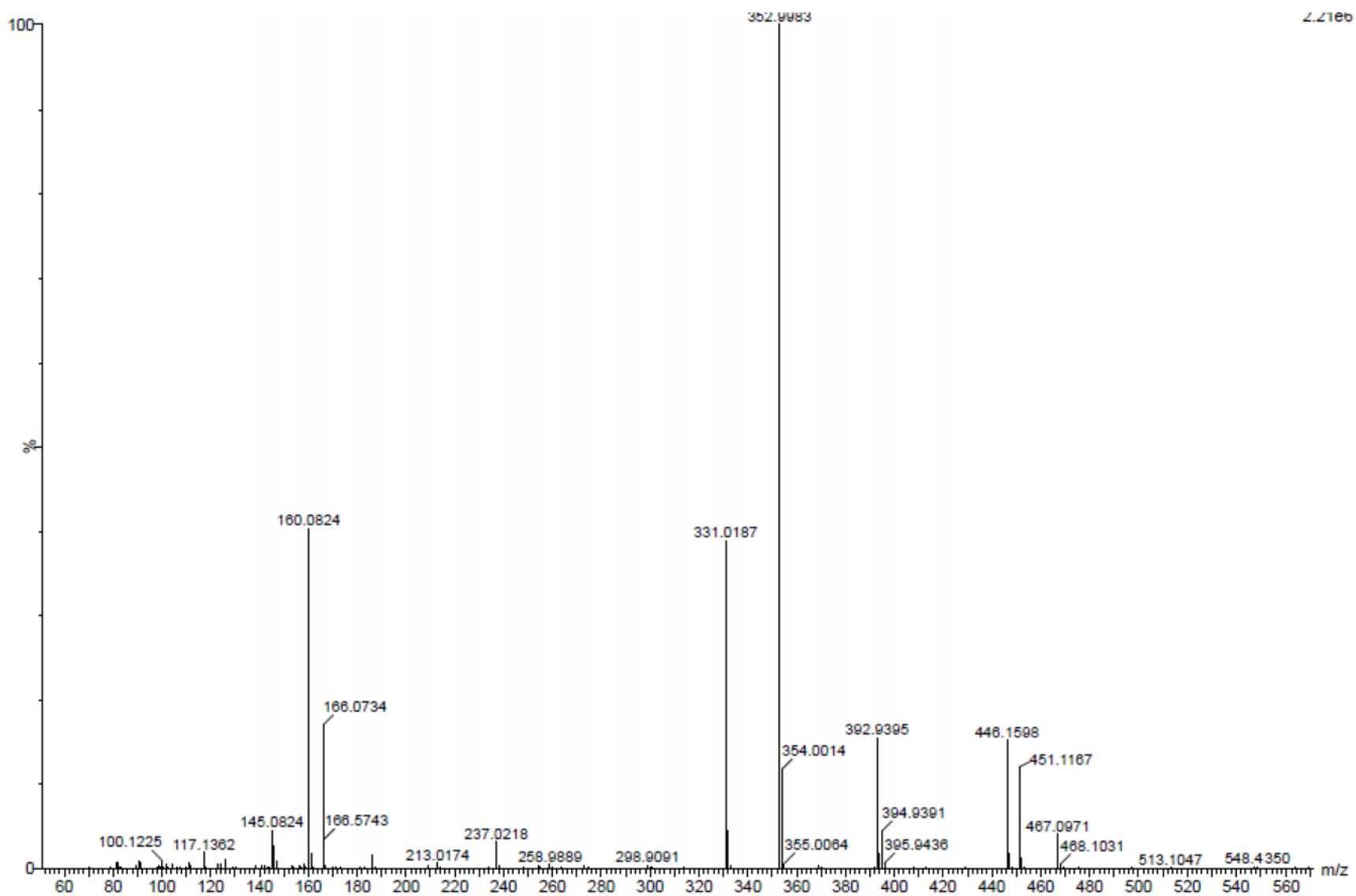
Figure 2.13 ESI mass spectra of complex (3)

JJ-TK-P-72 32 (0.558) AM (Cen,4, 80.00, Ht,10000.0,0.00,0.00); Cm (32:56)

TOF MS ES+
1.39e7

160.0829

560.4349

145.0824

161.0843

117.1362

100.1227

182.0345 237.0222

353.0002 380.9393

451.1172
467.0979

610.2592 663.4384

750.4234

822.5499 844.5347

921.5495
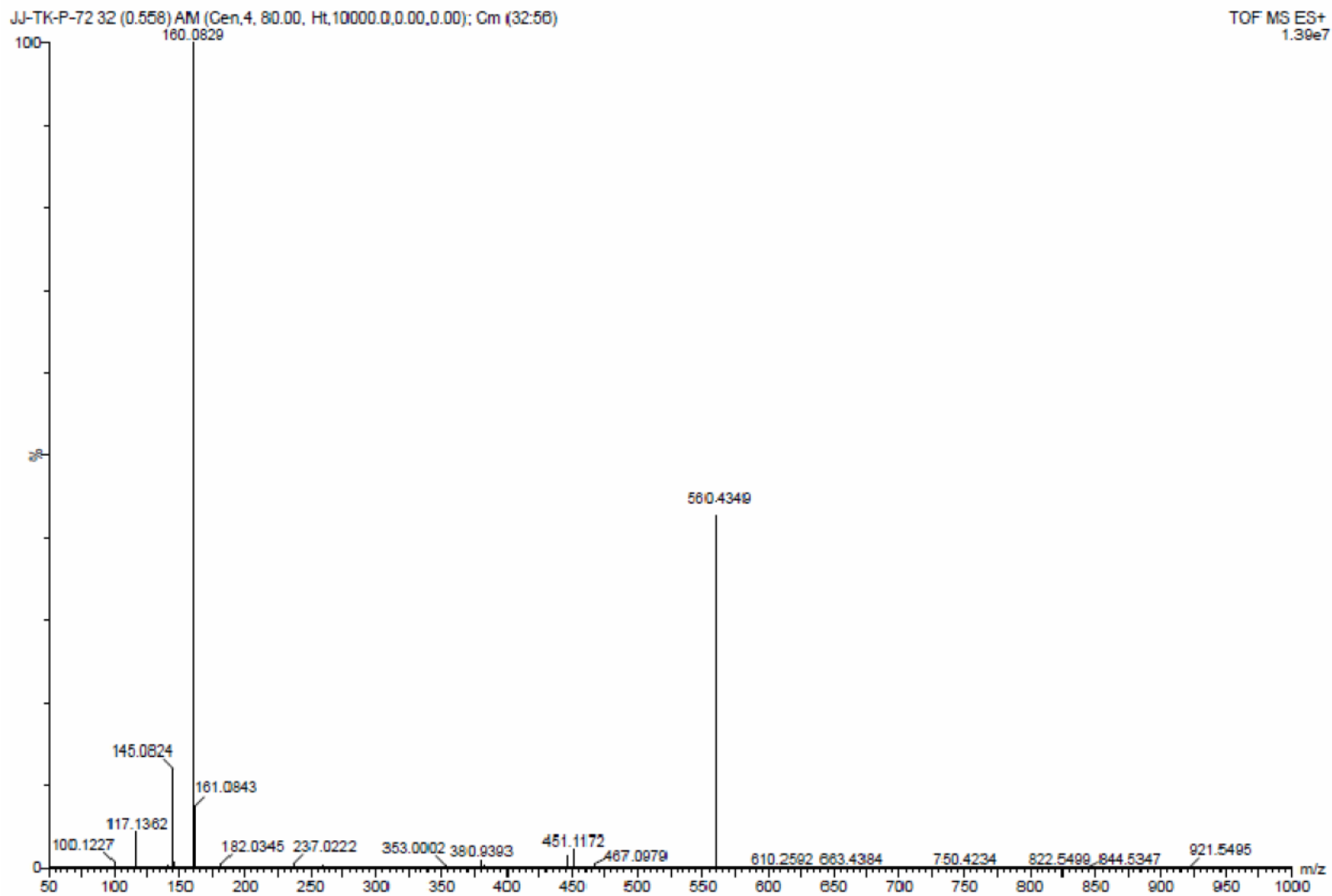
Figure 2.14 ESI mass spectra of complex (4)
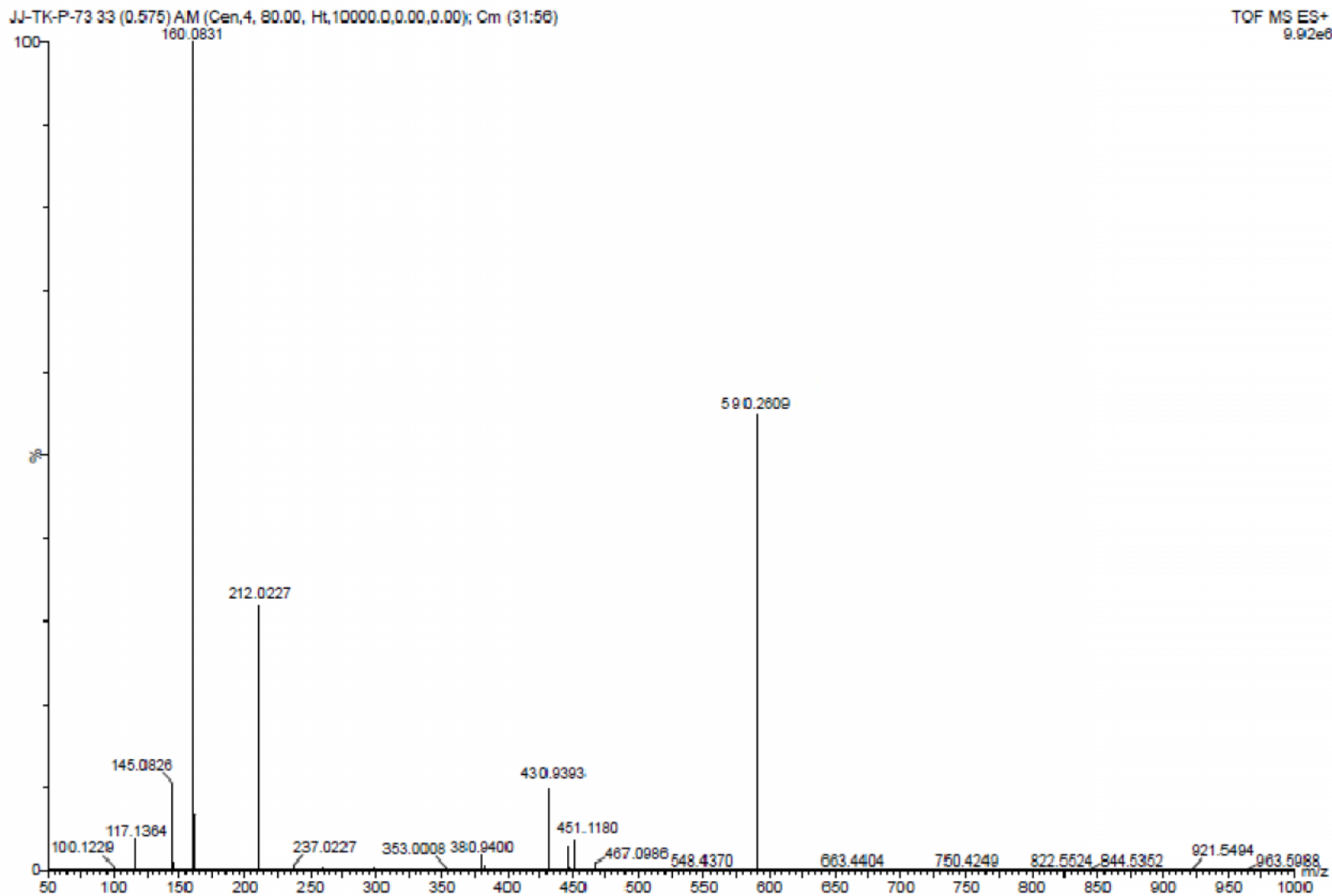
Figure 2.15 ESI mass spectra of complex (5)

JJ-RMI-09 29 (0.507) AM (Cen,4, 80.00, Ht,10000.0,0.00,0.00); Cm (29:53)
TOF MS ES+
1.79e6
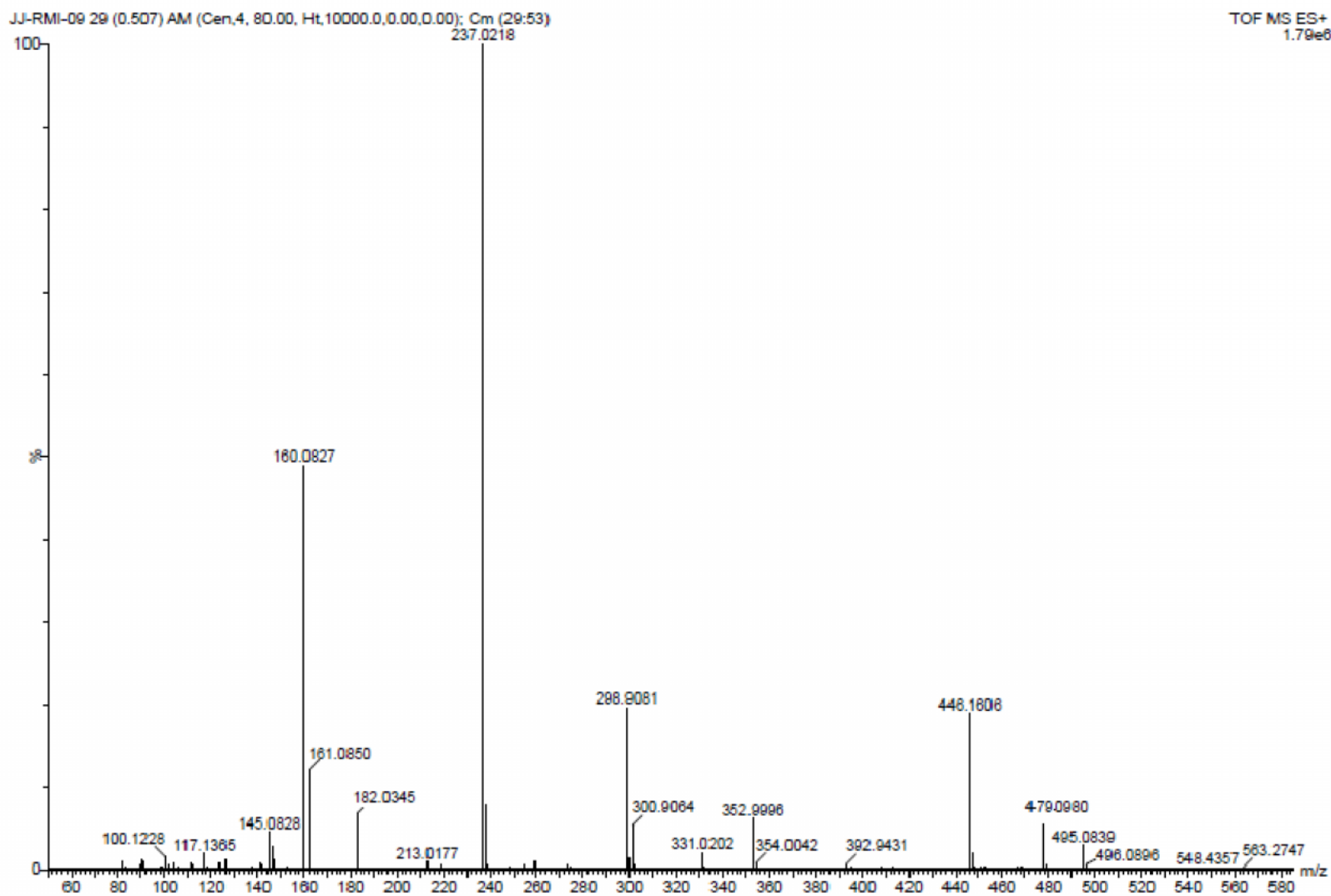
Figure 2.16 ESI mass spectra of complex (6)
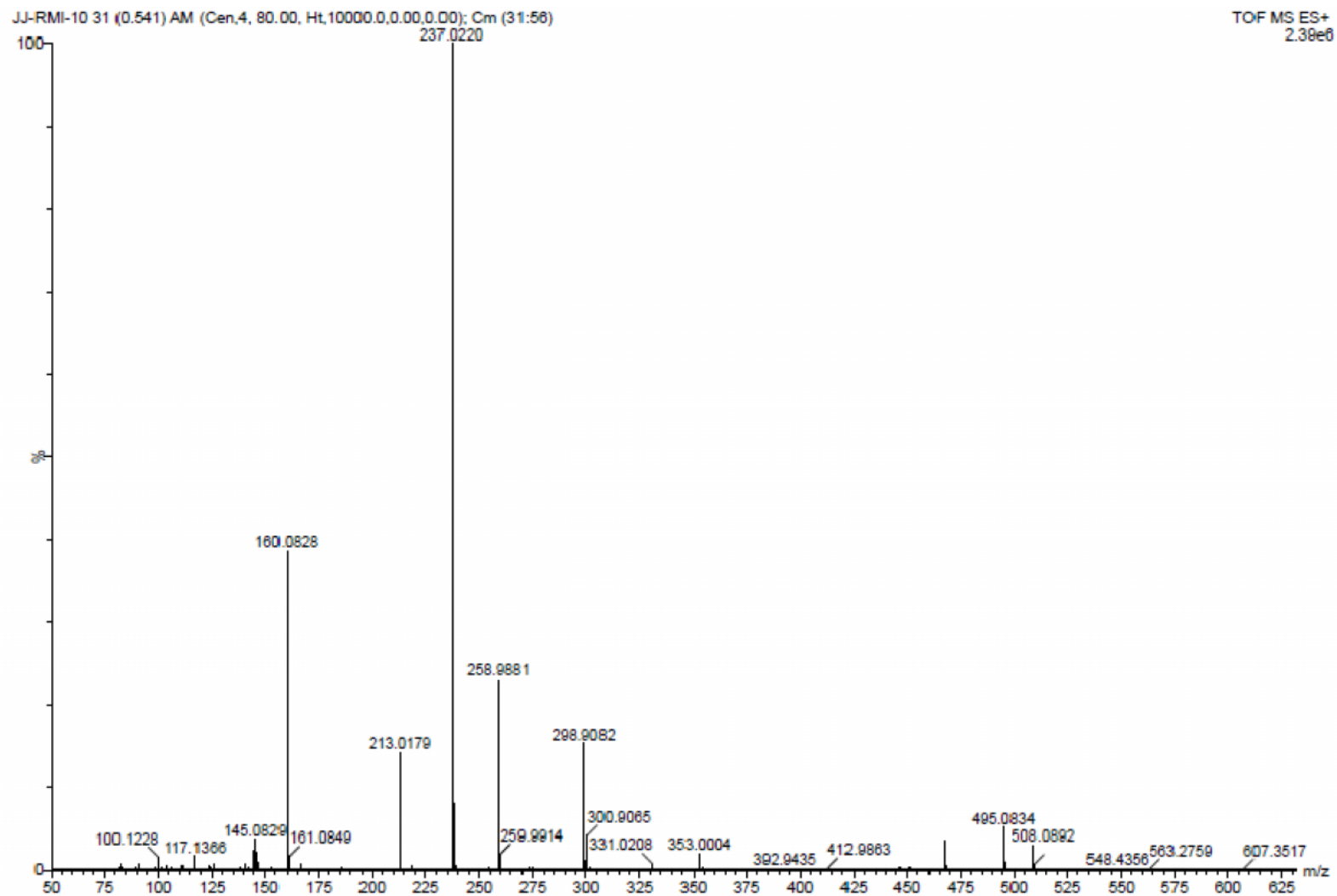
Figure 2.17 ESI mass spectra of complex (7)

JJ-TK-P-72 32 (0.558) AM (Cen,4, 80.00, Ht,10000.0,0.00,0.00); Cm (32:56)

TOF MS ES+
1.39e7
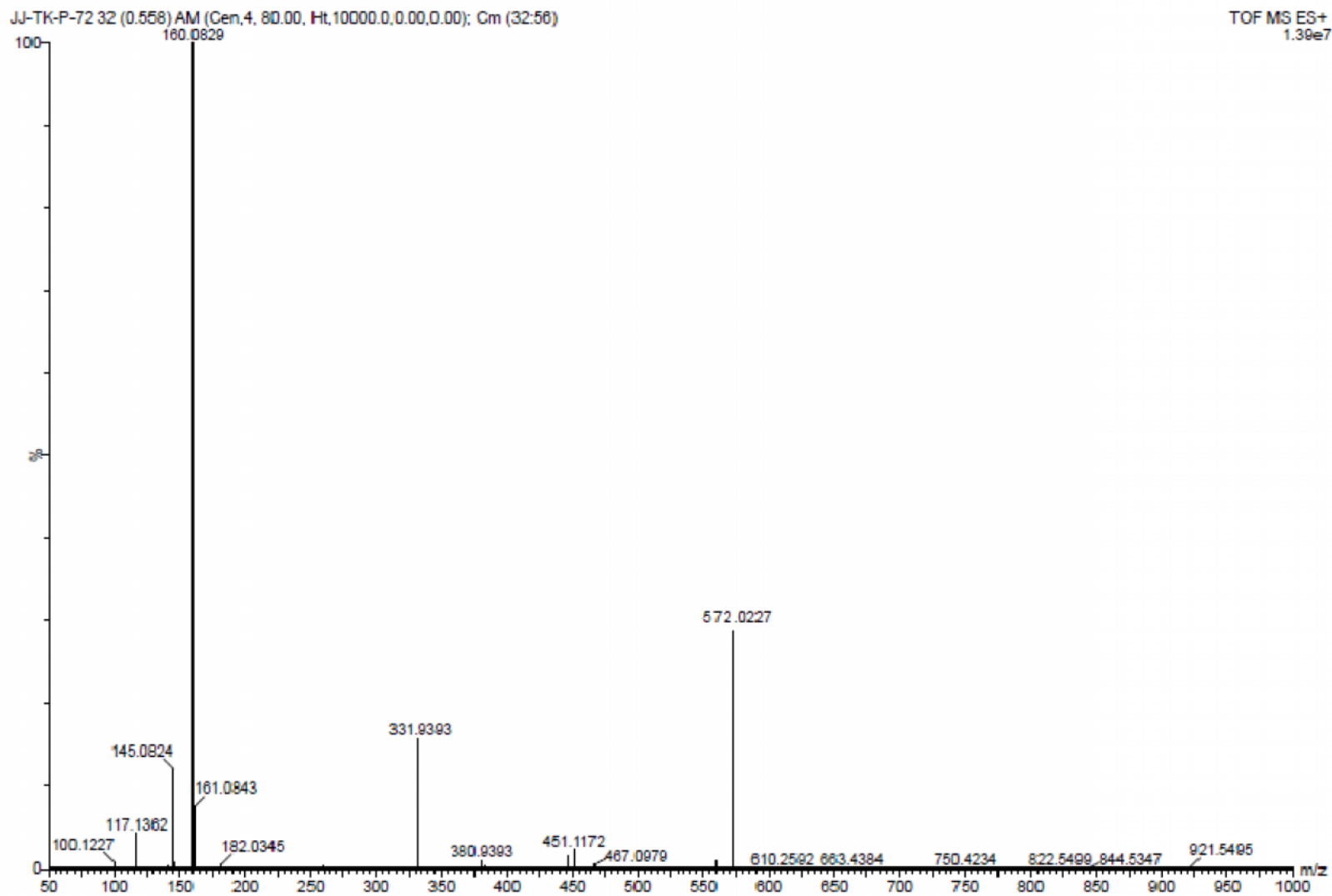
Figure 2.18 ESI mass spectra of complex (8)
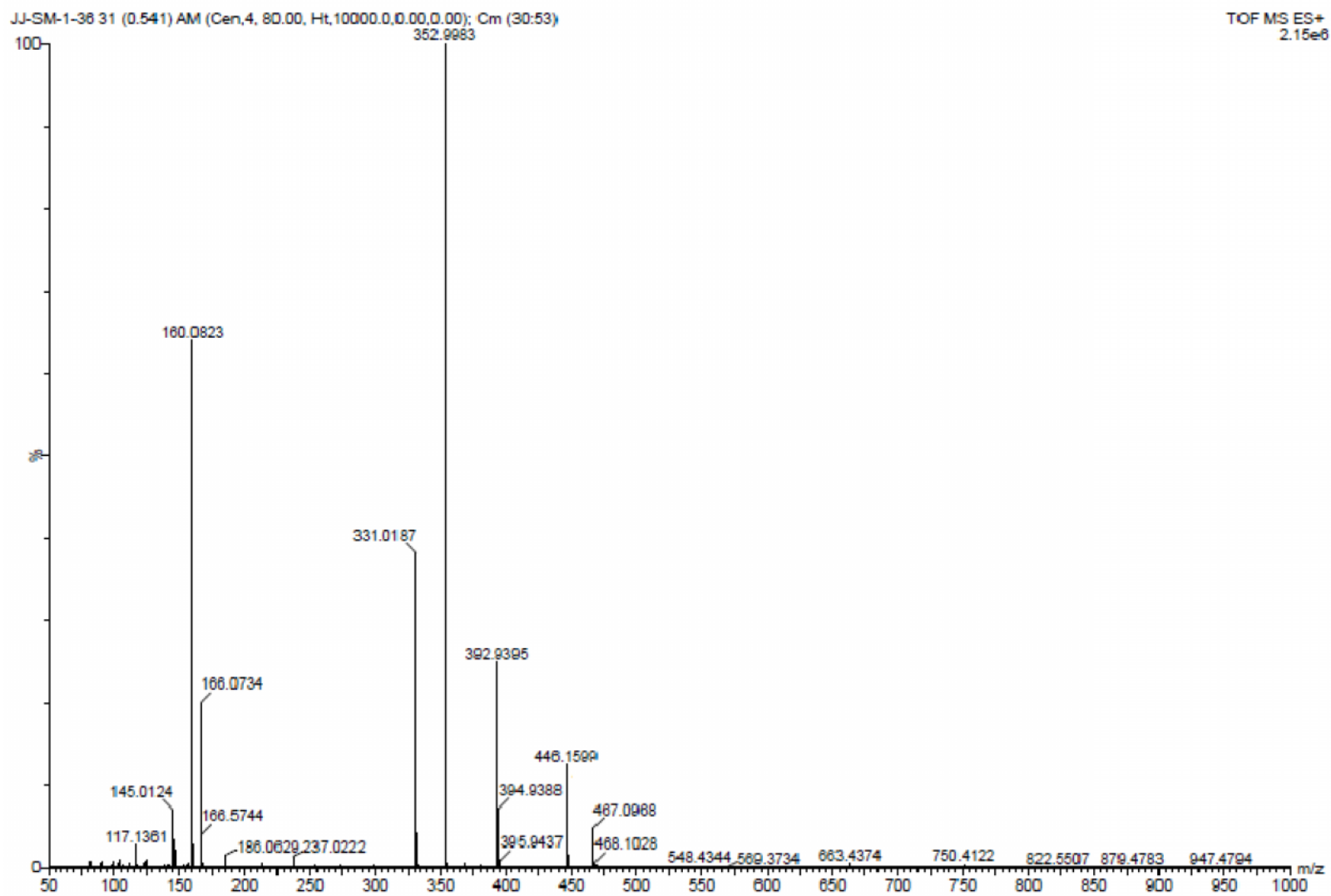
Figure 2.19 ESI mass spectra of complex (9)

2.4 References

[1]   S. Chabereck, A.E. Martell, Organic Sequestering Agents, Wiley, New York, 1959

[2]   A. E. Martell, M. Calvin, Chemistry of the Metal Chelate Compounds, Prentice Hall,   Englewood Cliffs, 1959

[3]   C.W. Tang, S.A. Van Slyke, Appl. Phys. Lett. 51 (1987) 913-915.

[4]   R.E. Bambury, Burger's Medicinal Chemistry, Part II, John Wiley, New York, 1979

[5]   R. Munteanu, K. Suntharalingam, Dalton Trans. 44 (2015) 13796-13808.

[6]   N. Shahabadi, S. Kashanian, F. Darabi, Eur. J. Med. Chem. 45 (2010) 4239-4245.

[7]   F. P. Dwyer, N.S. Gill, E.C. Gyarfas, F. Lions, J. Am. Chem. Soc. 74 (1952) 4188- 4193.

[8]   F.P. Dwyer, E.C. Gyarfas, W.P. Rogers, J.H. Koch, Nature 170 (1952) 190-191.

[9]   S. Tardito, A. Barilli, I. Bassanetti, M. Tegoni, O. Bussolati, R. Franchi-Gazzola, C. Mucchino, L. Marchio, J. Med. Chem. 55 (2012) 10448-10459.

[10]   P.C. Bruijnincx, P.J. Sadler, Curr. Opin. Chem. Biol. 12 (2008) 197-206.

[11]   T.W. Hambley, Dalton Trans. (2007) 4929-4937.

[12]   K.L. Haas, K.J. Franz, Chem. Rev. 109 (2009) 4921-4960.

[13]   E. Meggers, Chem. Commun. (2009) 1001-1010.

[14]   J.A. *S*chwartz, E.K. Lium, S.J. Silverstein, J. Virol. 75 (2001) 4117-4128.

[15]   E.L. Chang, C. Simmers, D.A. Knigh, Pharmaceuticals, 3 (2010) 1711-1728.

[16]   M. D. Hall, T.W. Failes, N. Yamamoto, T.W. Hambley, Dalton Trans. (2007) 3983- 3990.

[17]   F. Dimiza, A.N. Papadopoulos, V. Tangoulis, V. Psycharis, C.P. Raptopoulou, D. P. Kessissoglou, G. Psomas, Dalton Trans. 39 (2010) 4517-4528.

[18]   F. Dimiza, A.N. Papadopoulos, V. Tangoulis, V. Psycharis, C.P. Raptopoulou, D .P. Kessissoglou. J. Inorg. Biochem. 107 (2012) 54-56.

[19]   S. Tsiliou, L-A Kefala, F. Perdih, I. Turel, D.P. Kessissoglou, G. Psoma. Eur. J. Med. Chem. 48 (2012) 132-142.

[20]   S. Adewuyi, K.T. Kareem, A.O. Atayese, S.A. Amolegbe, C.A. Akinremi, Int J Biol Macromol. 48 (2011) 301-303.

[22]   M. Patel, M. Chhasatia, B. Bhatt, Med. Chem. Res. 20 (2011) 220-230.

[23]   J. F. Adediji, E.T. Olayinka, M.A. Adebayo, O. Babatunde, Int. J. Phys. Sci. 4 (2009) 529-534.

[24]   P.A. Ajibade, G.A. Kolawole. Synth. React. Inorg. Me. 40 (2010) 273-278.

[25]   P. Sathyadevi, P. Krishnamoorthy, M. Alagesan, K. Thanigaimani, P.T. Muthiah, N. Dharmaraj, Polyhedron. 31 (2012) 294-306.

[26]   S. Shreaz, R.A. Sheikh, R. Bhatia, K. Neelofar, S. Imran, A.A. Hashmi, N. Manzoor, S.F. Basir, L.A. Khan, BioMetals. 24 (2011) 923-933.

[27]   E. Khatiwora, K. Mundhe, N.R. Deshpande, R.V. Kashalkar, Der. Pharma. Chemica. 4 (2012) 1264-1269.

[28]   I. Ott, K. Schmidt, B. Kircher, P Schumacher, T. Wiglenda, R. Gust, J. Med. Chem. (2005) 622-629.

[29]   L. Randaccio, S. Geremia, N. Demitri, J. Wuerges, Molecules, 15 (2010) 228-3259.

[30]   A. Petrus, T.J. Fairchild, R.P. Doyle, Angew Chem. Int. Ed Engl. 48 (2009) 1022- 1028.

[31]   F. Zobi, O. Blacque, R.A. Jacobs, M.C. Schaub, A.Y. Bogdanova, Dalton Trans. 41 (2012) 370-378.

[32]   P. Ruiz-Sanchez, C. Koenig, S. Ferrari, R. Alberto, J. Biol. Inorg. Chem. 16 (2011) 33-44.

[34]   I. Ott, B. Kircher, C.P. Bagowski, D.H. Vlecken, E.B. Ott, J. Will, K. Bensdorf, W.S. Sheldrick, R. Gust, Angew Chem. Int. Ed. Engl. 48 (2009) 1160-1163.

[35]   I. Ott, T. Koch, H. Shorafa, Z. Bai, D. Poeckel, D. Steinhilber, R. Gust, Org. Biomol. Chem. 3 (2005) 2282-2286.

[36]   G. Rubner, K. Bensdorf, A. Wellner, B. Kircher, S. Bergemann, I. Ott, R. Gust, J. Med. Chem. 53 (2010) 6889-6898.

[37]   T.L. Deng, Y.W. Chen, N. Belzile, Anal. Chim. Acta, 432 (2001) 293-302.

[38]   G. Giraudi, C. Baggiani, C. Giovannoli, C. Marletto, A. Vanni, Anal. Chim. Acta. (999) 225-233.

[39]   S. N. Willie, H. Tekgul, R. E. Sturgeon, Talanta, 47 (1998) 439-445.

[40]   B. Paull, E. Twohill, W. Bashir. J. Chromatogr. A. 877 (2000) 123-132.

[41]   S. Tsakovski, K. Benkhedda, E. Ivanova, F.C. Adams. Anal. Chim. Acta 453 (2002) 143-154.

[42]   Y. P. Kovtun, Y.O. Prostota, A.I. Tolmachev, Dyes Pigment, 58 (2003) 83-91.

[43]   D.V. Nicolau, Curr. Appl. Phys. 4 (2004) 312-315.

[44]   Y.K. Han, S.U. Lee, Chem. Phys. Lett. 366 (2002) 9-16.

[45]   A. Burger. Medical Chemistry, 3rd Edn, p. 635, Wiley-Interscience, London (1970).

[46]   G. P. Cicileo, B.M. Rosales, F.E. Varela, J.R. Vilche, Corrosion Sci. 40 (1998) 1915-1926.

[47]   C. W. Tang, S.A. Van Slyke, Appl. Phys. Lett. 51 (1987) 913-915.

[48]   A. Mishra, P.K. Nayak, N. Periasamy, Tetrahedron Lett. 45 (2004) 6265-6268.

[49]   M.S. Xu, J.B. Xu, E.Z. Luo, Z. Xie. Chem. Phys. Lett. 374 (2003) 656-660.

[50]   L .M. Leung, W.Y. Lo, S.K. So, K. M. Lee, W. K. Choi, J. Am. Chem. Soc. 122 (2000) 5640-5641.

[51]   J.A. Cowan. In: Biological Inorganic Chemistry: Structure and Reactivity. I. Bertini, H.B. Gray, E.I. Stiefel, J.S. Valentine, editors. University Science Books; C. A. Sausalito (2007) 175

[52]   K. Li, Y. Li, D. Zhou, Y. Fan, H. Guo, T. Ma, J. Wen, D. Liu, L. Zhao, Bioorg. Med. Chem. 24 (2016) 1889-1897.

[53]   R. A. Muna, Al-Mandhary, P. J. Steel, Inorganica Chim. Acta 351 (2003) 7-11.

[54]   A. M. Trzeciak, H. Bartosz-Bechowski, Z. Ciunik, K. Niesyty, J.J. Ziokowski, Can.   J. Chem. 79 (2001) 752-759.

[55]   A. Bondi, J. Phys. Chem. 68 (1964) 441-451.

3.1 Introduction

The synthesis and biological investigation of inorganic complexes is an interesting developing area of bioinorganic chemistry [1–5]. In metal complexes, the central metal ion attached to the surrounding array of anions (ligands) has an important role in the development of anticancer metallodrug.

The interest in field of new transition metal based compounds are growing continuously after an incredible discovery of cisplatin [6] and lead to the synthesis and biological evaluation of palladium based heteroleptic derivatives containing oxo or chelating ligands. The palladium (II) complexes as nonplatinum metal complexes have drawn its attention of the recent researchers because of its significant biological activity as well as better anticancer properties with less side effects along with higher lipophilicity or solubility compared to cisplatin [7–10].

Generally Complexes of palladium with heterocyclic ligands are known to be potent anticancer agent [11]. Some palladium complexes derived from heterocyclic aromatic N/O-containing ligands e.g. derivatives of pyrazole, pyridine, quinoline, 1, 10-phenanthroline and hydroxyquinoline have shown highly proficient antitumor properties [12, 13]. Out of the many of the hydroxyquinoline ligands, 8-hydroxyquinoline is explored as the most interesting and efficient bidentate chelating ligand due to its multifunctional properties such as diverse bioactivities and therapeutic potentials [14].

Recently, various ligands bearing high flexibility have been designed and used to acquire non-rigid stereochemistries which could not be accessed by using lesser flexible ligands [15]. Various spacer groups like alkyl, ether and thioether are mostly bridged between two donor sites to establish this flexibility of the ligands, which allow the existence of variety of conformations of ligand [16].

Normally alkyl chains were widely employed for linking two monomer units of nitrogen heterocyclic ligands directly or via donor sites [17]. More recently, a large range of bridging ligands are reported in which a different spacer group propylene has been used to associate two pyridines [18] pyrazoles [19] and other heterocycles [20].

Covalently linked extra donor sites allows chelation at each of the metal centers which increase the stability of the resulting complexes due to multiple coordination. One of the well known subunit of this type of ligand is 2, 2 -bipyridine, which is one of the best known ligand among the bridged and N-heterocyclic systems with limited flexibility condition 2,2'-bipyridine is perhaps the most widely used chelating ligands [21-23].
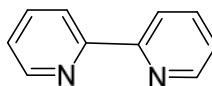
Figure 3.1 2,2'-bipyridine

Complexes of this ligand have been studied extensively for the photocatalytic activity e.g., tris(2,2 -bipyridine)iron(II) ($Fe(bpy)_3{}^{2+}$) and $Ru(bpy)_3{}^{2+}$ complexes represents an important class of compounds that possess a rich range of photocatalytic properties [24-25].
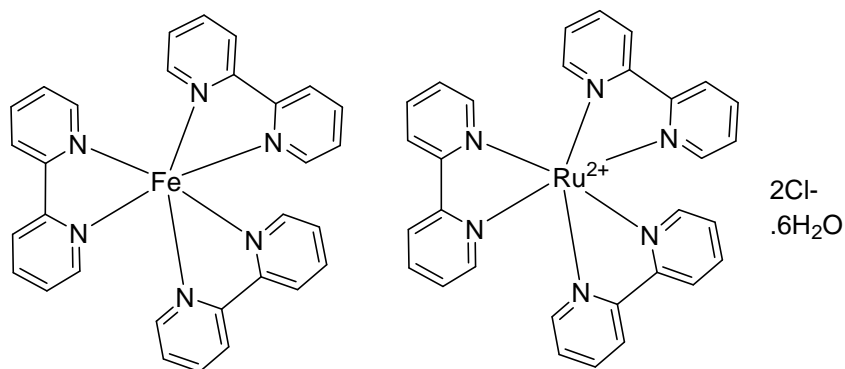
Figure 3.2 2,2'-bipyridine complexes with Fe^{2+} and Ru^{2+} showing photocatalytic property

Among the other ligands of this category used for coordination studies of bispyrazole derivatives have also been undertaken. The ligands of this type employed are both directly linked pyrazoles and pyrazoles linked via an alkyl group. The chemistry of linked pyridine ligands have also been studied extensively among which tripyridine is significant. Among the class of flexible ligands with bridged heterocyclic ligands the chemistry of quinoline has received limited attention [26]. This type of ligands has recently been well appraised [27]. Only few examples on linkage N-O donor chelating

subunits are described previously, however, N-O donor chelating ligands like 8-hydroxyquinoline were extensively used in coordination chemistry as ligands since very long time [28].
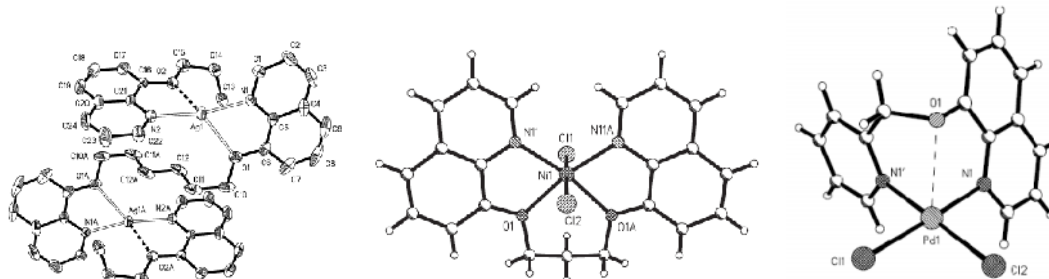
Figure 3.3 Ag, Ni and Cu complexes of bridged 8-hydroxyquinoline ligands

Synthesis of inorganic nanomaterials have drawn considerable attention in material science and nanotechnology over the last few decades owing to their distinctive properties as well as their utility in a number of fields for instance catalysis, optoelectronics, microelectronics, magnetic objects and many more [29-32].

The properties of inorganic nano materials such as catalytic activity and selectivity, thermodynamic, chemical and electrical properties mostly depend on the size of the particles and are quite dissimilar from the bulk material as a result of huge surface area and lesser volume of the nano particles [33]. Consequently, development of synthetic routes resulting in controlled particle size, highly dispersed and finely distributed morphology is very important.

Palladium oxide (PdO) is a significant metal oxide of Platinum group metals and the only well characterized oxide of palladium. It was usually used as catalysts for catalytic hydrogenation in organic synthesis. In recent years, the Palladium oxide (PdO) in its modified form was mainly used as catalysts in catalytic combustion of natural gases and liquid-phase oxidation of alcohols in presence of   oxygen [34-38].

Various traditional methods have been explored for the synthesis of nanosized PdO including heat decomposition [39], oil-bath heating [40], Microwave irradiation [41] and biosynthesis methods [42]. The synthesis of PdO was mostly done by heat decomposition

of $Pd(NO_3)_2$ which required a prolonged heating at higher temperature, during oil-bath heating considerably agglomerated particles were produced while the microwave method needs specific chemicals. The biosynthetic route may cause difficulty during purification and could manipulate the properties of the target nano materials [43]. However, so far there were very few synthetic routes reported for size-controlled preparation of PdO nanoparticles. Although some of the synthetic methods are available for the preparation of PdO nanoparticles some of which are discussed above, yet there is necessity for development of more a convenient and versatile technique for the synthesis of nanoparticles of desired sizes.

Currently, the synthesis of nanostructured material via sol gel method is attracting great interest because of the obvious benefits, such as economics, energy efficiency, and environmental friendliness [44-47]. This is a widely accepted method for the development of nanostructures like nanorods, nanowires and nanobelts as a consequence of the simplicity, easy handling process as well as ability of controlling particle size. This method can also control the structure of the crystal crystal as well as morphology of the particle by means of varying different parameters such as electronic environment of the precursor, pH, concentration and processing temperature [47-49].

Besides these parameters there are some other factors like nature of the ligands, coordination number of the central metal atom as well as rate of hydrolysis which also control the size of nano particles and their morphology [50, 51]. In the field of material chemistry, so far there is no report on synthesis of Palladium oxide using sol gel technique.

Palladium(II) complexes have been widely explored due to their remarkable structural variations and coordination geometries, which makes them prospective precursors for sol–gel method. Although, for the synthesis of nano particles of various metal oxides sol–gel method has been widely used however, the potential of this method for the preparation of nanosized palladium oxide has not been efficiently studied.

Consequently, in this chapter we have worked on the synthesis, characterization and the biological application of palladium complexes with bis(quinolinum) ligands in which

ligands contain two quinoline-oxo subunits linked by alkyl chains. One of the Pd derivatives from the above complexes was used as precursor for the synthesis of palldium oxide nanostructure using sol–gel method. It is worthy to mention that the preparation of stable palladium oxide (PdO) nano particles using sol–gel method, from bis(quinolinum) modified palladium complexes as precursors, is being reported here for the very first time to the best of our knowledge.

3.2 Experimental

3.2.1 General procedure and materials

Analytical grade 8-hydroxyquinoline (99%) was procured from Sigma-Aldrich and were used as received. Palladium (II) chloride was obtained from Thermo-fisher Scientific (India). Analytical grade solvents purchased from Rankem, India used in the experimental work and were purified by standard methods prior to use [52]. The preparation of the complexes (1-4) was carried out in anhydrous conditions under nitrogen. Ligands were synthesized using previously reported methods [53]. Palladium was estimated as PdO and nitrogen was estimated using Kjeldahl's method [52]. IR spectra [4,000–400 cm-1] were recorded using dry KBr pellets on a PerkinElmer Spectrum Version 10.4.00, FT-IR spectrometer. NMR [^{1}H and ^{13}C{^{1}H}] data were collected on JEOL FX 300 FT-NMR spectrometer in CDCl$_3$ or DMSO-d$_6$ solution at 400.4 MHz and 75.45 MHz frequencies for ^{1}H and ^{13}C{^{1}H} NMR spectra, respectively. ESI-mass spectra of the complexes were obtained from Water Xevo G2S Q-TOF with Ultra Performance Liquid Chromatography system, model UPLC-class using methanol as solvent. Thermogravimetric analyses (TGA) of palladium complexes were carried out on Perkin Elmer Pyris. The measurements were done under flowing nitrogen environment at a heating rate of 10°C/min from 30 to 800 °C. The XRD pattern of the samples were performed on Panalytical X'Pert PRO MPD diffractometer (model 3040). X-ray of wavelength 0.154 nm were generated using a sealed tube and the (Cu K-a). SEM and EDX were performed using powder samples on Carl-Zeiss (30 keV) make and model EVO. TEM was carried out on TECHNAI G^{2} 20 (FEI) North America, and Bruker, Germany. For TEM analysis particles of the sample were dispersed in the methanol and a drop of this dispersion was placed on the copper grid coated by carbon. This copper grid was further allowed to dry overnight before the TEM analysis. Raman spectra were

performed using STR-500CONFOCAL MICRO RAMAN SPECTROMETER (Raman system, USA) having excitation laser of k = 532 nm. Raman spectra were recorded in the range 200–1500 cm^{-1}. Absorption spectra of all the samples were obtained using LAMBDA 750 (Perkin Elmer) UV-Vis NIR spectrophotometer of wavelength range 400 to 800-nm. The C, H, N analyses were carried out using Thermo scientific Flash 2000.

3.2.2 Synthesis of ligands

3.2.2.1 Synthesis of 8-methoxyquinoline (MOQ), 1,3-bis(quinolin-8-yloxy)propane (PMOQ) and 8-(2-Pyridylmethoxy)quinoline (BQOP)

Synthesis and characterization of ligands 8-methoxyquinoline (MOQ), 1,3-bis(quinolin-8-yloxy)propane (PMOQ) and 8-(2-Pyridylmethoxy)quinoline (BQOP) were already discussed in the experimental section of previous chapter.

3.2.2.2 Synthesis of 1,6-bis(quinolin-8-yloxy)hexane (BQOH)

Tetracoordinating ligand 1, 6-bis(quinolin-8-yloxy)hexane (BQOH) was synthesized from 8-Hydroxyquinoline (2 mmol), 1,3-dibromopropane (1 mmol) and potassium carbonate (10 mmol) in dry acetone. The reaction mixture was refluxed with constant stirring for 12 hr on a hot plate magnetic stirrer and cooled. The resulting white solid was recrystallized from ethyl acetate/pet ether mixture. This ligand was characterized by proton NMR and single crystal X-ray analysis.
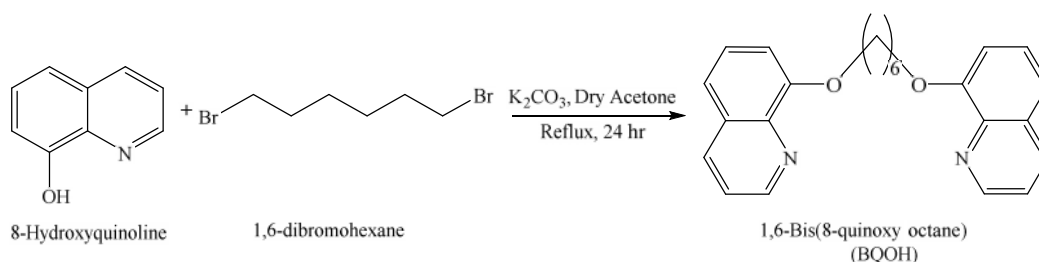
Scheme 3.1 Synthesis of 1,6-bis(quinolin-8-yloxy)hexane

The synthetic and analytical data of ligand (BQOH) are summarized below:

M.P.- 110 ^{o}C, Yield: 58%. Anal. (%) obs. (calc.) for $C_{24}H_{24}N_2O_2$ (372.18): C, 77.34 (77.39); H, 6.47 (6.50); N, 7.50 (7.52) %; ^{1}H NMR (CDCl$_3$ 400 MHz) : 8.43 (dd, 2H, -CH=N); 8.09 (dd, 2H, -CH=C-O); 7.40 (m, 6H, Ar proton); 7.05 (dd, 2H, -CH); 4.25 (t,

4H, -OCH$_2$); 1.65 (quintet, 4H, -CH$_2$-CH$_2$-CH$_2$). ^{13}C NMR (CDCl$_3$, 400.4 MHz): 154.9 (C-8); 149.4 (C-2); 140.5 (C-10), 135.9, 68.9 (C-11), 29.0 (C-12), 26.0 (C-13), 129.5, 126.7, 121.5, 1119.4, 108.7 (Ar. Carbon).

Crystal and molecular structure of 1, 6-bis(quinolin-8-yloxy)hexane, C$_{24}$H$_{24}$N$_2$O$_2$ (BQOH)

Transparent colorless good quality crystals of ligand (BQOH) were obtained from recrystallisation with isopropanol. A block crystal of C$_{24}$H$_{24}$N$_2$O$_2$ was mounted on glass fibres. X-Ray Crystallography data were collected on a 150 K on Bruker APEX-II CCD fitted with graphite-monochromated Mo-K radiation so that $_{max}$ = 29.01^o. Data collection and cell refinement gave cell constants corresponding to monoclinic cells whose dimensions and other experimental parameters are given in Table 3.1. The structures were resolved by direct methods and refinement was done on F^2 using data which had been corrected for absorption effects with an empirical procedure, with non-hydrogen atoms modeled with anisotropic displacement parameters with hydrogen atoms in their calculated positions. Molecular structure was drawn using ORTEP.

Table 3.1 Crystallographic data, data collection and structure refinement parameters for C$_{24}$H$_{24}$N$_2$O$_2$

Compound	Ligand (BQOH)
Empirical formula	C$_{24}$H$_{24}$N$_2$O$_2$
Formula weight	372.45
Temperature	100 K
Wavelength	0.71073 A
Crystal system, space group	Monoclinic, P 2(1)/n
Unit cell dimensions	a = 14.816(6)Å = 90
	7.573(3)Å = 90.797(5)
	17.874(8) Å = 90

Volume	2005.3(14)$\mathring{A}^3$
Z, Calculated density	4, 1.234 g cm^{-3}
Absorption coefficient	0.079 mm-1
F(000)	792
Crystal size	0.32 x 0.22 x 0.18 mm3
Theta range for data collection	1.77 to 29.010°
Limiting indices	-19<=h<=19, -10<=k<=10, -24<=l<=24
Reflections collected / unique	5238/2179 [R(int) = 0.1608]
Completeness to = 28.73	98.4%
Absorption correction	Multi-scan
Max. and min. transmission	0.9860 and 0.9752
Refinement method	Full-matrix least-squares on F2
Data / restraints / parameters	3800 / 0 / 190
Goodness-of-fit on F2	0.971
Final R indices [I>2 (I)]	R1 = 0.0549, wR2 = 0.1427
R indices (all data)	R1 = 0.1402, wR2 = 0.1848
Absolute structure parameter	0.83(4)
Largest diff. peak and hole	0.698d -0.452e.$\mathring{A}$-3

3.2.3   Synthesis of palladium (II) complexes

3.2.3.1 Synthesis of palladium complexes of 8-methoxyquinoline [(MOQ)$_2$ PdCl$_2$]

To a solution of 8-methoxyquinoline ligand (MOQ) (0.105g, 0.66 mmol in ~15 ml of methanol), PdCl$_2$ (0.058g, 0.33 mmol) was added. The mixture was stirred for 12 hours at atmospheric temperature. Resulting mixture was filtered using whatman quality filter paper yellow colored solid (2.43 g) obtained was re-crystallization from hot methanol and dried under reduced pressure.
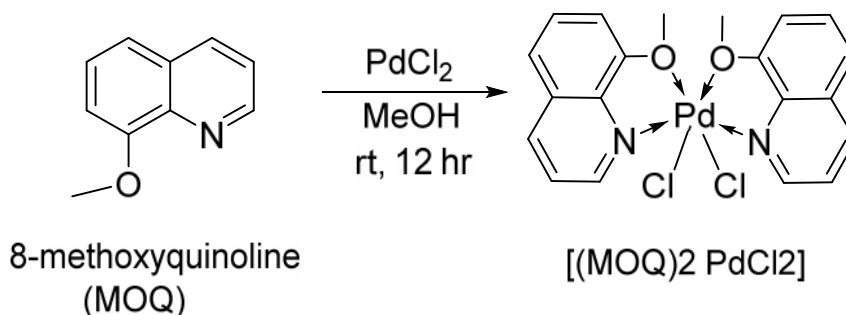
Scheme 3.2 Synthesis of palladium complexes of 8-methoxyquinoline

[(MOQ)$_2$PdCl$_2$): [Yield: 4.72 g, 58%], mp. 293°C, Elemental analysis (%) obs. (calc.) : C: 48.45 (48.46), H: 3.62 (3.66), N: 5.63 (5.65); M.W.: 501.21 (493.98), FT-IR, , cm–1: 2924 (C-H of O-CH$_3$); 1616 (C=N); 1510 (C=Car, asym); 1467 (C=Car, sym); 1372 (C-N-alkyl chain); 1270 (C-O-alkyl chain); 1052 (C-Oar), 537 (Pd-O), 420 (Pd-N), ^{1}H NMR (300.13 MHz, DMSO-d$_6$, at 25°C, ppm): 8.21 (d, H, H^2); 8.99 (d, H, H^7); 7.50-7.08 (m, 3H, other aromatic protons); 4.10 (t, 2H, H^{11})

3.2.3.2 Synthesis of palladium complexes of 8-(2-Pyridylmethoxy)quinoline [(PMOQ) PdCl$_2$]

PdCl$_2$ (0.32g, 1.35 mmol) was added to the MeCN solution of ligand 8-(2-Pyridylmethoxy)quinoline (0.24g, 1.35mmol in ~20 ml of MeCN) in 1:1 molar ratio and stirred for 5 minutes at atmospheric temperature. The resulting mixture was filtered and washed with dichloromethane and dried under vacuum to give dark orange colored solid, which was used as the source material for synthesizing Pd@PdO. Characterization of this sort of precursor has been reported in the literature [53].

[(PMOQ)PdCl$_2$]: [Yield: 0.43g, 76 %], mp. 231.4°C, analyses (%) obs. (calc.) : C: 43.55 (43.56), H: 2.93 (2.92), N: 6.73 (6.77); M.W.: 402.87 (411.94); FT-IR, , cm–1: 2926 (C-H); 1553 (C=N); 1613 (C=Car, asym); 1468 (C=Car, sym); 1386 (C-O-alkyl chain); 1111(C-Oar). 575 (Pd-O), 423 (Pd-N), ^{1}H NMR (400.13 MHz, DMSO-d$_6$, at 25°C, ppm): 8.11 (d, H, H^2); 8.98 (d, H, H^7); 8.61 (d, H, H of C=N Py); 7.64-7.05 (m, 7H, other aromatic protons); 5.56 (s, 2H, H of –O-CH$_2$-).
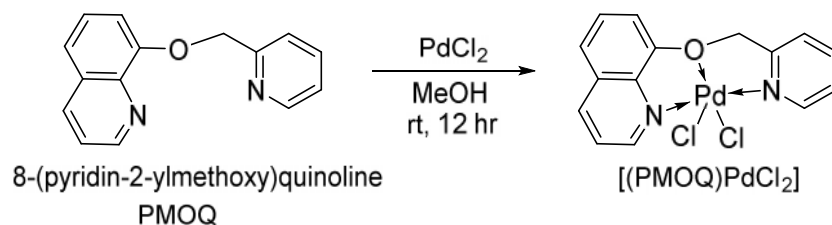
Scheme 3.3 Synthesis of palladium complexes of 8-(2-Pyridylmethoxy)quinoline

3.2.3.3 Synthesis of palladium complexes of 1, 3-bis (quinolin-8-yloxy)propane [(BQOP) PdCl₂]

An amount of 0.038g (0.21mmol) of PdCl₂ was added to the methanolic solution of ligand 1,3-bis(quinol-8-yloxy)propane (0.072g, 0.21mmol in ~20 ml of methanol) and stirred at atmospheric temperature overnight. The resulting yellow colored solid was filtered, washed with dichloromethane and dried under vacuum to give dark yellow colored solid.

Yield: 53%; mp. 274°C.
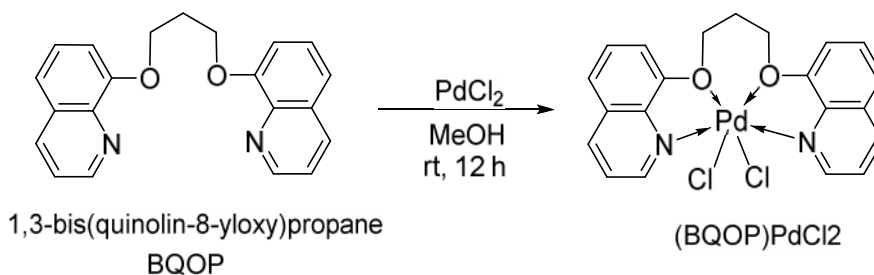
Scheme 3.4 Synthesis of palladium complexes of 1, 3-bis(quinolin-8-yloxy)propane

[(BQOP)PdCl₂]: [Yield: 4.72 g, 98.80 %], analyses (%) obs. (calc.) : C: 49.60 (49.68), H: 3.55 (3.57), N: 5.50 (5.52); M.W.: 498.87 (505.98); FT-IR, , cm–1: 2923 (C-H of O-CH₃); 1579 (C=N); 1511 (C=Car, asym); 1459 (C=Car, sym); 1378 (C-N-alkyl chain); 1267 (C-O-alkyl chain); 1051 (C-Oar), 535 (Pd-O), 423 (Pd-N), ^{1}H NMR (300.13 MHz, CDCl₃, at 25°C, ppm): 8.14 (d, H, H^2); 8.60 (d, H, H^7); 7.52-7.24 (m, 3H, other aromatic protons); 4.81 (t, 2H, H^{11}), 3.02 (m, 2H, H^{12}).

3.2.3.4 Synthesis of palladium complexes of 1,3-bis(quinolin-8-yloxy)hexane [(BQOH)PdCl₂]

A weighted amount of palladium dichloride (0.035g, 0.19 mmol) dissolved in methanol (~15 ml) to this mixture ligand (BQOH) 0.073 g (0.19 mmol) was added and stirred at room temperature. Stirring was continued for 12 hours at room temperature then bright yellow colored crystalline solid obtained was filtered, recrystallized with methanol and dried under reduced pressure.

[(BQOH)PdCl₂]: [Yield: 4.72 g, 58%], mp. 293°C, analyses (%) obs. (calc.) : C: 52.39 (52.43), H: 4.45 (4.40), N: 5.10 (5.10); M.W.: 540.42 (548.02), FT-IR, , cm–1: 2924 (C-H O-CH₃); 1568 (C=N); 1535 (C=Car,asym); 1466 (C=Car, sym); 1372 (C-N-alkyl chain); 1256 (C-O-alkyl chain); 1092 (C-Oar), 535 (Pd-O), 429 (Pd-N), ^{1}H NMR (300.13 MHz, DMSO-d₆, at 25°C,   ppm): 8.25 (d, H, H^2); 8.80 (d, H, H^7); 7.52-7.65 (m, 3H, other aromatic protons); 4.14 (t, 2H, H^{11}); 2.46 (m, 2H, H^{12}); 1.86 (m, 2H, H^{13}). ^{13}C NMR (CDCl₃, 400.4 MHz):   155.1 (C-8);   149.3 (C-2);   140.3 (C-10),   136.3,   69.0 (C-11), 29.2 (C-12), 25.9 (C-13), 129.6, 127.3, 122.2, 120.0, 110.2 (Ar. Carbon).

1,3-bis(quinolin-8-yloxy)hexane
BQOH

(BQOH) PdCl₂
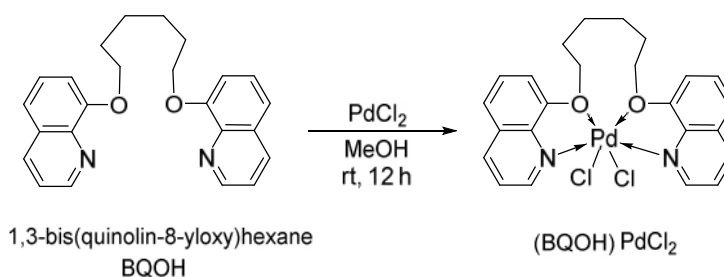
Scheme 3.5 Synthesis of [dichloro {1, 3-bis(quinolin-8-yloxy)hexane} Pd(II)]

3.2.4 Sol-gel transformation of PdCl₂ and [(PMOQ)PdCl₂] to pure palladium oxide (PdO) and Pd@PdO

[(PMOQ)PdCl₂] (0.32 g, 0.77 mmol) was dissolved in a mixture of ethanol (~ 20 ml) and THF (10 ml). Ammonia solution (2 ml) was added to this dirty yellow solution, color of mixture turned to dark yellow and instantaneously gelation occured. The reaction mixture was stirred for 24 hrs and then ~ 5 ml ammonia solution was added to it and was allowed to stir for two days to make sure hydrolysis completed. The resulting gel was

dried in a preheated oven (~100°C), dark greenish colored solid obtained was washed with deionized water several times followed by a mixture of acetone and n- hexane. This solid was sintered for 3 hrs at 600 °C resulting in dark green colored powder, which was characterized as pure Pd@PdO.

PdCl$_2$ was also hydrolyzed by the above discussed method and sintered at 600°C to yield the dark green colored powder and characterized as PdO.

3.3 Results and discussion

3.3.1 Synthesis and characterization

A systematic study of the reaction of palladium dichloride with ligands (L) in 1:1 molar ratio in MeOH have been carried out to give products of the type, [PdCl$_2$L] in quantitative yield . The general reaction scheme can be represented by the following equation:

$$PdCl_2 + L \xrightarrow[\text{Stirring}]{\text{MeOH}} [PdCl_2L]$$
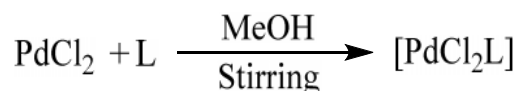
$$[\text{where, } L = C_{10}H_9NO(MOQ), C_{21}H_{18}N_2O_2(BQOP), C_{15}H_{12}Cl_2N_2O(PMOQ) \text{ and}$$
$$C_{24}H_{24}N_2O_2(BQOH)]$$

To characterize the complexes various analytical and spectral techniques were used including microanalysis at elemental level i.e. to detect the presence of Carbon, Hydrogen and Nitrogen, spectral studies NMR, IR, mass (ESI), UV-vis and TGA. All the thesized metal complexes are stable at room temperature, non-hygroscopic, partly soluble in ethanol and methanol but completely soluble in DMSO.

3.3.2   ESI mass spectra

The ESI mass spectral studies of all the complexes [**1-4**] indicate their monomeric nature. The distinctive fragmentation peaks for these compounds are listed in experimental section. Some peaks appeared at higher m/e as compared to the molecular ion peak can be assigned to reassociation of ions after fragmentation.

3.3.3 IR Spectra

The characteristic IR bands along with their assignments are shown in experimental section. These bands were assigned by evaluating IR spectra of metal complexes with IR spectra of their corresponding ligands. IR spectra of ligands exhibit strong bands near 2990-3050 cm^{-1}, attributing the symmetric stretching of O-CH$_2$ group vibrations. In the spectra of the ligands, the appearance of (C=N) stretching vibration at 1640–1665 cm^{-1} observed to be moved to region of lower-frequency (1568–1616 cm^{-1}) in the spectra of corresponding palladium complexes, signifying formation of coordinate bond of the nitrogen atom with the palladium, the appearance of new bands in the region (420–429 cm^{-1}) assigned to v(Pd–N further support coordination of ligand to the metal [54]. The band appeared in the region 535-537 cm^{-1} suggesting (Pd-O) vibrations, support the coordination of oxygen atom to the metal atom [55]. The band appeared in the region of 1256-1270 cm^{-1} of medium intensity in IR spectra of all the complexes is attributed to (C–O) of the alkoxy chain. The study and comparison of infrared spectra of ligands and their metal complexes imply that all the ligands behave as dibasic ligands.

3.3.4 NMR spectra

The ^{1}H-NMR spectra of ligands and their metal complexes were performrd in CDCl$_3$ and DMSO-d$_6$. The spectral data of all these palladium complexes are summarized in experimental section and interpreted by comparing with the spectra of parent organic ligands (MOQ, PMOQ, BQOP and BQOH) with their metal complexes. These comparisons indicate that -CH=N proton of the pyridine rings and proton of the phenoxy rings in ligands shifted to downfield in the complexes, this is consistent with coordination of nitrogen and oxygen. The other protons of the ligands did not show significant differences between ligands and its metal complexes and reveal characteristic signals at the expected positions with desired multiplicity.

The ^{13}C NMR spectra of ligands and their Pd(II) complexes were recorded in CDCl$_3$ and DMSO-d$_6$, are accessible in experimental section. The ^{13}C resonance signals have been assigned according to chemical shift theory. The considerable shielding (~2–3 ppm) takes place in the position of C-O and C=N in spectra of the above complexes as

compared to ligands, indicating coordination through the oxygen and the nitrogen to metal. These NMR spectral data uphold the informations acquired from IR data. All the other signals in the ^{13}C NMR spectra, appeared in the anticipated regions.

3.3.5 UV-Visible Absorption spectra

The UV-vis spectra of all the synthesized complexes (**1-4**) were recorded against their corresponding ligands (MOQ, PMOQ, BQOP and BQOH) blank. The absorption spectra of the ligands (MOQ, PMOQ, BQOP and BQOH) and their metal complexes are shown in Figure 3.4. The obtained spectra indicated that the complexes have maximum absorbance at 305 nm and ligands have maximum absorbance at 307 nm, respectively. The ligands have minimum absorbance at the maximum absorbance of its complexes and confirm the complexation between ligands and their complexes.
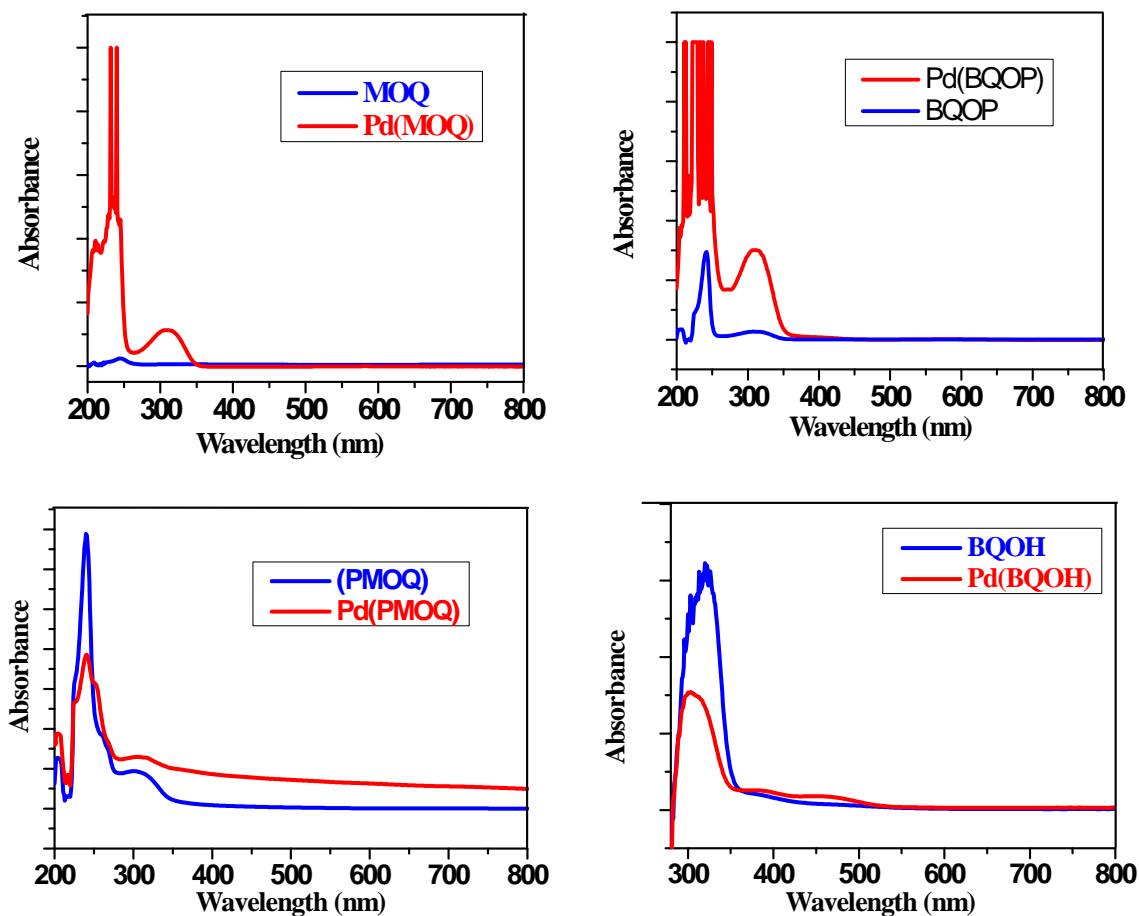
Figure 3.4 Absorption spectra of ligands and its complexes (against ligands)

Good quality Crystal could not be obtained for single crystal X-ray crystallography of all the complexes. However on ageing good quality crystals of the ligand (BQOH) were seprated out. In the absence of the single crystal structure of at least one of the complexes, it is hard to state upon the solid state structure of complexes. Nevertheless, the above studies signify the possible structures for all the synthesized palladium complexes shown in figure 3.5.

[(MOQ)2PdCl2]

[(BQOP)PdCl$_2$]

[(PMOQ)PdCl$_2$]
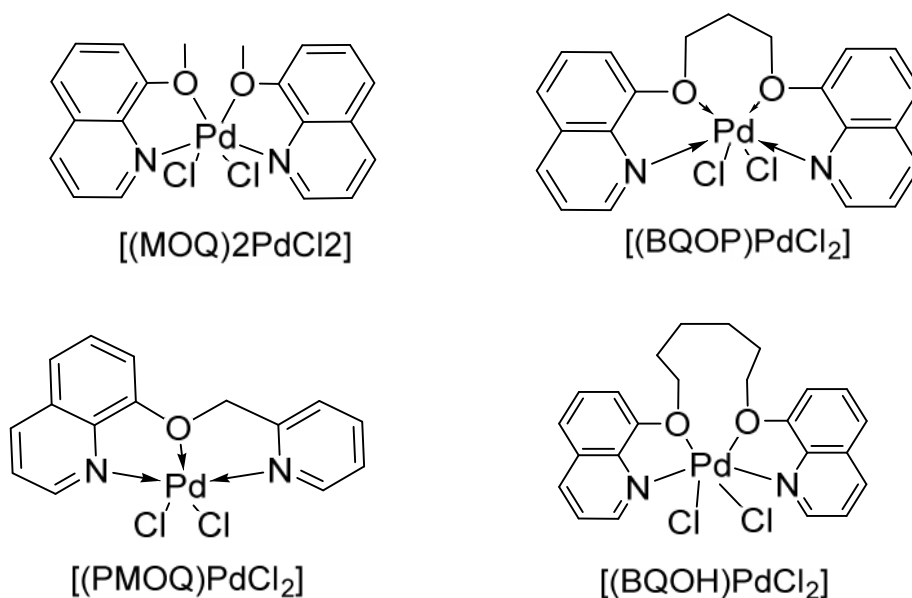
[(BQOH)PdCl$_2$]

Figure 3.5 Proposed structures of the complexes [(MOQ)$_2$PdCl$_2$], [(BQOP)PdCl$_2$], [(PMOQ)PdCl$_2$] and [(BQOH)PdCl$_2$]

3.3.6   Crystal and molecular structure of 1,6-bis(quinolin-8-yloxy)hexane (BQOH)

When the ligand C$_{24}$H$_{24}$N$_2$O$_2$ (BQOH) was recrystallized in isopropanol, crystals suitable for x-ray analysis were obtained. Single crystal X-ray diffraction study has been carried out for the ligand (L4) and the selected bond lengths and angles are summarized in Table 3.2. The ORTEP plot is displayed in Fig 3.6. The crystal system of C$_{24}$H$_{24}$N$_2$O$_2$ is monoclinic with space group P$_2$(1)/n. The molecular structure of C$_{24}$H$_{24}$N$_2$O$_2$ reveals presence of one formula units in the asymmetric cell. The crystal structure indicates that the ligand shows Z conformation and mirror plane symmetry. The structure of this molecule is approximately planar and demonstrates that two 8-hydroxy quinoline rings

are joined together by one hexyl linkage chains through two oxygen atoms. The geometrical parameters of the aromatic rings and other atoms for ligand structure are in good accord with each other as shown in table 3.2. Most of the important bond lengths and angles of ligand crystal are very similar to those values reported in literature [56, 57].
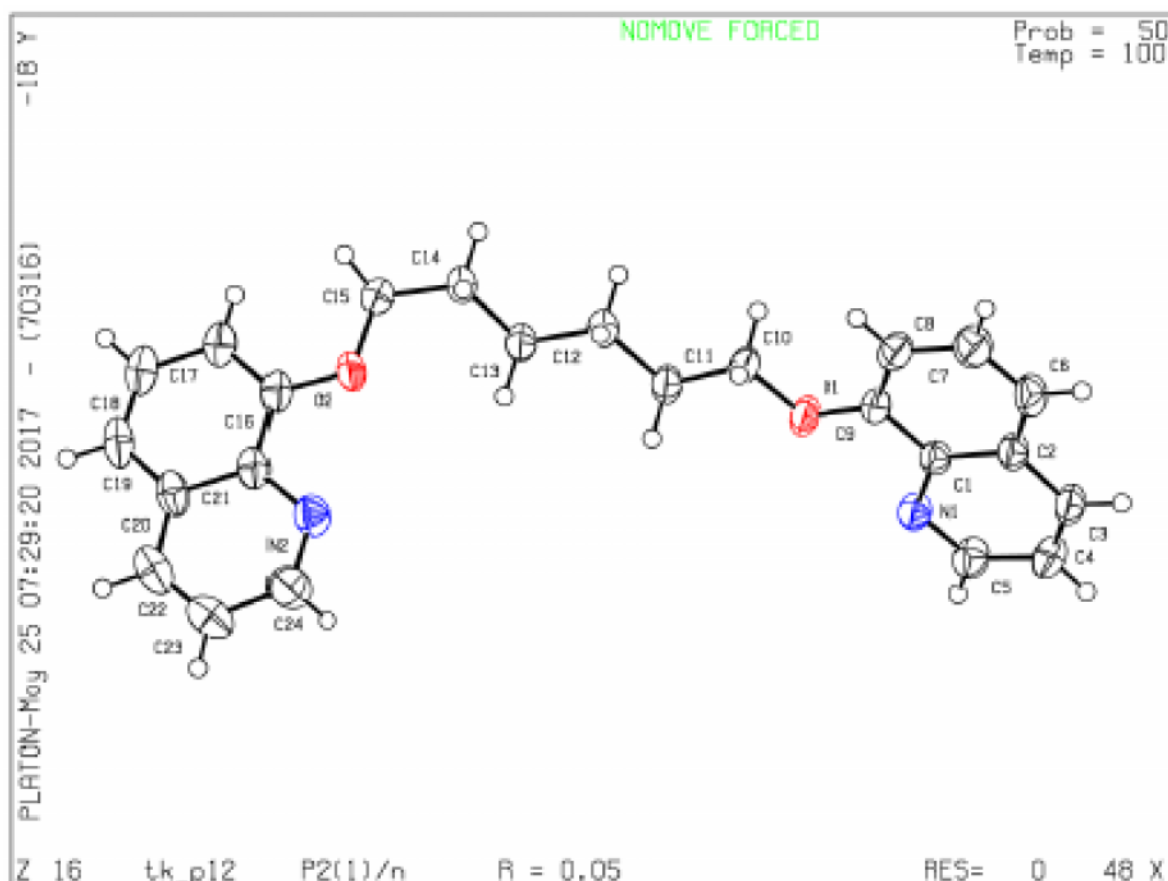
Figure 3.6 Crystal structure of ligand [1,6-bis(quinolin-8-yloxy)hexane]

Table 3.2 Important bond length and angles of ligand [1, 6-bis(quinolin-8-yloxy)hexane] (BQOH)

Bond lengths			
O(1)- C(9)	1.366(3)	O(1)- C(10)	1.442(3)
O(2)- C(16)	1.368(3)	O(2)- C(15)	1.438(3)
N(1)- C(5)	1.315(3)	N(1)- C(1)	1.374(3)
C(1)- C(2)	1.424(3)	C(1)- C(9)	1.434(3)
C(15)- C(14)	1.515(3)	C(15)- H(15A)	0.9700
C(15)- H(15B)	0.9700	C(10)- C(11)	1.519(3)
C(10)- H(10A)	0.9700	C(10)- H(10B)	0.9700
C(21)- N(2)	1.368(3)	C(21)- C(20)	1.429(3)
C(21)- C(16)	1.433(4)	C(16)- C(17)	1.370(3)
C(14)- C(13)	1.525(3)	C(14)- H(14A)	0.9700
C(14)- H(14B)	0.9700	C(11)- C(12)	1.534(3)
C(11)- H(11A)	0.9700	C(11)- H(11B)	0.9700
C(18)- C(19)	1.357(4)	C(18)- C(19)	1.357(4)
C(12)-C(13)	1.529(3)	C(18)- C(17)	1.416(3)
C(12)- H(12A)	0.9700	C(18)- H(18)	0.9300
C(12)- H(12B)	0.9700	C(19)- H(19)	0.9300
C(8)- C(9)	1.374(4)	C(17)- H(17)	0.9300
C(8)- C(7)	1.413(3)	C(6)- C(7)	1.362(4)
C(8)- H(8)	0.9300	C(6)- H(6)	0.9300
C(2)- C(6)	1.414(4)	C(22)- C(23)	1.353(4)
C(2)- C(3)	1.416(3)	C(22)- H(22)	0.9300
N(2)- C(24)	1.323(4)	C(7)- H(7)	0.9300
C(20)- C(22)	1.413(4)	C(23)- C(24)	1.408(4)
C(20)- C(19)	1.413(4)	C(23)- H(23)	0.9300
C(13)- H(13A)	0.9700	C(24)- H(24)	0.9300
C(13)- H(13B)	0.9700	C(5)- H(5)	0.9300
C(4)- C(3)	1.358(4)	C(3)- H(3)	0.9300

C(4)- C(5)	1.403(3)	C(4)- H(4)	0.9300
Bond Angles			
C(9)- O(1)- C(10)	116.29(19)	C10 C11 H11B	109.9
C(16)- O(2)- C(15)	117.36(19)	C12 C11 H11B	109.9
C(5)- N(1)- C(1)	117.0(2)	H11A C11 H11B	108.3
N(1)- C(1)- C(2)	122.5(2)	C13 C12 C11	114.5(2)
N(1)- C(1)- C(9)	118.8(2)	C13 C12 H12A	108.6
C(2)- C(1)- C(9)	118.7(2)	C11 C12 H12A	108.6
O(2)- C(15)- C(14)	107.4(2)	C13 C12 H12B	108.6
O(2)- C(15)- H(15A)	110.2	C11 C12 H12B	108.6
C(14)- C(15)- H(15A)	110.2	H12A C12 H12B	107.6
O(2)- C(15)- H(15B)	110.2	C9 C8 C7	120.4(2)
C(14)- C(15)- H(15B)	110.2	C9 C8 H8	119.8
H(15A)- C(15)- H(15B)	108.5	C7 C8 H8	119.8
O(1)- C(10)- C(11)	109.2(2)	O1 C9 C8	124.6(2)
O(1)- C(10)- H(10A)	109.8	O1 C9 C1	115.6(2)
C(11)- C(10)- H(10A)	109.8	C8 C9 C1	119.8(2)
O(1)- C(10)- H(10B)	109.8	C6 C2 C3	123.1(2)
C(11)- C(10)- H(10B)	109.8	C6 C2 C1	119.8(2)
H(10A)- C(10)- H(10B)	108.3	C3 C2 C1	117.1(2)
N(2)- C(21)- C(20)	122.5(3)	C24 N2 C21	117.1(2)
N(2)- C(21)- C(16)	118.8(2)	C22 C20 C19	124.1(2)
C(20)- C(21)- C(16)	118.7(2)	C22 C20 C21	116.8(3)
O(2)- C(16)- C(17)	124.8(2)	C19 C20 C21	119.1(3)
O(2)- C(16)- C(21)	115.0(2)	C14 C13 C12	110.6(2)
C(17)- C(16)- C(21)	120.2(2)	C14 C13 H13A	109.5
C(15)- C(14)- C(13)	114.7(2)	C12 C13 H13A	109.5
C(15)- C(14)- H(14A)	108.6	C14 C13 H13B	109.5
C(13)- C(14)- H(14A)	108.6	C12 C13 H13B	109.5

C(15)- C(14)- H(14B)	108.6	H13A C13 H13B	108.1
C(13)- C(14)- H(14B)	108.6	C6 C2 C3	123.1(2)
H(14A)- C(14)- H(14B)	107.6	C6 C2 C1	119.8(2)
C(10)- C(11)- C(12)	109.0(2)	C3 C2 C1	117.1(2)
C(10)- C(11)- H(11A)	109.9	C24 N2 C21	117.1(2)
C(12)- C(11)- H(11A)	109.9	C19 C18 H18	119.6
C(22)- C(20)- C(19)	124.1(2)	C17 C18 H18	119.6
C(22)- C(20)- C(21)	116.8(3)	C18 C19 C20	120.9(2)
C(19)- C(20)- C(21)	119.1(3)	C18 C19 H19	119.6
C(14)- C(13)- C(12)	110.6(2)	C20 C19 H19	119.6
C(14)- C(13)- H(13A)	109.5	C16 C17 C18	120.3(3)
C(12)- C(13)- H(13A)	109.5	C16 C17 H17	119.8
C(14)- C(13)- H(13B)	109.5	C18 C17 H17	119.8
C(12)- C(13)- H(13B)	109.5	C7 C6 C2	119.9(2)
H(13A)- C(13)- H(13B)	108.1	C7 C6 H6	120.0
C(3)- C(4)- C(5)	118.5(2)	C2 C6 H6	120.0
C(3)- C(4)- H(4)	120.8	C23 C22 C20	120.5(3)
C(5)- C(4)- H(4)	120.8	C23 C22 H22	119.7
C(4)- C(3)- C(2)	120.0(2)	C20 C22 H22	119.7
C(4)- C(3)- H(3)	120.0	C6 C7 C8	121.3(3)
C(2)- C(3)- H(3)	120.0	C6 C7 H7	119.3
N(1)- C(5)- C(4)	125.0(3)	C8 C7 H7	119.3
N(1)- C(5)- H(5)	117.5	C22 C23 C24	118.4(3)
C(4)- C(5)- H(5)	117.5	C22 C23 H23	120.8
C(19)- C(18)- C(17)	120.8(3)	C24 C23 H23	120.8

3.4 Sol–gel transformations of PdCl$_2$ and [PMOQPdCl$_2$] to pure palladium oxides (PdO) (a) and Pd encapsulated by PdO surface [Pd@PdO core-shell] (b) nanoparticles.

Precursors Sol–gel transformations of $PdCl_2$ and $[(PMOQ) PdCl_2]$ to pure palladium oxides (**a**) and Pd@PdO core shell (**b**), respectively have been carried out by following method:
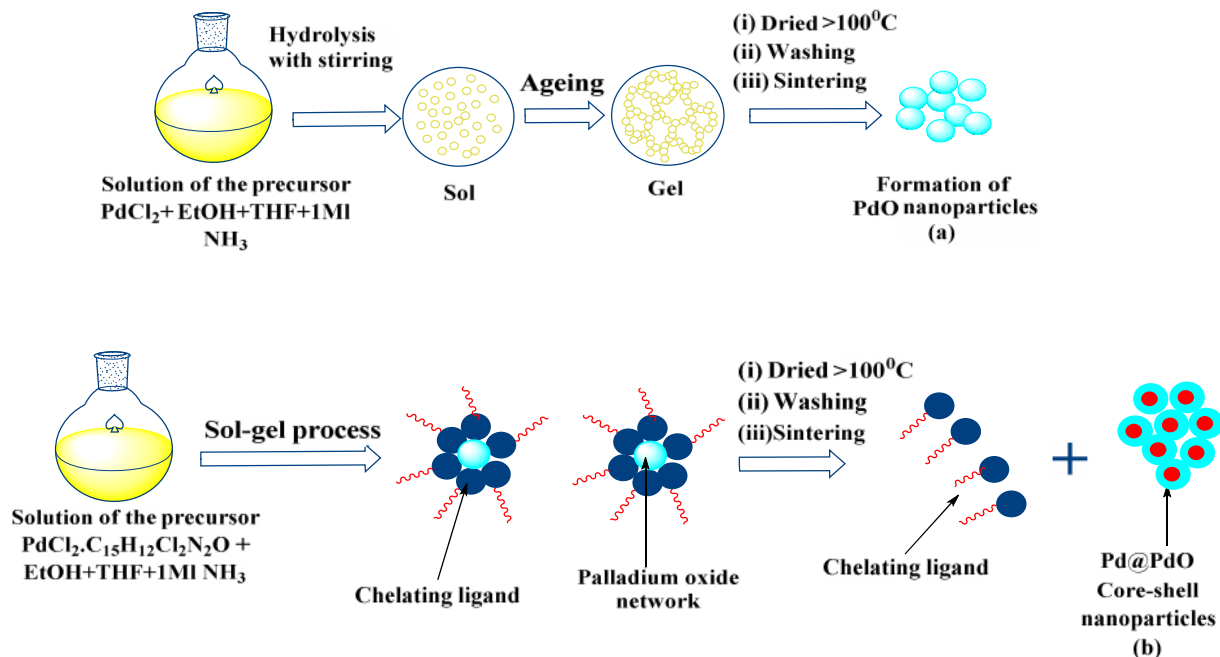
Scheme 3.6 Formation of PdO and Pd@PdO nanoparticle by sol-gel method

The composition and purity of resulting palladium oxides (**a**) and (**b**) were characterized by FT-IR and EDX spectral analysis. The crystal structure, size of crystal and phases were studied by XRD and further HRTEM confirmed the results. The morphological study of the prepared PdO and Pd@PdO nanoparticle were made by FE-SEM analysis. The XRD patterns of the samples were recorded in the range $2\theta = 20–70°$ using a step size of 0.02 Degree.

The powder X-ray diffraction patterns of synthesized palladium oxide samples (a) and (b) are shown in Fig.3.7. A comparative study of the XRD spectra of both the samples indicate the formation of PdO (tetragonal phase) for (a) and Pd@PdO (cubic and tetragonal phase for Pd and PdO, respectively) for (b). In the XRD pattern of sample (a), reflection peaks at $2\theta = 33.75, 41.80, 54.61, 60.06,$ and 60.65 belong to the pure tetragonal phase PdO obtained, indexed to the planes (100), (101), (110), (112), (103) and

(200) (JCPDS#85-0713) [58]. The XRD pattern of the sample (b), indicated both the formation of cubic (fcc) Pd and tetragonal PdO phase; reflections from the (111), (200) and (220) planes of Pd(0) and (101), (110), (112), (103) and (200) planes of PdO were observed (JCPDS # 46-1043 and 85-0713) [58]. The lattice parameters calculated were a= 3.02 Å b= 3.02 Å c= 5.31 Å for samples (**a & b**) (tetragonal) and a = b = c = 3.89 Å for Pd of Pd@PdO of sample (**b**) (cubic). The appearance of a core–shell structure comprising of a PdO shell encapsulating a Pd(0) core (shown by blue trace in Fig.3.6) suggesting that there is incomplete oxidation of Pd to PdO occured even at high temperature (600˚C). The average crystalline size of both the PdO and Pd@PdO samples {~30.1 nm (**a**), and ~33.01 nm (**b**)} were calculated taking reflections planes (101), (110), and (111), by using the Debye-Scherrer equation [59]. The full-width at half maximum (FWMH) of the spectral peaks in both the samples are sharp, which proposes crystalline nature of the samples.
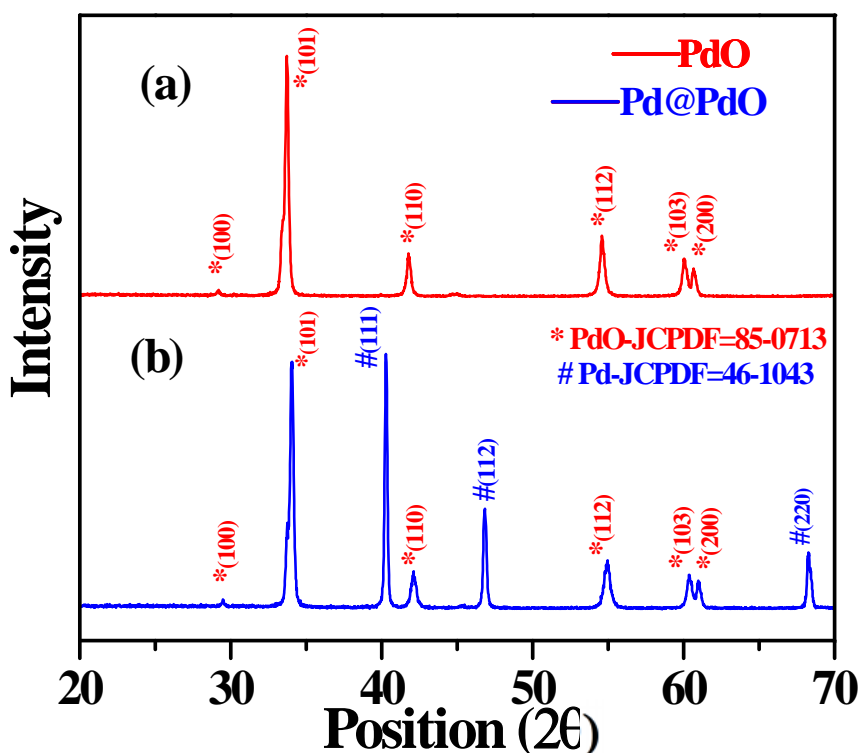
Figure 3.7 Powder XRD pattern of (a) PdO and (b) Pd@PdO formed by [PdCl$_2$] and [(PMOQ)PdCl$_2$] respectively using sol-gel technique at 600 ˚C

In the FT-IR spectra of palladium oxide samples, the absorption bands observed around at 606-608 cm^{-1} and at 661-666 cm^{-1}, appeared because of the Pd-O stretching and bending vibrations. These peaks further supported the formation of PdO in both the samples [56]. The appearance of absorption band between the region of 3430-3439 and 1631-1652 cm^{-1} point out the stretching mode and bending vibrational mode of hydroxyl group (-OH) because of the absorption of atmospheric moisture during sample handelling [60].

The surface morphology of the prepared samples were studied using scanning electron micrographs (SEM) technique, the SEM images are shown in Fig.3.9. These images suggest agglomerated granular morphologies for both the samples (**a**) and (**b**) with nano sized crystallite. SEM image shows the homogeneity of particles and the particles of good quality having approximately consistent diameter, confirming the reproducibility of the method.

In order to investigate the composition of samples, energy dispersive X-ray analysis (EDX) (Fig.3.9) of these samples were performed which signified the formation of pure PdO and Pd@PdO in desired composition.

The formation of core–shell Pd@PdO structure was established by using electron microscopy studies. Further characterization of the core–shell nano materials was carried out using transmission electron microscopy (TEM) and the selected area electron diffraction (SAED) pattern as shown in Fig.3.10 (a). The TEM images of the PdO sample (**a**) indicates formation of polygonal shaped granules of different sizes ranging from 20 to 90 nm where as the TEM image of Pd@PdO core–shell sample (**b**) shows the broad distribution of spherical type morphology with average diameter of varying from 10-100 nm with presence of nano-sized crystallites. The SAED pattern of samples (a) and (b) indicates polycrystalline nature of both the samples and this result was supported by XRD data. The SAED pattern of Pd@PdO core–shell [3.10(b)] identified the formation of both Pd and PdO phases.

The HRTEM images of (**a**) & (**b**) signify occurrence of multiple crystals signifying their polycrystalline nature (Fig. 3.11). The d-spacing measured by HRTEM and the

planes obtained by SAED patterns were corroborated with the XRD results of the samples. Thus the results obtained from integrated powder XRD and electron microscopy (HRTEM & SAED) indicated the generation of a Pd@PdO core–shell structure for sample (b) and tetragonal for (a).

The UV-visible absorption spectra of both the samples are shown in fig.3.13. It demonstrate that UV absorption data for both the samples are inadequate and unclear so the comparison with literature data is not possible. However, this data for PdO is consistent with those reported for PdO obtained from Feng Ling and col [61].

A typical full Raman spectrum for PdO and Pd@PdO samples were recorded at atmospheric temperature and are shown in fig.3.14. PdO is strongly Raman-active substance while metallic Pd is Raman inactive, and on the basis of the reported literature, it is confirmed that PdO can be identified by Raman scattering spectroscopy even without the use of any supporting factor [62].

As shown in figure 3.14, main three moderately intense Raman active modes appeared at the Raman shifts: 647 cm-1, 424 cm-1 and 275 cm-1 which were allocated to the B1g, Eg and X_8 modes respectively [63,64]. Commonly, PdO has two Raman active modes B1g and Eg which are related to the unit cell of the tetragonal phase of PdO crystal [62, 63]. The main symmetric and sharp peak centered at 647 cm^{-1} is assigned to the B_1g mode, which again confirms the formation of tetragonal PdO particles in the samples. Another Raman scattering mode at 422 cm−1 is recognized as the Eg mode, also a very sensitive indicator of the nature of PdO oxide [64].

Energy band gaps for both the samples (a) & (b) were ploted using the Tauc relation (2) [65]. h   versus (h)^2 plot shown in Figure 3.14 of the PdO samples (a) and (b) exhibit   band gaps at 1.89 and 1.43 eV respectively. The bandgap of the Pd@PdO nanoparticles is very near to the optimal bandgap (~ 1.5 eV) of absorber layer in the solar cell [66] which suggests its possible use in solar applications. According to Brus approximation the band gap of the substance is decreases with increase in the particle size [67]. Therefore, here increase in the energy band gap indicates decreased size of the particle.
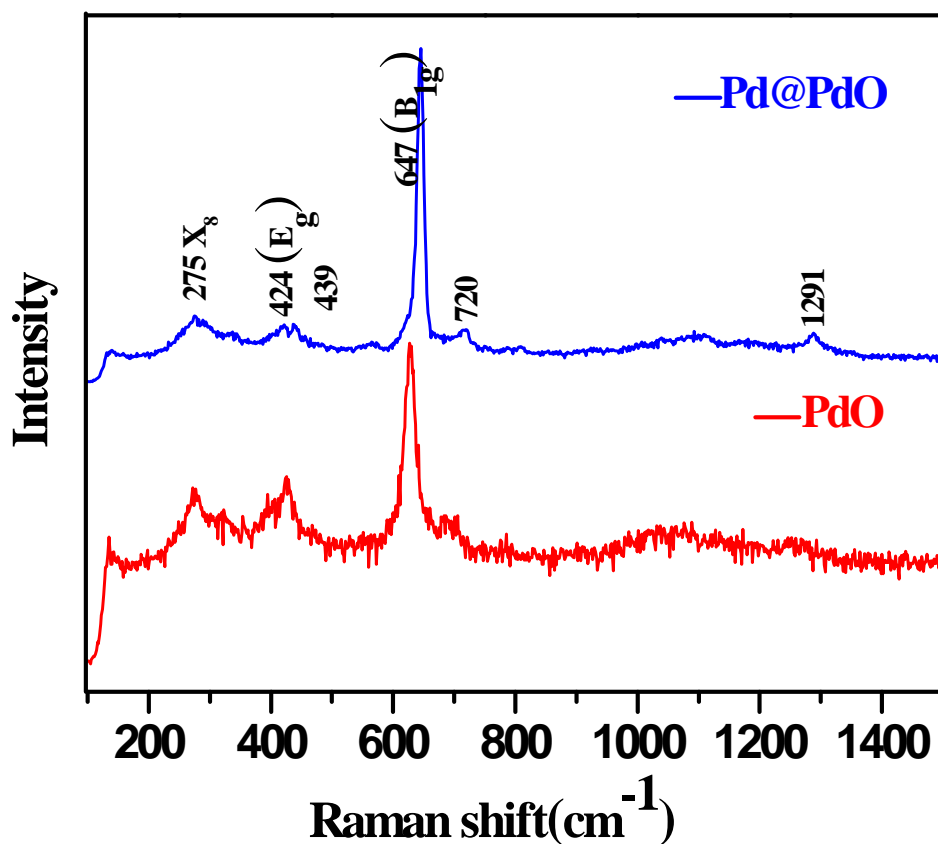
Figure 3.8 Raman shift of PdO and Pd@PdO core-shell

3.5 Thermal study

The thermogravimetric analysis (TG) of two representative complexes [PdCl$_2$.(C$_9$H$_6$NO)$_2$(CH$_2$)$_3$] (**1**) and [PdCl$_2$.C$_{15}$H$_{12}$Cl$_2$N$_2$O] (**3**) were carried out under nitrogen atmosphere, and the TG curves is shown in Fig. 3.12. The onset decomposition of the precursors started at 170 ˚C and they decomposed in different steps due to multiple weight loss steps and organic pyrolysis events. The decomposition appears to be completed at about 800 ˚C. Here PdO was obtained as a final products [25.04 % (24.21 %)] and [28.49 % (29.78 %)].
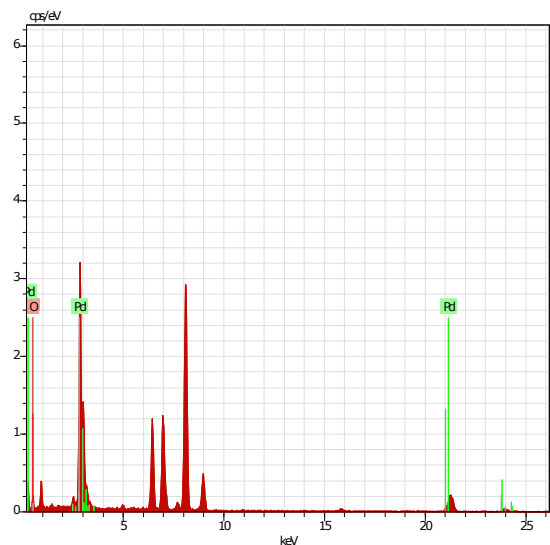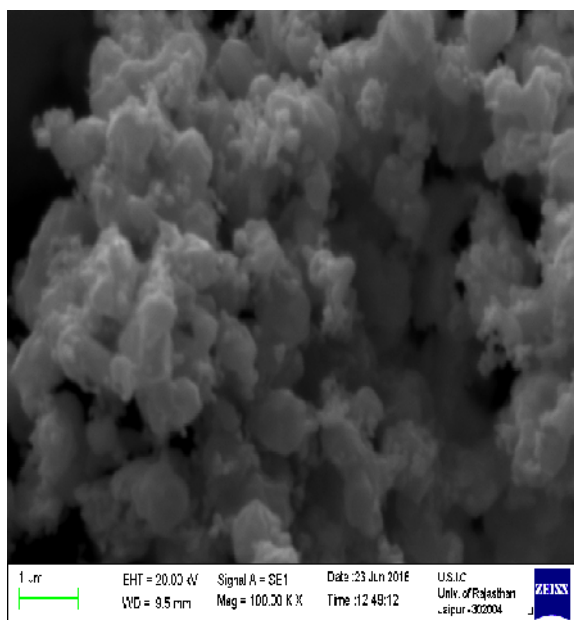
Figure 3.9 (a) SEM and EDX images of (a) PdO formed by [PdCl$_2$] by sol-gel method at 600 ˚C
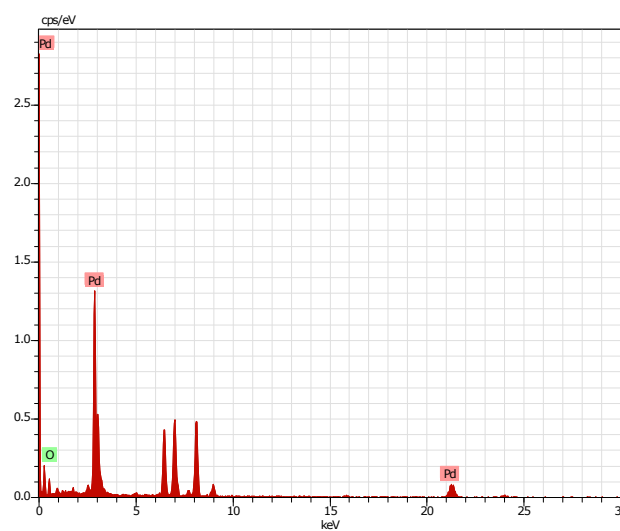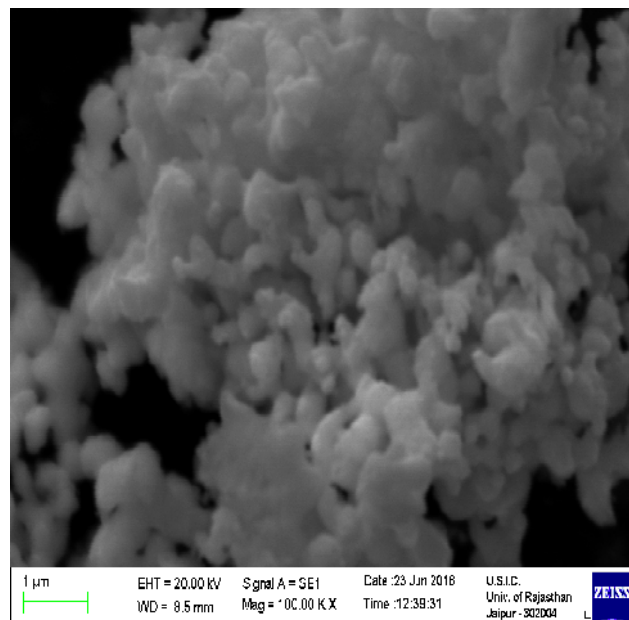
Figure 3.9 (b) SEM and EDX images Pd@PdO formed by [PdCl$_2$.C$_{15}$H$_{12}$Cl$_2$N$_2$O] (3) by sol-gel method at 600 ˚C
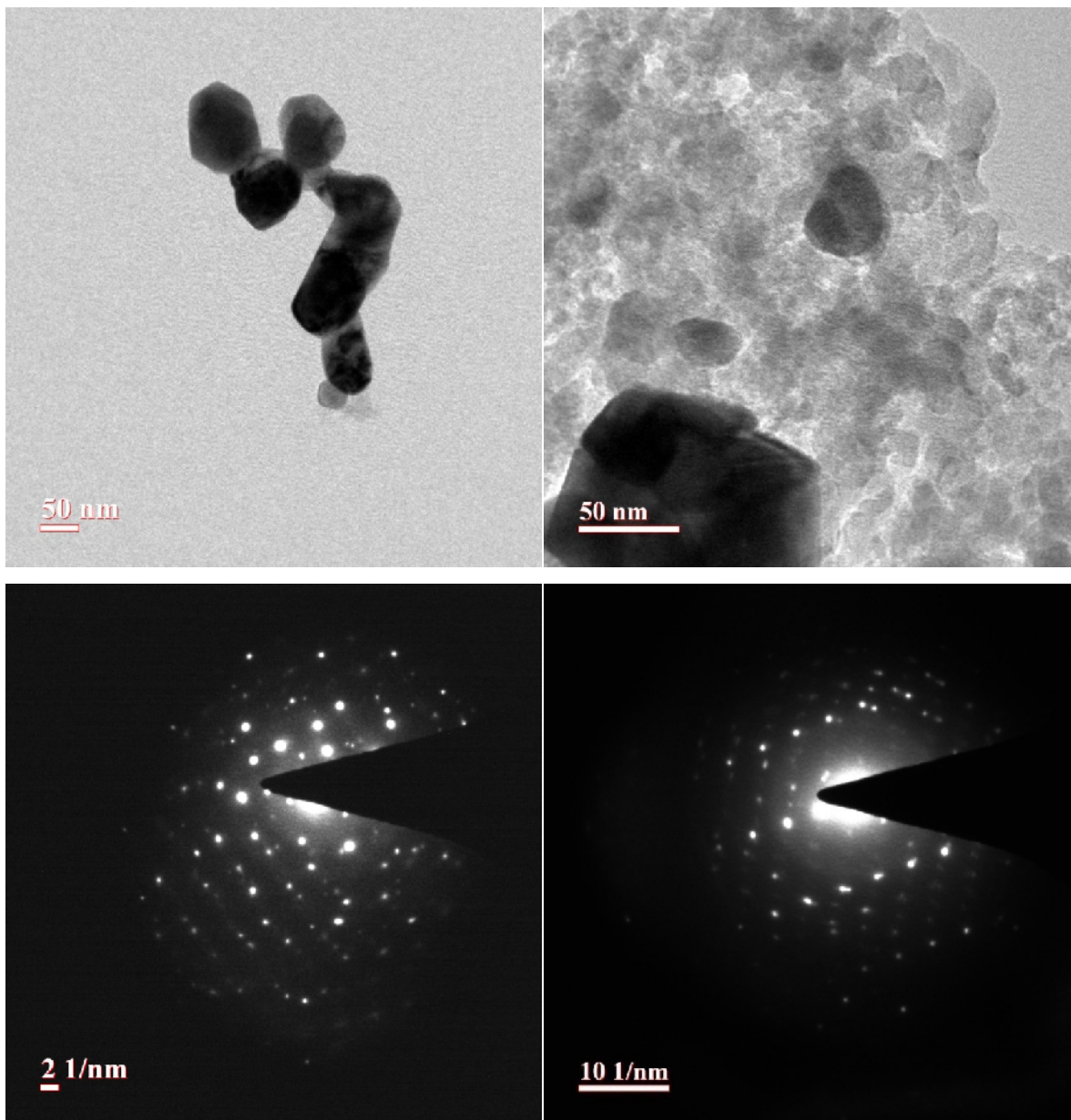
Figure 3.10 (a) TEM and SAED pattern of PdO formed by [PdCl$_2$] by sol-gel method at 600 ˚C

Figure 3.10 (b) TEM and SAED pattern of Pd@PdO formed by [PdCl$_2$.C$_{15}$H$_{12}$Cl$_2$N$_2$O] (3) by sol-gel method at 600 ˚C
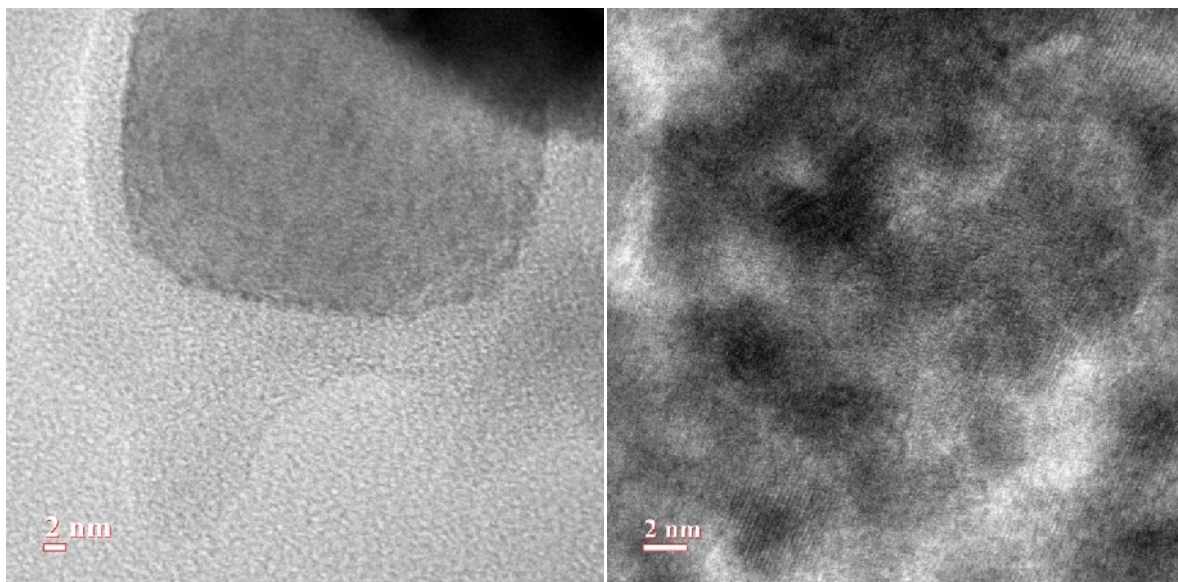
Figure 3.11 (a) HRTEM pattern of PdO formed by [PdCl$_2$] by sol-gel method at 600 ˚C

Figure 3.11 (b) HRTEM pattern of Pd@PdO formed by [PdCl$_2$.C$_{15}$H$_{12}$Cl$_2$N$_2$O] (3) by sol-gel method at 600 ˚C
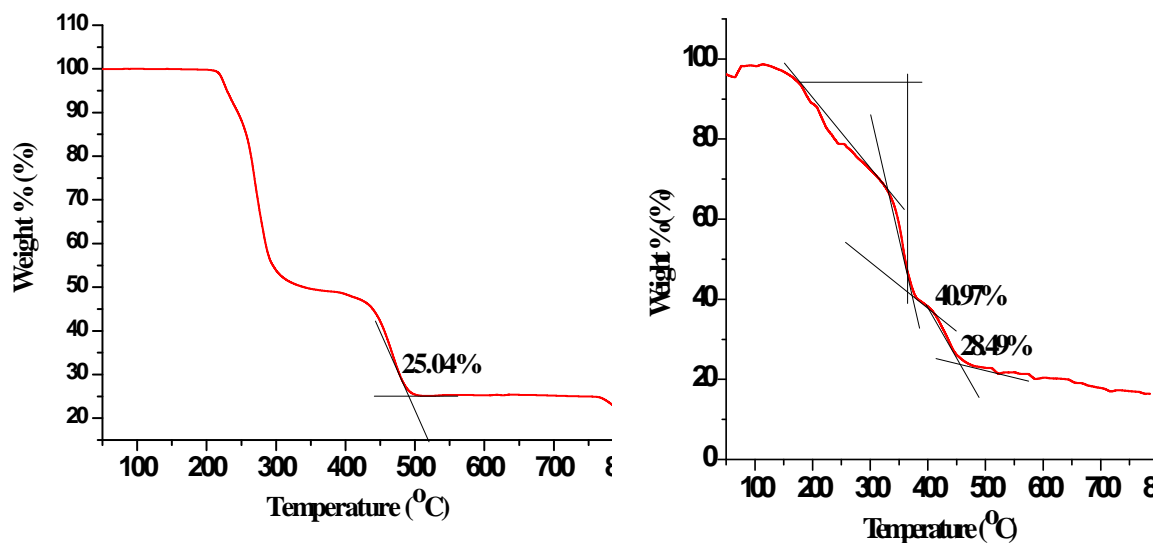
Figure 3.12 TG curves obtained from [PdCl$_2$.(C$_9$H$_6$NO)$_2$(CH$_2$)$_3$] (1) and [PdCl$_2$.C$_{15}$H$_{12}$Cl$_2$N$_2$O] (3)
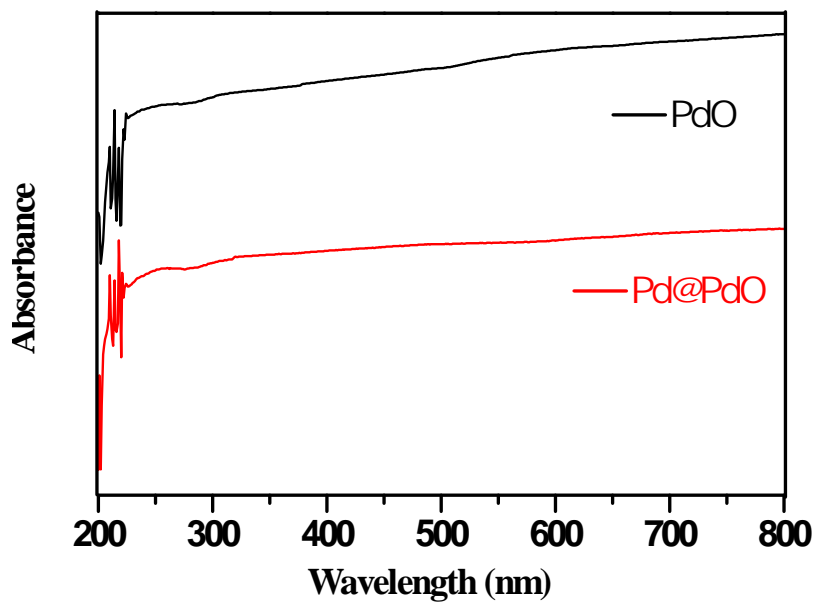
Figure 3.13 UV-visible spectra of PdO and Pd@PdO from the precursors (a) [PdCl$_2$] and (b) [PdCl$_2$.C$_{15}$H$_{12}$Cl$_2$N$_2$O](3)
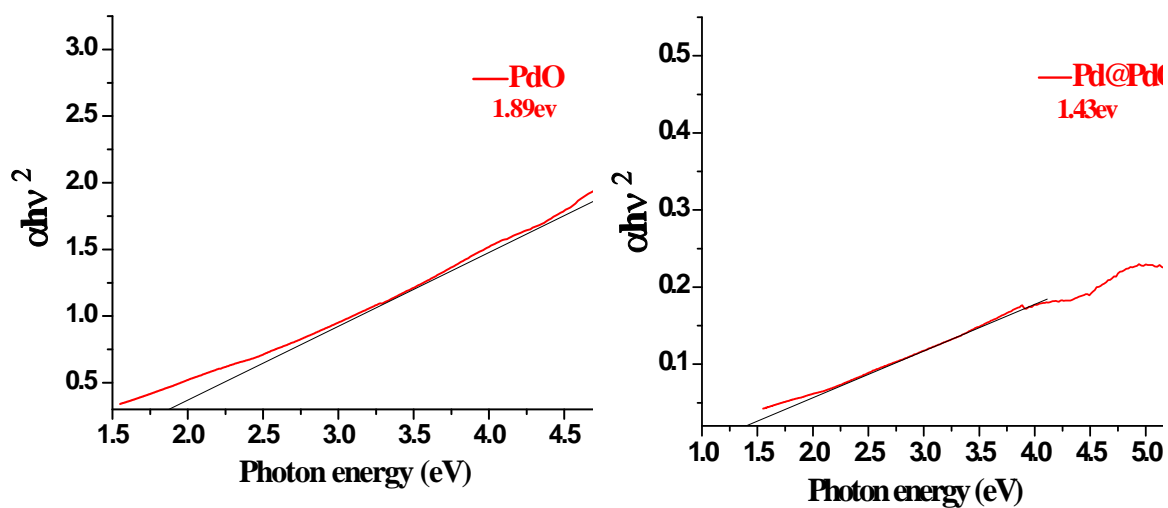
Figure 3.14 hν vs (αhν)^2 plot for samples (a) and (b)

Spectrum
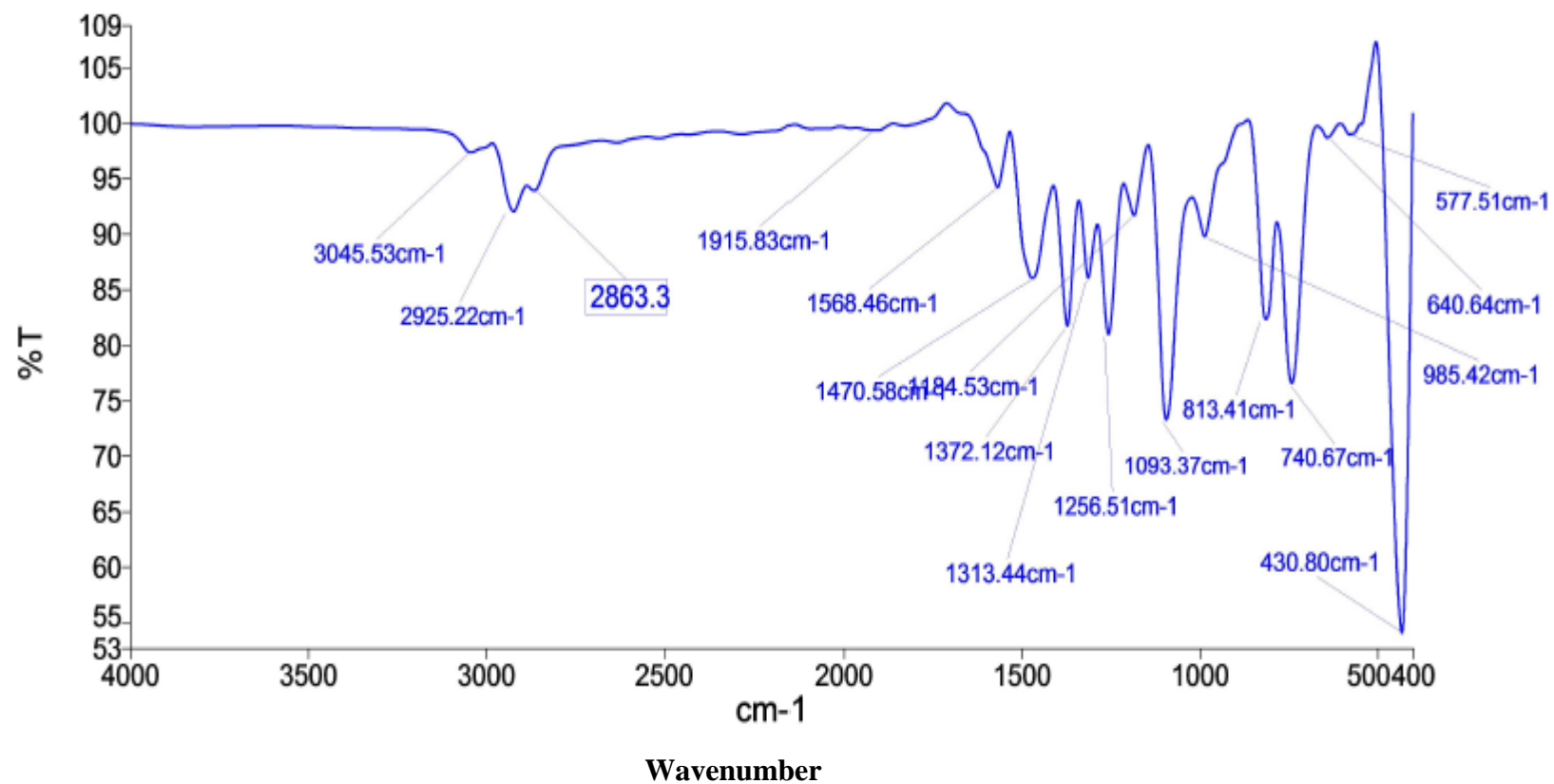
Figure 3.15 FT-IR spectra of the ligand, 1,6-bis(quinolin-8-yloxy)hexane (BQOH)
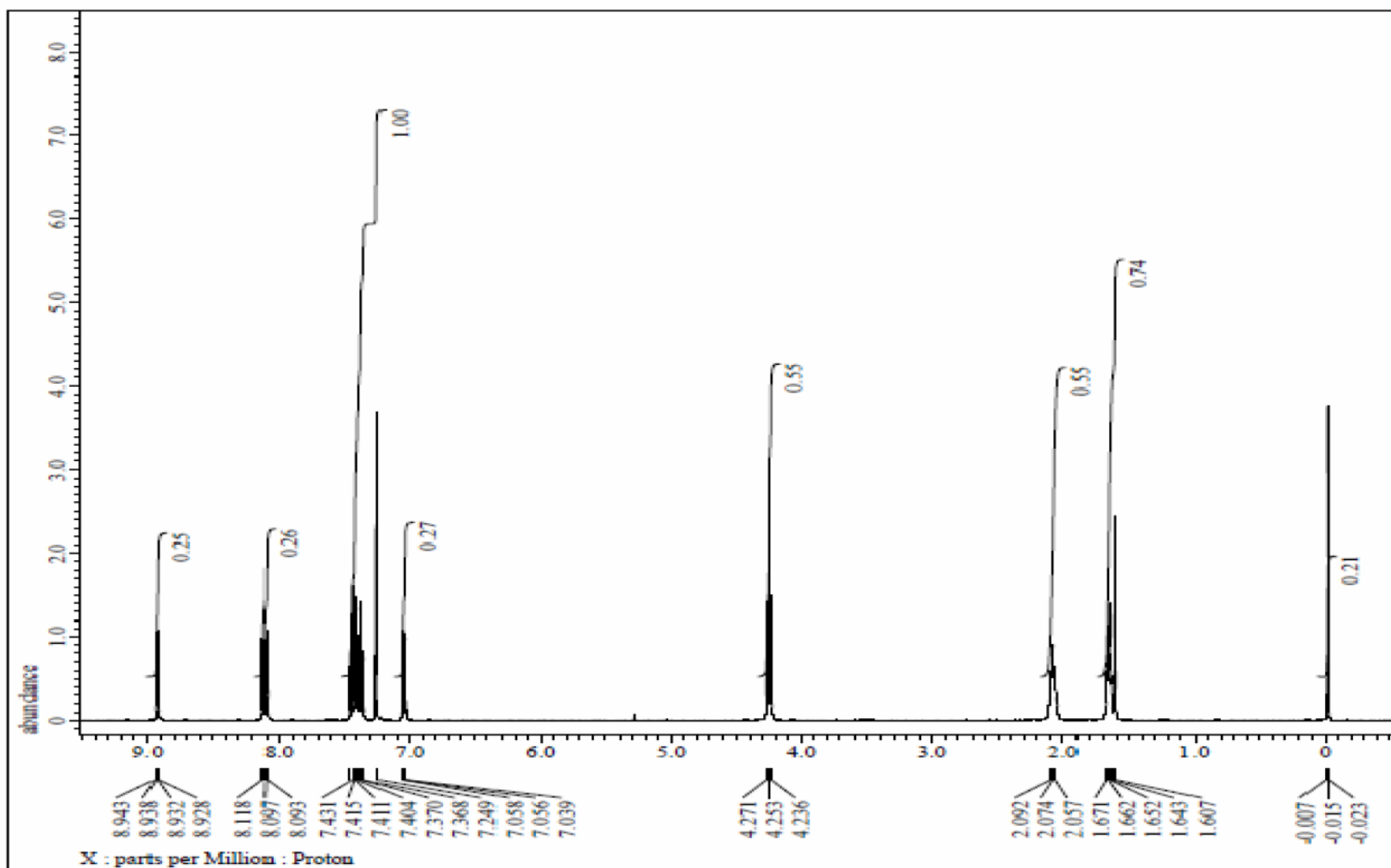
Figure 3.16 ^{1}H NMR spectra of the ligand 11,6-bis(quinolin-8-yloxy)hexane (BQOH) in CDCl3
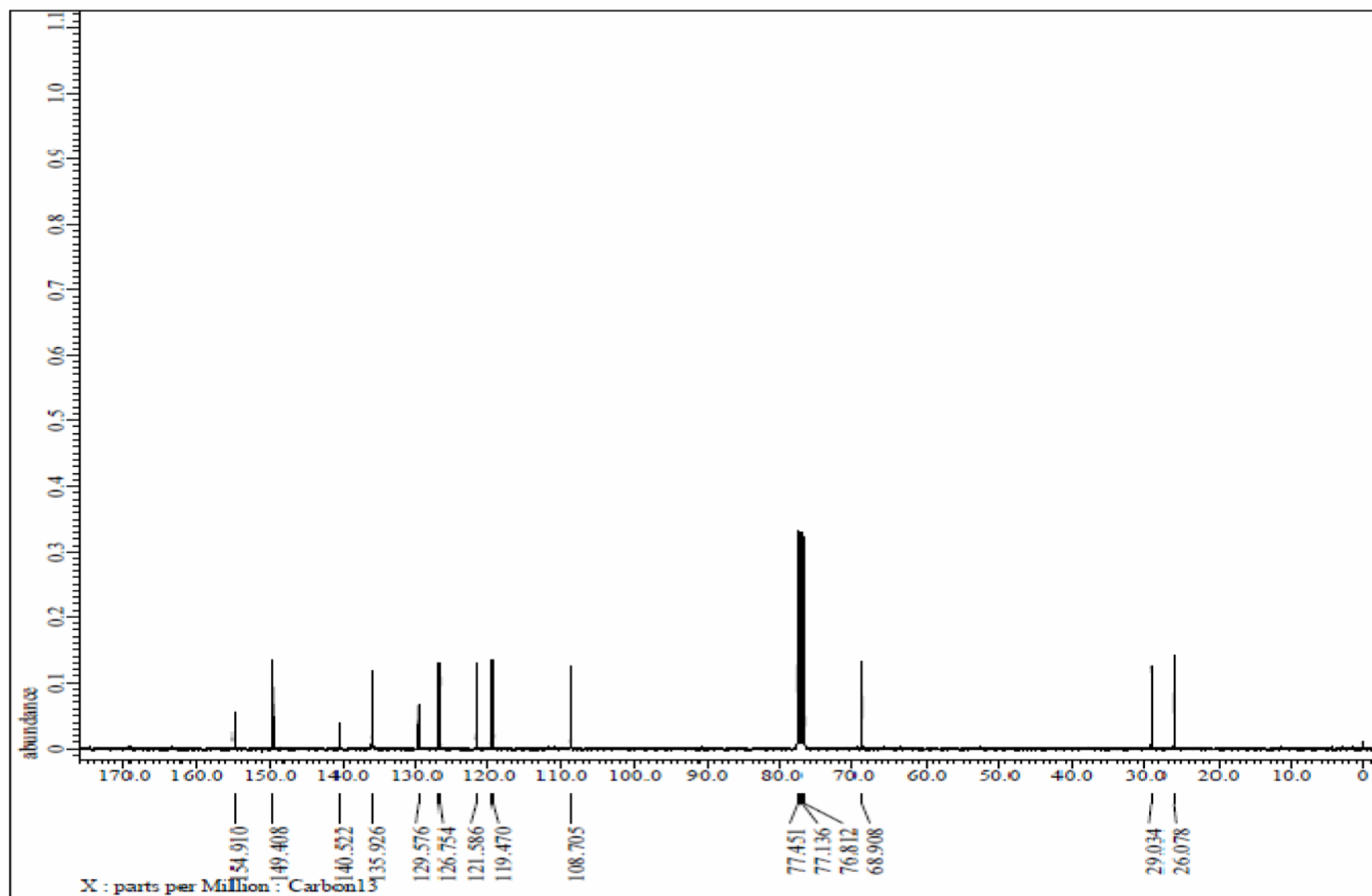
Figure 3.17 ^{13}C NMR spectra of the ligand 1,6-bis(quinolin-8-yloxy)hexane (BQOH) in CDCl3
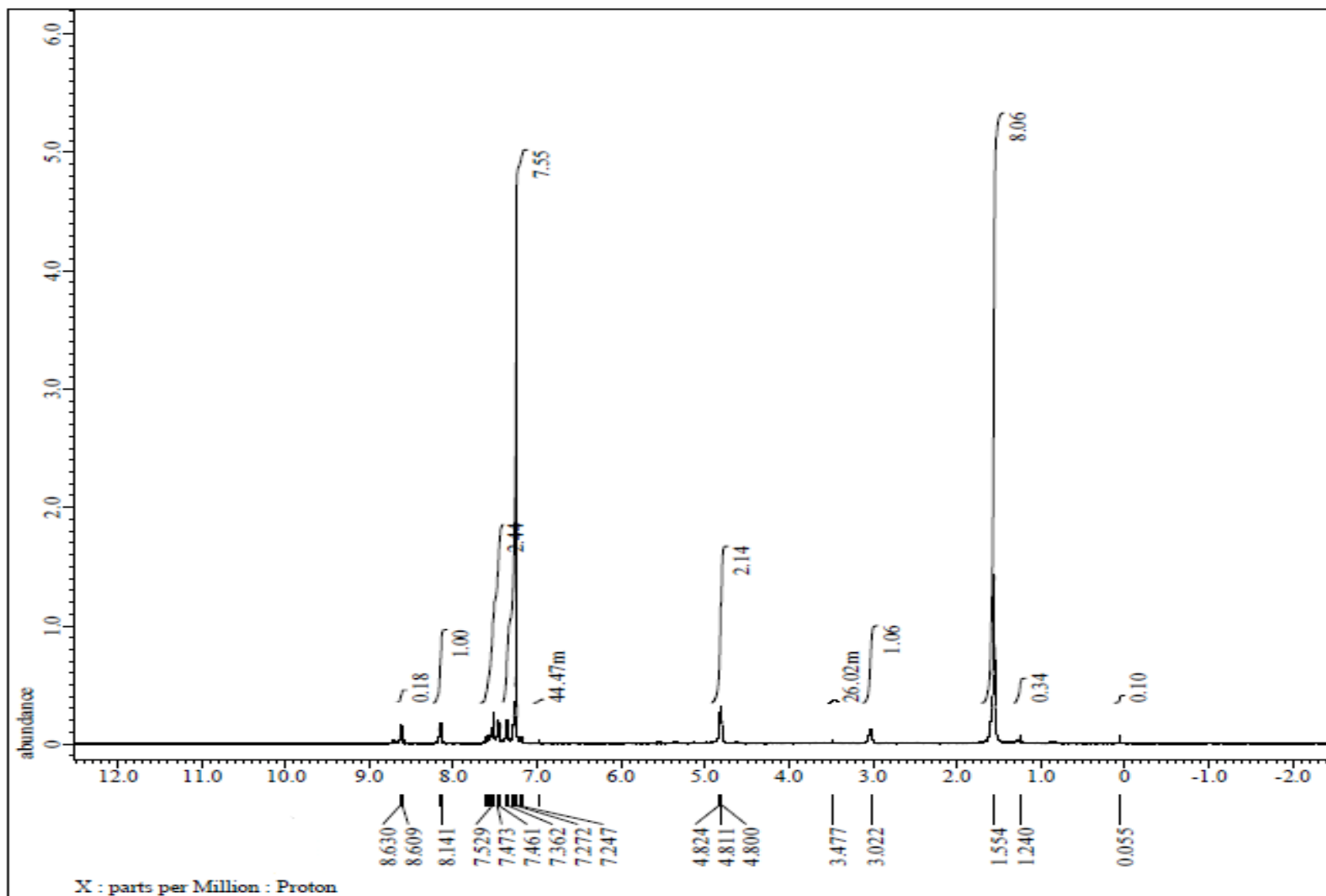
Figure 3.18 ^{1}H NMR spectra of the Pd(II) complex with 8-methoxyquinoline [(MOQ)$_2$PdCl$_2$] in DMSO-d6

JJ-TK-P-83 6 (0.118) AM (Cen,4, 80.00, Ht,10000.0,0.00,0.00); Cm (4:10)   TOF MS ES+
                                                                                2.46e7
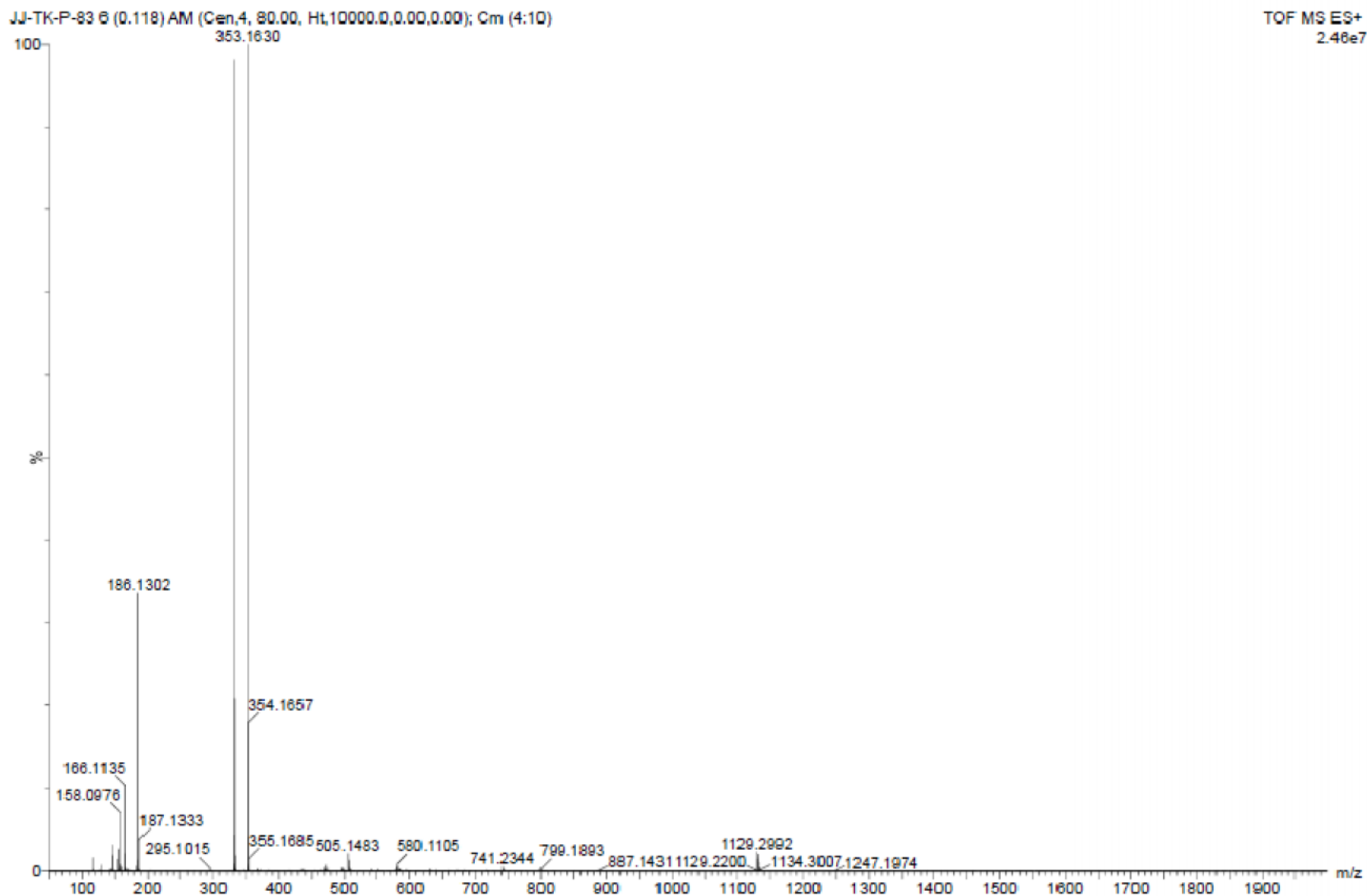
Figure 3.19 ESI mass spectra of the Pd(II) complex with 8-methoxyquinoline [(MOQ)$_2$PdCl$_2$]

PerkinElmer Spectrum Version 10.4.00
Tuesday, February 06, 2018 3:04 PM
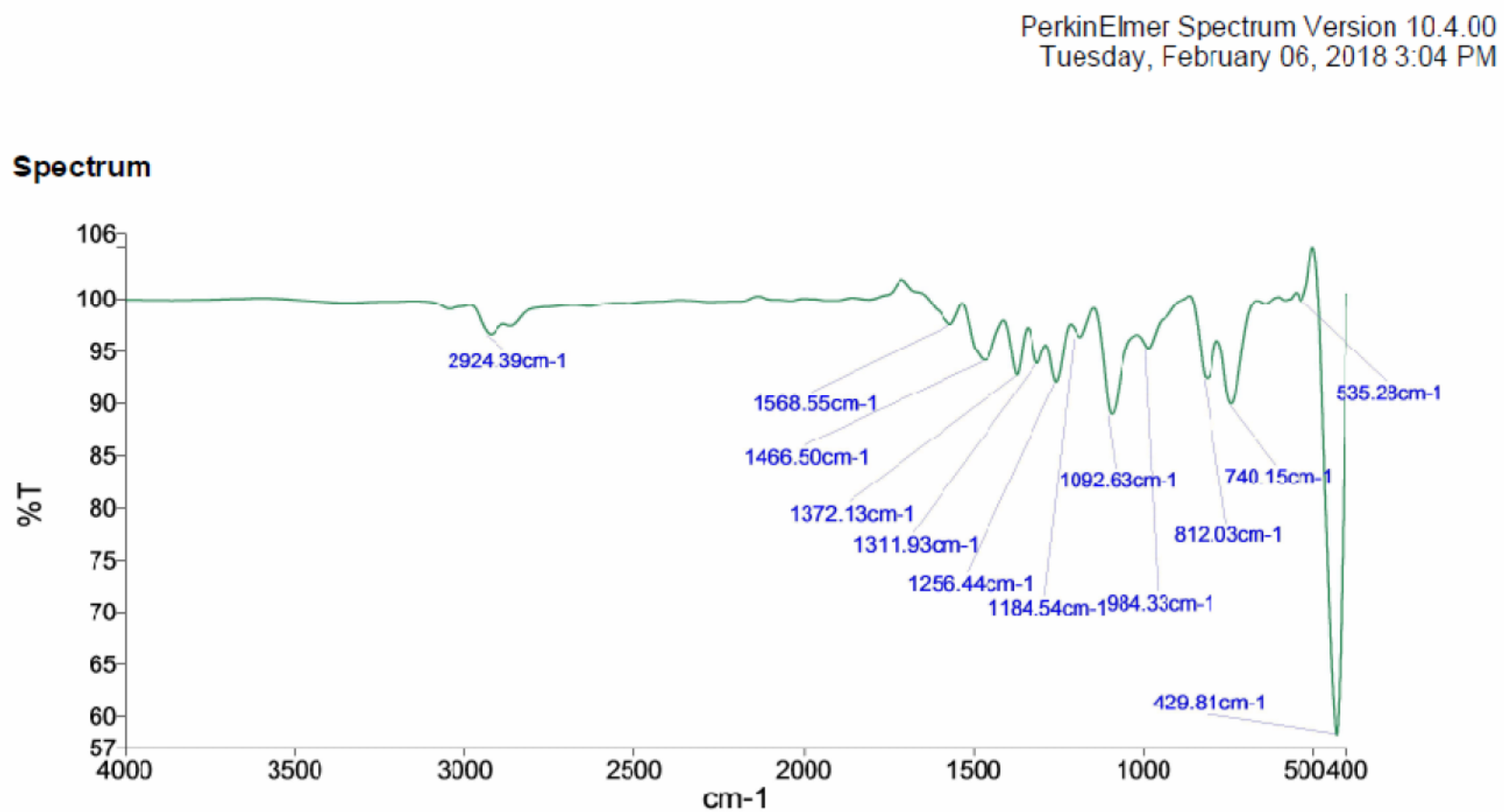
Figure 3.20 FT-IR spectra of the complex Pd(II) complex with 1,6-bis(quinolin-8-yloxy)hexane[(BQOH)PdCl2]
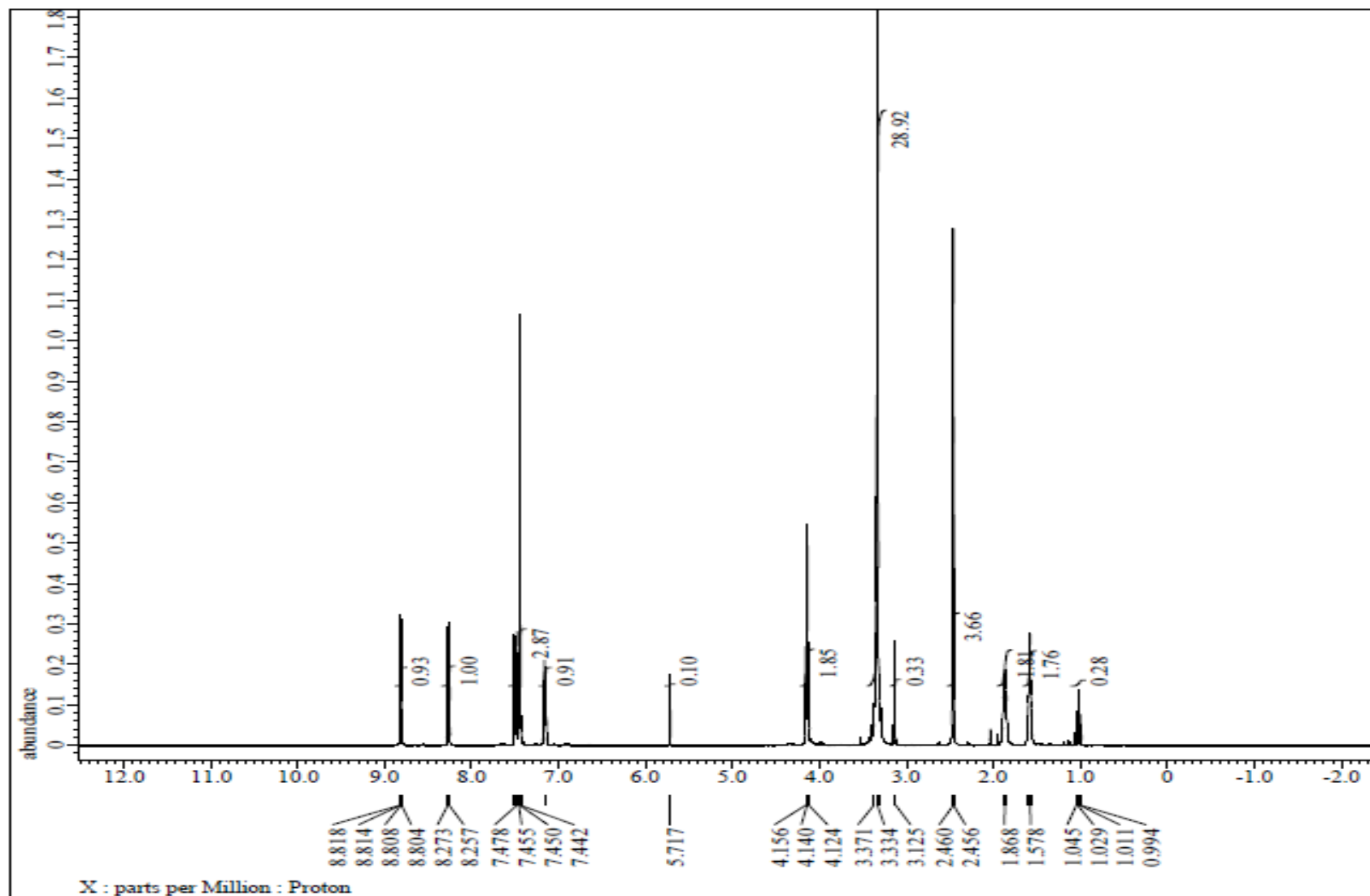
Figure 3.21 ^{1}H NMR spectra of the Pd(II)complex with 1,6-bis(quinolin-8-yloxy)hexane [(BQOH)PdCl${}_2$] in DMSO-d6

JJ-TK-P-84 4 (0.085) AM (Cen,4, 80.00, Ht,10000.0,0.00,0.00); Cm (4:9)

TOF MS ES+
1.53e7
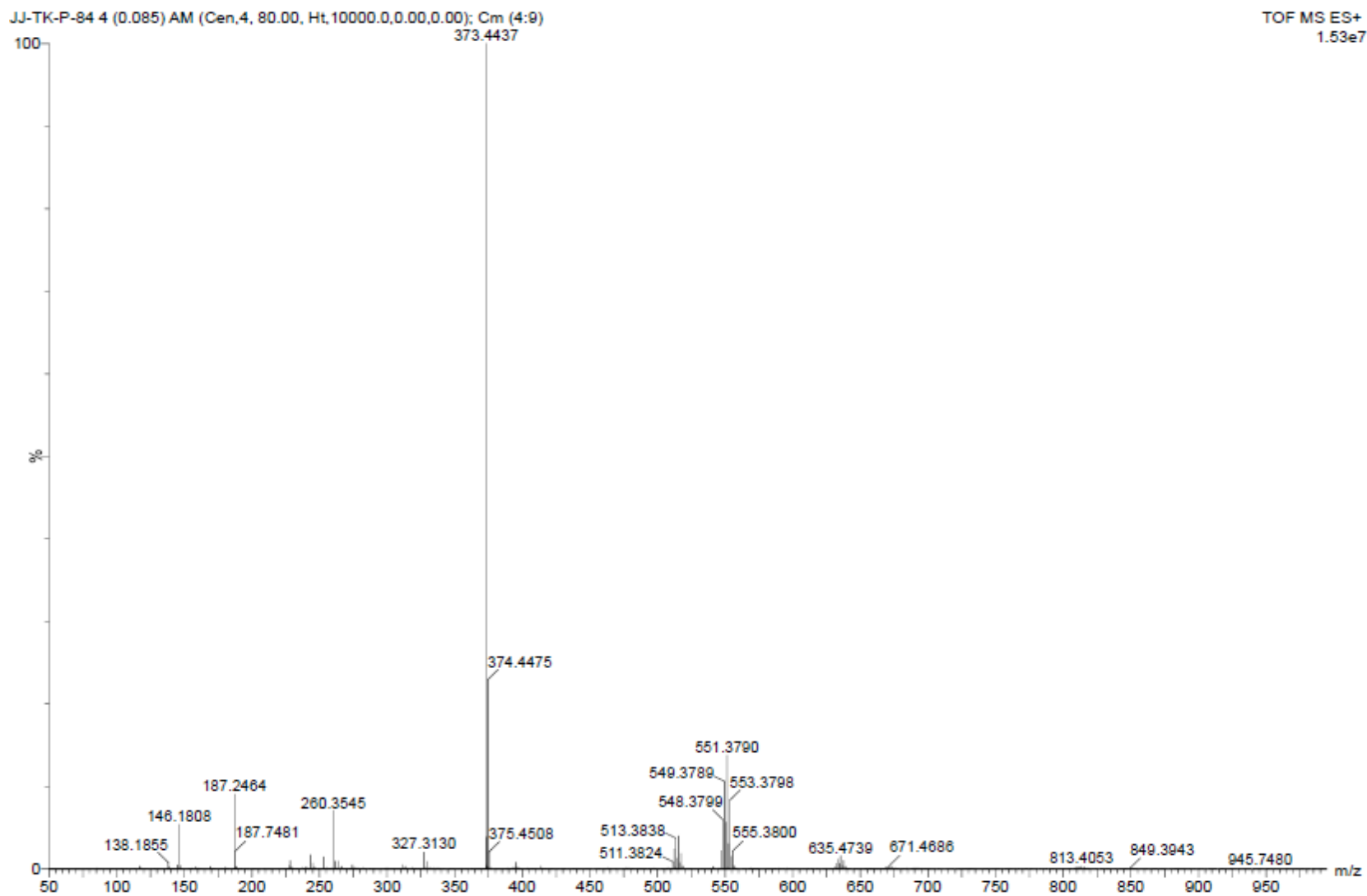
Figure 3.22 ESI mass spectra of the Pd(II) complex with 1,6-bis(quinolin-8-yloxy)hexane [(BQOH)PdCl$_2$]
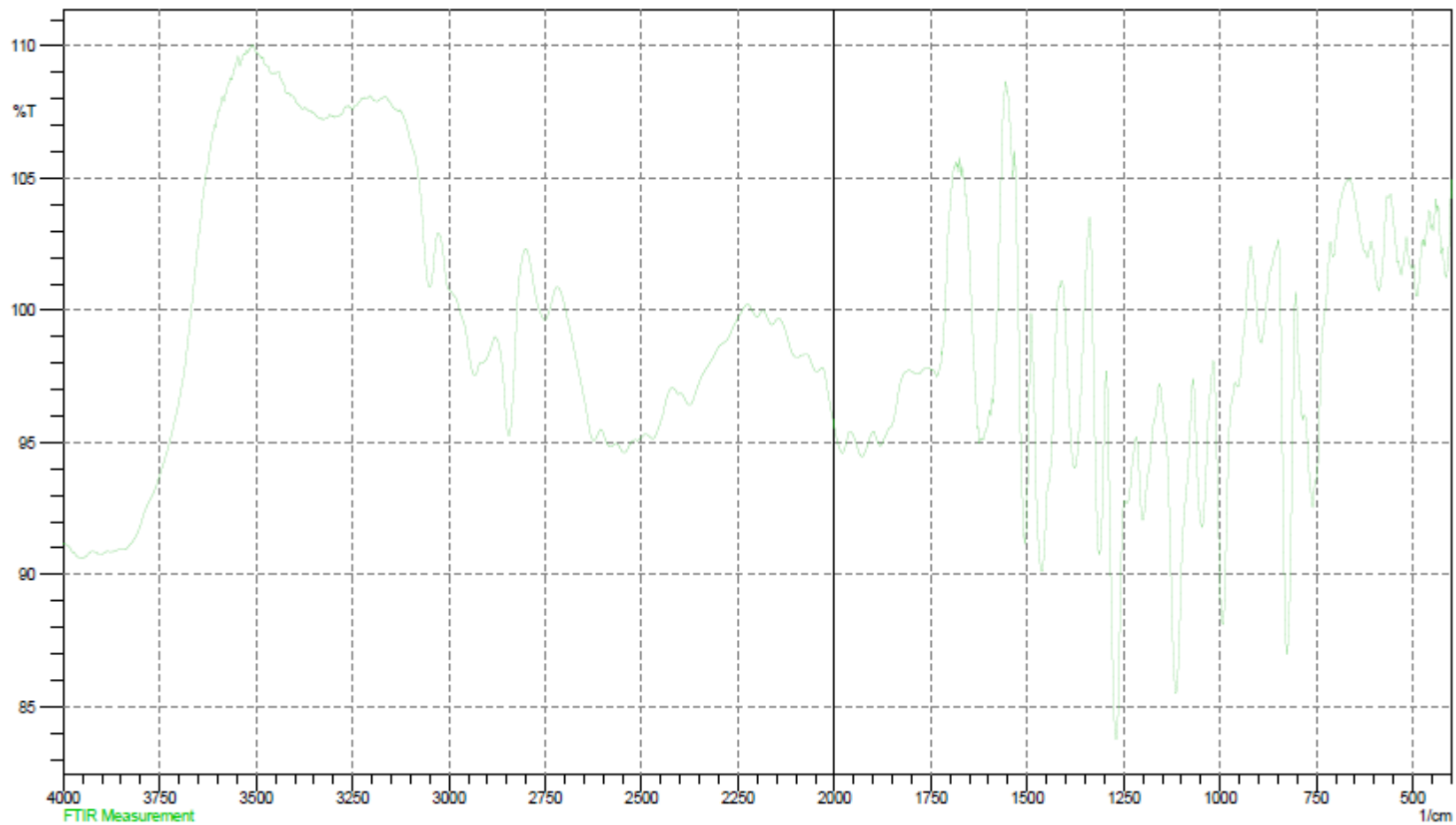
Figure 3.23 FT-IR spectra of the Pd(II) complex with 8-(2-Pyridylmethoxy)quinoline [(PMOQ)PdCl$_2$]
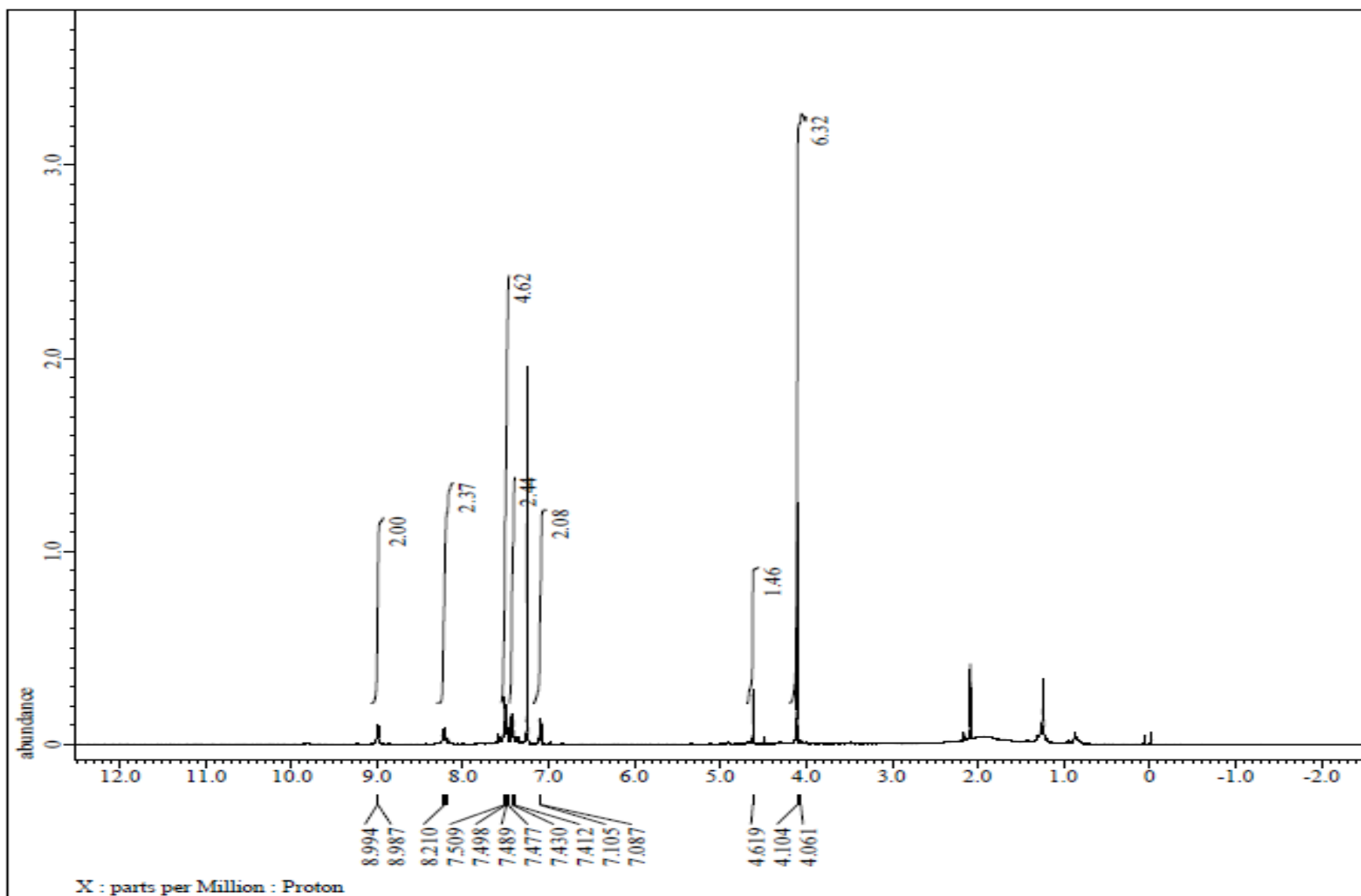
Figure 3.24 ^{1}H NMR spectra of the Pd(II) complex with 8-(2-Pyridylmethoxy)quinoline [(PMOQ)PdCl$_2$] in DMSO-d6

3.6 References

[1] I. Ott, Coord. Chem. Rev. 253 (2009) 1670- 1683.

[2] A. Bindoli, M. P. Rigobello, G. Scutari, C. Gabbiani, A. Casini, L. Messori, Coord. Chem. Rev. 253 (2009) 1692.

[3] C. Orvig, M. J. Abrams, Chem Rev 99 (1999) 2201-2204.

[4] A. Colak, Ü. Terzi, M. Col, Eur J Med Chem. 45 (2010) 5169–5175.

[5] S. Mathur, S. Tabassum. Cent Eur J Chem. 4 (2006) 502–522.

[6] B. Rosenberg, L. Vancamp, J. Trosko, V. Mansour, Nature 222 (1969) 385.

[7] A. S. Abu-Surrah, H. H. Al-Sadoni, M. Y. Abdalla, Cancer Therapy 6 (2008) 1.

[8] Lj. Tusek-Bozic, I. Matijasic, G. Bocelli, G. Calestani, A. Furlani, V. Scarcia, A. Papaioannou, J. Chem. Soc. Dalton Trans. (1991) 195.

[9] M. Curic, Lj. Tusek-Bozic, D. Vikic-Topic, V. Scarcia, A. Furlani, J. Balyarini, E. De Clercq, J. Inorg. Biochem. 63 (1996) 125.

[10] H. Eagle, Proc. Soc. Exp. Biol. Med. 89 (1955) 362.

[11] J. G. Kellof, J. Cell. Biochem. 26S (1996) 54.

[12] G. R. Newkome, W. E. Puckett, G. E. Kiefer, V. K. Gupta, F. R. Fronzkie, D. C. Pantaleo, G. L. McClure, J. B. Simpson, W. A. Deutsch, Inorg. Chem. 24 (1985) 811.

[13] F. Z. Wimmer, S. Wimmer, P. Castan, S. Cros, N. Johnson, E. Colacio-Rodrigez, Anticancer Res. 9 (1989) 791.

[14] M. Yamato, K. Hashigaki, Y. Yasumoto, J Med Chem. 30 (1987) 1897–1900.

[15] K. Maruoka, N. Murase and H. Yamamoto, J. Org. Chem. 58 (1993) 2938.

[16] O. J. Gelling, F. V. Bolhuis, B. L. Feringa, Chem. Commun. (1991) 918

[17] E. C. Constable, M. G. B. Drew, M. D. Ward, Chem. Commun., (1987) 1600

[18] E. C. Constable, M. D. Ward, J. Am. Chem. Soc. 112 (1990) 1256.

[19] E. C. Constable, A. J. Edwards, P. R. Raithby, J. V. Walker, Angew. Chem., Int. Ed. Engl., 32 (1993) 1465.

[20] E. C. Constable, A. J. Edwards, M. J. Hannon, P. R. Raithby, Chem. Commun. (1994) 1991.

[21]   N. C. Fletcher, J. Chem. Soc. Perkin Trans. 1 (2002) 1831.

[22] J.-M. Lehn, Angew. Chem. Int. Ed. Engl., 27 (1988) 89.

[23] A. Juris, V. Balzani, F. Barigelletti, S. Campagna, P. Belser, A. von Zelewsky, Coord. Chem. Rev. 84 (1988) 85.

[24] W. H. Quayle, J. H. Lunsford, Inorg. Chem. 21 (1982) 97–103.

[25] K. Mori, M. Kawashima, K. Kagohara, H. Yamashita, J. Phys. Chem. C, 112 (2008) 19449–19455.

[26] M. Munakata, G. L. Ning, Y. Suenaga, K. Sugimoto, T. Kurodasowa, M. Maekawa, Chem. Commun. (1999) 1545.

[27] S. Liao, C. Y. Su, C. H. Yeung, A. W. Xu, H. X. Zhang, H. Q. Liu, Inorg. Chem. Commun. 3 (2000) 405.

[28] S. Liao, C. Y. Su, A. W. Xu, Z. F. Zhang, X. P. Yang, B. S. Kang, H. Q. Liu, Chem. Res. Chin. Univ. 27 (2000) 273; C. Y. Su, B. S. Kang, Q. G. Wang, T. C. W. Mak, Dalton Trans. (2000) 1831.

[29] M. R. Hoffmann, S.T. Martin, W. Choi, D.W. Bahnemann, Chem. Rev. 95 (1995) 69.

[30] P.V. Kamat, Chem. Rev. 93 (1993) 267.

[31] J. Livage, M. Henry, C. Sanchez, Prog. Solid State Chem. 18 (1988) 259.

[32] Juan J. Giner-Casares, Malou Henriksen-Lacey, Marc Coronado-Puchau, Luis M. Liz- Marzán, Materials Today, 19, (2016) 19-28.

[33] Oskam, G. Journal of Sol-Gel Science and Technology, 37 (2006) 161–164.

[34] J. Tsuji, Palladium Reagents and Catalysts New Perspectives for the 21st Century (Wiley, Chichester, 2004)

[35] R. Narayanan, M.A. El-Sayed,. J. Catal. 234, (2005) 348–355.

[36] O.M. Wilson, M.R. Knecht, J.C. Garcia-Martinez, R.M. Crooks, J. Am. Chem. Soc. 128, (2006) 4510–4511.

[37] J. Huang, Y. Liu, H. Hou, T. You, Biosens. Bioelectron. 24 (2008) 632–637.

[38] D. Sil, J. Hines, U. Udeoyo, E. Borguet ACS Appl. Mater. Interfaces 7(10), (2015) 5709– 5714.

[39] Y. Ozawa, Y. Tochihara, M. Nagai, S. Omi, Chem. Eng. Sci. 58 (2003) 671–677.

[40] T.L. Stuchinskaya, I.V. Kozhevnikov, Catal. Commun. 4 (2003) 417–422.

[41] X. Xu, W. Yang, J. Liu, L. Lin, Adv. Mater. 12 (2000)195–204.

[42] E. Ismail, M. Khenfouch, M. Dhlamini, S. Dube, M. Maaza, J. Alloy. Compd. 695

(2017) 3632– 3638.

[43] B. L. Justus, R.J. Tonucci, A. D. Berry, Appl. Phys. Lett. 61 (1992) 3151–3153.

[44] S. Sakka, Handbook of Sol-Gel Science and Technology: Characterization and Properties of Sol-Gel Materials and Products (Springer, Switzerland, 2005)

[45] V. G. Kessler, G.I. Spijksma, G.A. Seisenbaeva, S. Hakansson, D.H.A. Blank, H .J. M. Bouwmeester, J. Sol-Gel Sci. Technol. 40 (2006) 163–179.

[46] D. Avnir, T. Coradin, O. Lev, J. Livage, Recent bio-applications of sol–gel materials. J. Mater. Chem. 16, (2006) 1013–1030.

[47] A .E. Danks, S.R. Hall, Z. Schnepp, Mater. Horiz. 3 (2016) 91–112.

[48] F. L. Li, H.J. Zhang, Materials 10 (2017) 995–1011.

[49] L. L. Hench, J.K. West, Chem. Rev. 90, (1990) 33–72.

[50] C. J. Brinker, G.W. Scherer, Sol–Gel Science: The Physics and Chemistry of Sol–Gel Processing (Academic Press, California, 1990)

[51] M. K. Atal, R. Sharma, A. Saini, V. Dhayal, M. Nagar, J. Sol-Gel Sci. Technol. 79 (2016) 114–121.

[52] A. I. Vogel, A Text Book of Quantitative Inorganic Analysis, 5th edn. (Longman, London, 1989)

[53] R.A. Muna, A. Al-Mandhary, P.J. Steel, Inorg. Chim. Acta. (2003) 351, 7–11.

[54] A. M. Tajuddin, H. Bahron, K. Kassim, W. Nazihah, W. Ibrahim, B.M. Yamin, Malays. J. Anal. Sci. 16 (2012), 79–87.

[55] M. J. Tura, P. Regull, L. Victorit, D.D. Castellar, Surf. Interface Anal. 11 (1988) 447–449.

[56] K. Searles, B. L. Tran, M. Pink, C.-H. Chen, D. J. Mindiola, Inorg. Chem. 52 (2013) 11126–11135

[57] A. K. Bar, C. Pichon, J.-P. Sutter, Coord. Chem. Rev. 308 (2016) 346–380

[58] D. Jose, B.R. Jagirdar, J. Solid State Chem. 183 (2010) 2059– 2067.

[59] B.E. Warren, X-Ray Diffraction (chap. 13) (Dover Publication, New York, 1990).

[60] X. Wei, D. Chen, Mater. Lett. 60 (2006) 823–827.

[61] W. Shockley, H.J. Queisser, J. Appl. Phys. 32 (1961) 510–519.

[62] R. Bardhan, A. Schwartzberg, C.L. Pint, J. Phys. Chem. C **117**, 21558–21568 (2013).

[63] G. W. Graham, D. Uy, W.H. Weber, H. Sun, X.Q. Pan, Catal. Lett. 79 (2002) 99–105.

[64] J. R. McBride, K. C. Hass, W. H. Weber, Matter Mater. Phys. 44 (1991) 5016–5029.

[65] J Tauc, Amorphous & Liquid Semiconductors (Plenum, New York, 1974).

[66] W. Shockley, H.J. Queisser, J. Appl. Phys. 32 (1961) 510–519.

[67] W.L. Wilson, P.J. Szajowski, L.E. Brus, Science 262, 1242–1244 (1993).

4.1 Introduction

Among the various nano sized materials, titania (TiO_2) has gained attraction due to its wide range applications including in solar cells, photocatalysts, gas sensors, biomolecules, biomaterials, etc. [1-7]. The properties of nano materials are entirely decided by shape and size of the nano particles, morphology as well as their composition [8-9]. Titania exhibits three distinct crystallographic phases: anatase, brookite, and rutile. Out of three, anatase titania has been established to show an excellent catalytic activity in photodecomposition and solar energy conversion [6, 7].

There have been several methods reported for the synthesis of nano-materials [10-15], out of which low temperature aqueous sol-gel technique is the simplest and cost effective [15-18]. This method has been considered to be most useful because nanoparticles of high homogeneity and good uniformity can be synthesized at calcination temperature [19, 20].

Usually metal alkoxides have been used as molecular precursors in sol-gel method for the synthesis of nano particles, owing to their solubility in common organic solvents. However, most of the metal alkoxides of transition metals are highly moisture sensitive and they react instantaneously with water, resulting in unwanted products, which causes the formation of a polymeric gel instead of a colloidal gel that is not suitable for the nano material preparation [18, 21-23] therefore, adequate precaution have to be taken for using them as starting metal for nano synthesis.

Designing of new molecular metallo-organic precursors obtained from substitution of one or more alkoxy groups present in metal alkoxides with chelating ligands such as Schiff's bases, -ketoesters, -diketones, Oximes 8-hydroxyquinoline etc. [8,24-27] which may induce remarkable structural changes, are being considered as an alternative approach for sol gel synthesis of nanoparticles [16,17].

In this chapter, we report the synthesis and optical properties of nano-sized anatse titania by low temperature aqueous sol–gel technique. It is commendable to mention here that synthesis of stable anatase TiO_2 by aqueous sol–gel route, using precursors 8-

hydroxyquinoline modified titanium(IV)bis(acetylacetonate) diisopropoxide, is being reported for the first time to the best of our knowledge.

4.2 Experimental

4.2.1 Materials and Methods

Analytical grade 8-hydroxyquinoline (99%) was procured from Sigma-Aldrich and were used as received. Analytical grade solvents used in the experimental work were procured from Rankem, India. All solvents were purified by standard methods before use. The synthesis of complexes [{acac}$_2$Ti{OPr^i}{ONC$_9$H$_6$}] (**1**) and [{acac}$_2$Ti{ONC$_9$H$_6$}$_2$] (**2**) were performed in strictly moisture free environment. All the reagents were dried using conventional methods prior to use [27]. Titanium(IV) isopropoxide and [{acac}$_2$Ti{OPr^i}$_2$] were synthesized as reported in the literature [28, 29] and used freshly. Estimation of Titanium done as TiO$_2$ [27], nitrogen was estimated using Kjeldahl's [27] and isopropanol was estimated by benzene azeotrope using oxidimetric method [30].

IR spectra were obtained from SHIMADZU, FT-IR 8400 spectrometer ranging 400-4000 cm^{-1} using dry KBr pellets. NMR (^{1}H and ^{13}C) data were recorded on JEOL FX 300 FT-NMR spectrometer in CDCl$_3$ solution at frequencies 300.4 MHz for ^{1}H and 75.45 MHz for ^{13}C. Molecular weights were measured by determining the freezing point depressions of anhydrous benzene using a Beckmann's Thermometer (Einstellthermometer n-Bek) fitted in a glass assembly (supplied by JSGW, India). The XRD patterns were recorded on P'analyticalmake X'Pert PRO MPD diffractometer (model 3040). The X-ray were produced using a sealed tube and the wavelength of X-ray was 0.154 nm (Cu K-a). SEM and EDX was performed on Carl-Zeiss (30 keV) make and model EVO. The powder samples were used for SEM and EDX..TEM was carried out on TECHNAI 20, FEI, North America and Bruker, Germany. UV-visible spectra of the samples were recorded using LAMBDA 750 (Perkin Elmer) spectrophotometer of wavelength range 200 to 800 nm.

4.2.2 Synthesis of Precursors

4.2.2.1 Synthesis of [{acac}$_2$Ti{OPr^i}{ONC$_9$H$_6$}] (1)

Solution of [{acac}$_2$Ti{OPr^i}$_2$] (1.78 g, 4.8 mmol in anhydrous benzene) was added dropwise to the solution of 8-hydroxyquinoline (C$_9$H$_6$NOH) (0.70 g, 4.8 mmol) in anhydrous benzene. The light Yellow colored solution obtained was refluxed. Continuous oxidimetric analysis of the liberated isopropanol in the azeotrope of benzene verified progress of the reaction. Excess of the solvent was removed upon completion of the reaction under reduced pressure to give a reddish brown color solid (2.09g). The product obtained was re-crystallized using n-hexane and dichloromethane mixture.

4.2.2.2 Synthesis of [{acac}$_2$Ti{ONC$_9$H$_6$}$_2$] (2)

A similar route as discussed above was employed for the synthesis of [{acac}$_2$Ti{ONC$_9$H$_6$}2] (2) derivative using a 1:2 molar ratio of the [{acac}$_2$Ti{OPr^i}$_2$] and C$_9$H$_6$NOH. The physical and analytical data of the complexes (1) and (2) are summarized in Table-4.1.

4.2.3 Hydrolysis of [{acac}$_2$Ti{OPr^i}{ONC$_9$H$_6$}] (1), [{acac}$_2$Ti{ONC$_9$H$_6$}$_2$] (2) and [Ti{OPr^i}$_4$] (A)

To the transparent solution of Precursor [{acac}$_2$Ti{OPr^i}{ONC$_9$H$_6$}] (**1**) (1.1 g) in anhydrous 2-propanol 3-4 drops of (1:1) mixture of water-isopropanol was added and the resultant mixture was constantly stirred for ~2 h., a brownish color sol formation was observed. In order to ensure absolute hydrolysis small portions of water added constantly in stoichiometric ratio (0.18g) {~ 10 ml} with uninterrupted stirring for ~ 5 h. and this mixture was further allowed to stir for 24 h. The gel formed was filtered and dried in an oven previously heated (~100°C), resulting in the formation of an off white solid. To remove organic/inorganic impurities, the solid was washed with distilled water and subsequently with acetone and sintered at ~600°C for ~4 h yielding a white powder. The resulting white powdered solid was characterized as pure nano-sized anatase TiO$_2$.

Compound (**2**) and [Ti{OPr^i}$_4$] (A) were also hydrolyzed by using similar method and the product obtained were also characterized as anatase TiO$_2$.

Table 4.1 Physical and analytical data for 8-hydroxyquinoline complexes of titanium(IV)bis(acetylacetonate) diisopropoxide

Reactants (g)			Complexes	Colour/ Physical state	Yield (g) Found [Calculated]	Liberated Pr^iOH(g) [Found (Calculated)]	% Analysis found (Calculated)			Molecular weight Found (Calculated)
A	B	Molar ratio					OPr^i	Ti	N	
1.78	0.70	1:1	[{acac}$_2$Ti{OPr^i} {ONC$_9$H$_6$}] **[1]**	Reddish brown/ solid	2.09 [2.18]	0.30 [0.29]	13.1 [13.2]	10.4 [10.5]	3.0 [3.1]	436 [455]
0.91	0.71	1:2	[{acac}$_2$Ti {ONC$_9$H$_6$}$_2$] **[2]**	Pale yellow/ solid	1.26 [1.33]	0.29 [0.29]	-	8.8 [8.9]	5.2 [5.2]	526[540]

4.3 Result and Discussion

4.3.1 Synthesis and characterization of precursor

Reactions of $[(acac)_2Ti(OPr^i)_2](A)$ with stoichiometric amount of 8-hydroxyquinoline (B) in (molar ratios 1:1 and 1:2) were carried out in anhydrous benzene, yielding the complexes of the type $[(acac)_2Ti\{OPr^i\}_{2-n}\{Q\}_n]$ as shown below:

$$[(acac)_2Ti(OPr^i)_2] + nQH \xrightarrow{\text{benzene}/\triangle} [(acac)_2Ti\{OPri\}_{2-n}\{Q\}_n] + nPr^iOH \uparrow$$

Titanium diisopropoxide bis(acetylacetonate)   8-Hydroxyquinoline   Titanium diisopropoxide acetylacetonate quinolinate   Isopropanol
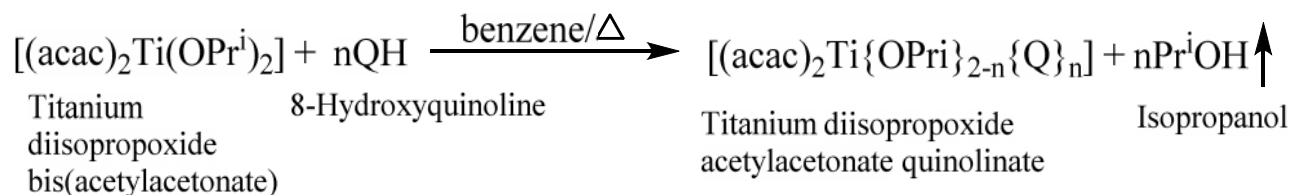
[Where, n = 1 (**1**) or n=2 (**2**)]

These reactions were observed to be reasonably facile and quantitative, yielding reddish brown/pale yellow colored solids. Complexes formed are hygroscopic in nature and found to be soluble in common organic solvents. Progress of the reaction was examined by analyzing the released isopropanol which formed azeotrope with benzene, using oxidimetric method [27]. Monomeric nature of both the complexes (1) and (2) were suggested by measurement of their molecular weight in freezing benzene [30].

4.3.2 IR spectra

Some important IR absorption bands for the complexes are listed in the Table- 4.2. The IR spectral bands of the compounds (**1**) & (**2**) have been inferred by comparing their IR spectra with the IR spectra of free acetylacetone, free 8-hydroxyquinoline and other $[(acac)_2Ti(OPr^i)_2]$ complexes [26,31]. IR spectra of these compounds show strong bands due to v(C-O) and v(C-C) stretching vibrations at 1505-1490 and 1460-1445 cm^{-1} respectively while in free acetylacetonate it is observed at 1680 cm^{-1} [31]. These observed shifts in the carbonyl stretching frequencies towards lower frequencies in the formed derivative suggest chelation of acetylacetonate moieties in bidentate manner.

Absence of broad band at (3,194-3,358 cm^{-1}) due to hydroxyl group absorption and appearance Ti-O bond (644-650 cm^{-1}) has been observed in the IR spectra of these

derivatives [18]. ν(C=N) stretching frequency observed towards lower frequencies (~ 1575-1576 cm^{-1}) in comparison to free 8- hydroxyquinoline indicating the coordination of nitrogen to the titanium. In the region of 535-540 cm^{-1} band observed which can be assigned to (Ti-N) mode in both the complexes [18]. The intermediate intensity band appeared at ~ 1015 cm^{-1} in complex (**2**) can be allocated to ν(C-O) of the 2-propanol group.

4.3.3 NMR spectra

The ^{1}H and ^{13}C chemical shifts of derivatives (**1**) & (**2**) were performed and evaluated against spectra of free acetylacetone, free 8-hydroxyquinoline and other [(acac)$_2$Ti(OPr^i)$_2$] complexes [26,31]. Some of the important NMR peaks are listed in Table- 4.3 & 4.4. The peak for hydroxyl proton (8.6-9.23) were absent in ^{1}H NMR spectra of both the derivatives, indicating coordination of 8-hydroxyquinoline with titanium atom in deprotonated form.

The methyl signals of the acetylacetone moiety appeared as a doublet in the 1.92–2.07 and 2.02– 2.15 ppm ranges, indicating the non-equivalent nature of the two methyl groups. Methine signals of the acetylacetone moiety appeared at 5.49-6.52 in both the derivatives.

In the NMR spectra of all the complexes presence of methyl proton observed at 1.21-1.33 and methine proton in the region of 4.72-4.74 ppm. Their ^{13}C resonances appear at 24.95 and at 64.53 ppm. The ^{13}C NMR chemical shift of C=N and C-O appeared in the region 144.73-162.78 ppm respectively indicating formation of Ti-N and Ti-O bond.

Two signals for the carbonyl carbon of the acetylacetone moiety in both of these precursors have been observed at 191.15–191.31 ppm. Similarly, two signals for the methyl and methine carbon of the acetylacetone moiety have also been observed at 24.79– 26.35 and 100.43-100.56 ppm, respectively.

Attempts to grow crystals of the complexes suitable for X-ray analysis were failed. In the absence of single crystal X-ray structures, it is hard to state on the solid state

structure of the complexes. However, on the basis of the above mentioned spectral studies following are the possible structures of the compounds (Fig.4.1).

(1)   **(2)**
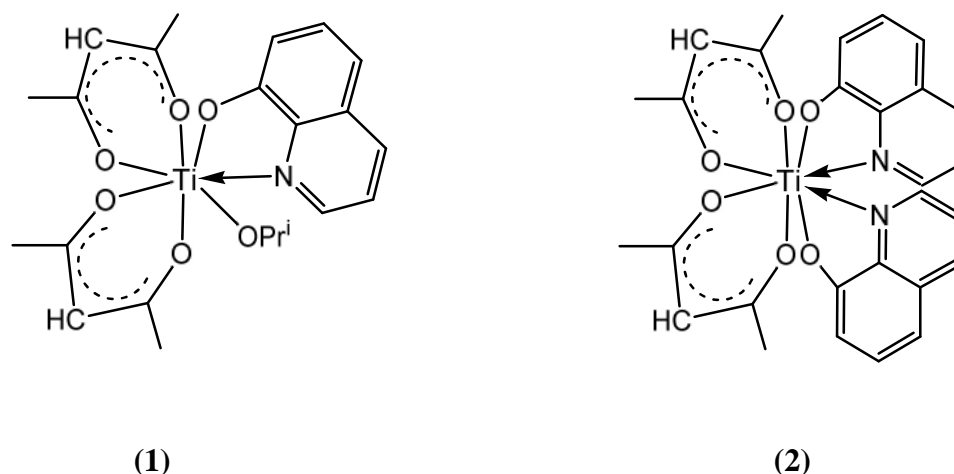
Figure 4.1 Proposed structures for complexes (1) & (2)

4.4 Hydrolytic studies of [Ti{OPr^i}$_4$], [{acac}$_2$Ti{OPr^i}{ONC$_9$H$_6$}] (1) and [{acac}$_2$Ti{ONC$_9$H$_6$}$_2$] (2), using low temperature sol-gel route in organic medium

[Ti{OPr^i}$_4$ and Precursors **(1)** and **(2)** were hydrolyzed via low temperature aqueous sol-gel method in organic medium to get titania samples **(a), (b)** and **(c),** respectively. Schematic representation of the hydrolytic process is depicted in fig. 4.2.
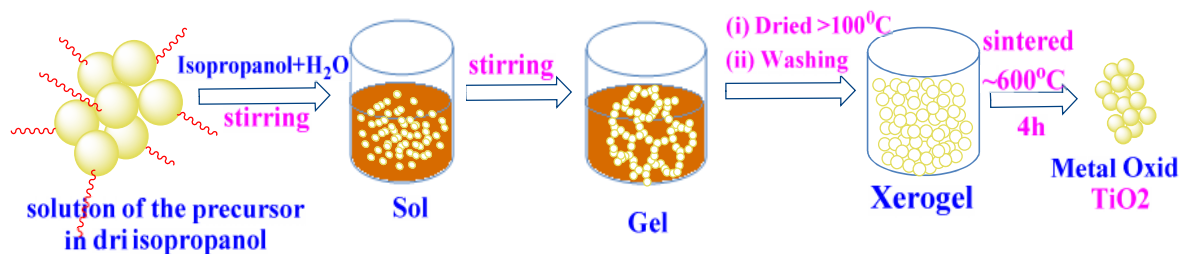
Figure 4.2 Schematic representation of the hydrolytic process

XRD patterns of the formed titania samples (a), (b) and (c) along with standard pattern (JCPDF # 89-4921) have been shown in Fig. 4.3, suggest the formation of anatase phase of pure titania in all the three samples [32]. The lattice parameters calculated area, a = b = c = 5.129 Å and the average crystallite size of titania samples were calculated from the (101) and (200) reflections ~26.47 nm for sample (a), 11.70 nm for sample (b) and ~8.25 nm for sample (c), using Debye Scherrer equation [33]. The observed values of 2 for the main peaks in the XRD patterns of titania samples, d spacing as well as their analogous hkl planes are shown in Table-4.5. The crystallite size of oxides indicates that, the substitution of isopropoxy group by the chelating ligand in the precursor molecule tends to decrease particle size of the titania. The shifting in the peaks in sample (b) and (c) can be seen towards low 2 values due to accumulation of strains in the samples due to presence of the finer particles and smaller crystallites in the samples than sample (a).

Further samples (**b**) and (**c**) were characterized by transmission electron microscopy (TEM) and the selected area electron diffraction (SAED) shown in Fig. 5. The TEM images of the samples (**a**), (**b**) and (**c**) reveal the spherical nano-sized crystallites formation of titanium oxides of average particle size ~ 15 nm, ~ 9 nm & ~ 7 nm, respectively. The SAED patterns of samples (**b**) and (**c**) indicate that both the oxides are poly-crystalline in nature. All these results obtained from TEM and SAED supported the findings acquired from XRD data. The size of crystallite obtained from the XRD data was a little higher than the size of crystal calculated from TEM analysis due to presence of stresses in the samples.

The surface morphology of all prepared samples was investigated by SEM images (Fig. 4.4). SEM micrograph of all the samples (a), (b) and (c) indicated the formation of agglomerated granular morphology formed by nano-sized particles. Though, particle size in all the samples is of sub-micron range. Energy dispersive X-ray (EDX) analyses were also performed which indicated the formation of pure TiO_2 (Fig.4.5). The particle size in the sample (b) and (c) is much lesser than the particle size in sample (a) as can be seen in Fig.4. The reduction in particle size is due to presence of the branched chelating agents in the modified precursors, not allowing growth of titania nuclei thus inhibiting the increase in particle size.The morphology of the particles in sample (b) and (c) is granular than

flake-shaped in sample (a). The granular morphology is due to stabilizing the surface energy of the formed nuclei to particles very swiftly under the influence of chelating agents which was not present in the precursor of the sample (a).The particle size in the sample (a) is ~ 1μm approximately where in sample (b) and (c), the particle size is ~ 100 nm.

The formation of anatase phase of the titanaia samples was further confirmed by IR spectral studies. The bands around at 400-800 cm $^{-1}$ are appeared due to O-Ti-O vibrations in all the sample (a), (b) and (c) in IR spectra as shown in Fig. 6 [18]. In sample (a) and (b) bands appeared at 470□cm $^{-1}$ and 730□cm $^{-1}$ and in sample (c) bands appeared at 479□cm^{-1} and 682□cm^{-1} are the characteristic of O–Ti–O bonding in contributions of the anatase TiO_2 nanoparticles [18]. The (-OH) absorption in the region of 3,450 cm^{-1} and 1,633 cm^{-1} in sample (a) and (b) indicate the stretching and bending vibrations, due to the absorption of moisture, possibly owing to the atmospheric H_2O, which could be adsorbed during the preparation and processing of FTIR samples in the ambient atmosphere [32]. There is no peak in this range was observed for sample (c) showing absence of moisture in sample (c). Absence of the peak around at 2900□cm $^{-1}$regarding C–H stretching bands, indicate that all organic compounds were removed from all the samples after calcinations.

The absorption spectra of samples (a), (b) and (c) shown in Fig. 4.7 illustrates excellent UV absorption bands for these samples and are in good agreement with anatase titania as reported in literature [18]. Energy band gaps of all the titania samples have been determined with the help of Tauc relation [34]:

$$(h)^n = (h - E_g)A$$

Here, represents an absorption coefficient, Eg is band gap, is the frequency of incident light and h signifies Plank's constant. Graph plotted for h against (h)^2 shown in Fig. 4.8. All the titania (a), (b) and (c) exhibit energy band gaps 2.9 , 3 and 3.1eV, respectively. According to Brus approximation the energy band gap is inversely proportional to the size of the particles [35]. Therefore here, raised energy band gap proposes decrease in the size of nano particles. At nano scale each particle is constituted

of very few atoms, subsequently when the size of the particle decreases, the number of energy levels overlapping tends to decrease resulting in finer width of the band and this causes rise in energy gap between the valence band and the conduction band. The results confirm the synthesis of semiconducting nanoparticles [36]. It also suggests possible synthesis of titania nanoparticles with varied bandgaps.

Table 4.2 Some important IR spectral data (cm^{-1}) assigned for 8-hydroxyquinoline complexes of titanium (IV)bis(acetylacetonate)diisopropoxide

Complex	Acetylacetonate moity		Isopropoxy moiety	8-hydroxyquinoline moiety				
	(C-O)	(C-C)	(C-O)	(C-H)	(C=C)/(C=N)	(Ar-O)	(Ti-O)	(Ti-N)
[{acac}$_2$Ti{OPr^i}{ONC$_9$H$_6$}] , [1]	1490	1445	1015	3050 (m)	1585/1545 (s)	1110 (m)	644 (s)	535 (vs)
[{acac}$_2$Ti{ONC$_9$H$_6$}$_2$], [2]	1505	1460	-	3040 (m)	1595/1560 (s)	1115 (m)	650 (s)	540 (vs)

(vs= very strong, s= strong, m= medium)

Table 4.3 ^{1}H NMR data (ppm) for for 8-hydroxyquinoline complexes of titanium(IV)bis(acetylacetonate)diisopropoxide

Compound	Acetylacetonate moiety		Isopropoxy moiety		8-hydroxyquinoline moiety			
	-CH$_3$	-CH	CH$_3$	-OCH<	CH(2)	CH(7)	OH	Other aromatic protons
[{acac}$_2$Ti{OPr^i} {ONC$_9$H$_6$}], **[1]**	2.02, 2.14 (d, 12H)	5.70 (s, 2H)	1.21-1.25 (d, 6H) merged	4.72-4.74 (m, 1H)	8.05,d(1H)	8.22, d(1H)	-	7.21-7.49, m(4H)
[{acac}$_2$Ti{ONC$_9$H$_6$}$_2$], **[2]**	2.07, 2.15 (d, 12H)	5.48 (s, 2H)	-	-	8.02,d(2H)	8.64, d(2H)	-	7.40-7.45, m(8H)

s = singlet; d = doublet; m = multiplet

Table 4.4 $^{13}C\{^1H\}$ NMR data (ppm) for 8-hydroxyquinoline complexes of titanium(IV)bis(acetylacetonate)diisopropoxide

Compound	Acetylacetonate moiety			Isopropoxy moiety		Ligand moiety (8-hydroxyquinoline)			
	-CH$_3$	-CH	-CO	-CH$_3$	-OCH<	C (8)	C(9)	C (2)	Other aromatic carbons
[{acac}$_2$Ti{OPr^i} {ONC$_9$H$_6$}] [1]	26.35	100.56	191.31	24.95	64.53	162.96	146.40	138.91	129.83 (C-4), 129.53 (C-10), 128.41 (C-6), 121.91 (C-3), 117.40 (C-5), 111.14 (C-7)
[{acac}$_2$Ti{ONC$_9$H$_6$}$_2$] [2]	24.79	100.43	191.15	-	-	162.78	144.73	136.98	129.34 (C-4), 129.18 (C-10), 128.12 (C-6), 120.60 (C-3), 114.50 (C-5), 111.20 (C-7)

Table 4.5 XRD data of titania samples (a), (b) and (c)

Titania	XRD data			
(TiO$_2$)	2	d(Å)	hkl	crystal type
(a)	25.551	3.4841	101	Tetragonal
	47.947	1.8958	200	
(b)	24.706	3.6006	101	Tetragonal
	47.531	1.9114	200	
(c)	25.648	3.4705	101	Tetragonal
	48.335	1.8815	200	
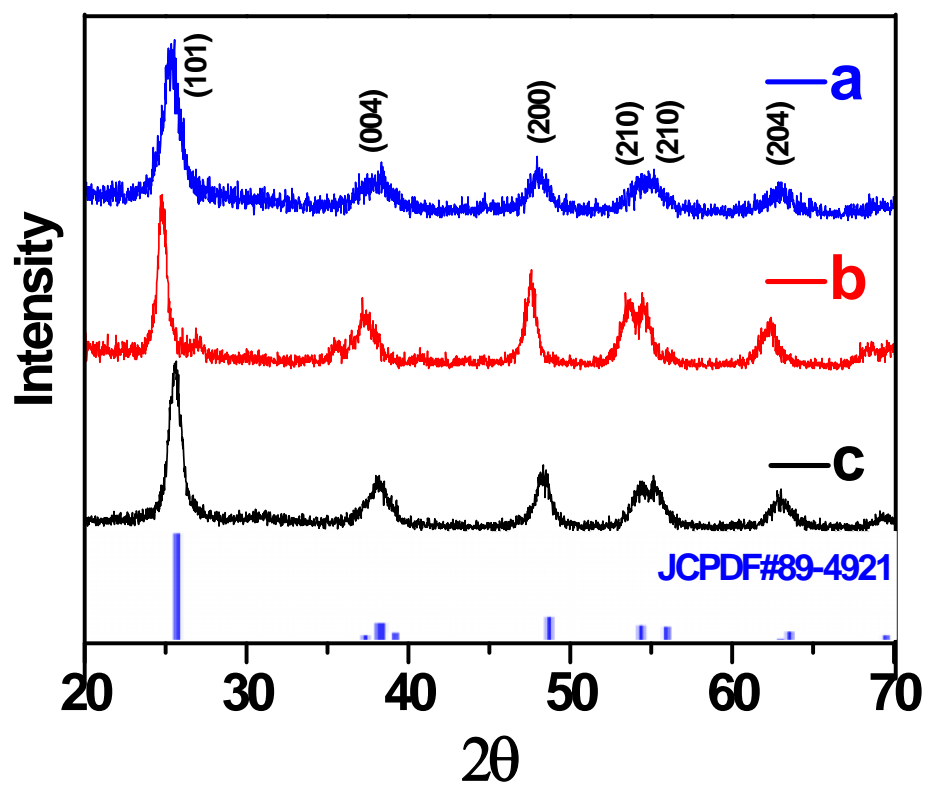
Figure 4.3 XRD patterns of titania samples (a), (b), (c) and reference pattern PDF# 89-4921
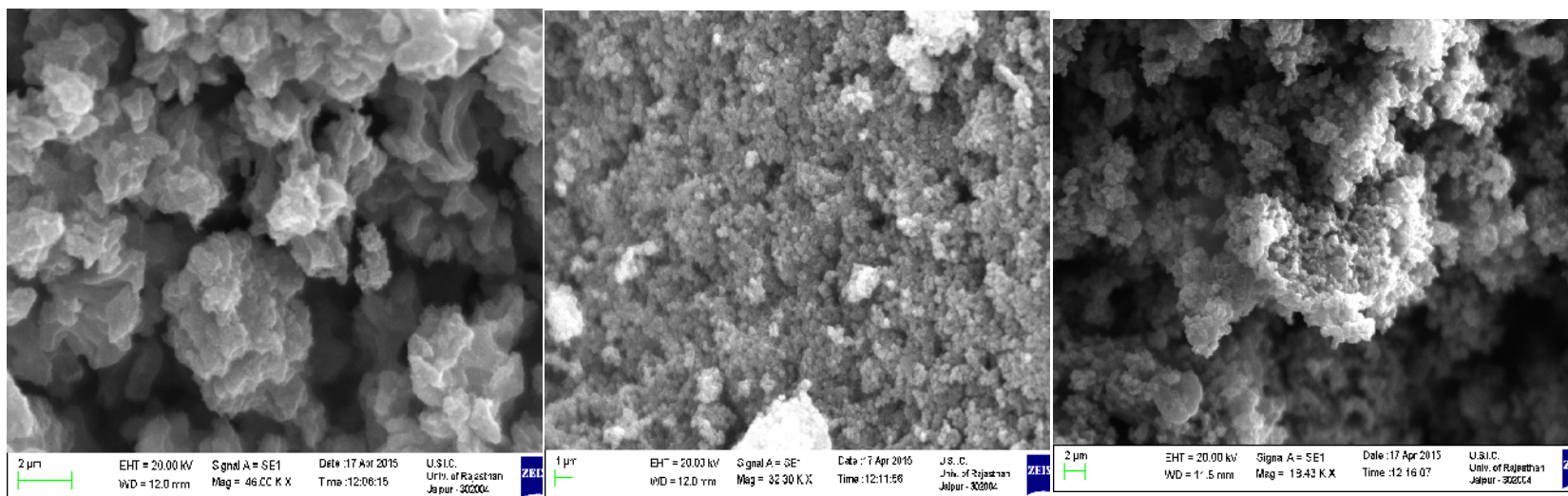
(**a**)   (**b**)   (**c**)

Figure 4.4 SEM image of titania samples (a), (b) and (c)
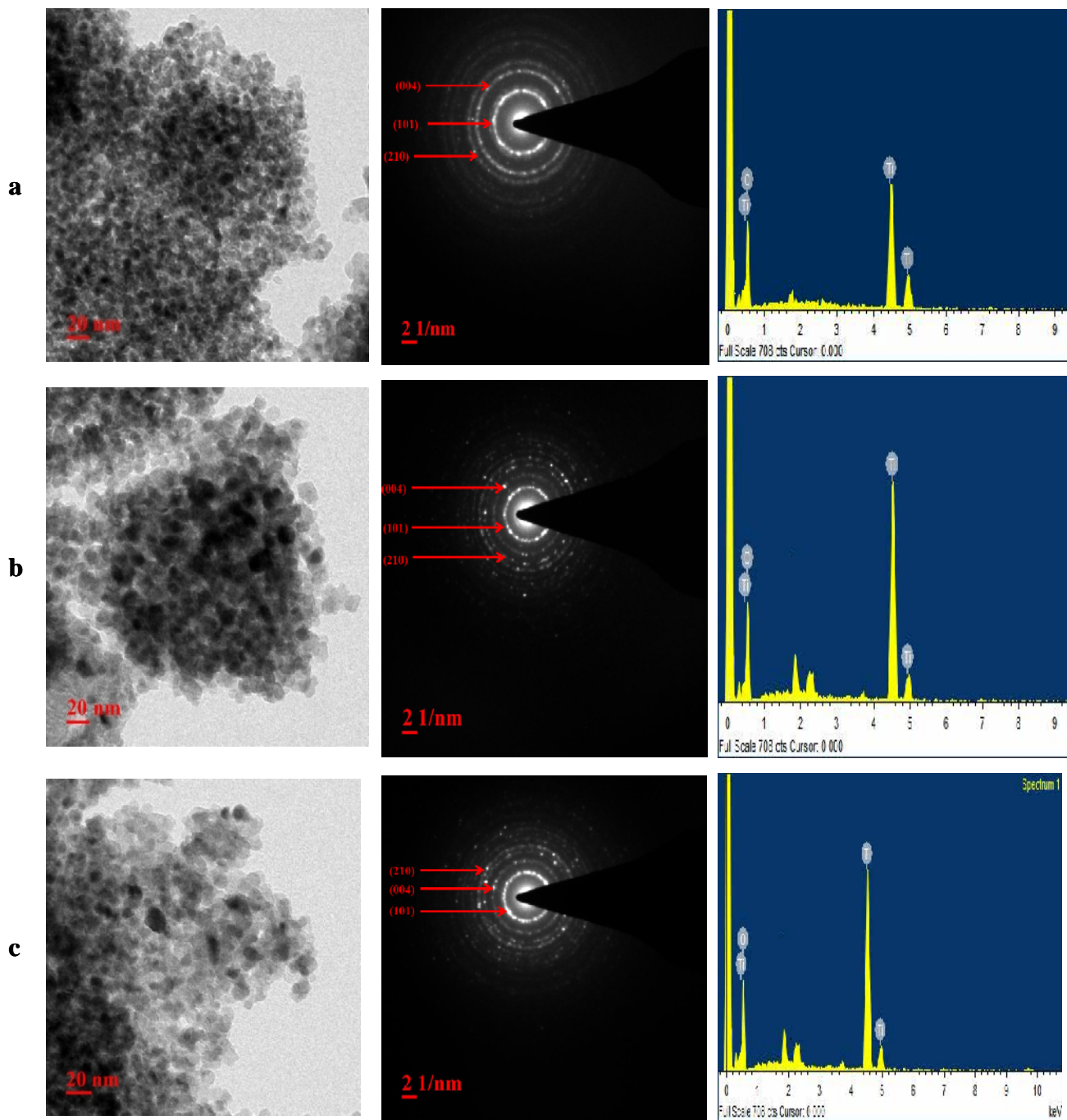
Figure 4.5 TEM, SAED patterns and EDX images of sample **(a),** (**b**) & (**c**) of nano-sized titania obtained from sol–gel transformation
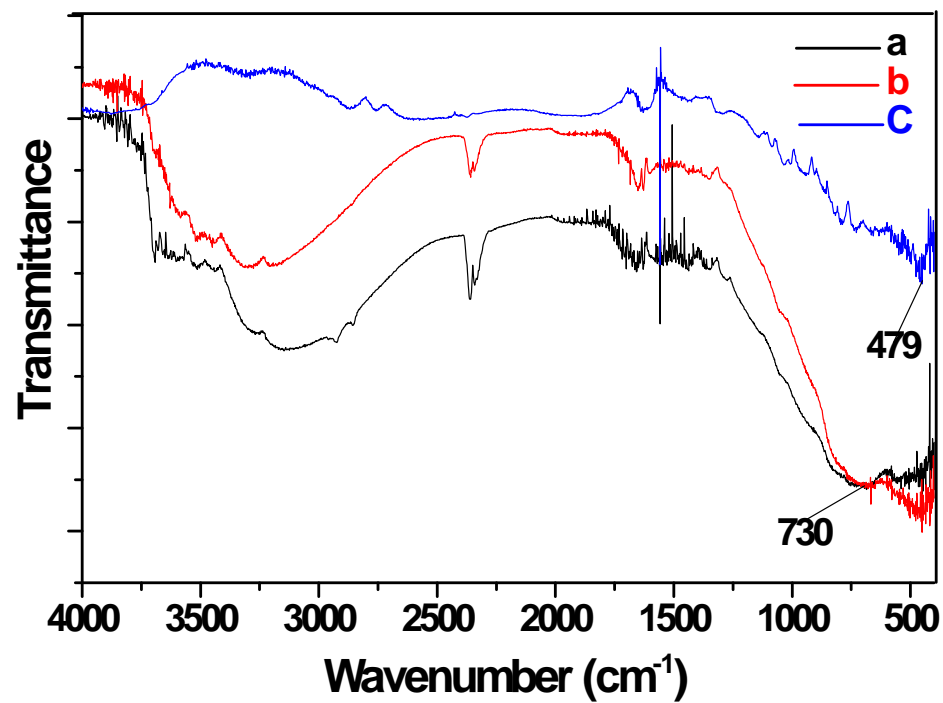
Figure 4.6 IR patterns of titania samples (a), (b) and (c)
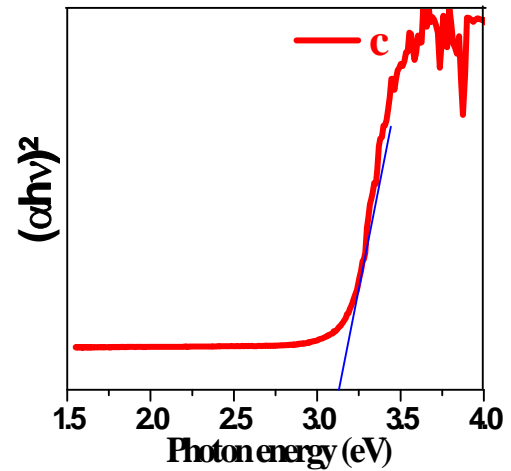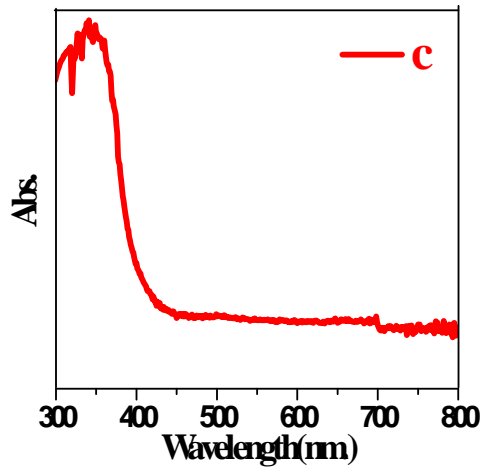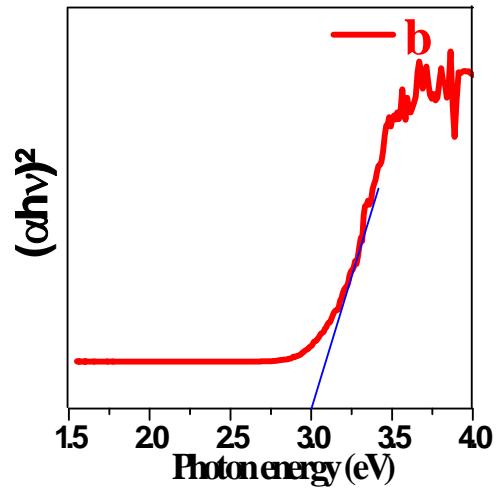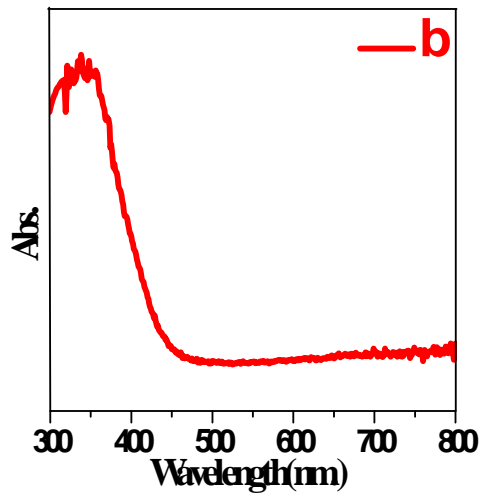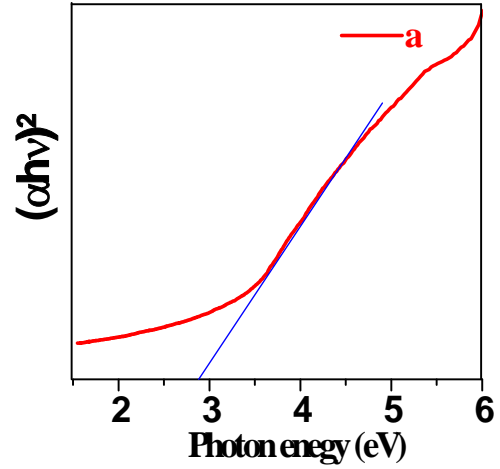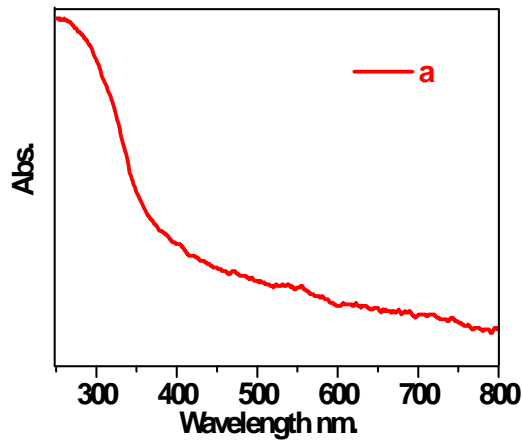
Figure 4.7 Absorption spectra of titania samples (a), (b) and (c)

Figure 4.8 Plot of h vs (h)^2 of titania samples (a), (b) and (c)
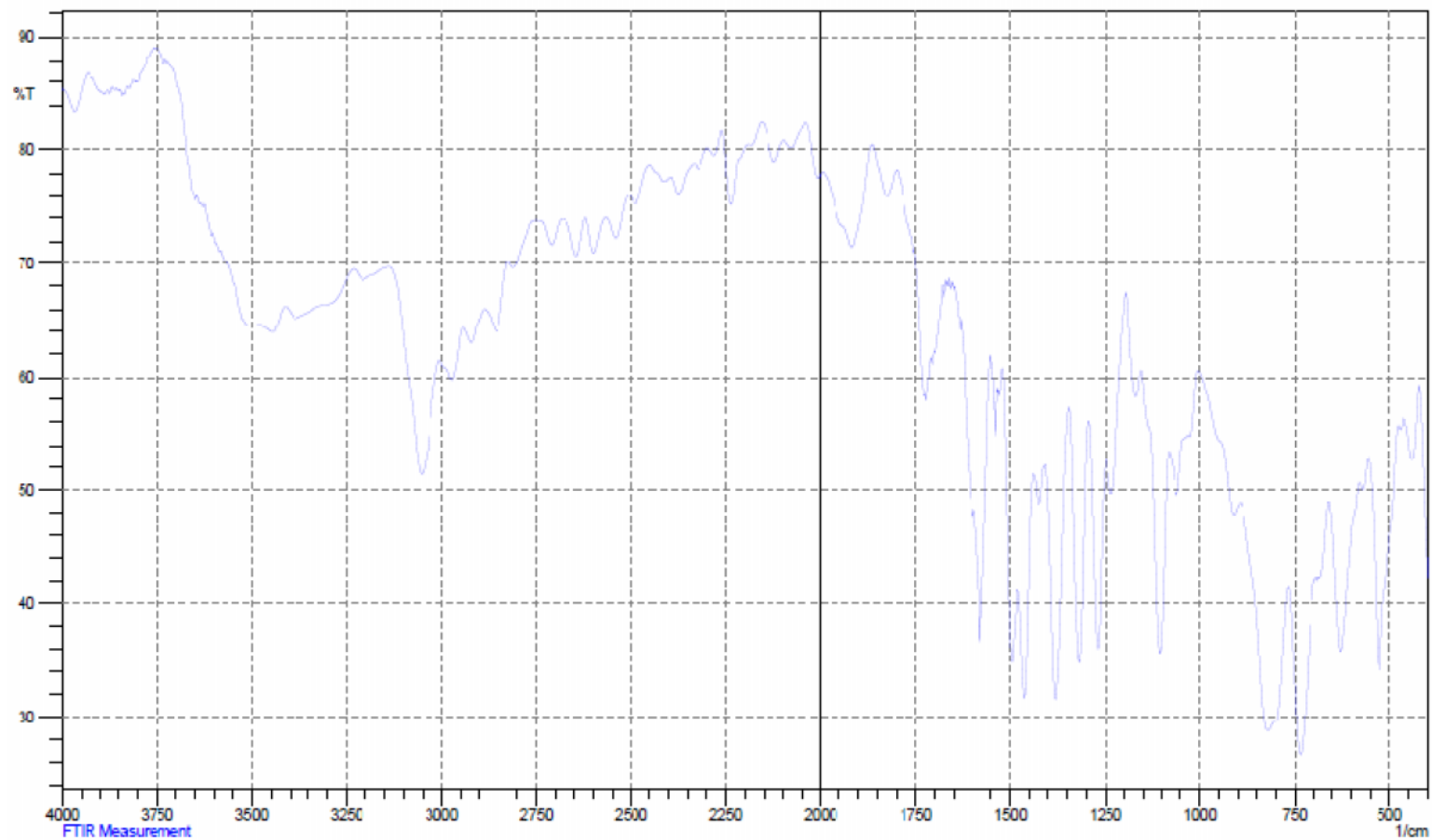
Figure 4.9 FT-IR spectra of the complex Titanium isopropoxide acetylacetonate 8-hydroxy quinolinate (1)
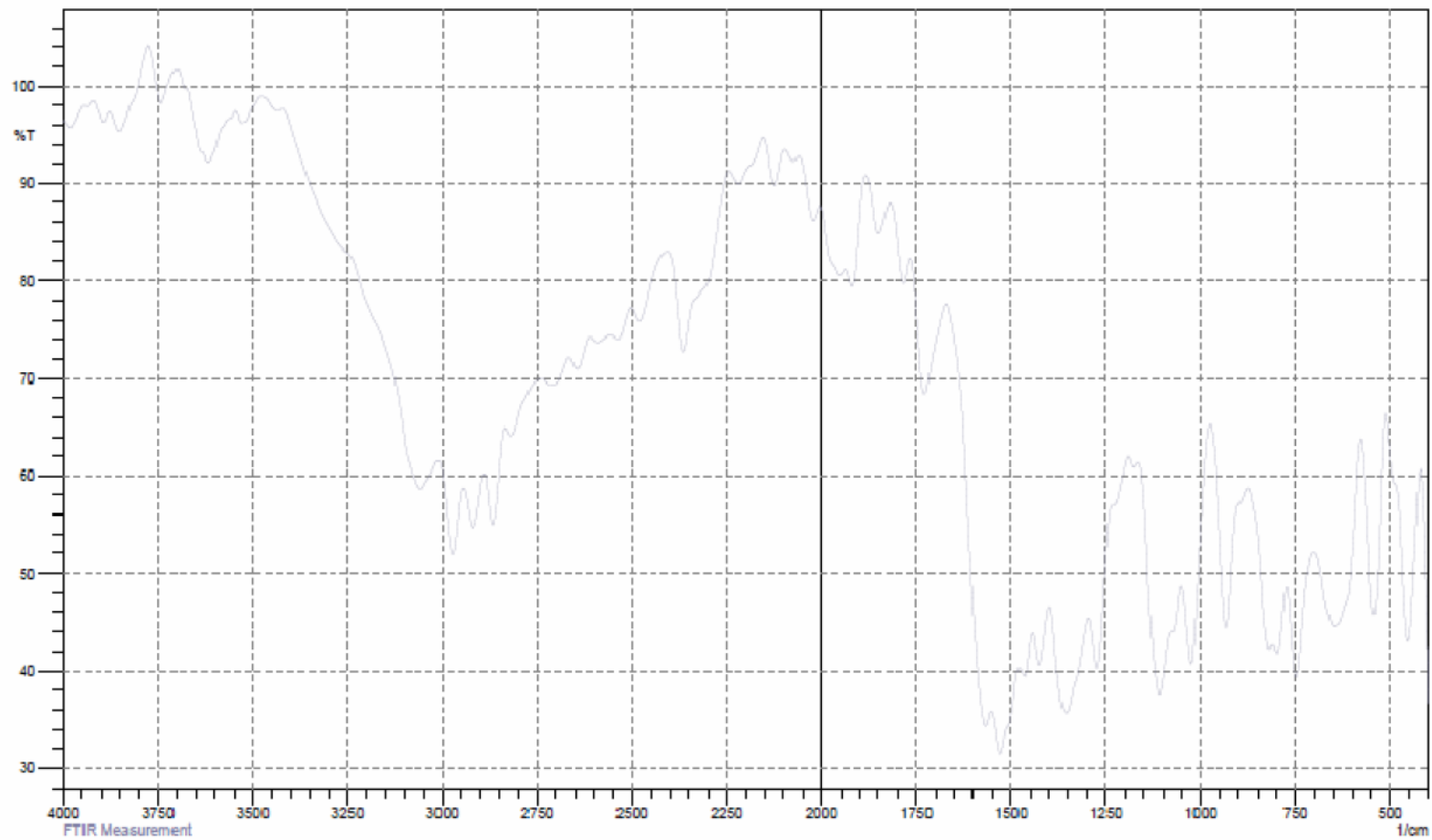
Figure 4.10 FT-IR spectra of the complex Titanium isopropoxide acetylacetonate bis (8-hydroxy quinolinate) (2)
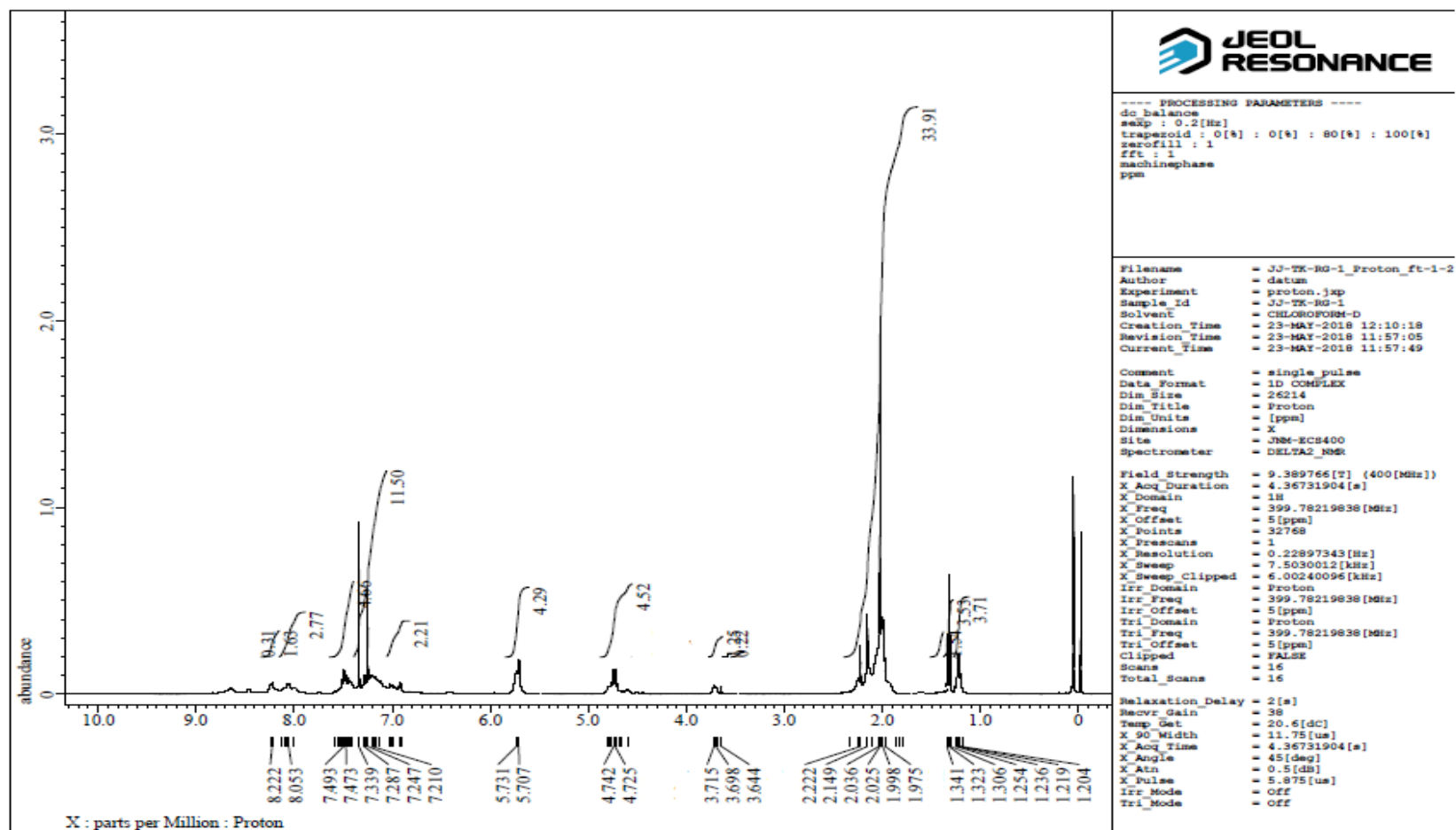
Figure 4.11 ^{1}H NMR spectra of the complex Titanium isopropoxide acetylacetonate 8-hydroxy quinolinate (1) in CDCl$_3$
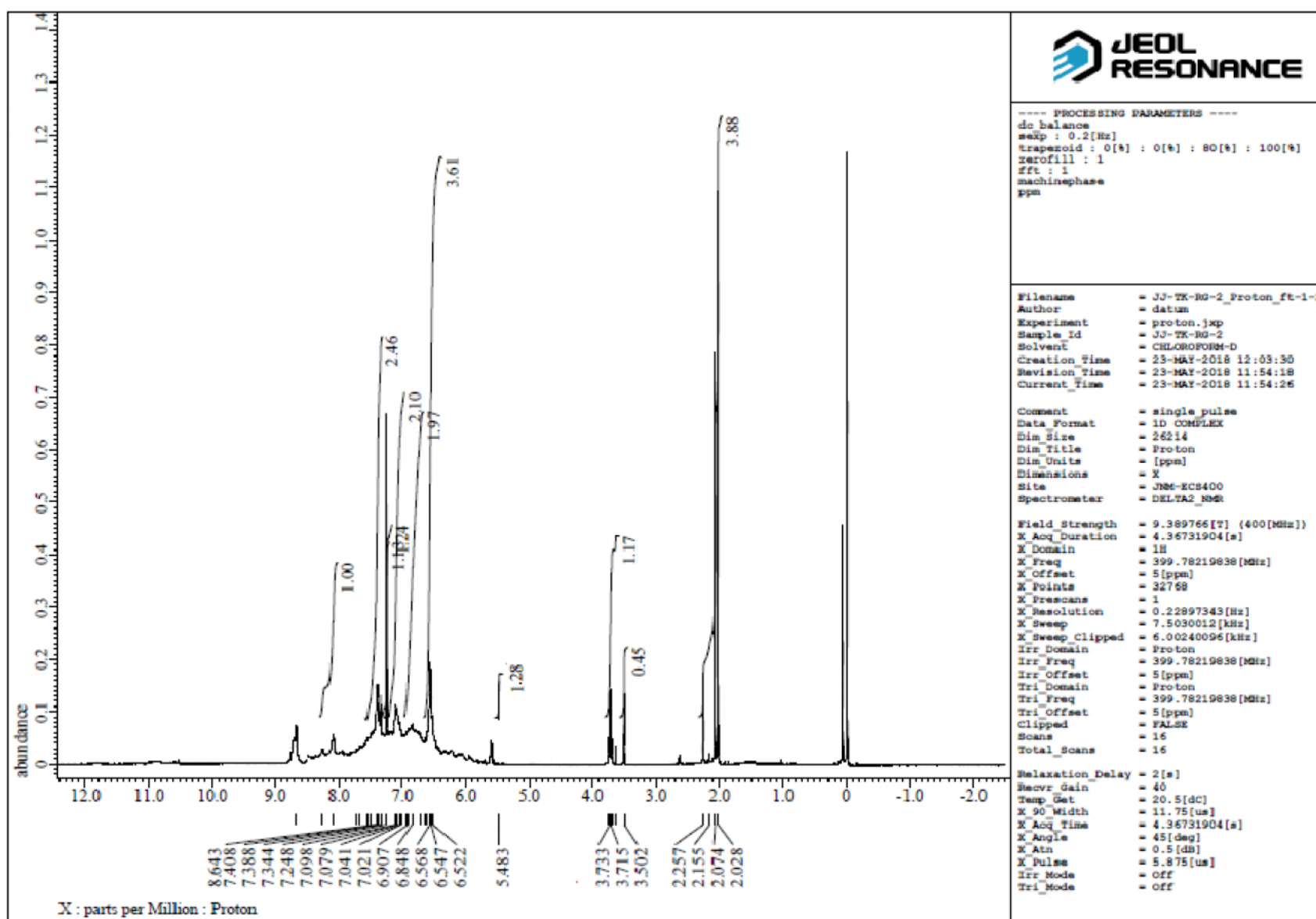
Figure 4.12 ^{1}H NMR spectra of the complex Titanium acetylacetonate bis (8-hydroxy quinolinate) (2) in CDCl$_3$
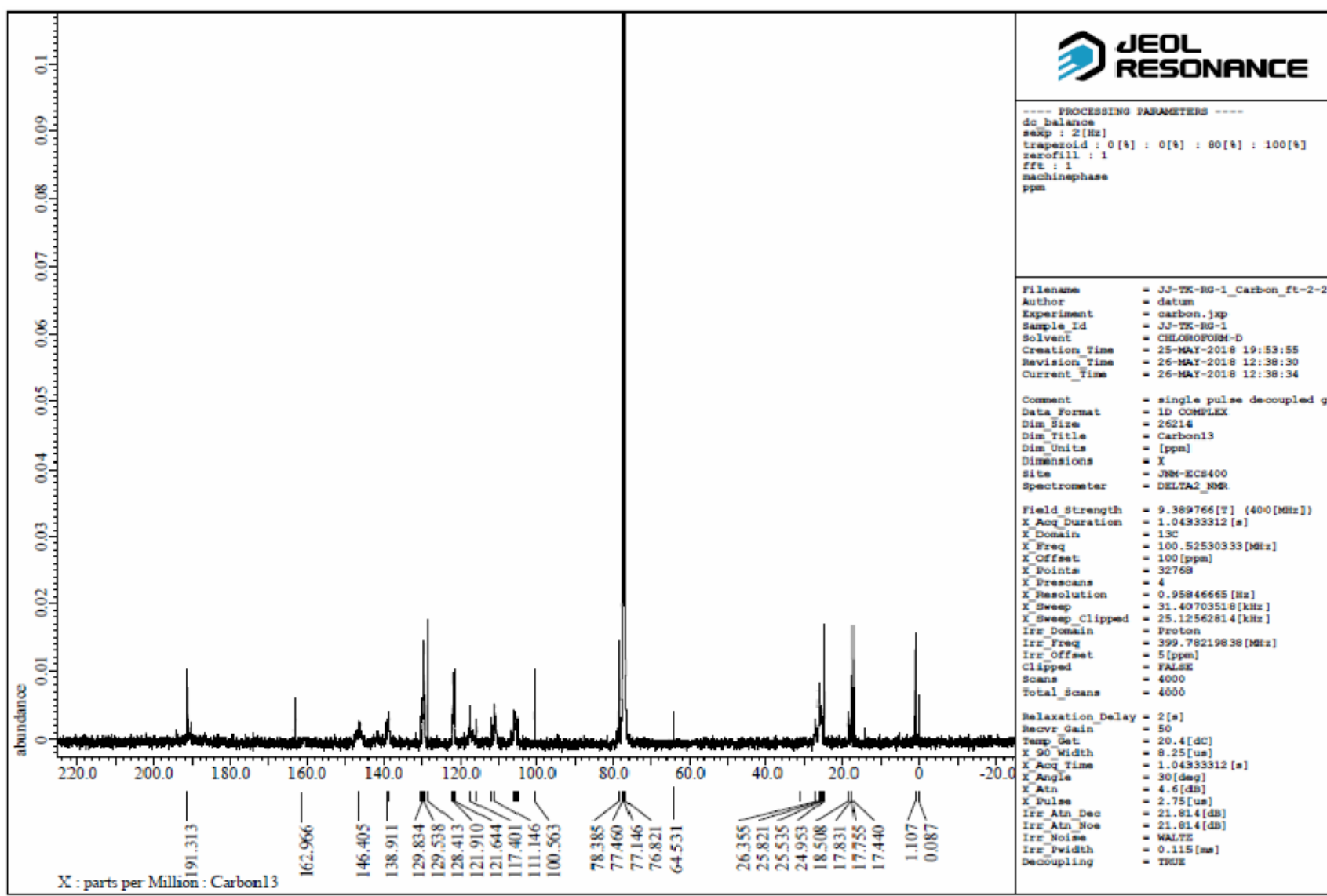
Figure 4.13 ^{13}C NMR spectra of the complex Titanium isopropoxide acetylacetonate 8-hydroxy quinolinate (1) in CDCl$_3$
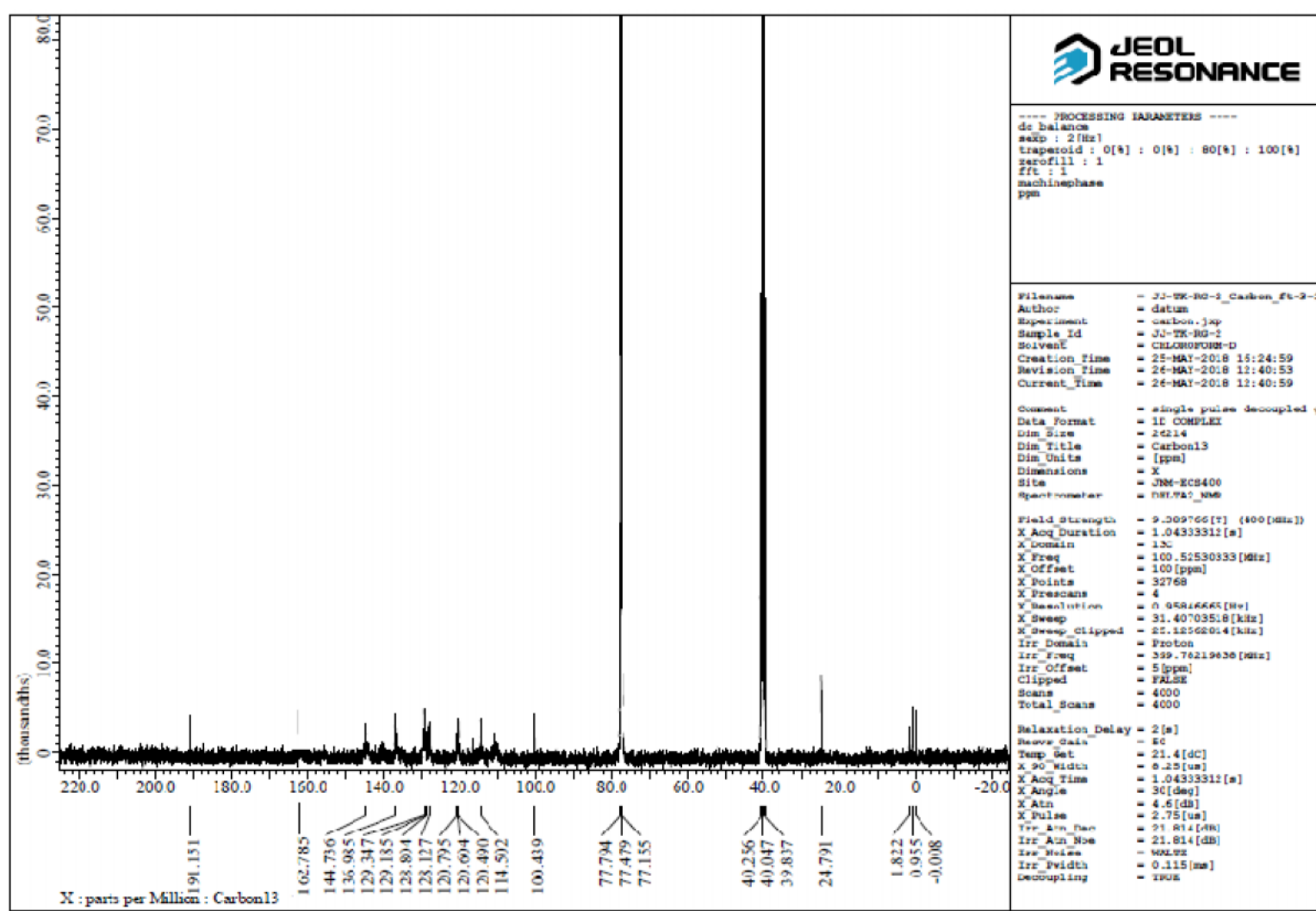
Figure 4.14 ^{13}C NMR spectra of the complex Titanium isopropoxide acetylacetonate 8-hydroxy quinolinate (1) in CDCl$_3$

4.5 References

[1] R. Zhang, A.A. Elzatahry, S.S. Al-Deyab, D. Zhao, Nano Today. 7 (2012) 344-366.

[2] J. Bai, B. Zhou, Chem. Rev. 114 (2014) 10131-10176.

[3] W. Maziarz, A. Kusior, A. Trenczek-Zajac, Beilstein J. Nanotechnol. 7 (2016) 1718- 1726.

[4] M. Pagliaro, G. Palmisano, R. Ciriminna, V. Loddo, Energy Environ. Sci. 2 (2009) 838- 844.

[5] F.U. Rehman, C. Zhao, H. Jiang, X. Wang, Biomater. Sci. 4 (2016) 40-54.

[6] H. Kisch, G. Burgeth, W. Macyk, Adv. Inorg. Chem. 56 (2004) 241-259.

[7] D.A.H. Hanaor, C.C. Sorrell, J Mater. Sci. 46 (2011) 855-874.

[8] U. Schubert, Acc. Chem. Res. 40 (2007) 730-737.

[9] M. Niederberger, Acc. Chem. Res. 40 (2007) 793-800.

[10] M. Rehan, X. Lai, G.M. Kale, Cryst. Eng. Comm. 13 (2011) 3725-3732.

[11] R. Gegova, Y. Dimitriev, A. Bachvarova-Nedelcheva, R. Iordanova, A. Loukanov, T. Iliev, J. Chem. Technol. Metall. 48(2) (2013) 147-153.

[12] J.C. Colmenares, E. Kuna, P. Lisowski, Top Curr. Chem.(Z) 59 (2016) 374-375.

[13] S. Ding, X. Yin, X. Lu , Y. Wang, F. Huang, D. Wan, ACS Appl. Mater. Interfaces. 4 (2012) 306-311.

[14] H. Yao, M. Fan, Y. Wang, G. Luo, W. Fei, J. Mater. Chem. A 3 (2015) 17511-17524.

[15] S. Sakka, (eds) Handbook of sol-gel science and technology: Characterization and properties of sol-gel materials and products. Springer, Switzerland (2005)

[16] V.G. Kessler, G.I. Spijksma, G.A. Seisenbaeva, S. Hakansson, D.H.A. Blank, H.J.M. Bouwmeester, J. Sol-Gel Sci. Technol. 40 (2006) 163-179.

[17] U. Schubert, J. Mater. Chem. 15 (2005) 3701-3715.

[18] A. Chaudhary, V. Dhayal, M. Nagar, R. Bohra, S.M. Mobin, P. Mathur, Polyhedron. 30 (2011) 821-831.

[19] E.A. Olevsky, R. Bordia, (eds) Advances in sintering science and technology. John Wiley & Sons, (2010) p.211.

[20] B. Basu, K. Balani, (eds) Advanced Structural Ceramics. John Wiley & Sons,

(2011).

[21] V. Dhayal, A. Chaudhary, B.L. Choudhary, M. Nagar, R. Bohra, S.M. Mobin, P. Mathur, Dalton Trans. 41 (2012) 9439-9450.

[22] J. Livage, M. Henry, C. Sanchez, Prog. Solid State Chem. 18 (1988) 259.

[23] L.L. Hench, J.K. West, Chem. Rev. 90 (1990) 33-72.

[24] D.C. Bradley, R.C. Mehrotra, I.P. Rothwell, A. Singh, (eds) Alkoxo and aryloxo derivatives of metals. Academic Press, London (2001)

[25] A. R. Sanwaria, N. Sharma, A. Chaudhary, M. Nagar, J. Sol-Gel Sci. Technol. 68 (2013) 245-253.

[26] R. Gopal, J. Jain, A. Goyal, D.K. Gupta, M. Nagar, J. Aust. Ceram. Soc. doi.org/10.1007/s41779-018-0198-z

[27] A .I. Vogel, A Text Book of Quantitative Inorganic Analysis fifth ed. Longman, London (1989).

[28] D.C. Bradley, D.C. Hancock, W. Wardlaw, J. Chem. Soc. (1952) 2773-2778.

[29] D.M. Puri, K.C. Pande, R.C. Mehrotra, J. Less Common Mets. 4 (1962) 393-398.

[30] D. C. Bradley, F.M. Abd-el-Halim, R.C. Mehrotra, W. Wardlaw, J. Chem. Soc. 0 (1952) 4609-4612.

[31] M. Pathak, R. Bohra, R.C. Mehrotra, Transit. Metal Chem. 28 (2003) 187-192.

[32] X. Tong, P. Yang, Y. Wang, Y. Qin, X. Guo, Nanoscale. 6 (2014) 6692-700.

[33] B. E. Warren, X-ray Diffraction (Chapter 13). Dover Publication, New York (1990) (eds).

[34] J. Tauc, Amorphous & liquid semiconductors. Plenum, New York (1974).

[35] W.L. Wilson, P.J. Szajowski, L.E. Brus, Science. 262 (1993) 1242-1244.

[36] M.-C. Daniel, D. Astruc, Chem. Rev. 104 (2004) 293–346.

5.1 Introduction

The design and synthesis of hybrid materials composed of organic–inorganic framework have involved significant attention in the field of chemistry due to their interesting structural aspect as well as their prospective applications in various fields such as medicine, electrical conductivity, photochemistry, surface phenomenon, magnetism and catalysis [1-4].

Ionic compounds comprising of organic cations in combination with inorganic anions bearing typically diffused charges which have low melting points are often termed as ionic liquids (ILs) [5]. Ionic liquids have shown to exhibit numerous distinctive properties, for instance high thermal stability, exceptionally low vapour pressure, wide range of liquid-state temperature and non-flammability [6, 7]. Due to these prosperities currently ionic liquids are broadly used in several areas of electrochemistry and various other branches of chemistry including organic synthesis and biochemistry [8-13].

Pendleton et. al. in 2015 published a review study paying attention to the potential of ionic liquids in the field of biological activity [14]. Antimicrobial activities of ionic liquids were well explored for Bacteria due to short time required for their generation in comparison to other living micro organisms [15, 16]. This study revealed that several ionic liquids exhibit potential anti-bacterial activity. Roslonki ewicz et al. [17] and Pernak et al. [18] have also studied antibacterial activity of ionic liquids against a variety of bacteria and identified a tendency of increase in antibacterial activity with the increase in the length of alkyl chain substituent present in the cationic organic part of the compound [19, 20].

Among various ionic liquids studied to date mostly are derived from organic cations like pyridinium or imidazolium in combination with simple inorganic anions, for instance chloride (Cl^-), pentafluorophosphate (PF_6^-), bis(trifluoromethanesulfonyl) amide (NTf_2^-) etc. These ionic liquids do not show adequate thermal stability which is required for their use in gas chromatography. In order to advance the thermal stability, a number of ionic compounds have been designed by connecting two cationic moieties resulting in a dication which is charge satisfied by simple anions, these type of ionic salts are called as

dicationic ionic liquids [21,22]. It has been observed that thermal stability of these dicationic ionic salts is considerably enhanced. Even though most of these dicationic salts have melting points more than 100 ˚C, still for simplicity they are termed as ionic liquids [23, 24]. Above mentioned dicationic ionic liquids could be classified in two categories one is germinal, in which two linked monocations forming a dication are identical, such as a dication formed by bridging two imidazolium with alkyl or ether bridge. Another category is unsymmetrical, where two different monocations are present such as, imidazolium and pyridinium ions linked with spacer groups.

1,1'-(propane-1,3-diyl)bis(pyridin-1-ium)   1-(3-(1-methyl-1*H*-imidazol-3-ium-3-yl)propyl)
bromide   pyridin-1-ium bromide

(1)   (2)
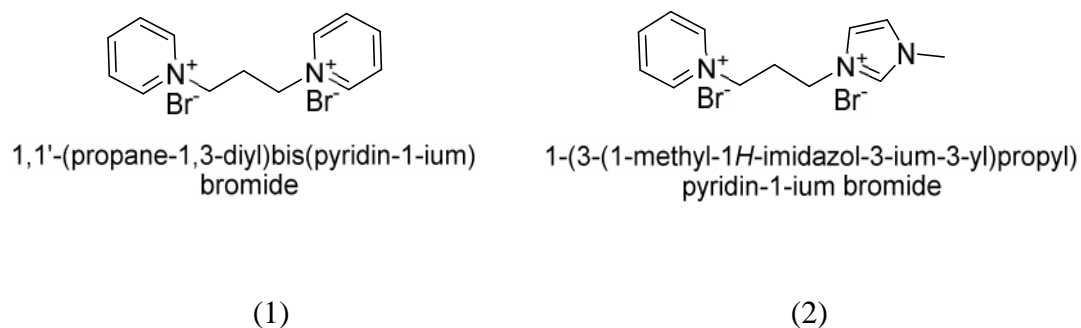
Figure 5.1 (1) Geminal ionic liquid & (2) Unsymmetrical ionic liquid

It has been reported that geminal ionic liquids which have symmetrical cationic surfactants bears specific properties and have potential applicability in several fields. Moreover, studies have shown that the variation in chain length of spacer groups and the aliphatic chains drastically affect the properties of Gemini ionic liquids [25]. Even though several geminal ionic liquids containing spacer groups of different chain length have been reported [11, 14, 26], geminal ionic liquids having longer aliphatic chains have not been investigated much. Therefore designing of different types of geminal ionic liquids as well as investigating their applications in various fields is an interesting area of research.

Hence, we have attempted synthesis and antimicrobial study of the new type of geminal ionic liquids having varied alkyl chain length. Here, we report the synthesis, structural characterization and in-vitro antimicrobial activities of 8-hydroxyquinolenium based cyclic geminal Dicationic Ionic Liquids.

5.2 Experimental

5.2.1 Material and methods

All the reagents and solvents in used of the best grade available and were used without further purification. Precursors (PMOQ, HMOQ & BQOP) were prepared using previously reported method [20]. IR spectra were recorded as dry KBr pellets on a Perkin Elmer Ultra Two, FT-IR spectrometer [4,000–400 cm^{-1}]. ^{1}H NMR data were collected on JEOL FX 300 FT-NMR spectrometer in CDCl$_3$ and DMSO-d$_6$ solution at 400.4 MHz frequency. ESI-mass spectrums were obtained on Xevo G2-SQ TOF Waters, USA spectrometer in the electron spray mode, using methanol solvent. X-ray crystal structures were performed on Bruker APEX-II CCD system. The elemental analyses were performed on a Thermo Scientific Flash 2000. The absorption spectra of compounds (200-800 nm) were recorded in methanol using Perkin Elmer, Lambda 750, UV–Vis spectrophotometer.

5.2.2 Synthesis of bromide anions salt containing geminal dications $[(C_9H_6NO)_2(CH_2)_3]^{2-}2Br^-$ (1)

1, 3-Bis(8-quinoxy propane) (PMOQ) synthesized by previously reported method [27]. The excess amount of dibromopropane was added to the solution of compound (PMOQ) (0.447 g, 1.35 mmol) and refluxed with stirring at 110°C for 8 hr. After stirring this reaction mixture, a yellow coloured precipitate was filtered off and rinsed with ethyl acetate followed by hexane several times to obtain pure compound (1).

The synthetic and analytical details are summarized below:

$[(C_9H_6NO)_2(CH_2)_3]^{2+}2Br^-]$ **[1]:** Yellow solid, yield 88%, mp 240°C, soluble in chloroform, DMSO, DMF, methanol, and ethanol. C$_{24}$H$_{24}$N$_2$O$_2$Br$_2$: % Found (Calculated): C 54.34 (54.56), H 4.41 (4.55), N 5.21 (5.26); FT-IR, , cm–1: 1599 (C=N); 1535 (C=Car,asym); 1463 (C=Car, sym); 1390 (C-N-alkyl chain); 1285(C-O-alkyl chain); 1110(C-Oar). ^{1}H NMR (300.13 MHz, DMSO d$_6$, at 25°C, ppm): 9.46 (d, H, H^2); 9.45 (d, H, H^4); 8.82 (dd, H, H^3); 7.84-7.87 (m, 3H, aromatic); 3.46 (t, 2H, H^{11}); 2.35 (m, 2H,

H^{12}); 5.14 (t, 2H, H^{14}); 2.89 (m, 2H, H^{15}). ^{13}C NMR (DMSO-d$_6$): 21.149 (C^{13}); 28.45 (C^{15}), 59.34 (C^{14}), 72.24 (C^{11}), 113.94 (C^7), 117.725 (C^5), 123.36 (C^3), 130.87 (C^6), 132.49 (C^{10}), 145.79 (C^4), 148.45(C^9), 150.22 (C^2), 152.49 (C^8). MS(ESI): 451 [M/z-Br]$^+$, 331 [(C$_9$H$_6$NO)$_2$(CH$_2$)$_3$]$^+$, 255 [(C$_9$H$_6$NO)(CH$_2$)$_3$(C$_3$H$_3$N)]$^+$, 227 [(C$_9$H$_6$NO)(CH$_2$)$_3$(C$_2$H)]$^+$, 186 [(C$_9$H$_6$NO)(CH$_2$)$_3$]$^+$, 158 [(C$_9$H$_6$NO)CH$_2$]$^+$, 146 [(C$_9$H$_6$NO)]$^+$.

5.2.3 Synthesis of bromide anions salt containing geminal dications [(C$_9$H$_6$NO)$_2$(CH$_2$)$_6$]$^{2-}$ 2Br$^-$ (2)

Synthesis of compound 1, 6-Bis(8-quinoxy hexane) (HMOQ) achieved by previously reported method [28].To synthesize geminal dications [(C$_9$H$_6$NO)$_2$(CH$_2$)$_6$]$^{2-}$2Br$^-$ (2), compound (HMOQ) (0.100g, 0.26 mmol) was added to excess amount of dibromohexane (3 ml) and this solution was stirred at 110°C for 8 hr. After stirring this reaction mixture, a pale yellow coloured precipitate was filtered off and washed several times with ethyl acetate and hexane to obtain pure compound (**2**).

[(C$_9$H$_6$NO)$_2$(CH$_2$)$_6$]$^{2-}$2Br$^-$ [2]: Yellow solid, yield 82%, mp 200°C, soluble in chloroform, toluene, DMSO, DMF, methanol, and ethanol. C$_{30}$H$_{36}$N$_2$O$_2$Br$_2$: % Found (Calculated): C 58.39 (58.45), H 5.81 (5.89), N 4.51 (4.54); FT-IR, , cm–1: 1598 (C=N); 1535 (C=Car,asym); 1460 (C=Car, sym); 1385 (C-N-alkyl chain); 1283 (C-O-alkyl chain); 1111 (C-Oar). ^{1}H NMR (300.13 MHz, DMSO d$_6$, at 25°C, ppm): 9.48 (d, H, H^2); 9.42 (d, H, H^4); 9.18 (dd, H, H^3); 7.78-7.96 (m, 3H, aromatic); 4.32 (t, 2H, H^{11}); 2.15 (m, 2H, H^{12}); 1.35 (m, 2H, H^{13}); 5.17 (t, 2H, H^{18}); 2.46 (m, 2H, H^{19}); 1.94 (m, 2H, H^{20}). ^{13}C NMR (75 MHz, DMSO-d$_6$): 25.840 (C^{13}), 28.89 (C^{12}), 32.48 (C^{19}), 52.35 (C^{18}), 63.301 (C^{17}), 69.89 (C^{11}), 117.62 (C^7), 122.807 (C^5), 129.45 (C^3), 130.57 (C^6), 140.36 (C^{10}), 145.79 (C^4), 148.18 (C^9), 150.114 (C^2), 152.05 (C^8). MS(ESI): 537 [M/z-Br]$^+$, 455 [M/z-Br]$^+$, 414 [(C$_9$H$_6$NO)$_2$(CH$_2$)$_6$(CH$_2$)$_3$]$^+$, 372 [(C$_9$H$_6$NO)$_2$(CH$_2$)$_6$]$^+$, 350 [(C$_9$H$_6$NO)(CH$_2$)$_6$(C$_7$H$_5$NO)]$^+$, 319 [(C$_9$H$_6$NO)(CH$_2$)$_6$(C$_6$H$_3$O)]$^+$, 269 [(C$_9$H$_6$NO)(CH$_2$)$_6$(C$_2$HO)]$^+$, 228 [(C$_9$H$_6$NO)(CH$_2$)$_6$]$^+$, 187 [(C$_9$H$_6$NO)(CH$_2$)$_3$]$^+$, 146 [(C$_9$H$_6$NO)]$^+$.

5.2.4 Synthesis of bromide anions salt containing geminal dications $[(C_9H_6NO)_2(C_6H_6N)(CH_2)_3]^{2-}2Br^-$ (3)

Compound 8-(2-Pyridylmethoxy)quinoline (BQOP) (0.24g, 1.35mmol) was dissolved in excess of dibromopropane (~3 ml) and this solution was stirred at 110^oC for 12 hr. Upon cooling brown coloured solid precipitated was washed several times with ethyl acetate followed by n-hexane to get pure compound (**3**).

$[(C_9H_6NOCH_2)(C_6H_4N)(CH_2)_3]^{2+}2Br^-$ **[3]:** Dark Brown solid, yield 86%, mp 214°C, soluble in chloroform, DMSO, DMF, methanol, and ethanol. $C_{18}H_{18}Br_2N_2O$: % Found (Calculated): C 49.37 (49.34), H 4.12 (4.14), N 6.36 (6.39); FT-IR, , cm–1: 1590 (C=N); 1534 (C=Car,asym); 1465 (C=Car, sym); 1398 (C-N-alkyl chain); 1274 (C-O-alkyl chain); 1114 (C-Oar). ^{1}H NMR (400.13 MHz, DMSO d_6, at 25°C, ppm): 8.84 (d, H, H^2); 8.56 (d, H, H of C=N Py); 8.29 (d, H, H^7); 7.84-7.25 (m, aromatic H); 5.34 (s, 2H, H of $-O-CH_2-$); 2.84 (t, 2H, $-N-CH_2$); 2.68 (m, 2H, $-N-CH_2-\underline{CH_2}-CH_2-$); 2.46 (m, 2H, $-N-CH_2-CH_2-\underline{CH_2}-$). MS(ESI): 451 $[M/z-Br]^+$, 331 $[(C_9H_6NO)_2(CH_2)_3]^+$, 255 $[(C_9H_6NO)(CH_2)_3(C_3H_3N)]^+$, 227 $[(C_9H_6NO)(CH_2)_3(C_2H)]^+$, 186 $[(C_9H_6NO)(CH_2)_3]^+$, 158 $[(C_9H_6NO)CH_2]^+$, 146$[(C_9H_6NO)]^+$.

5.2.5 General procedure for synthesis of 8-hydroxyquenolenium based geminal dicationic ionic liquids $[(C_9H_6NO)_2(CH_2)_3]^{2-}2PF_6^-$ [1a], $[(C_9H_6NO)_2(CH_2)_6]^{2-}2PF_6^-$ (2a) and $[(C_9H_6NO)_2(C_6H_6N)(CH_2)_3]^{2-}2PF_6^-$ (3a)

Dicationic compound (**1**) (0.447 g, 1.35 mmol) was reacted with NH_4PF_6 in 1:2 molar ratio in methanol and stirred at room temperature for 24 hr. After stirring, the resulting solid product was filtered off, washed with distilled water and recrystallised with MeCN to give a pure compound (**1a**).

A similar procedure has been applied for preparing other ionic compounds (2a) and (3a). Colorless transparent crystals of only compound (1a) suitable for single crystal X-ray analysis were obtained from slow evaporation of MeCN solution and characterized by X-ray analysis.

The synthetic and analytical details of compounds (1a), (2a) and (3a) are summarized below:

$[(C_9H_6NO)_2(CH_2)_3]^{2-}2PF_6^-$ [1a]: Off white solid, yield 86%, mp 218°C, soluble in chloroform, toluene, DMSO, DMF, methanol, and ethanol. $C_{24}H_{24}F_{12}N_2O_2P_2$: % Found (Calculated): C 43.41 (43.52), H 3.49 (3.65), N 4.21 (4.23); FT-IR, , cm–1: 1600 (C=N); 1536 (C=Car,asym); 1463 (C=Car, sym); 1393 (C-N-alkyl chain); 1286(C-O-alkyl chain); 1113(C-Oar); 829 (P–F). ^{1}H NMR (300.13 MHz, DMSO d$_6$, at 25°C, ppm): 9.35 (d, H, H^2); 9.19 (d, H, H^4); 8.27 (dd, H, H^3); 7.98-7.85 (m, 3H, aromatic); 4.57 (t, 2H, H^{11}); 2.03 (m, 2H, H^{13}); 5.39 (t, 2H, H^{14}); 3.34 (m, 2H, H^{15}). ^{13}C NMR (75 MHz, DMSO-d$_6$): 21.2 (C^{13}), 28.615 (C^{15}), 59.699 (C^{14}), 72.178 (C^{11}), 117.78 (C^5), 123.22 (C^3), 129.45 (C^6), 130.930 (C^{10}), 132.53 (C^4), 148.56 (C^9), 149.97 (C^2), 152.47 (C^8). ^{31}P-NMR (161 MHz), DMSO-d$_6$: = -143.5 (hept, J = 710 Hz). MS(ESI): 372 [M/z-2PF$_6$]$^+$, 329 $[(C_9H_6NO)_2(CH_2)_3]^+$, 298 $[(C_9H_6N)_2(CH_2)_3]^+$, 284 $[(C_9H_6N)(C_8H_4N)(CH_2)_3]^+$, 254 $[(C_9H_6N)(C_6H_3N)(CH_2)_3]^+$, 237 $[(C_9H_6N)(C_4H_3N)(CH_2)_3]^+$, 212 $[(C_9H_6N)(C_2H_2N)(CH_2)_3]^+$, 200 $[(C_9H_6N)(CH_2N)(CH_2)_3]^+$, 175 $[(C_9H_6N)(H)(CH_2)_3]^+$, 117 $[(C_8H_6N)]^+$.

$[(C_9H_6NO)_2(CH_2)_6]^{2-}2PF_6^-$ [2a]: off white solid, yield 89%, mp 142°C, soluble in chloroform, toluene, DMSO, DMF, methanol, and ethanol. $C_{30}H_{36}F_{12}N_2O_2P_2$: % Found (Calculated): C 48.15 (48.27), H 4.90 (4.86), N 3.69 (3.75); FT-IR, , cm–1: 1600 (C=N); 1535 (C=Car,asym); 1464 (C=Car, sym); 1389 (C-N-alkyl chain); 1288 (C-O-alkyl chain); 1112 (C-Oar); 831 (P–F). ^{1}H NMR (300.13 MHz, DMSO d$_6$, at 25°C, ppm): 9.24 (d, H, H^2); 9.09 (d, H, H^4); 8.63 (dd, H, H^3); 7.33-7.84 (m, 3H, aromatic); 4.20 (t, 2H, H^{11}); 2.21 (m, 2H, H^{12}); 1.43 (m, 2H, H^{13}); 5.10 (t, 2H, H^{18}); 2.46 (m, 2H, H^{19}); 1.82 (m, 2H, H^{20}). ^{13}CNMR (DMSO): 25.51 (C^{13}), 28.65 (C^{12}), 32.24 (C^{19}), 52.13 (C^{18}), 63.48 (C^{17}), 70.73 (C^{11}), 117.48 (C^7), 122.66 (C^5), 129.10 (C^3), 130.84 (C^6), 132.61 (C^{10}), 140.12 (C^4), 148.27 (C^9), 150.09 (C^2), 152.00 (C^8). ^{31}P-NMR (161 MHz), DMSO-d$_6$: = -143.6 (hept, J = 710 Hz). MS(ESI): 456 [M/z-2PF$_6$]$^+$, 414 $[(C_9H_6NO)_2(CH_2)_6(CH_2)_2]^+$, 372 $[(C_9H_6NO)_2(CH_2)_6]^+$, 309 $[(C_9H_6NO)(CH_2)_6(O)]^+$, 228 $[(C_9H_6NO)(CH_2)_6]^+$, 187 $[(C_9H_6NO)(CH_2)_2CH_3]^+$, 146$[(C_9H_6NO)]^+$.

[(C₉H₆NOCH₂)(C₆H₄N)(CH₂)₃]²⁺2PF₆⁻ [3a]: Dark Brown solid, yield 84%, mp 183°C, soluble in chloroform, DMSO, DMF, methanol, and ethanol. $C_{18}H_{18}F_{12}N_2OP_2$: % Found (Calculated): C 38.03 (38.04), H 3.14 (3.19), N 4.89 (4.93); FT-IR, , cm⁻¹: 1593 (C=N); 1536 (C=Car, asym); 1471 (C=Car, sym); 1385 (C-N-alkyl chain); 1273 (C-O-alkyl chain); 1115 (C-Oar). ¹H NMR (400.13 MHz, DMSO d₆, at 25°C,   ppm): 8.72 (d, H, H²); 8.53 (d, H, H of C=N Py); 8.31 (d, H, H⁷); 7.81-7.32 (m, aromatic H); 5.71 (s, 2H, H of –O-CH₂-); 2.82 (t, 2H, -N-CH₂); 2.71 (m, 2H, -N-CH₂-CH₂-CH₂-); 2.51 (m, 2H, -N-CH₂-CH₂-CH₂-). MS(ESI): 451 [M/z-Br]⁺, 331 [(C₉H₆NO)₂(CH₂)₃]⁺, 255 [(C₉H₆NO)(CH₂)₃(C₃H₃N)]⁺, 227 [(C₉H₆NO)(CH₂)₃(C₂H)]⁺, 186 [(C₉H₆NO)(CH₂)₃]⁺, 158 [(C₉H₆NO)CH₂]⁺, 146[(C₉H₆NO)]⁺.

5.2.6 Crystal structure analysis of [(C₉H₆NO)₂(CH₂)₃]²⁻2PF₆⁻ (1a)

Transparent crystals of compound (1a) were obtained upon slow evaporation of its solution in acetonitrile. The single crystal X-ray data for (1a) were obtained at temperature 150 K on Bruker APEX-II CCD system equipped with a temperature lowering attachment. All the data were gathered using graphite-monochromated Mo Ka radiation (ka = 0.71073 Å). Bruker APEX2 software was used for the evaluation of collected data. X-ray data for analysis were obtained from standard '□-□' scan methods and CRYSALISPRO RED software was used for reduction and scaling of the data collected. The molecular structure was resolved by direct methods using SHELXS-97 and structural refinements were done by using full matrix least squares with SHELXL-2014, F^2. All the atomic positions were determined using direct methods. All atoms other than hydrogen were anisotropically refined and the hydrogen atoms were positioned in geometrically hindered sites and were refined isotropically with temperature aspects of usually 1.2×9 Ueq. Ortep program was used to obtain the H-bonding interactions, mean plane analyses and foe molecular drawings. Atomic coordinates, bond lengths and angles, and thermal parameters have been deposited at the Cambridge crystallographic data center. Symmetry transformations used to generate equivalent atoms: 'x, y, z '-x+1/2, y+1/2, -z+1/2' '-x, -y, -z' 'x-1/2, -y-1/2, z-1/2'. The crystal data and refinement are summarized in table 5.1.

Table 5.1. X-ray and structural refinement data for **(1a)**

Complex	$[(C_9H_6NO)_2(CH_2)_3]^{2-}2PF_6^-$
Empirical formula	$C_{24}H_{24}F_{12}N_2O_2P_2$
Formula weight	662.39
Temperature	100(2) K
Wavelength	0.71073 A
Crystal system, space group	Monoclinic, P 2(1)/n
Unit cell dimensions	a = 10.145(3) Å = 90
	b = 15.764(4)Å = 103.587
	c = 17.802(5)Å = 90
Volume	2767.3(13)Å^3
Z, Calculated density	4, 1.590Mg m^{-3}
Absorption coefficient	0.265 mm^{-1}
F(000)	1345.92
Crystal size	0.41 x 0.15 x 0.11 mm^3
Theta range for data collection	2.21 to 28.73°
Limiting indices	-13<=h<=13, -21<=k<=21, -23<=l<=23
Reflections collected / unique	7069/3443 [R(int) = 0. 0.0901]
Completeness to = 28.73	98.4%
Absorption correction	Semi-empirical from equivalents
Max. and min. transmission	0.9714 and 0.8991
Refinement method	Full-matrix least-squares on F^2

Data / restraints / parameters	7069 / 0 / 379
Goodness-of-fit on F^2	1.020
Final R indices [I>2 (I)]	R1 = 0.0626, wR2 = 0.1456
R indices (all data)	R1 = 0.1402, wR2 = 0.1848
Absolute structure parameter	0.83(4)
Largest diff. peak and hole	0.698d -0.452e.Å^{-3}

5.3 Result and discussion

5.3.1 Synthesis of new quinolinium based ionic compounds

New quinolinium based geminal dicationic ionic liquids were synthesized using a three steps route as depicted in Scheme 5.1. In the first step, two molecule of 8-hdroxyquinoline reacted with suitable dibromo alkane to form precursors PMOQ, HMOQ and BQOP. In the second step, these precursors acting as strong nucleophile was reacted to the different dibromo alkanes to give corresponding quinolinium based geminal dicationic bromide ionic compounds (1), (2) and (3). In the third step Br⁻ ions in the product of the second step exchanged by hexafluorophosphate ions involving exchange metathesis by reacting with a small excess of ammonium hexafluorophosphate resulting in ionic compounds (1a), (2a) and (3a).

The structural elucidations of all these newly designed geminal dicationic ionic compounds were done by ^{1}H NMR, FT-IR, ESI-Mass, UV-Vis spectroscopy, elemental analysis and X-ray crystal structure. All the characterization data are given in the experimental section.
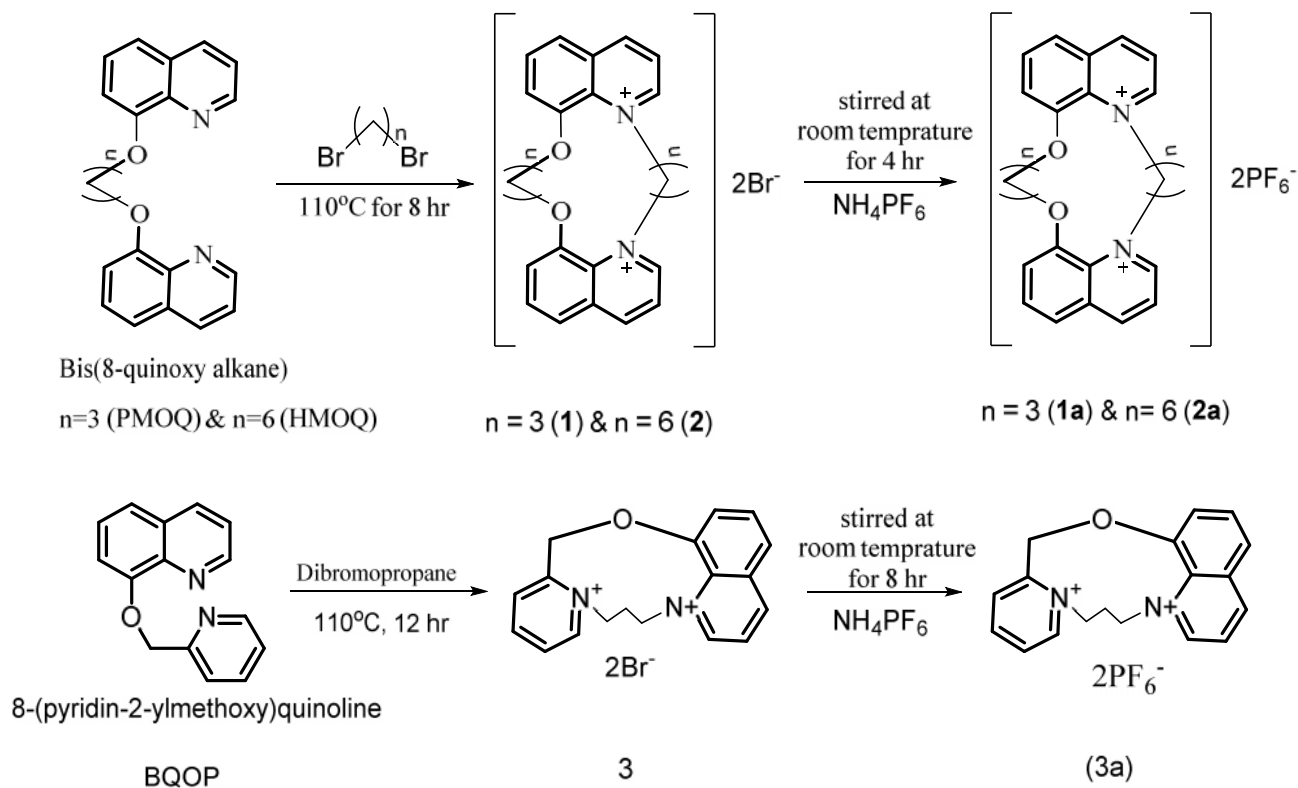
Scheme-5.1 General procedure for synthesis of ionic compounds

All the above reactions were found to be pretty feasible and quantitative, resulting in off white/yellow powders. All the ionic liquids are stable in air and water and decompose on heating at ~220 C. These compounds are slightly soluble in common organic solvents but readily soluble in coordinating solvents like THF and DMSO. Both the compounds (**2a**) and (**3a**) are relatively more stable in solution than their geminal dication bromide salt. The ionic compound (**1a**) can be re-crystallized by slow evaporation of MeCN solution. The ESI-mass spectral data of of compounds (1), (1a), (2), (2a), (3) and (3a) suggest monomeric nature.

5.3.2 Single crystal X-ray analysis of compound (1a)

The ORTEP plot of the ionic liquid $[(C_9H_6NO)_2(CH_2)_3]^{2+}2PF_6^-$ [**1a**] is shown in Fig. 5.2 Important bond lengths and bond angles for (**1a**) are given in Table 2. The crystal system of compound (**1a**) is monoclinic with space group P2(1)/n restraining a pair of ions in the symmetric component $[(C_9H_6NO)_2(CH_2)_3]^{2+}$ dication and two PF$_6^-$

counterions. Both the PF_6^- demonstrates geometry close to octahedral, where the P atom is situated at the E site symmetry and six fluorine atoms surrounding the P atom. All the axial and equatorial P–F bond lengths ranging from 1.577 to 1.590 Å (average 1.585 Å) and *cis*-F–P–F angular distortions observed are less than 3˚. These data are in good accord with those ranges observed in other PF_6^- derivatives (1.577 to 1.590 Å) [23].

The crystal structure indicates that the $[(C_9H_6NO)_2(CH_2)_3]^{2+}$ dication has boat like cyclic configuration. The structure of this dication demonstrated that two 8-hydroxy quinoline rings are joint together by two propyl linkage chains with two oxygen and two nitrogen atoms. The bond lengths and bond angles obtained for $[(C_9H_6NO)_2(CH_2)_3]^{2+}$ moiety are as per expected. Hydrogen bond formation between a F atom of PF_6^- and the H atom of dication $[(C_9H_6NO)_2(CH_2)_3]^{2+}$ has not been observed in the present study. To the best of our knowledge, this type of ionic liquid has been structurally characterized first time in which a symmetrical dication observed in cyclic form. The geometrical parameters of the aromatic rings and other atoms for germinal dication structure are in good accord with each other as shown in table 5.2. All the important bond lengths and angles of dication are pretty close to those previously reported values [24].

Table 5.2. Important bond length and angles of ionic compound $[(C_9H_6NO)_2(CH_2)_3]^{2+}2PF_6^-$ [**1a**]

Bond lengths			
P(1)-F(1)	1.590(2)	O(1)-C(13)	1.361(4)
P(1)-F(2)	1.579(2)	O(1)-C(12)	1.447(4)
P(1)-F(3)	1.588(2)	O(2)-C(9)	1.359(4)
P(2)-F(12)	1.560(3)	O(2)-C(10)	1.438(4)
P(2)-F(9)	1.577(3)	C(5)-C(9)	1.429(4)
P(2)-F(7)	1.585(3)	C(18)-C(13)	1.426(4)
N(1)-C(1)	1.329(4)	C(5)-C(4)	1.433(5)
C(5)-N(1)	1.409(4)	C(18)-C(17)	1.426(4)
N(1)-C(24)	1.497(4)	C(9)-C(8)	1.380(4)

N(2)-C(21)	1.330(4)	C(13)-C(14)	1.386(4)
N(2)-C(22)	1.499(4)	C(12)-C(11)	1.498(5)
N(2)-C(18)	1.402(4)	C(21)-C(20)	1.389(5)
Bond Angles			
F(5)-P(1)-F(3)	88.06(15)	C(21)-N(2)-C(18)	121.2(3)
F(5)-P(1)-F(4)	90.18(18)	C(21)-N(2)-C(22)	114.4(3)
F(4)-P(1)-F(6)	90.59(16)	C(18)-N(2)-C(22)	124.4(3)
F(3)-P(1)-F(6)	179.24(16)	C(1)-N(1)-C(5)	120.9(3)
F(5)-P(1)-F(2)	179.76(17)	C(1)-N(1)-C(24)	115.4(3)
F(11)-P(2)-F(7)	90.42(16)	C(5)-N(1)-C(24)	123.6(3)
F(12)-P(2)-F(8)	87.82(14)	C(9)-C(5)-C(4)	119.2(3)
F(9)-P(2)-F(8)	91.76(16)	C(9)-O(2)-C(10)	117.2(3)
F(11)-P(2)-F(8)	178.58(16)	C(13)-O(1)-C(12)	118.2(3)
F(10)-P(2)-F(7)	176.47(19)	O(1)-C(13)-C(14)	123.0(3)
F(12)-P(2)-F(9)	179.58(17)	O(1)-C(13)-C(18)	118.3(3)
N(1)-C(5)-C(4)	116.4(3)	O(2)-C(9)-C(5)	118.6(3)
N(2)-C(18)-C(17)	116.6(3)	O(2)-C(9)-C(8)	123.0(3)
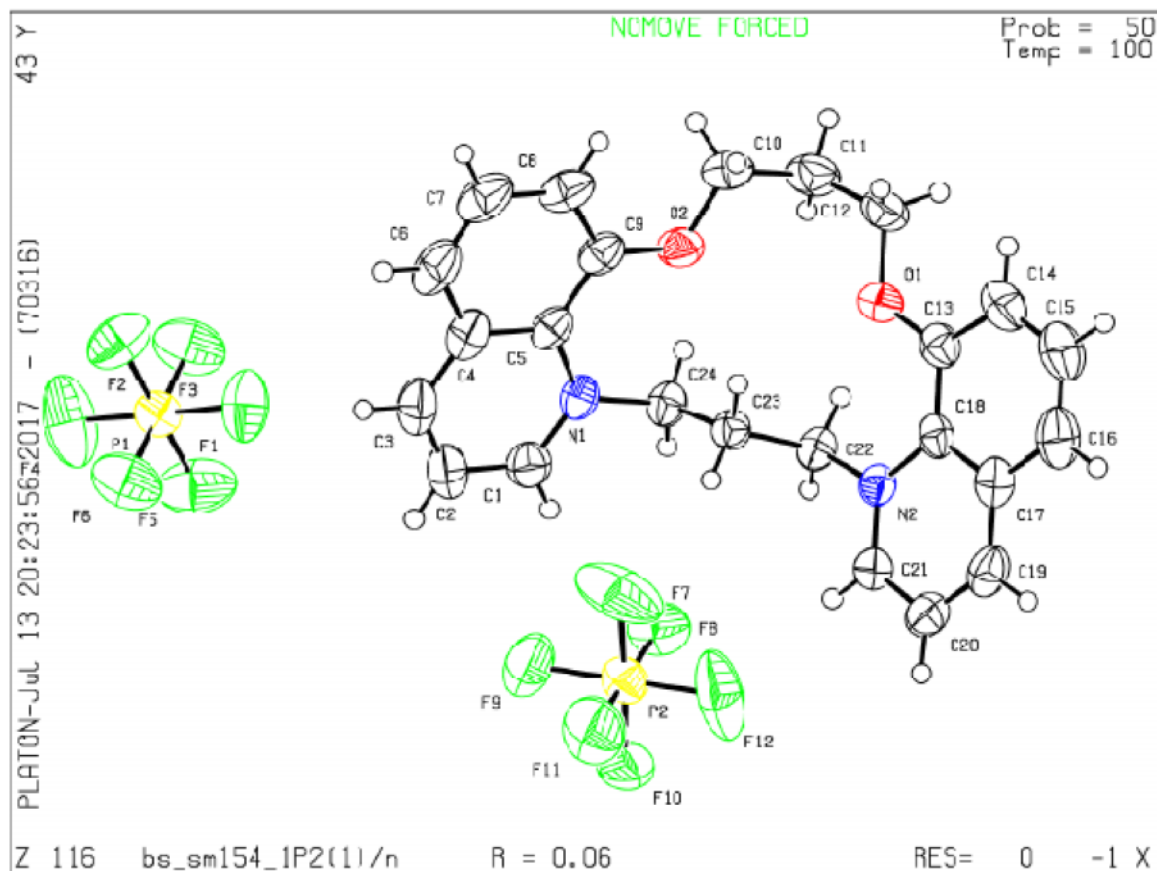
Figure 5.2 ORTEP diagram of $[(C_9H_6NO)_2(CH_2)_3]^{2+}$ and $2PF_6^-$ in the

$[(C_9H_6NO)_2(CH_2)_3]^{2+}2PF_6$ (2a) structure with an atom numbering scheme

5.3.3 IR and NMR spectra

The IR and ^{1}H NMR spectral data of all these ionic liquids are summarized in experimental section and deduced by comparing them with the spectra of parent organic compound (PMOQ, HMOQ & BQOP) and 8-hydroxyquinoline. In the NMR spectra of ionic compounds, all the signals are observed at the desired position with desirable multiplicities in all the derivatives. The proton NMR spectra did not show significant differences between parent organic compound and its ionic compounds. In the IR spectra, all the absorption appeared to the expected position. ATR/FTIR spectroscopy measurements were carried out to support the occurrence of the anion exchange reaction.

Since bromide anions are invisible in ATR/FTIR, only the absorption bands of parent dication can be recorded in the spectra. For ionic compound (1a), (2a) and (3a) carrying PF_6^- as anion, the broad peak at 830 cm^{-1} can be assigned to the symmetric stretching of the PF_6^- anion. Therefore, ATR/FTIR spectra offered solid evidence of the anion exchange.

The ^{31}P NMR spectra of ionic compounds containing PF_6^- (1a, 2a & 3a) were recorded in DMSO-d$_6$ and ^{31}P-NMR shift values were approximately the same as expected in the ionic compounds. The presence of the PF_6^- in ionic compound were confirmed by the one sets of septate which observed at   -143.6 and   -143.5 (for 1a & 2a) as shown in figures 5.10, 5.11. Based on above ^{31}P NMR data, observed at expected positions, supporting the crystal structure in which organic ligands and a PF_6^- anion linked as counter ion.

5.3.4   UV-Vis. Absorption spectra

The absorption spectrum of all the ionic liquids was recorded against the precursor (PMOQ, BQOP & BQOH) blank. The absorption spectra of the precursors BQOP, BQOH and their ionic compounds are shown in Figure 5.1. The obtained spectra indicated that the ionic compounds have maximum absorbance at 365 nm and precursors have maximum absorbance at 313 nm, respectively. The precursors have minimum absorbance at the maximum absorbance of its ionic compounds and confirm the complexation between precursors and ionic salts.

(a)

(b)

(**c**)
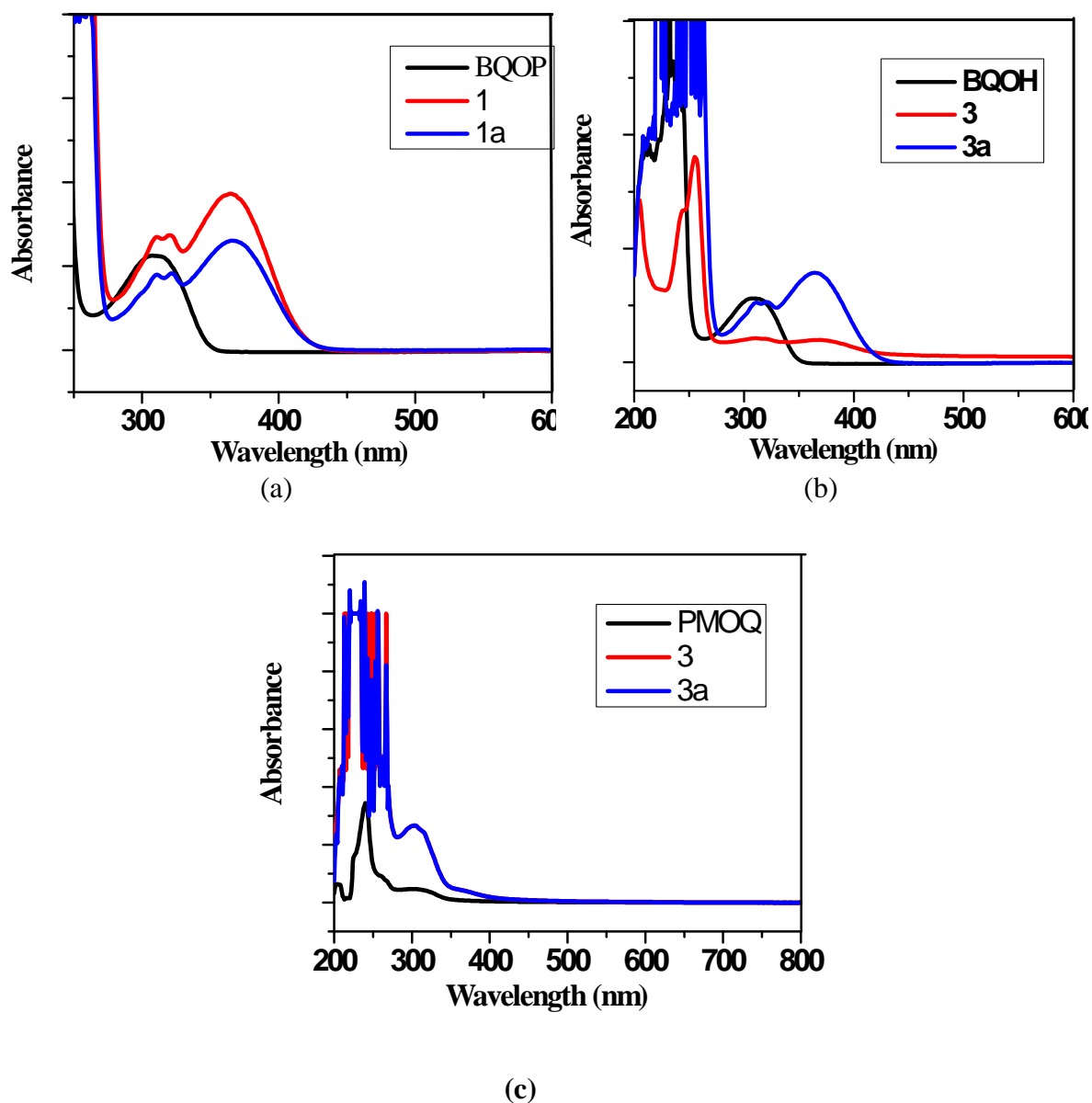
Figure 5.3 (a) Absorption spectra of precursor BQOP and its ionic compounds **(b)** Absorption spectra of precursor BQOH and its ionic compounds **(c)** Absorption spectra of precursor PMOQ and its ionic compounds (against precursor PMOQ)
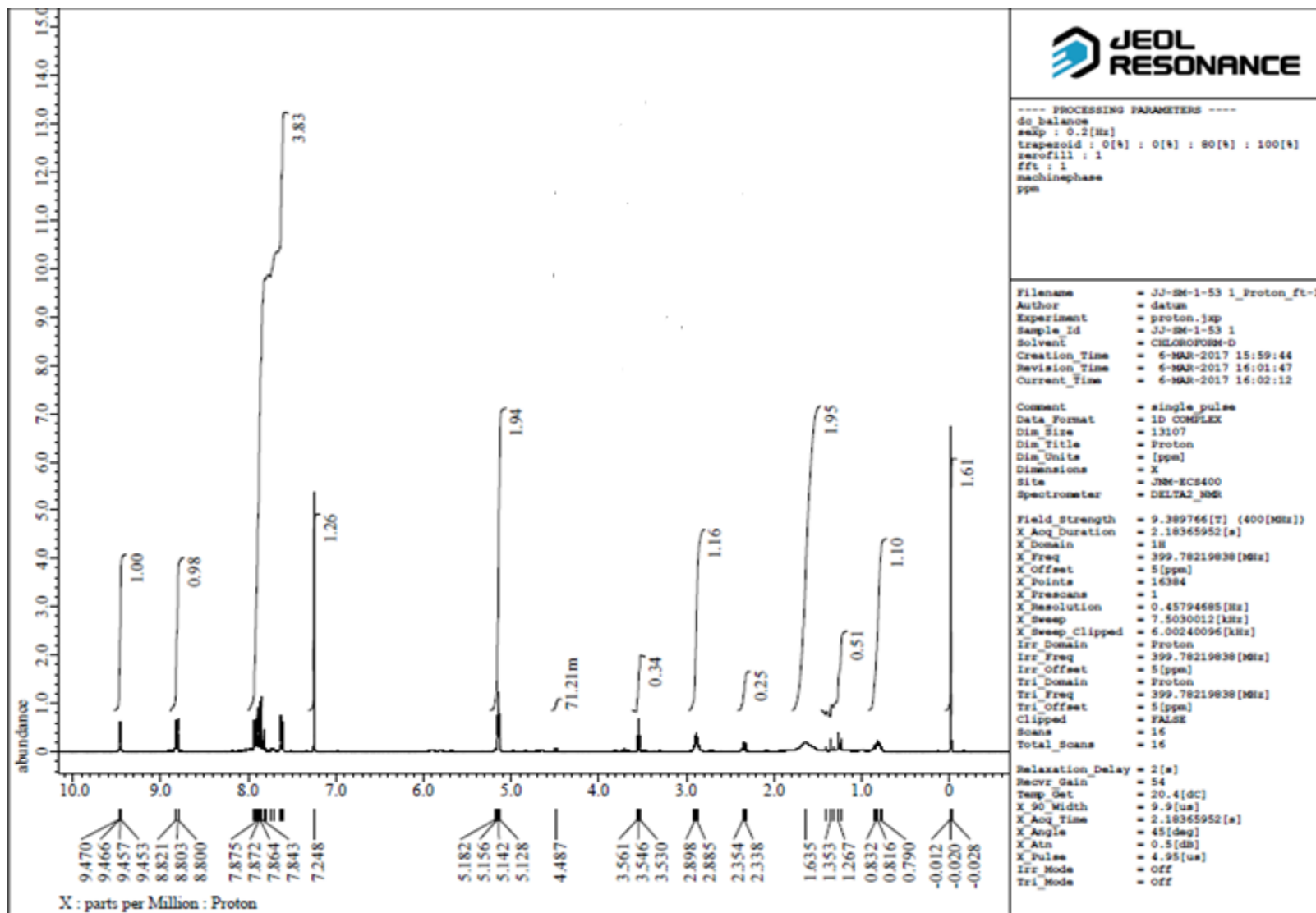
Figure 5.4 ^{1}H NMR spectra of the ionic complex (1) in DMSO-d$_6$
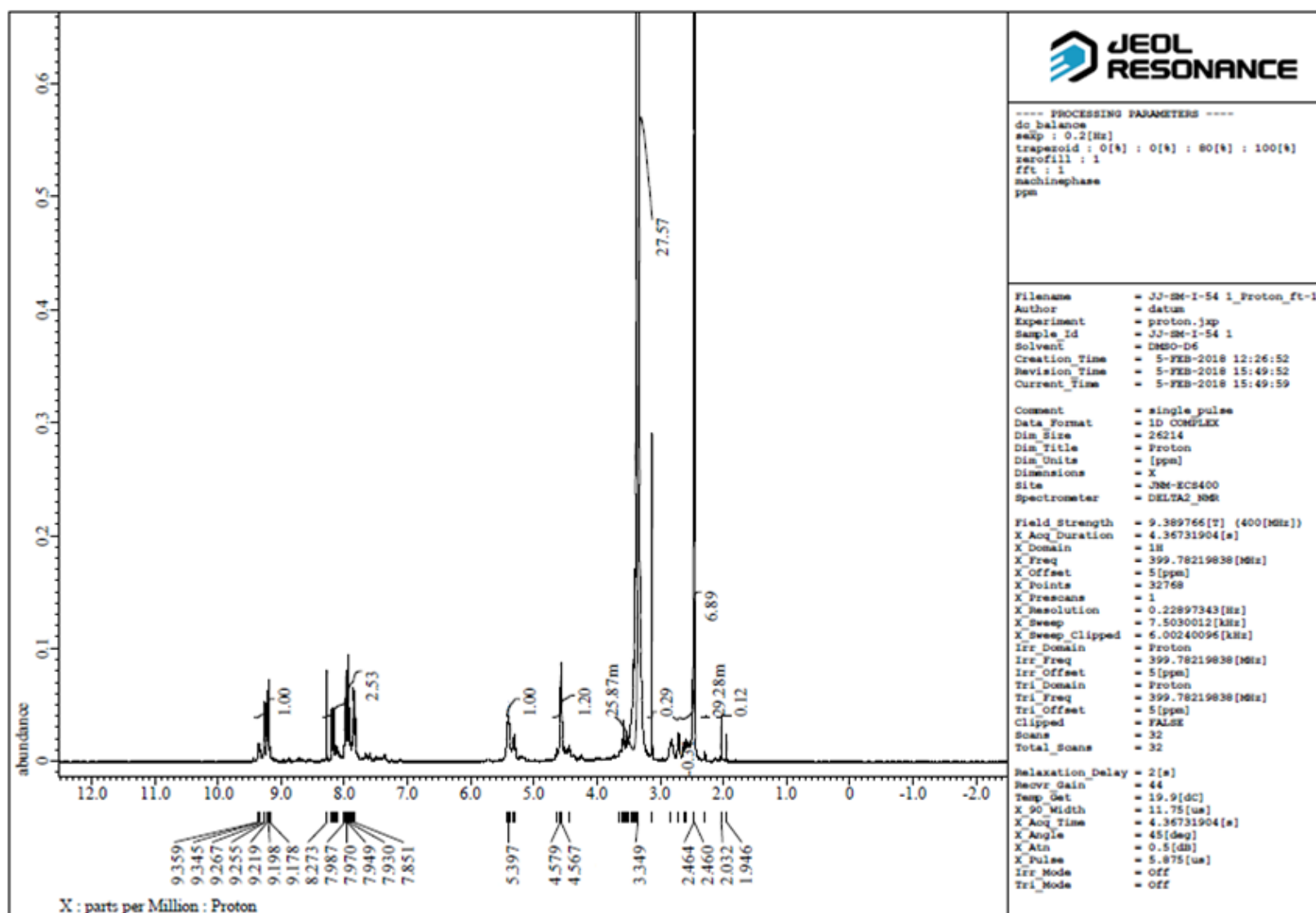
Figure 5.5 ^{1}H NMR spectra of the ionic complex (1a) in DMSO-d$_6$
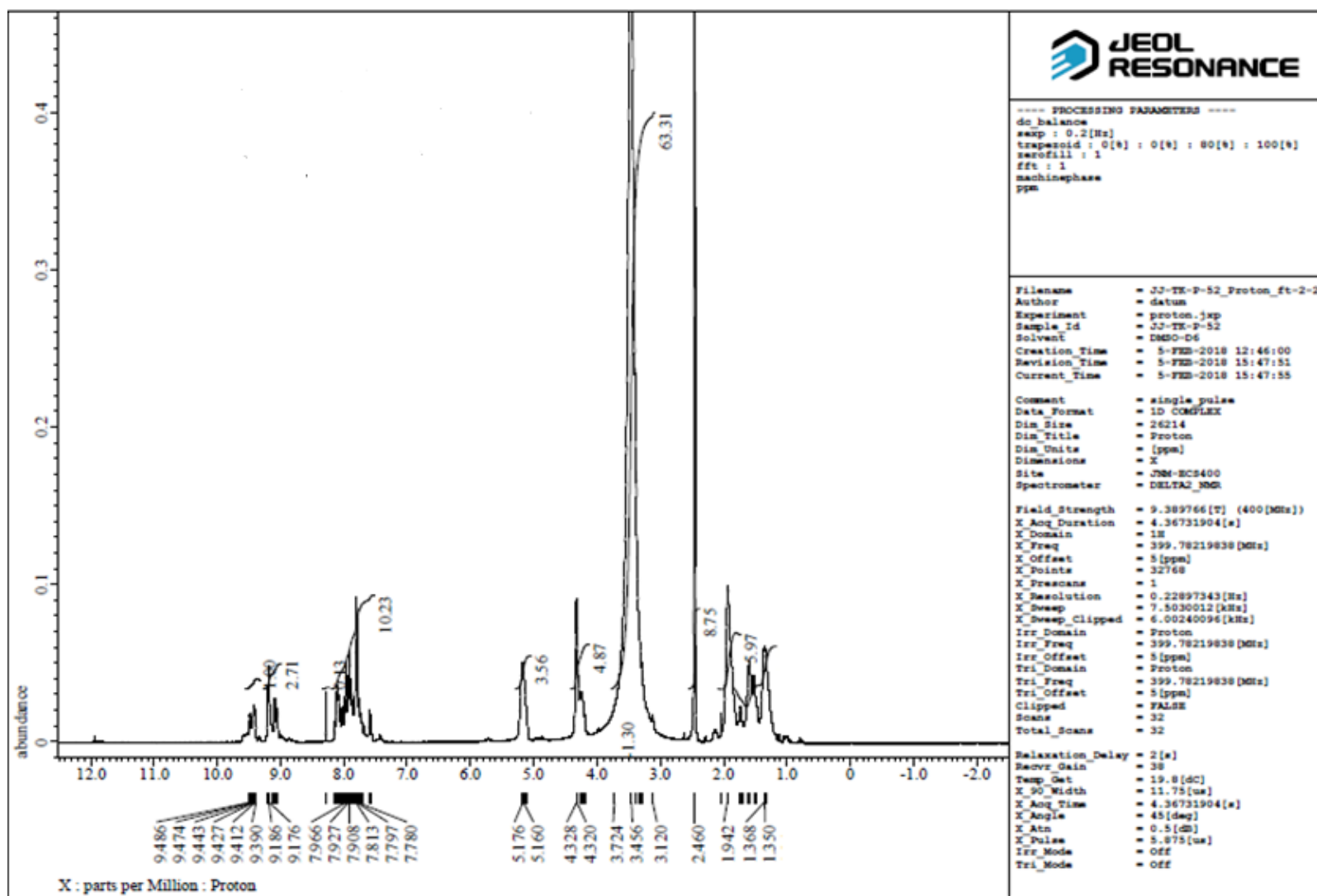
Figure 5.6 ^{1}H NMR spectra of the ionic complex (2) in DMSO-d$_6$
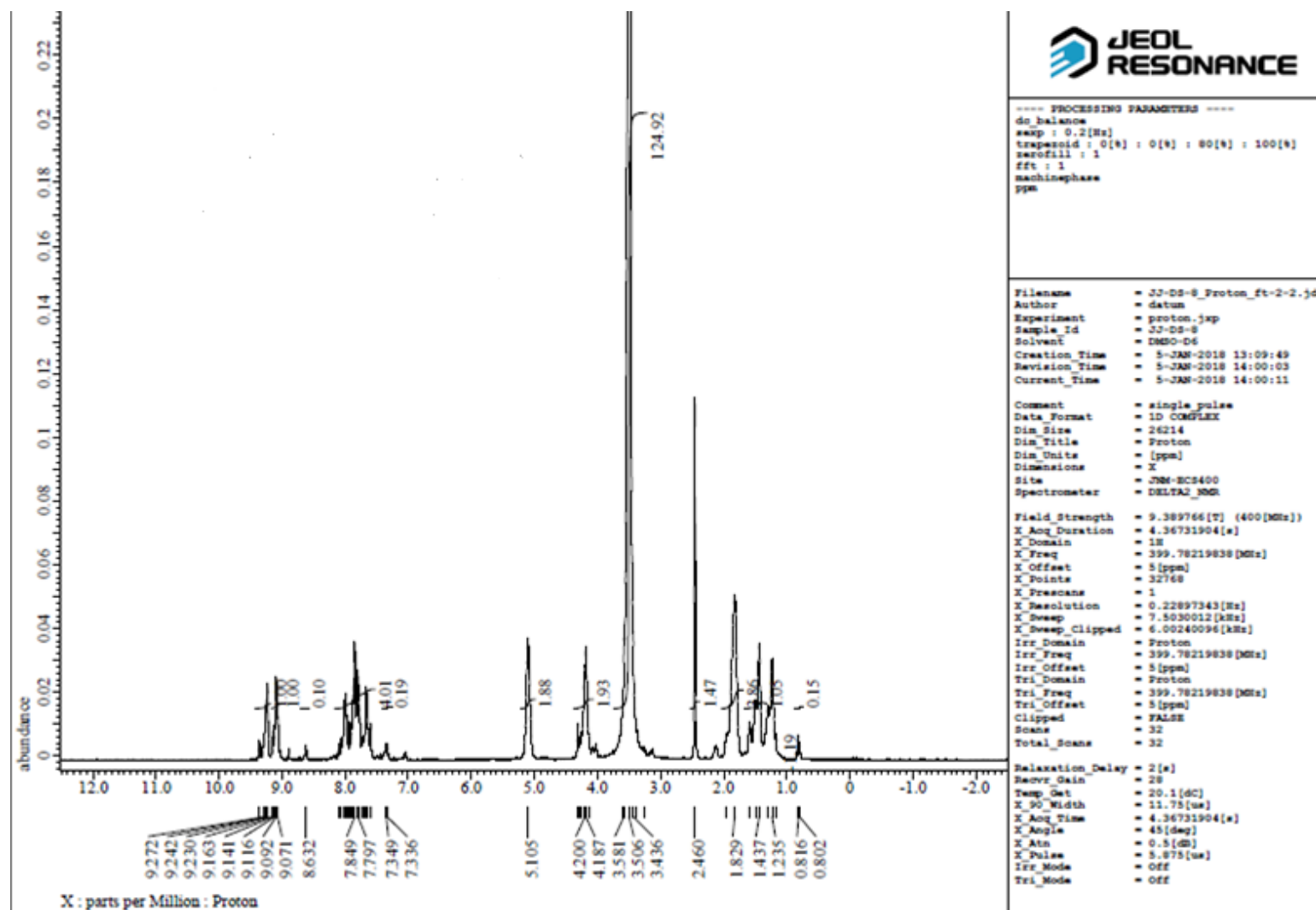
Figure 5.7 ^{1}H NMR spectra of the ionic complex (2a) in DMSO-d$_6$
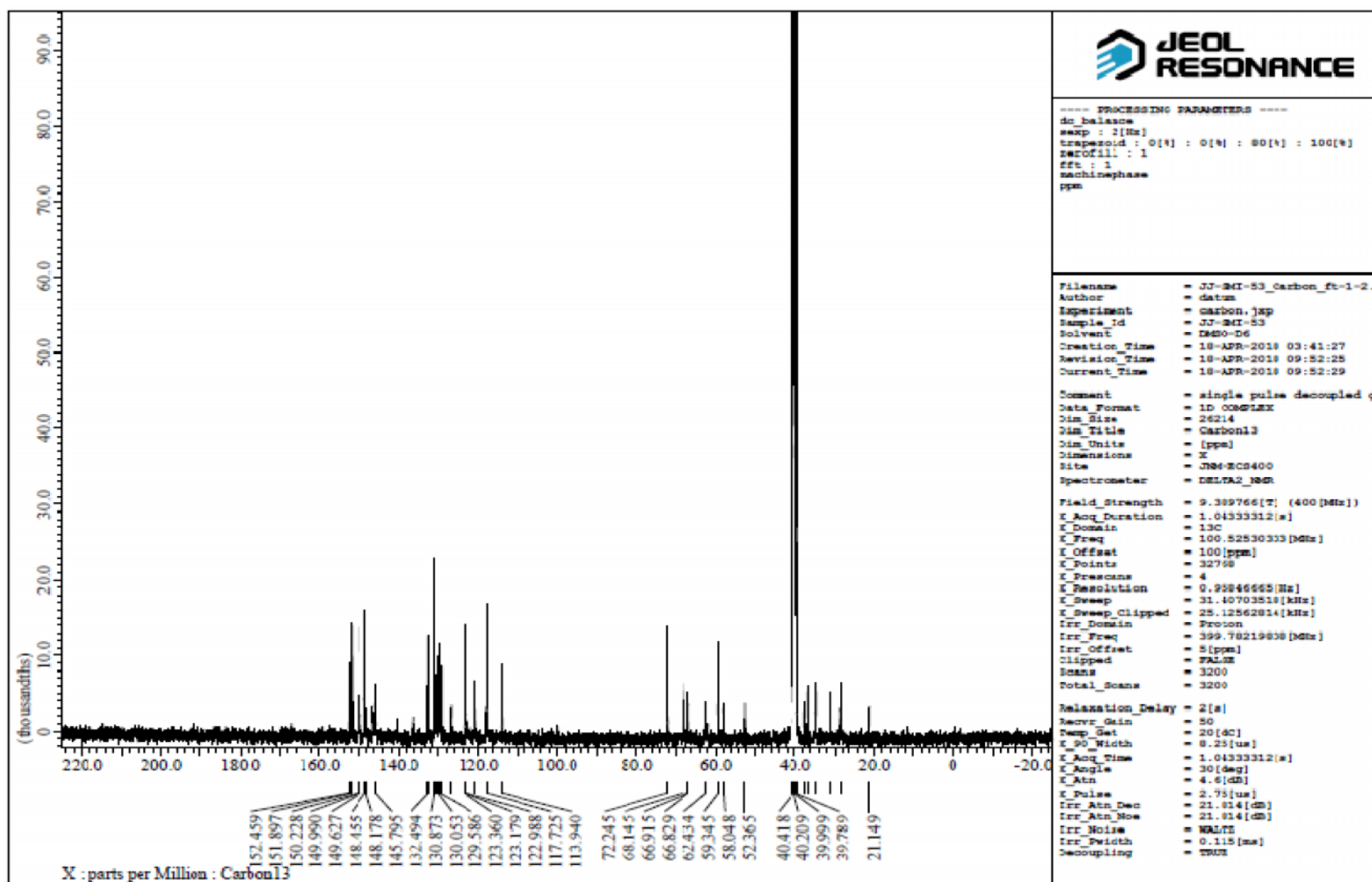
Figure 5.8 ^{13}C NMR spectra of the ionic complex (1) in DMSO-d$_6$
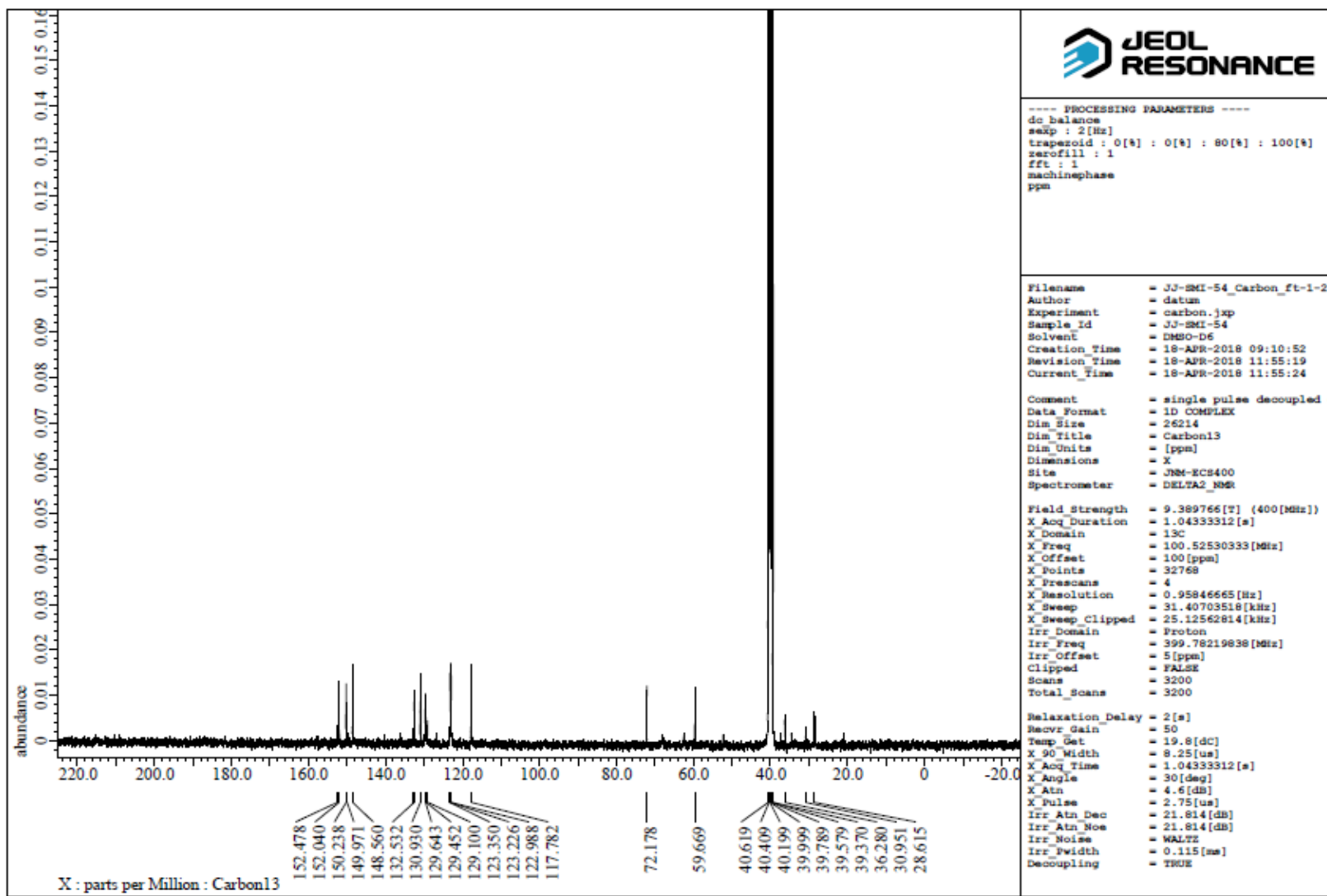
Figure 5.9 ^{13}C NMR spectra of the ionic complex (1a) in DMSO-d$_6$
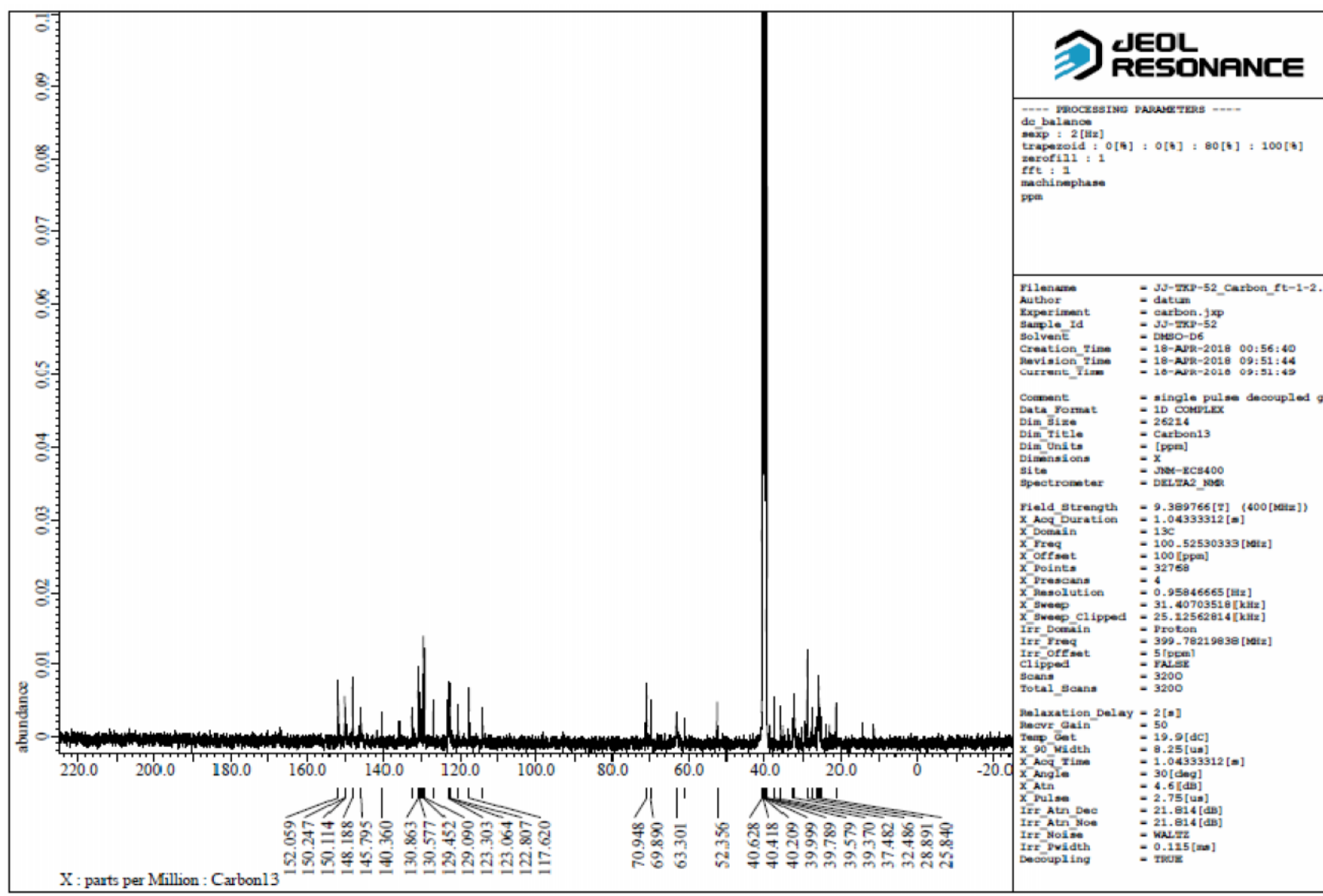
Figure 5.10 ^{13}C NMR spectra of the ionic complex (2) in DMSO-d$_6$
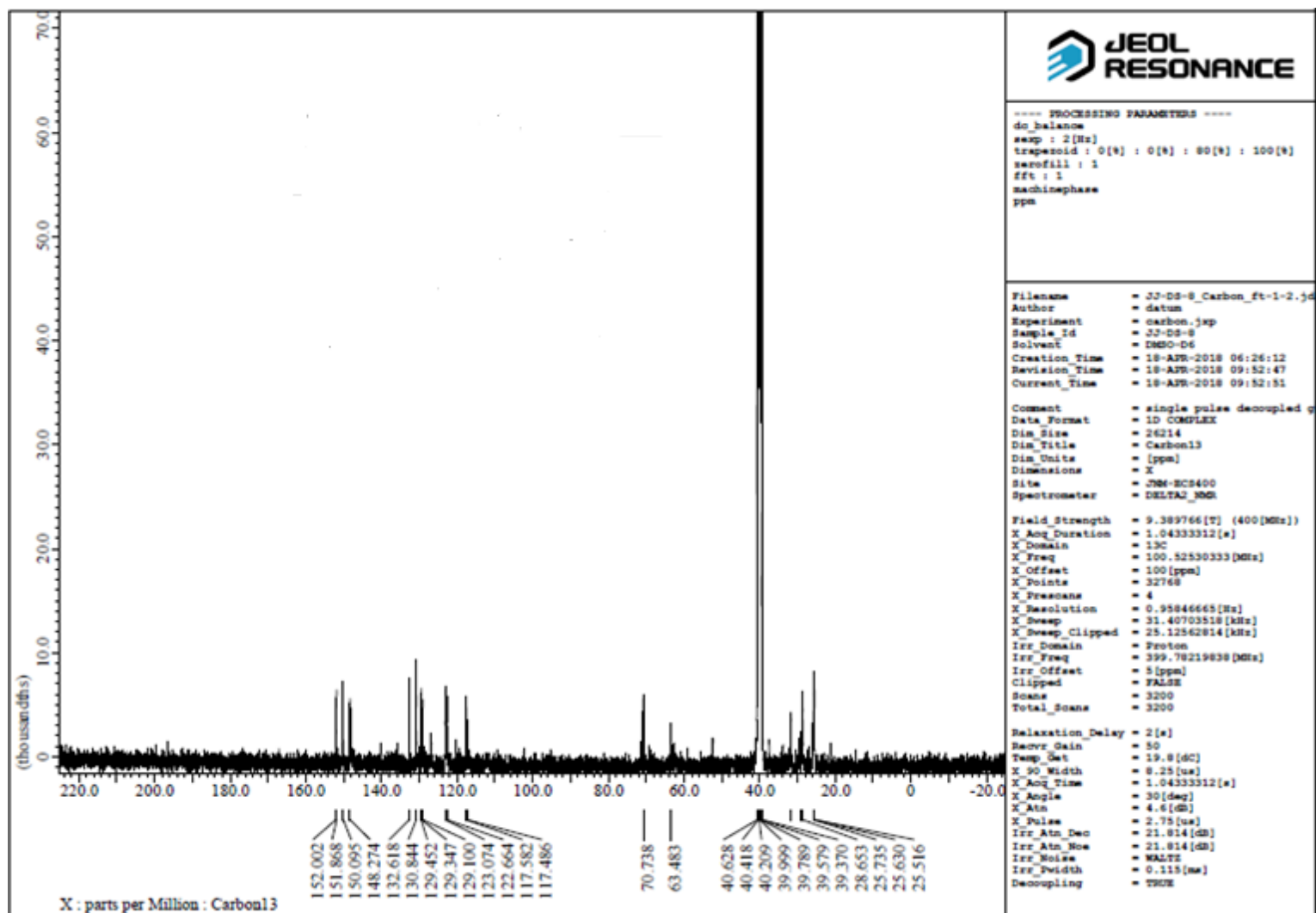
Figure 5.11 ^{13}C NMR spectra of the ionic complex (2a) in DMSO-d$_6$
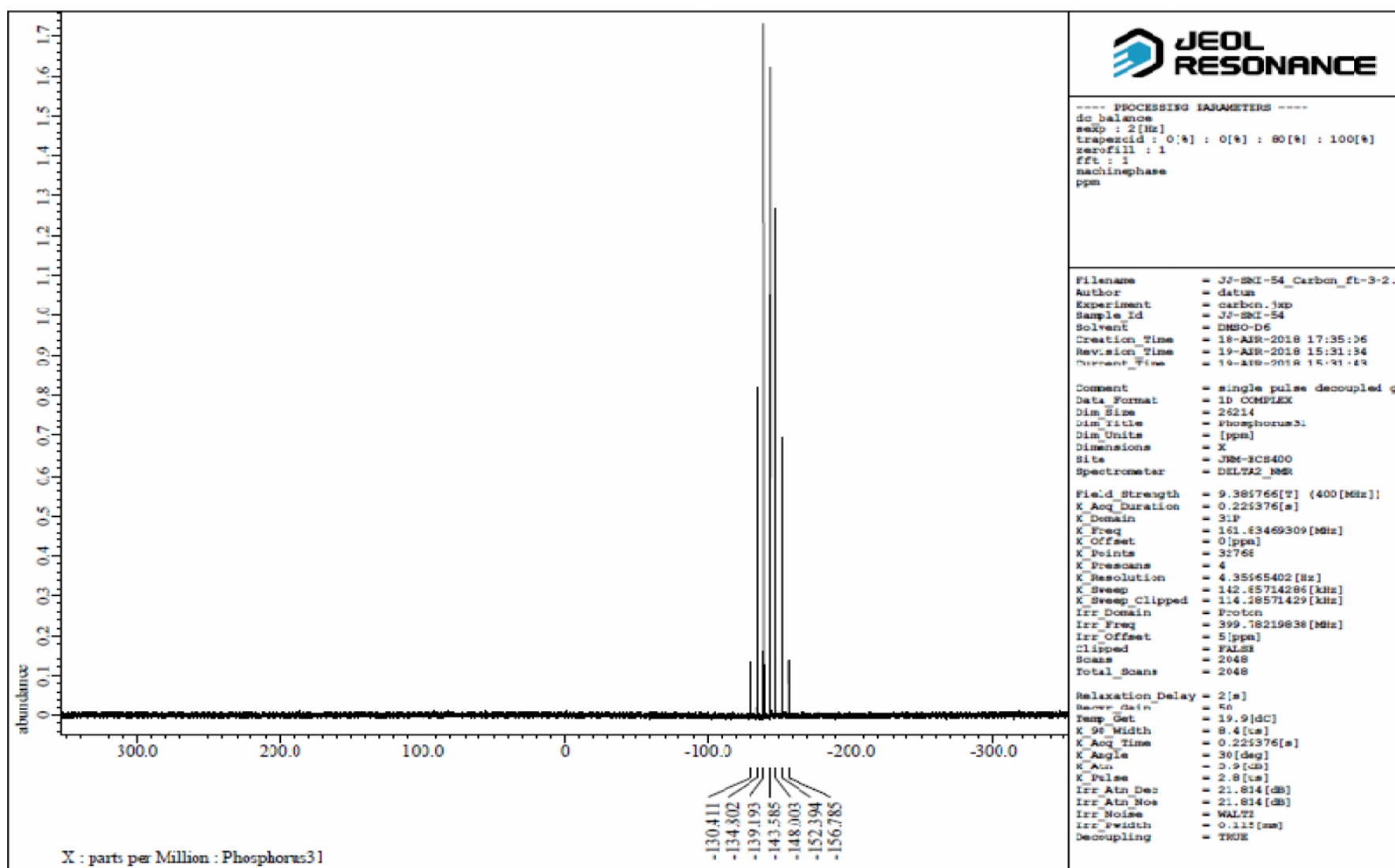
Figure 5.12 ^{31}P NMR spectra of the ionic complex (1a) in DMSO-d$_6$
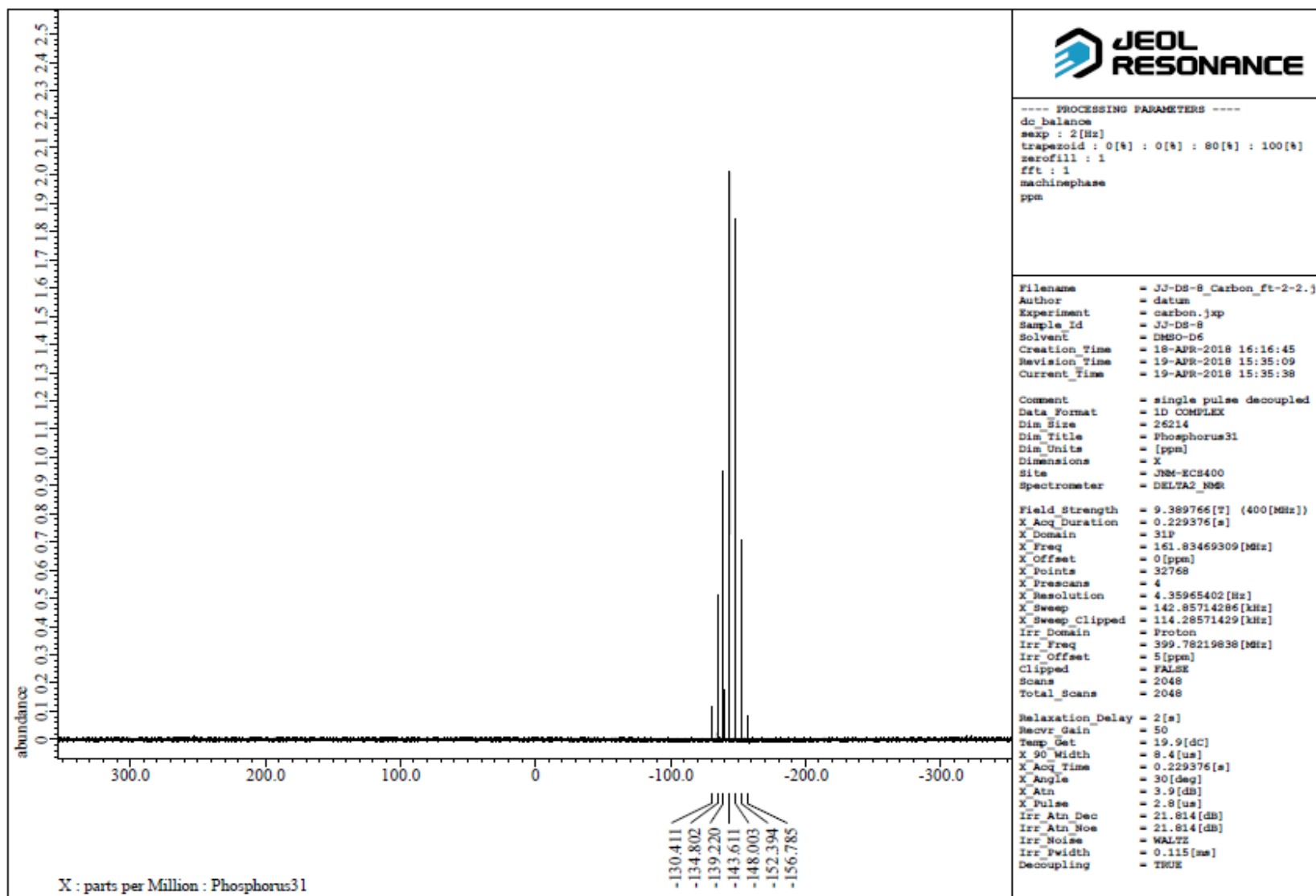
Figure 5.13 ^{31}P NMR spectra of the ionic complex (2a) in DMSO-d$_6$

5.4 References

[1] S. Sowmiah, V. Srinivasadesikan, M.C. Tseng, Y.H. Chu, Molecules 14 (2009) 3780-3813.

[2] M. Freemantle, An Introduction to Ionic Liquids, Royal Society of Chemistry, 2010.

[3] B. Kirchner, Ionic Liquids, Springer, 2009.

[4] P. Wasserscheid, T. Welton, Ionic Liquids in Synthesis, Wiley-VCH, 2008.

[5] T. Welton, Coord. Chem. Rev. 248 (2004) 2459–2477.

[6] J. K. Chang, M.T. Lee, C.W. Cheng, W.T. Tsai, M.J. Deng, Y.C. Hsieh, I.W. Sun, J. Mater.Chem. 19 (2009) 3732-3738.

[7] C. Zefer, K. Ocakoglu, C. Ozsoy, S. Icli, Electrochim. Acta 54 (2009) 5709-5714.

[8] H. Ohno, Electrochemical Aspects of Ionic Liquids; Wiley: Hoboken, NJ, 2005.

[9] S. Letaief, C.J. Detellier, Mater. Chem. 17 (2007) 1476-1484.

[10] M. Freemantle, An Introduction to Ionic Liquids, Royal Society of Chemistry, 2010.

[11] P. Wasserscheid, T. Welton, Ionic Liquids in Synthesis, Wiley-VCH, 2008.

[12] S. P. Gou, I.W. Sun, Electrochim. Acta 53 (2008) 2538-2544.

[13] J. K. Chang, M.T. Lee, C.W. Cheng, W.T. Tsai, M.J. Deng, Y.C. Hsieh, I.W. Sun, J. Mater. Chem. 19 (2009) 3732-3738.

[14] C. Zefer, K. Ocakoglu, C. Ozsoy, S. Icli, Electrochim. Acta 54 (2009) 5709-5714.

[15] Y.N. Hsieh, R.S. Horng, W.Y. Ho, P.C. Huang, C.Y. Hsu, T.J. Whang, C.H. Kuei, Chromatographia 67 (2008) 413-420.

[16] J. N. Pendleton, B.F. Gilmore, Int. J. Antimicrob. Agents. 46 (2015) 131-139.

[17] M. Y. El-Naggar, S.A. El-Assar, S.M. Abdul-Gawad, J. Microbiol. Biotechnol.19 (5) (2009) 468–473.

[18] M. I. Hossain, M. El-Harbawi, Y.A. Noaman, M.A.B. Bustam, N.B.M. Alitheen, N. A. Affandi, G. Hefter, C.Y. Yin,. Chemosphere 84 (2011) 101–104.

[19] J. Pernak, K. Sobaszkiewicz, I. Mirska, Green Chem. 5 (2003) 52–56.

[20] A. C. Roslonkiewicz, J. Pernak, J.K. Feder, A. Ramani, A.J. Robertsond, K.R. Seddon, Green Chem. 7 (2005) 855–862.

[21] J. L. Anderson, R. Ding, A. Ellern, D.W. Armstrong, J. Am. Chem. Soc. 127 (2005) 593- 604.

[22] M. Borse, V. Sharma, V.K. Aswal, P.S. Goyal, S. Devi, J. Colloid Interface Sci. 284

(2005) 282–288.

[23] C.M. Jin, C. Ye, B.S. Phillips, J.S. Zabinski, X. Liu, W. Liu, J.M. Shreeve, J. Mater. Chem. 16 (2006) 1529–1535.

[24] R. Wang, C.M. Jin, B. Twamley, J.M. Shreeve, Inorg. Chem. 45 (16) (2006) 6396–6403.

[25] S. Mastoor, S. Faizi, R. Saleema, B.S. Siddiqui, Magn. Reson. Chem. 52 (2014) 115–121.

[26] C. Perez, M. Paul, P. Bazerque, Acta. Biol. Med. Exp. 15 (1990) 113-115.

[27] B. Shadidi, S. Aghighi, N.A. Karimi, Iran. J. Biol. Sci. 4 (2005) 405-412.

[28] J. Fuller, R.T. Carlin, H.C. De Long, D. Haworth, J. Chem. Soc., Chem. Commun. 0 (1994) 299-300.

6.1 Introduction

The coordination chemistry of nitrogen-oxygen donor ligands and its complexes is an exciting area of research since long time due to their significant antioxidant activity [1-3] and biological activity against a number of bacteria and fungi [4-6]. The pharmacological evaluation of metal complexes derived from biologically important N-O donor ligands have been of utmost importance since some of the metal ions play active role in various metabolic reactions [7-9]. These metals act as vital metallic element and display immense biological activity upon association with certain metal-protein complexes by taking part in transport of oxygen and in redox reactions. These properties have created great interest in the development and study of these metal complex systems [10]. Several synthetic metal complexes have known to work as antioxidants which provide antioxidant defences from reactive oxygen species (ROS) damage and reinstate the balance by reducing the reactive groups [11-13]. Other than being antioxidants they acquired massive importance owing to their significant ability to prevent several diseases [14]. Bacteria show resistance toward many drugs which reduces the efficiency of antimicrobial treatment using existing antibiotics, thus there is an immense need today for the development of more competent drugs [15].

Numerous reported studies revealed that metal chelates are more active biologically than those of free ligands; this shows that upon chelation polarity of metal ions reduces which enhances the hydrophobic property of the complex and thus supports the diffusion through lipid cell membrane of the microorganisms [16]. Therefore, it can be inferred that interaction of metal ions with organic ligands increases biological activity than free ligands, this conclusion validates the several ongoing research work towards synthesis of new drugs of which mechanism of action are still not well established [15-17]. The newly developed metal complexes tend to have immense potential against many pathogenic bacteria [18]. Several studies have demonstrated an increase in antimicrobial activity following the interaction of several ligands with metal ions [19]. Metal chelation occurs in several significant biological processes where the coordination takes place between various metal ions and a broad variety of ligands [19-21]. Several categories of ligands and their metal chelates have been explored broadly which show their applications in the

field of medicine [22-24]. The complexes of copper with pyridazin derivatives and complexes of Ag(I), Co(II), Ni(II) and Cu(II) with *sulfamethoxypyridazine* were shown to have remarkable anti-inflammatory and antimicrobial activity [25-28].

8-Hydroxyquinoline is a small planar organic molecule having lipophilic property. It is an excellent N-O donor bidentate chelating ligand and having ability to form complexes with various bivalent metal ions through chelate formation [29]. 8-Hydroxyquinoline and its derivatives were reported to exhibit significant biological activity towards a number of microorganisms. Potential bioactivities of 8-hydroxyquinoline and its complexes can be attributed to their chelating ability. Metal discrepancy is one of the important reasons for several diseases; 8-hydroxyquinoline being a potent chelator could reinstate metal balance and therefore can be applicable in the treatment of metal imbalance related diseases. Numerous 8-hydroxyquinoline and its derivatives have potential applicability in medicinal field such as antineuro degenerative, anticancer, antioxidant, antimicrobial, anti-inflammatory, and antidiabetic activities [30]. Considering the above discussed biological properties of the nitrogen and oxygen containing ligands and their transition metal complexes, in the presented work we have undertaken the antioxidant, antibacterial and antifungal activity of the N-O donor ligands derived from 8-hydroxyquinoline and their metal complexes synthesized in previous chapters.

6.1.1   Antioxidant Activity

Antioxidants are the compounds which play a crucial rule in terminating effect of reactive species such as free radicals which are produced during the oxidation process. Formation of reactive oxygen species or free radicals during metabolic processes and other activities which are outside the range of antioxidant capability of a biological system generate oxidative stress [31]. This Oxidative stress plays key part in causing heart diseases, neurodegenerative diseases, cancer as well as in the aging process. The complexes exhibiting antioxidant activity avert these reactive species and in this way can control early ageing process and other diseases arising due to oxidative damage inside the body [32].

Antioxidative property of synthesized metal complexes can be investigated by studying the scavenging ability of those complexes towards trapping free radicals. The free radical scavenging method is one of the most commonly used techniques and provides first move towards assessment of antioxidant activity. These active species can oxidise biomolecules viz. lipids, proteins, nucleic acids, DNA, tissue damage and therefore cause degenerative diseases. Human diseases like cancer, emphysema, cirrhosis and arthritis etc. may be caused by oxidative damage [33, 34]. Up to a few extent most of the living organisms get protected from damages caused by free radical from some enzyme like super-oxide dismutase and catalase or other compounds like ascorbic acid, tocopherols, phenolic acids, polyphenols, flavonoids and glutathione [35-37]. However, antioxidant supplements may provide required protection to the body from the destructive effect of active species [36]. E. ribes has been reported as a potential antioxidant for diabetic animals [38-40].

6.1.1.1 Antioxidant activity using DPPH and ABTS radical scavenging activity

Free radical scavenging activity of methanolic solutions using 1, 1-diphenyl-2-picryl hydrazyl (DPPH) Assay

Antioxidant activity can be screened using a variety of the methods having different mechanisms, including hydrogen atom transfer (HAT), single electron transfer (ET), reducing power, and metal chelation among others. DPPH radical scavenging technique is one of the most used techniques and it provides first approach for evaluating antioxidant activity. The DPPH radical is one of the few stable organic nitrogen radicals. It is commercially available and does not have to be generated before assay. The stable DPPH radical have been used for determination of free radical-scavenging property of the compounds, according to the procedure described by Hatano et al., 1986 [41]. In this method compounds are dissolved in acetone/water (70:30) mixture, and a different concentration of each compound was added to methanolic solution of DPPH (0.1mM) at room temperature. After 30 minutes, the absorbance was recorded at 517 nm. This experiment repeated three times using Ascorbic acid and quercetin as standard antioxidants. IC_{50} value represents the inhibitory concentration of sample, which is

required to scavenge 50% of DPPH free radicals.Percentage inhibition calculated using following formula,

% scavenged DPPH radical = [($A_{control}$ - A_{sample})] / ($A_{control)}$] × 100

Where, $A_{control}$ is the absorbance of DPPH radical with blank; A_{sample} is the absorbance of DPPH radical + tested compound.

ABTS radical scavenging activity

Free radical scavenging ability of compounds can also be determined by using 2, 2´-azinobis [3-ethylbenzthiazoline]-6-sulfonate (ABTS) method. In this method 7.0 mM solution of ABTS in methanol and 2.45 mM potassium persulfate solution is prepared in water and used as separate stock solutions. Then the working solution prepared by mixing these two stock solutions in equal amount, and placed in dark for 12 hrs. at room temperature. To this solution further 1.0 ml of $ABTS^{.+}$ solution in methanol is added and mixed to get the absorbance 0.702 ± 0.001 units, at wavelength 734 nm. 1.0 ml solution of the compounds in methanol reacted with ABTS solution (1.0 ml) for 10 minutes and then absorbance recorded at 734 nm. The ABTS scavenging capacity for the tested compounds compared with standard antioxidants ascorbic acid and quercetin. Percentage scavenging capacity of the compounds calculated as,

% scavenged ABTS radical = [($A_{control}$ - A_{sample})] / ($A_{control)}$] × 100

Where, $A_{control}$ is the absorbance of ABTS radical + blank; A_{sample} is the absorbance of ABTS radical + compounds/standard

6.1.2   Antimicrobial activity

In recent time, multi-drug resistant microorganisms have caused serious threat in many countries across the world [42, 43]. Several recent clinical studies have depicted the increase in development of *Staphylococcus aureus* resistant to meticillin (MRSA), *enterococci* resistant to drug *vancomycin* (VRE) and many other infectious microorganisms which develop resistance for antibiotics [44]. Diseases originated due to such microorganisms posed a serious problem for the researchers working in the field of medicine and the necessity for successful treatment of these diseases, development of

new efficient drugs is required. Antimicrobial agents either kill or inhibit the harmful microbes [45]. Numerous antimicrobial agents have been developed and examined. Antimicrobial agents may be anti-bacterial, anti-fungal or antiviral and for all of them mechanism of action are different for curbing the infection. Advancement in identification of novel natural products and development of new synthetic compounds showing antimicrobial property as well as expansion in diversity of antibiotic agents are providing chemical leads for new drugs.

6.1.2.1 Strains of bacteria

In the present work antibacterial activity of complexes have been screened against gram positive (*Stapylococcus aureus*) and gram negative (*Escherichia coli*) bacteria using ciprofloxacin as a standard antibacterial agent. The bacteria selected for screening are known to cause diseases in human. *Staphylococus aureus* have known to cause staph-related illness, internal abscess and food poisoning while *Escherichia coli* causes bloody diarrhea, dermatitis, soft tissue infections, bacteremia and urinary tract infections.

Escherichia coli (E. coli)

Escherichia coli is a gram negative rod (*bacillus*), facultative anaerobic and non-sporulating in the family *Enterobacteriaceae* (Fig 6.1). *Escherichia coli* normally present in the lower intestine of living organisms having warm blood (endotherms). Most of the *E.coli* is not harmful, but some of them may cause severe food poisoning. The risk-free *E.coli* strains belongs to the regular flora of the gut, and can assist their hosts by producing vitamin K2 and by preventing the establishment of pathogenic bacteria inside the intestine [46]. *E. coli* represents approx 0.1% of gut flora, and fecal-oral diffusion is the most common route for diseases caused by infectious strains of *E. coli* bacteria [47].
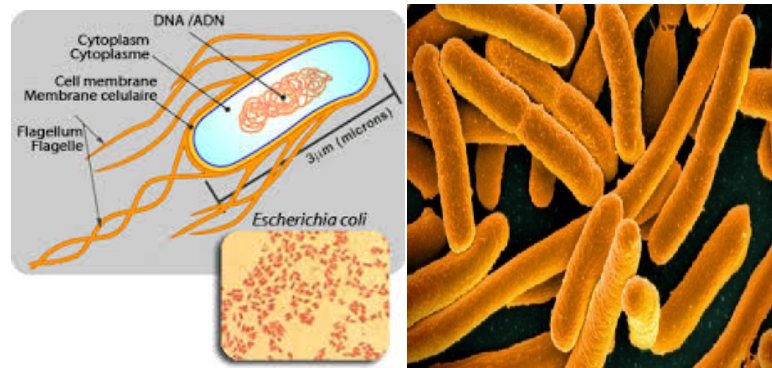
Figure 6.1: Structure of *E.Coli*

Staphylococcus aureus (S. aureus)

Staphylococcus aureus is a gram positive, non-motile and non-spore forming facultative anaerobes that belongs to the *Staphylococcace* (Figure 6.2) [48]. It mostly remains associated with skin, skin glands, and mucous membranes [49]. *Staphylococcus aureus* is an opportunistic pathogen often carried asymptomatically on the human body. Nearly 20-30% of whole population is the carrier of *S.aureus*. It forms golden colonies of intermediate size on thick medium. These golden colonies often cause - hemolysis on sheep blood agar plates. The golden colour of *S. aureus* colonies occur due to the caratenoids and are reportedly play significant role in guarding the pathogen from oxidants formed by the immune system [50].
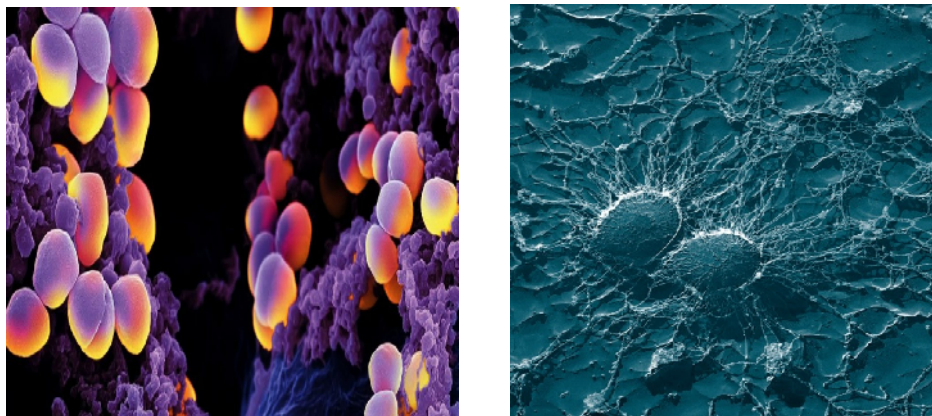
Figure 6.2: Structure of *Staphylococcus aureus*

6.1.2.2 Fungal Strains

Antifungal activity was screened against two fungal species *Trichoderma reesei* and *Fusarium* by using *Ketokenazole* as standard antifungal agents. The selected fungal species are known to cause human.

Trichoderma reesei

Trichoderma reesei is a mesophilic filamentous fungus (figure 6.3) originally isolated from the Solomon Islands during the Second World War. It is an anamorph of the fungus *Hypocrea jecorina*. *T. reesei* has the capacity to secrete large amounts of cellulolytic enzymes. It is well known for its ability to produce large amounts of cellulases and hemicellulases, which are critical for this microorganism to acquire energy from the environment [51]. The filamentous fungus *Trichoderma reesei* is today a paradigm for commercial scale production of different cellulases and hemicellulases and is well adapted to fermenter cultivations [52]. It is also a distinguished biological source of cellulolytic and hemicellulolytic enzymes to degrade the plant cell wall, and thus, is widely used in the industry for production of renewable carbon source.
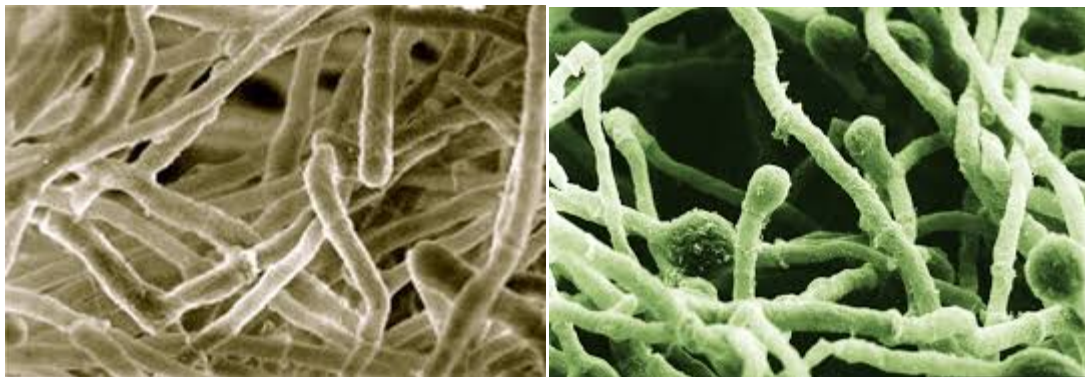
Figure 6.3: Structure of *Trichoderma reesei*

Fusarium

Fusarium is a large and diverse genus of filamentous fungi (Figure 6.4) that includes a number of economically important plant pathogens, including *F. graminearum*, *F. oxysporum*, and *F. solani*. Most of the *Fusarium* species belongs to soil

fungi and are distributed worldwide. Some of these species are plant pathogens which damages root, stem, vascular wilt and fruit. Several species have emerged as important opportunistic pathogens in humans causing hyalohyphomycosis, mycotic keratitis and onychomycosis [53]. Some other species act as mycotoxin producers. Even though many species of *Fusarium* can behave as infectious pathogens in humans not having sound immunity, mycotoxicoses have caused most of the health problems to the animal and human. There have been more than 50 species of *Fusarium* which infect mostly plant and animals and to some extent humans. Twelve species were found to be infectious; the most harmful is *Fusarium solani* (50% of cases) then Fusarium oxysporum (in 20% cases) followed by *Fusarium verticillioidis* and *Fusarium moniliforme* (10% each) [54, 55].
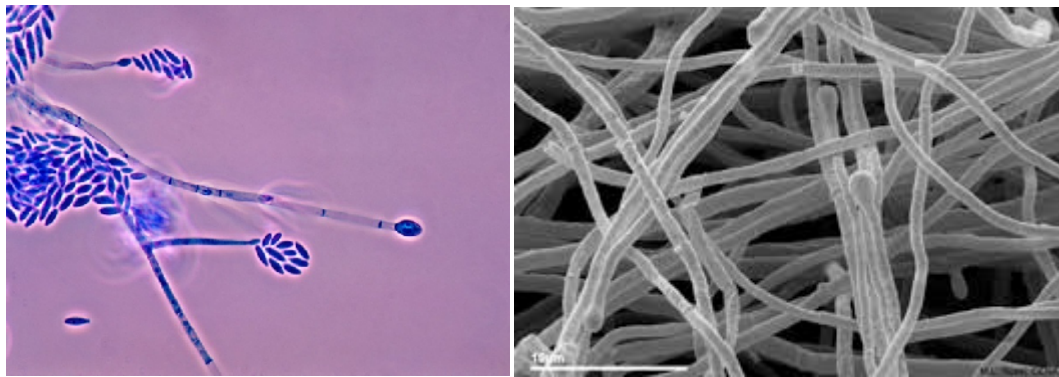
Figure 6. 4: Structure of *Fusarium*

Penicillium

Penicillium, saprophytic fungus, commonly known as blue or green mold is one of the most common fungi appearing in a wide range of habitats like air, soil, covered environments vegetation and many other food merchandises (figure 6.5). *Penicillium* colonies occur in various colours like blue-green, white, yellow and pink with a velvety to powdery texture. Their growth is very fast and releases a strong musty odour. It is distributed worldwide and has a big impact on economy. In nature key role of *Penicillium* is to decompose the organic compounds, and causes rots food crops as pre- and post harvest pathogens and forms various mycotoxins. *Penicillium* acts as a common allergen causing hypersensitivity, pneumonitis, fever, nasthma. Most of the *Penicillium* is usually not pathogenic however, there are some exclusions. Some of

the *Penicillium* species can produce microbial volatile organic compounds (MVOCs) and toxins which can harm human health particularly upon continuing exposure. The most common species of *Penicillium* are *Penicillium marneffei*, *Penicillium purpurogenum*, *Penicillium chrysogenum*, and *Penicillium janthinellum*.

Figure 6.5 Structure of *Penicillium*

6.2 Determination of Antimicrobial Assay

6.2.1 Evaluation of antibacterial activity by inhibition zone technique

In vitro antibacterial activity of all the ligands and the metal complexes synthesized were tested against two bacterial strains *Staphylococcus aureus* Gram (+ve) and *Escherichia coli* Gram (-ve) by the agar well diffusion technique [56]. Mueller Hinton agar no. 2 (Hi Media, India) was used as the medium for bacteria. Bacterial extracts were diluted in 100% Dimethylsulphoxide (DMSO) to make the concentration of 5 mg/mL. The Mueller Hinton agar was liquefied, then cooled to 48 – 50 ℃, standardized inoculums (1.5×108 CFU/mL, 0.5 McFarland) and after that mixed to the molten agar. This mixture was filled into sterilized petri dishes which resulted into solid plate. To the incubated agar plates wells were made of diameter 6 mm. The compounds to be tested (100 µl) were placed into the well and the plates were incubated at 37℃ for 12 h. The antimicrobial activity of the compounds against bacterial species was determined by measuring diameter of zones formed around the well. The zone of inhibition diameter (measured in mm) generated by the tested compounds were compared with those formed

by standard antibiotics, streptomycin. The control zones were subtracted from the test zones and the resulting zone diameter was measured with antibiotic zone reader to nearest mm. The procedure was repeated thrice in order to diminish the error and the mean values taken.

6.2.2 Evaluation of antifungal activity by agar well diffusion method

Anti fungal activity of the all the compounds was investigated against fungal strains, *Fuseriumsemitectum*, *Trichoderma reesei* and *Penicillium* by using agar well diffusion method [57]. The fungi were subcultured onto Sabouraud's dextrose agar, SDA (Merck, Germany) and cultivated at 37°C for 24 h and 25°C for 2 - 5 days. Spores of fungi were suspended in sterile PBS and the concentration was maintained to 106 cells/ml. To this fungal suspension sterile swab was dipped and spread on the agar medium surface. These plates were allowed to dry at room temperature for 15 min. In the culture media wells having diameter of 10 mm and at approximately 7 mm distant were perforated with the help of disinfected glass tube. Very diluted fresh extracts (0.1 ml) \was poured to fullness for each well. Further these plates were incubated at 37°C for 24 h and after that activities of compounds were tested by measuring the diameter of zone of inhibition (in mm). All experiments were performed thrice and mean values were calculated.

6.3   Result and discussion

6.3.1   Antioxidant activity of cobalt complexes and ligands (Chapter 2)

Free radical scavenging activity of compounds using DPPH and ABTS assay

Varity of derived 8-Hydroxyqunoline ligands on complexation with cobalt metal show good antioxidant activity. In order to test *in vitro* antioxidant activity, scavenging effect of the compounds upon radicals DPPH and ABTS have been used as an easy and trustworthy method. The free radical scavenging activities of methanolic solutions of tested compounds at different concentrations are shown in Tables 6.1 & 6.2 and graph (figure 6.6 & 6.7).

It is evident from the results that free radical scavenging activity of these compounds was concentration dependent. From the data it is clearly indicated that the increase in radical scavenging activity of these compounds is dose dependent. At higher concentration (more than 80-100 µg/ml) all the compound except ligands (MOQ, PMOQ

and BQOP) scavenge more than 95 % DPPH and ABTS radicals and show potent antioxidant properties at this concentration level. It is evident that among the compounds tested the complexes (**8**) and (**9**) exhibited strong interactive ability with DPPH and ABTS, respectively. Compound (**8**) exhibited maximum free radical scavenging activity (98.69%) for DPPH radicals while compound (**9**) displayed highest free radical scavenging activity (98.26%) for ABTS radicals. The ligands MOQ, PMOQ and BQOP showed lower antioxidant activity (35.07), (34.53), (32.43) and (38.45), (35.77), (30.33) for DPPH and ABTS radicals respectively, comparatively to the AA and QRT as a standard is shown by graphs (Figure 6.6). The compounds which have low IC-50 value are good antioxidant. The standards [i.e. AA (40.4, 38.4 µg/mL) and QRT (41.9, 41.8 µg/mL) for DPPH and ABTS radicals, respectively] have higher IC-50 value than that of complexes and lower than ligands at higher concentrations. On the basis of IC-50 data, it can be assigned that complexes are more potent antioxidant than the ligand. The comparative antioxidant activity of compounds against AA, and QRT as a standard is shown by graphs (Figure 6.6). All DPPH and ABTS scavenging activities were carried out only to evaluate the relative antioxidant activities. The antioxidant activities of compounds under consideration are significant which indicates that among the tested compounds complexes show potent antioxidant activity.

6.3.2 Antioxidant activity of palladium complexes and ligands (Chapter 3)

Free radical scavenging activity of methanolic solutions using DPPH and ABTS assay

The free radical scavenging activity data of methanolic solutions of ligands and their palladium complexes at various concentrations are depicted in Tables 6.3 & 6.4. On the basis of the result it is clearly observed that all the free radical scavenging data of these synthetic complexes was concentration dependent. All the ligands (MOQ, BQOP, BQOH) revealed IC-50 value of 65.77, 64.48, 69.82 and 63.47, 64.77, 65.90 for DPPH and ABTS radicals, respectively which is moderately higher than the standard AA and QRT as shown in table 6.3 & 6.4 and graph (figure 6.8 & 6.9).

Present result of antioxidant data and graph for DPPH and ABTS radicals clearly confirmed that, the palladium complexes show more potent antioxidant activity than the ligands.   [Pd(PMOQ)Cl$_2$] complex displayed higher antioxidant property among all the

ligands and complexes for both DPPH and ABTS radicals which is just about close to the standard. Complex [Pd(MOQ)$_2$Cl$_2$] exhibited lower antioxidant activity, complex [Pd(BQOP)Cl$_2$] and the ligands displayed moderate activity. The results also confirmed that the free ligands and their metal complexes showed significant free radicals scavenging activity.

Table 6.1: Antioxidant activity of synthesized Co(II) complexes and ligands (DPPH assay)
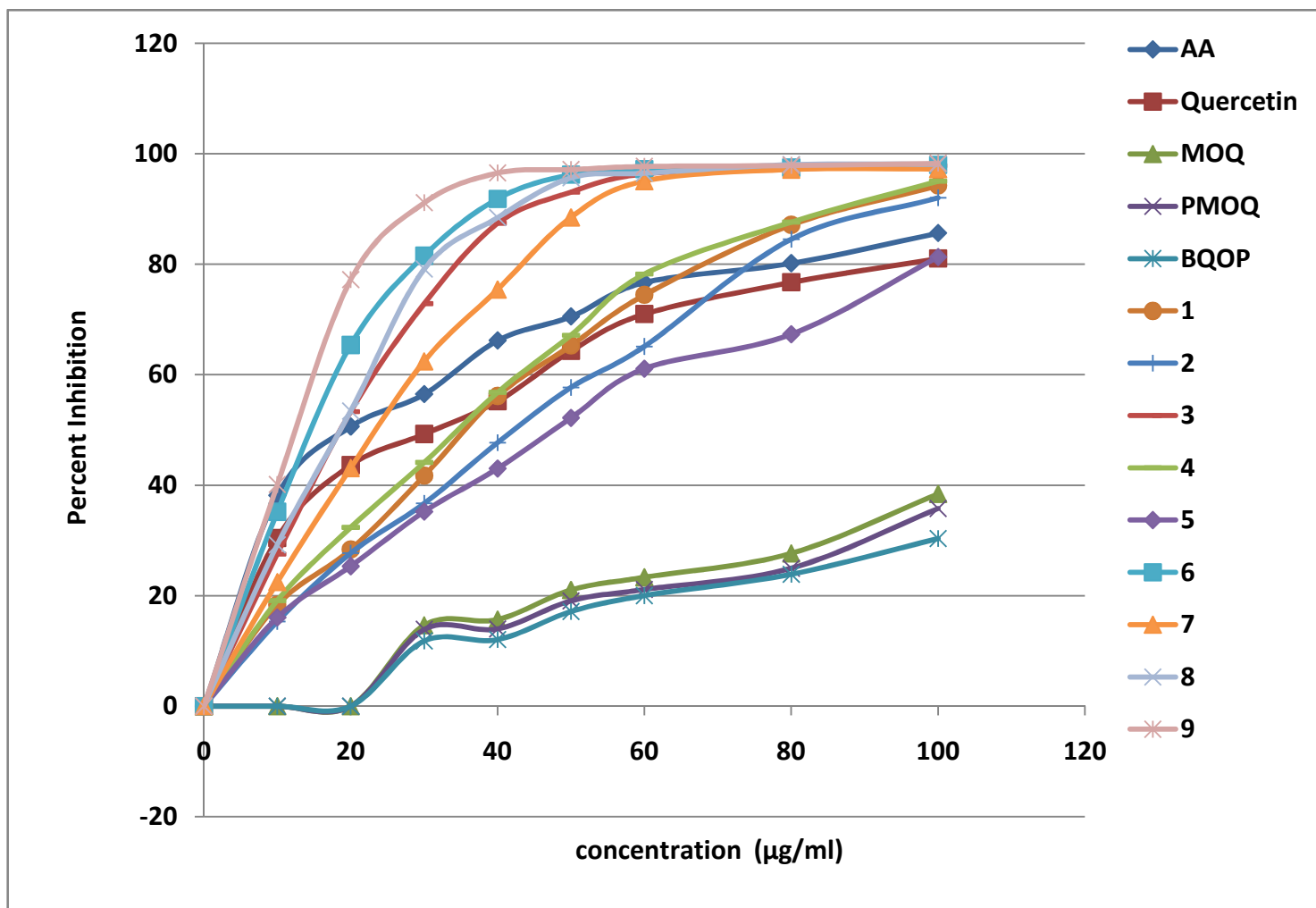
Compounds	Concentration (µg/ml) DPPH									
	0	**10**	**20**	**30**	**40**	**50**	**60**	**80**	**100**	**IC-50 µg/ml**
Ascorbic acid (AA)	0	6.97	11.26	16.40	19.48	22.10	29.31	36.95	41.86	40.4
Quercetin	0	5.65	10.31	14.73	17.59	20.01	26.87	31.98	35.07	41.9
MOQ	0	0	0	11.78	12.46	16.86	20.55	23.73	34.53	54.3
PMOQ	0	0	0	9.70	11.78	15.87	19.68	21.22	32.43	53.2
BQOP	0	0	0	8.86	10.48	13.97	18.73	20.12	30.33	51.7
1	0	15.54	26.58	36.46	48.03	59.65	69.64	85.01	92.42	38.5
2	0	12.73	23.40	30.68	41.78	53.65	60.43	77.01	91.32	44.9
3	0	23.24	42.74	64.65	81.60	90.34	95.56	97.05	98.12	21.6
4	0	15.13	26.86	38.46	51.86	62.14	72.44	87.74	94.32	22.3
5	0	31.45	58.34	72.96	91.53	96.14	97.01	97.74	98.52	36.9
6	0	19.58	36.44	55.86	65.18	79.10	92.97	96.45	98.03	15.8
7	0	25.68	47.02	71.09	86.58	96.32	97.15	97.86	98.43	25.3
8	0	35.26	68.33	91.02	95.48	96.45	98.01	98.24	98.69	19.9
9	0	18.37	35.25	53.37	67.80	81.24	91.32	95.57	97.86	12.8

Table 6.2: Antioxidant activity of synthesized Co(II) complexes and ligands (ABTS assay)

Compounds	Concentration (µg/ml) ABTS									
	0	**10**	**20**	**30**	**40**	**50**	**60**	**80**	**100**	**IC-50 µg/ml**
Ascorbic acid (AA)	0	38.17	50.62	56.48	66.20	70.53	76.70	80.17	85.63	38.4
Quercetin	0	30.43	43.62	49.26	55.19	64.31	70.98	76.72	81.02	41.8
MOQ	0	0	0	14.65	15.68	21.05	23.35	27.68	38.45	55.1
PMOQ	0	0	0	13.89	13.99	19.06	21.13	24.97	35.77	52.4
BQOP	0	0	0	11.79	12.05	17.13	20.01	23.87	30.33	50.6
1	0	18.34	28.37	41.71	56.15	65.29	74.44	87.11	94.22	34.5
2	0	15.34	27.70	36.69	47.71	57.69	65.12	84.52	92.02	40.8
3	0	27.53	53.30	72.84	87.38	93.04	96.33	97.25	97.81	18.5
4	0	19.12	32.36	44.11	56.79	67.14	78.21	87.61	95.02	32.8
5	0	16.05	25.34	35.23	43.03	52.20	61.11	67.33	81.32	45.9
6	0	35.19	65.38	81.55	91.84	96.22	97.20	97.49	97.98	14.2
7	0	22.47	43.12	62.41	75.42	88.48	95.05	97.14	97.21	22.7
8	0	29.21	53.41	79.10	88.43	95.62	96.47	98.02	98.11	18.6
9	0	40.12	77.21	91.11	96.52	97.14	97.71	97.88	98.26	12.3
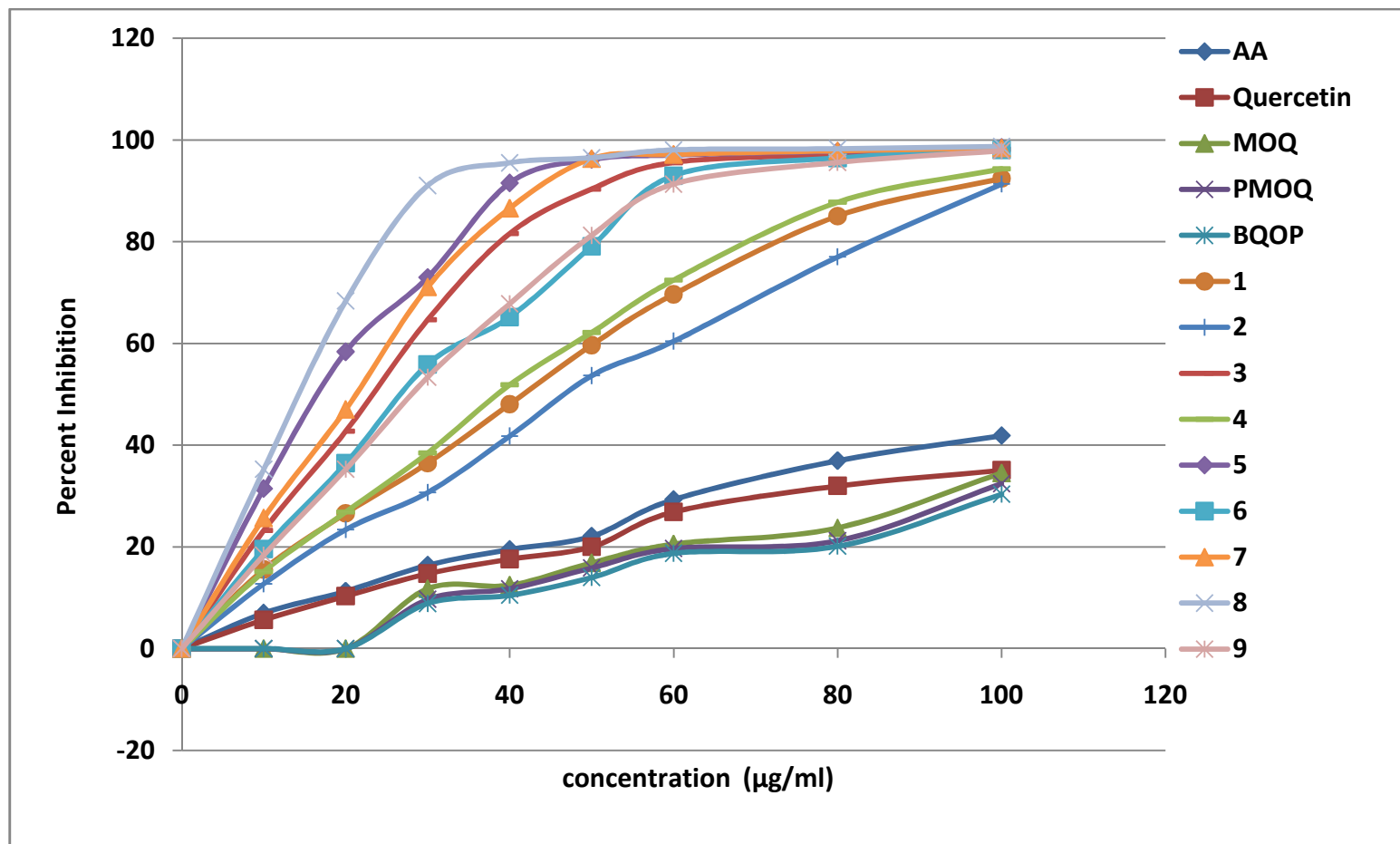
Figure 6.6 Antioxidant activities of synthesized cobalt complexes and ligands (DPPH assay)

Figure 6.7: Antioxidant activity of synthesized cobalt complexes and ligands (ABTS assay)

Table 6.3: Antioxidant activity of synthesized Pd(II) complexes (DPPH assay)

Compound	Concentration (µg/ml) DPPH												
	0	10	20	30	40	50	60	80	100	150	200	500	IC-50 µg/ml
Ascorbic acid (AA)	0	6.97	11.26	16.40	19.48	22.10	29.31	36.95	41.86	52.10	67.73	84.73	62.19
Quercetin	0	5.65	10.31	14.73	17.59	20.01	26.87	31.98	35.07	45.26	56.83	80.28	66.21
MOQ	0.0	0.0	0.0	11.78	12.46	16.86	20.55	23.73	34.53	47.65	59.16	84.23	65.77
PMOQ	0.0	0.0	0.0	9.47	11.78	15.87	19.68	21.22	32.43	47.68	63.67	85.98	64.48
BQOP	0.0	0.0	0.0	8.86	10.48	13.97	18.73	20.12	30.33	45.98	61.47	71.87	69.82
[Pd(MOQ)$_2$Cl$_2$]	0.0	0.0	0.0	11.83	14.71	17,65	23.45	27.63	36.13	53.72	66.03	89.21	61.53
[Pd(PMOQ)Cl$_2$]	0.0	0.0	12.44	15.87	21.68	26.67	31.78	40.82	51.68	71.53	89.30	91.42	60.89
[Pd(BQOP)Cl$_2$]	0.0	14.56	24.64	32.45	39.67	46.28	55.56	67.46	74.78	86.78	92.96	96.71	57.39

Table 6.4: Antioxidant activity of synthesized palladium complexes (ABTS assay)

Compounds	Concentration (µg/ml) ABTS												
	0	10	20	30	40	50	60	80	100	150	200	500	IC-50 µg/ml
Ascorbic acid (AA)	0	38.17	50.62	56.48	66.20	70.53	76.70	80.17	85.63	91.02	93.23	94.58	50.19
Quercetin	0	30.43	43.62	49.26	55.19	64.31	70.98	76.72	81.02	87.37	91.33	92.17	51.38
MOQ	0.0	0.0	0.0	14.65	15.68	21.05	23.35	27.68	38.45	54.65	72.44	89.76	63.47
PMOQ	0.0	0.0	0.0	13.89	13.99	19.06	21.13	24.97	35.77	51.93	67.61	79.62	64.77
BQOP	0.0	0.0	0.0	11.79	12.05	17.13	20.01	23.87	33.61	48.89	64.53	76.54	65.90
[Pd(MOQ)2Cl$_2$]	0.0	0.0	0.0	18.28	20.63	23.04	24.73	32.46	40.14	61.72	74.69	85.62	57.93
[Pd(PMOQ)Cl$_2$]	0.0	0.0	13.94	17.32	24.64	29.42	34.82	45.73	56.97	83.46	91.20	93.76	54.42
[Pd(BQOP)Cl$_2$]	0.0	13.79	22.57	29.56	34.35	46.28	52.79	64.79	74.97	84.75	91.80	93.86	53.09
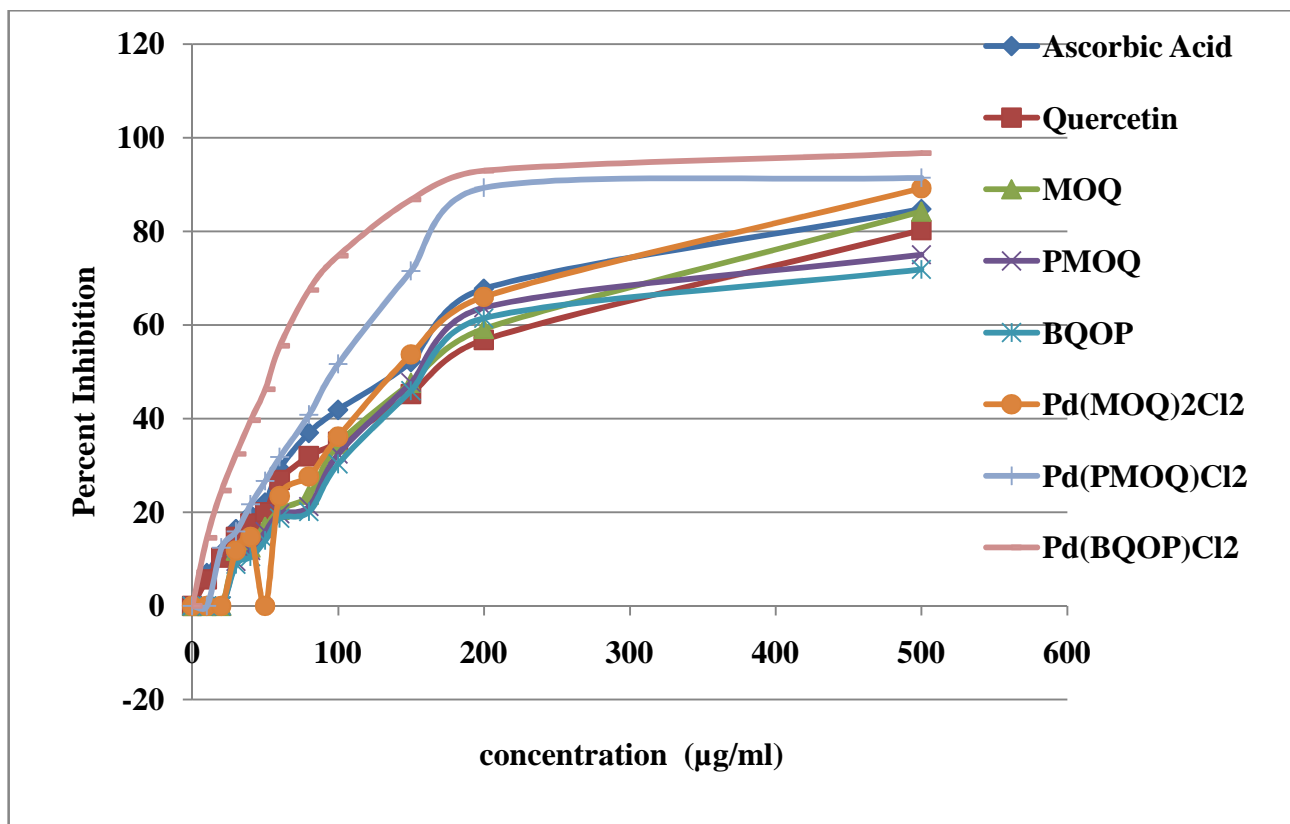
Figure 6.8: Antioxidant activity of synthesized Pd(II) complexes (DPPH assay)
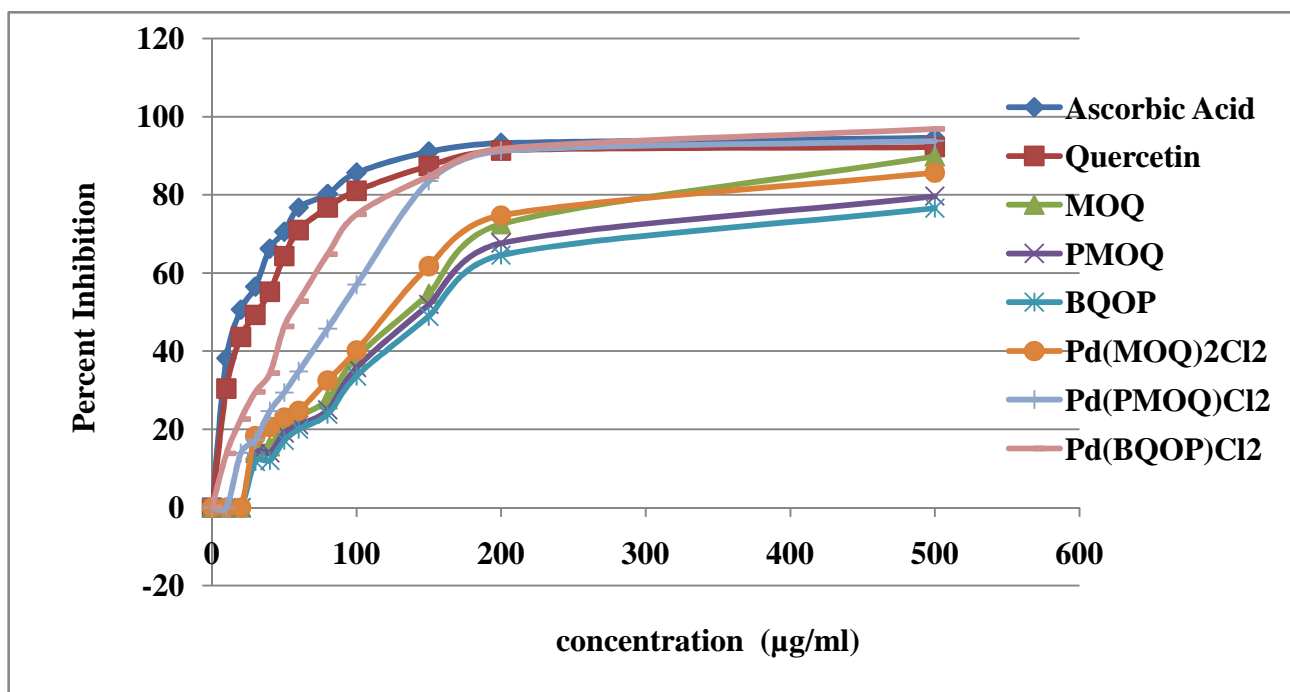
Figure 6.9: Antioxidant activity of synthesized Pd(II) complexes (ABTS assay)

6.3.3 Antimicrobial activity of ionic compounds (Chapter 5)

In order to test antimicrobial activity of ionic compounds, it is easier to start with antibacterial activities owing to the short generation time of bacteria as compared to other living organisms [58, 59]. In 2015 a review studies of Pendleton et. al [60] focused on the antimicrobial potential of ionic compounds. This has indirectly led to the realization that some ILs exhibit anti-bacterial activity. Antimicrobial activity of new ionic liquid and their precursor were investigated against two bacteria *S. aureus* (G$^+$) & *E. coli* (G$^-$) and two fungai, *T. reesei* (G$^+$) & *Penicillinium* (G$^-$). The results of the antimicrobial activity are shown in table 6.5 and figures 6.10 & 6.11.

The parent compound BQOH has not shown any anti-bacterial and antifungal activity against any of the tested microorganisms and fungi while the compound BQOP has shown all activity against *E. coli* (G$^-$) and fungi *T. reesei* (G$^+$) & *Penicillinium* (G$^-$) except *S. aureus* (G$^+$) bacteria. The parent compound BQOH has not shown any activity against any of the screened microorganisms and fungi but their ionic liquids (**2**) and (**2a**) showed both the activities against all tested microorganisms and fungi. In general ionic liquid (**1**) showed high activity against all G– or G+ bacteria and fungi was most potent compound as shown in table. The antimicrobial activity of ionic compounds (**1**) and (**2**) are much higher than the compound (**1a**) and (**2a**). This effect indicates that the brominated ionic liquids are highly active comparatively to the hexaflorophosphate containing ionic liquid. For G$^-$ or G$^+$ bacteria and fungi, the PF$_6^-$ containg ionic liquids (**1a**) and (**2a**) recorded higher activity against *E. coli* (G$^-$) & *T. reesei* and lower against *Penicillin*(G$^-$) *S. aureus* (G$^+$).

Table 6.5 Antibacterial activity data for ligands and its anionic complexes after 24 hours.

Compounds	Concentration (mg/Disc)	Average value of bacteriostatic diameter (mm)*		Average value of fungal static diameter (mm)*	
		S. aureus	*E. coli*	*T. reesei*	*Penicillin*
BQOP	2	0	8	4	8
BQOH	2	0	0	0	0
(**1**)	2	10	20	14	10

(1a)	2	2	10	8	1
(2)	2	16	18	24	26
(2a)	2	1	8	12	2
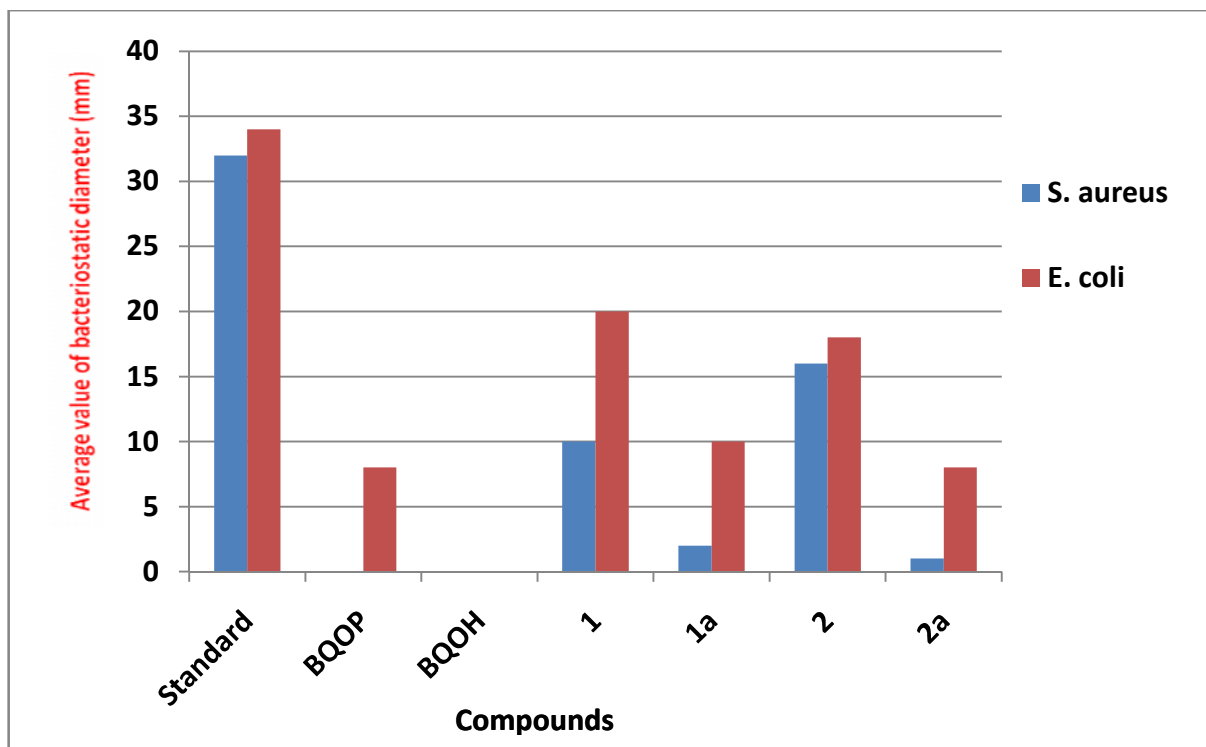
Figure 6.10 Bar graph showing the relative antibacterial activity of the ligands and ionic compounds

6.1.1   Antimicrobial activity of ligands and their cobalt complexes (Chapter 2)

The antibacterial activity of ligands and their corresponding cobalt complexes were tested against *S. aureus* and *E. coli* and antifungal activity against *T. reesei* and *Fusarium.* Both the antibacterial and antifungal results are shown in table 6.6. From the results it is revealed that some of the synthesized cobalt complexes show better activity than that of ligands while some complexes do not show any activity against the same microorganism. The enhanced antimicrobial activity of the metal complexes can be attributed to the effect of metal ion on the normal cell processes.

Tweedy's chelation theory may be a possible explaination for enhanced antimicrobial activity of the complexes [61-64]. According to this theory due to chelation

polarity of the metal ion reduces significantly since the positive charge gets partly shared with the chelating ligands and the delocalization of - electron. This increases the lipophilic property of the metal atom, consequently, enhances its permeability to the cell membrane through lipid layer.
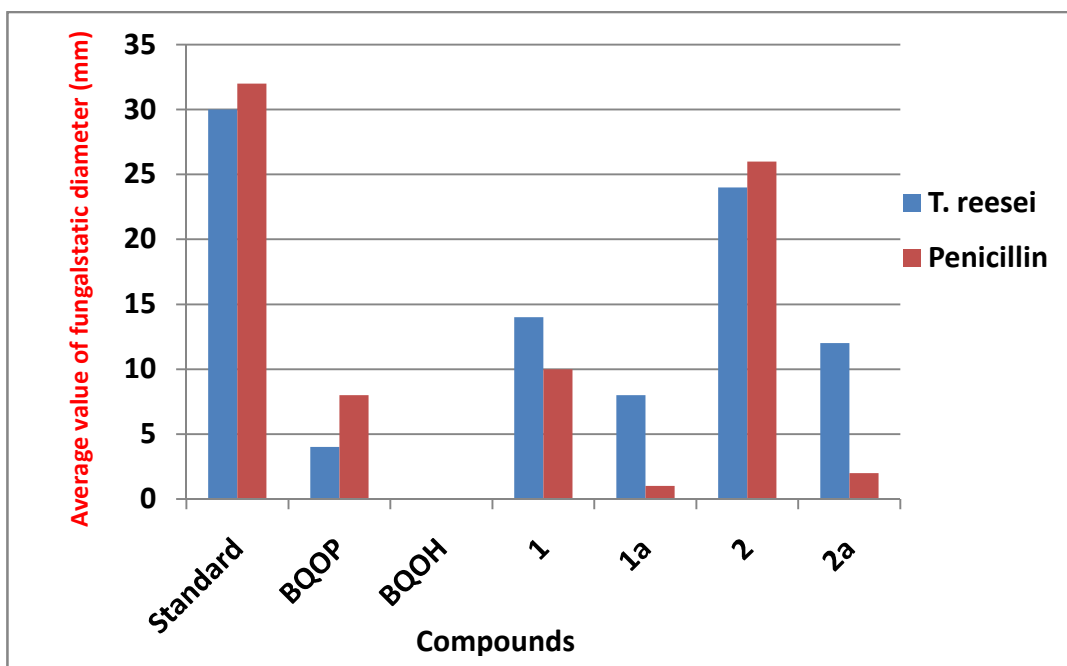
Figure 6.11 Bar graph showing the relative antifungal activity of the ligands and ionic compounds.

The results shown in table 6.5 and graphs (fig. 6.12 & 6.13) clearly show that the complexes (3), (6), (8) and (9) exhibited significant bacterial growth against *S. aureus* (Gram +ve) and *E. coli* (Gram -ve) bacteria at a concentration of 1 mg/ml while no bacterial growth was observed in case of complexes (1), (2), (4) and (5). In case of complex (7), the growth of the organism was observed against only in Gram –ve bacteria *E. coli* at concentration 1 mg/ml. The complexes having substituted fluorine containing groups with cobalt metal displayed to be the more effective antibacterial activity compared to the parent complexes and ligands.

In the study of the antifungal activity, chelating cobalt complexes tested against the fungal strains, *T. reesei* and *Fusarium,* were observed higher activity at concentrations 1 mg/ml. All the results shown in table 6.5 and figure 6.12 & 6.13 clearly show that all

these complexes exhibit higher activity than their parent ligands. In the case of the *T. reesei*, except complex (2) and (5), all the other complexes demonstrate significant high antifungal activity. With respect to the results of complexes (3), (8) and (9), no bacterial growth was observed against fungi *Fusarium.* The complexes (3) and (9) showed the same activity against the *T. reesei* while the complexes (5) and (6) showed similar activity against the gram -ve fungi *Fusarium*.

Even though there is an adequate rise in the activities of the complexes against bacteria and fungi than their corresponding free ligands, however, some complexes could not exhibit significant activity as compared to standard antifungal and antibacterial agents. From the data it is evident that the cobalt complexes having fluorine substituted group exhibit better activity and the synthesized Co(II) complexes are more active against fungi than the various strains of bacteria (Table 6.5).

Table 6.5 Antibacterial activity data for ligands and its cobalt complexes after 24 hours.

Compound	Concentration (mg/Disc)	Average value of bacteriostatic diameter (mm)*		Average value of fungal static diameter (mm)*	
		S. aureus	*E. coli*	*T. reesei*	*Fusarium*
Standard (Ciprofloxacin)	2	39	40	-	36
MOQ	2	2	8	2	8
PMOQ	2	3	6	0	6
BQOP	2	-	8	4	8
[(MOQ)2CoCl2](1)	2	-	-	-	18
[(PMOQ)CoCl2](2)	2	-	-	12	15
[(BQOP)CoCl2](3)	2	25	17	38	-
[(MOQ)2Co(OC6F5)$_2$](4)	2	-	-	34	40

[(MOQ)2Co(OC3F7)$_2$](5)	2	-	-	-	24
[(PMOQ)Co(OC$_6$F$_5$)$_2$](6)	2	16	10	27	24
[(PMOQ)Co(OC$_3$F$_3$)$_2$](7)	2	-	7	32	20
[(BQOP)Co(OC$_6$F$_5$)$_2$](8)	2	13	10	30	-
[(BQOP)Co(OC$_3$F$_3$)$_2$](9)	2	18	20	37	-
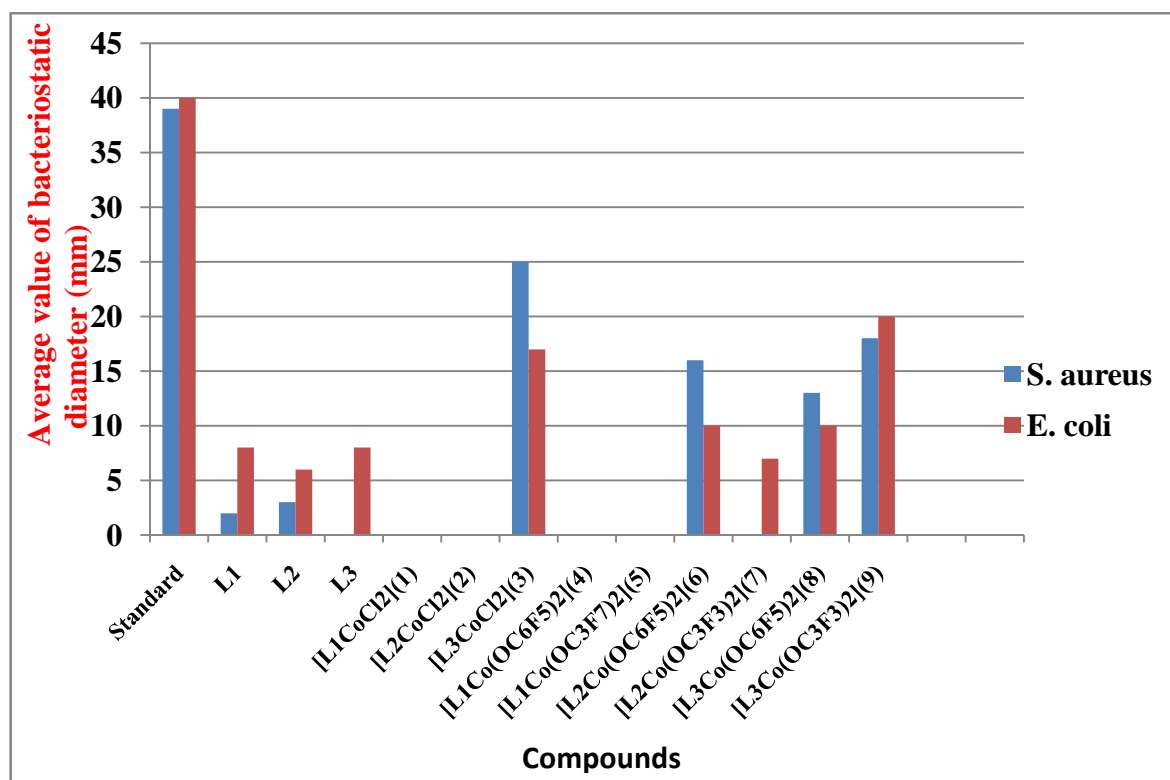
Figure 6.12 Bar graph showing the relative antibacterial activity of the ligands and Co(II) complexes
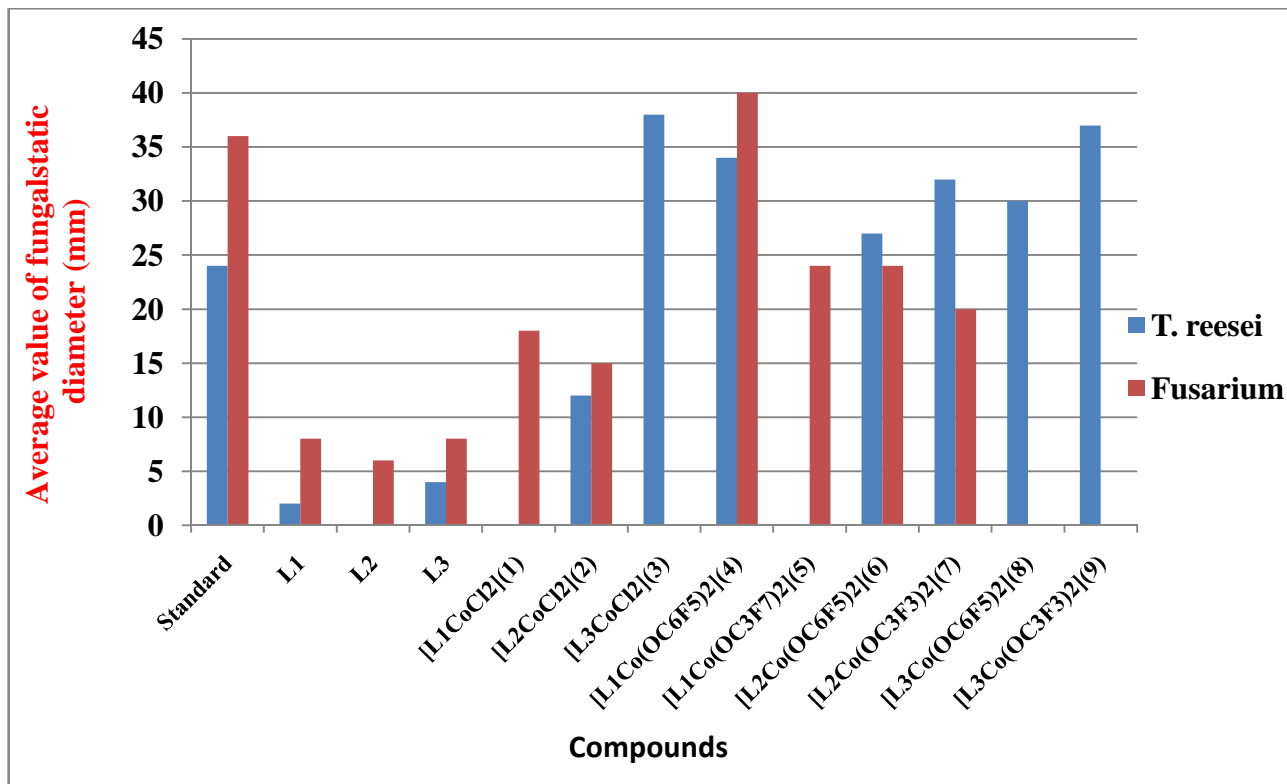
Figure 6.13 Bar graph showing the relative antifungal activity of the ligands and Co(II) complexes

(a) Antibacterial activity of cobalt complexes (1), (4) and (5) against *S. aureus*	(b) Antibacterial activity of cobalt complexes (2), (6) and (7) against *S. Aureus*	(c)Antibacterial activity of cobalt complexes (3), (8) and (9) against *S. Aureus*
(d) Antibacterial activity of cobalt complexes (1), (4) and (5) against *E. coli*	(e) Antibacterial activity of cobalt complexes (2), (6) and (7) against *E. coli*	(f) Antibacterial activity of cobalt complexes (3), (8) and (9) against *E. Coli*
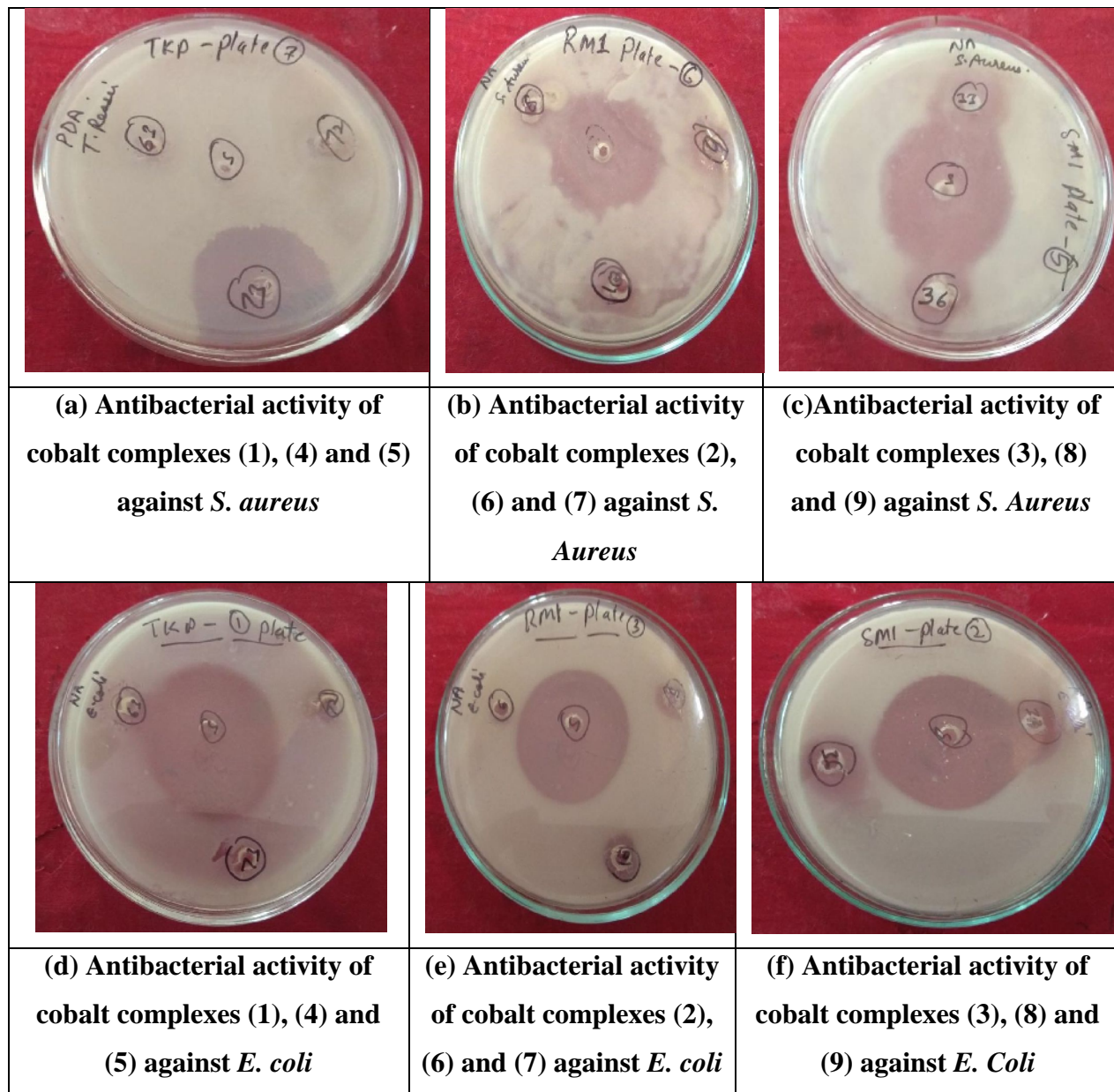
Figure 6.14 (a-f) Antibacterial activity of newly synthesized cobalt complexes against *S. aureus* and *E. coli* after 24 hrs

(a)Antifungal activity of cobalt complexes (1), (4) and (5) against *T. reesei*	**(b) Antifungal activity of cobalt complexes (2), (6) and (7) against *T. reesei***	**(c) Antifungal activity of cobalt complexes (3), (8) and (9) against *T. reesei***
(d)Antifungal activity of cobalt complexes (1), (4) and (5) against *Fusarium*		**(e)Antifungal activity of cobalt complexes (2), (6) and (7) against *Fusarium***
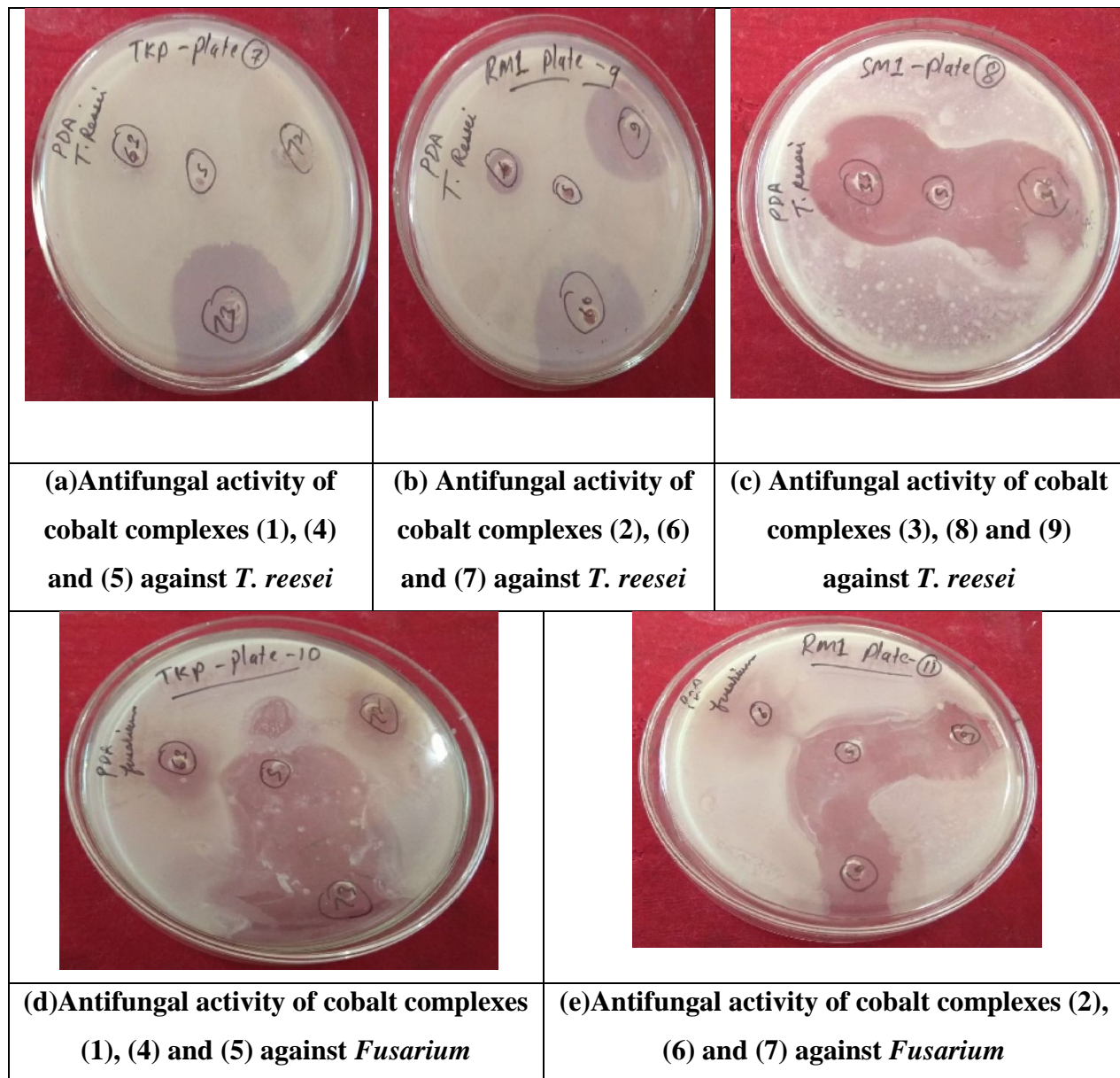
Figure 6.15 (a-e) Antifungal activity of newly synthesized cobalt complexes against *T. reesei* and *Fusarium* after 24 hrs

(a) Antibacterial activity of compounds (1), and (BQOP) against *S. aureus*	(b) Antibacterial activity of compound (2) and (2a) against *S. Aureus*
(c)	(d)

(e) Antibacterial activity of compounds (1), and (BQOP) against *E. Coli*	(f) Antibacterial activity of compounds (2), and (2a) against *E. Coli*
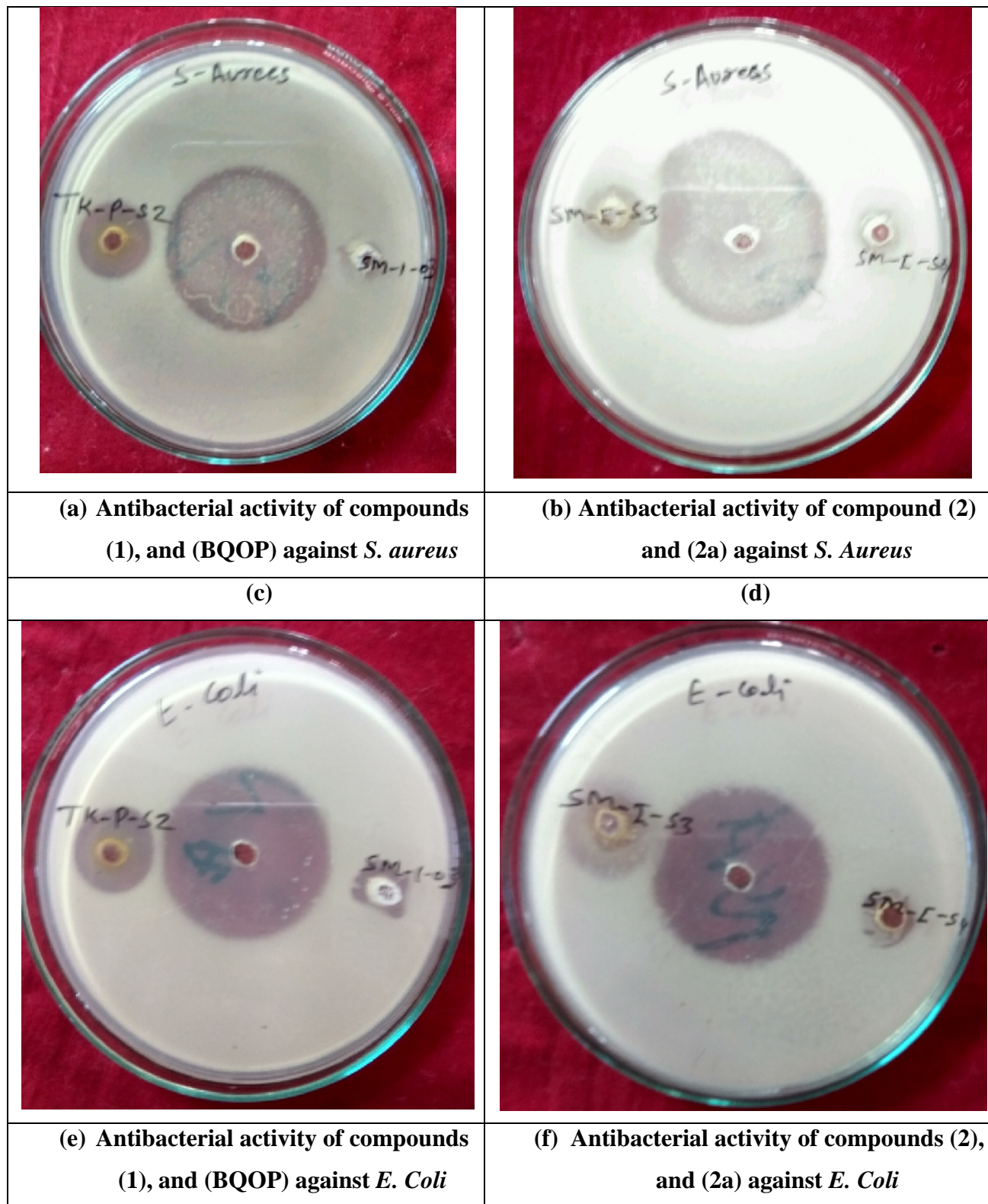
Figure 6.16 (a-d) Antibacterial activity of newly synthesized ionic compound against *S. aureus* and *E. coli* after 24 hrs

(a) Antifungal activity of compounds (1) and (BQOP) against T. Ressei	**(b)Antifungal activity of compound (2) and (2a) against T. Ressei**	**(c)Antifungal activity of compound (BQOH) and (2a) against *T. Ressei***
(d)Antifungal activity of compounds (BQOP) and (1a) against *penicillium*	**(e)Antifungal activity of compound (BQOH) and (2a) against *penicillium***	**(f)Antifungal activity of compounds (2) and (BQOP) against *penicillium***

Figure 6.17(a-f) Antifungal activity of newly synthesized ionic compound against *T. reesie* and *pencillium* after 24 hrs

6.4 References

[1] M. Jafari, M. Salehi, M. Kubicki, A. Arab, A. Khaleghian, Inorganica Chim. Acta. 462 (2017) 329-335.

[2] A. Choudhary, R. Sharma, M. Nagar, M. Mohsin, J. Enzyme Inhib. Med. Chem. 26 (2011) 394–403.

[3] T. Bal-Demirci, M. Sahin, E. Kondakçi, M. Özyürek, B. Ülküseven, R. Apak, Spectrochim. Acta. A Mol. Biomol. Spectrosc. 138 (2015) 866-872.

[4] J.R. Anacona, C. Toledo, Transition Met. Chem. 26 (2001) 228–231.

[5] M. Sönmez, I. Berber, E. Akbas, Eur. J. Med. Chem. 41 (2006) 101–105.

[6] P.V.A. Lakshmi, P.S. Reddy, V.J. Raju, Spectrochim. Acta. A Mol. Biomol. Spectrosc. 74 (2009) 52–57.

[7] R.J.P. Williams, R. Inst. Chem. Rev. 1 (1968) 13-38.

[8] W.F. Beyer, I. Fridovich, (1986).Manganese in metabolism and enzyme function (193-219). New York: Academic Press.

[9] M. Tümer, H. Köksal, M.K. Sener, S. Serin, Transition Met. Chem. 24 (1999) 414-420.

[10] G. Albertin, E. Bordignon, A.A. Orio, Inorg. Chem. 14 (1975) 1411-1413.

[11] D.X. Tan, L.C. Manchester, R. Sainz, J.C. Mayo, F.L. Alvares, R.J. Reiter, Expert. Opin. Ther. Pat. 13 (2003) 1513.

[12] W. Dröge, Physiol. Rev. 82 (2002) 47-95.

[13] N. Noguchi, Free Radic. Biol.Med. 33 (2002) 1480-1489.

[14] WHO, 2012. Promoting Access to Medical Technologies and Innovation Intersections between public health, intellectual property and trade. World Health Organization, World Intellectual Property Organization and World Trade Organization.

[15] G.T. Javier, G.J. Javier, R. Cortos, T. Rojo, M.K. Urtiaga, I. Arriotua, Inorganica. Chim. Acta. 249 (1996) 25-32.

[16] U. Abram, K. Ortner, K. Sommer, J. Chem. Soc., Dalton Trans. (1999) 735-742.

[17] C. Sulpizio, J. Breibeck, A. Rompel, Coord. Chem. Rev. 374 (2018) 497-524.

[18] L. Ronconi, P.J. Sadler, Coord. Chem. Rev. 251 (2007) 1633-1648.

[19] R.R. Crichton, (2008). Biological Inorganic Chemistry an Introduction (2). Boston:

Elsevier Science.

[20] R.M. Roat-Malone, (2002). Bioinorganic Chemistry: A short Course. New York: John Wiley & Sons, Inc.

[21] D. Gamovskii, A.L. Nivorozhkin, V.I. Mimkin, Coord. Chem. Rev. 126 (1993) 1-69.

[22] M. Sönmez, Polish J. Chem. 77 (2003) 397-402.

[23] M. Sönmez, M. Sekerci, Synth. React. Inorg. Met. Org. Chem. 33 (2003) 1747-1761.

[24] J.H. Pandya, M.K. Shah, IJSC 1 (2008) 133–136.

[25] M. Dorneanu, E. Stefanescu, O. Paduraru, M. Pavelescu, A. Hriscu, Rev. Med. Chir. Soc. Med. Nat. Iasi. 100 (1996) 167–171.

[26] S.C. Chaturvedi, S.H. Mishra, K.L. Bhargava, Y. Avadhoot, Indian Drug 16 (1979) 178– 181.

[27] L.J. Bellamy, (1978). The Infrared Spectra of Complex Molecules. London: Chapman and Hall.

[28] A. Choudhary, R. Sharma, M. Nagar, Int. Res. J. Pharm. Pharmacol. 1 (2011) 172-187.

[29] S.D. Rubbo, A. Albert, M.I. Gibson, Br. J. Exp. Pathol. 31 (1950) 425-441.

[30] V. Prachayasittikul, S. Prachayasittikul, S. Ruchirawat, V. Prachayasittikul, Drug. Des. Devel. Ther. 7 (2013) 1157-1178.

[31] G. Zengin, Y.S. Cakmak, G.O. Guler, A. Aktumsek, Rec. Nat. Prod. 5 (2011) 123-132.

[32] C.A. Rice-Evans, N.J. Miller, G. Paganga, Free Rad. Biol. Med. 20 (1996) 933-956.

[33] B. Halliwell, J.M. Gutteridge, Biochem. J. 219 (1984) 1-14.

[34] S.R. Maxwell, Drugs 49 (1995) 345-361.

[35] M. Valko, M. Izakovic, M. Mazur, C.J. Rhodes, J. Tesler, Mol. Cell. Biochem. 266 (2004) 37-56.

[36] D. S. Raja, N.S.P. Bhuvanesh, K. Natarajan, Eur. J. Med. Chem. 46 (2011) 4584-4594.

[37] Y. Byun, D. Darby, K. Cooksey, P. Dawson, S. Whiteside, Food Chem. 124 (2011) 615- 619.

[38] U. Bhandari, R. Kanojia, K.K. Pillai, Int. J. Exp. Diabetes Res. 3 (2002) 159-162.

[39] U. Bhandari, N. Jain, K.K. Pillai, Exp. Diabetes Res. 15 (2007) 1-6.

[40] Y.L. Nene, P.N. Thapliyal, (1993). Fungicides in plant diseases control. New Delhi: Oxford and IBH.

[41] T. Hatano, R. Edamatsu, M. Hiramatsu, A. Mori, Y. Fujita, T. Yasuhara, T. Yoshida, T. Okuda, Chem. Pharm. Bull. 37 (1989) 3177-3180.

[42] D. L. Mayers, S.A. Lerner, M. Ouelette, J.D. Sobel (Eds.). (2009). Antimicrobial Drug Resistance: Clinical and Epidemiological Aspects (681–1347). London: Springer Dordrecht Heidelberg.

[43] A. Guschin, P. Ryzhikh, T. Rumyantseva, M. Gomberg, M. Unemo, BMC Infect. Dis. 15 (2015) 1–7.

[44] M.Z. David, R.S. Daum, Clin. Microbiol. Rev. 23 (2010) 616–687.

[45] J. Rai, G.K. Randhawa, M. Kaur, Int. J. Appl. Basic Med. Res. 3 (2013) 3–10.

[46] J.M. Conly, K. Stein, Prog. Food Nutr. Sci. 16 (1992) 307–343.

[47] P. B. Eckburg, E.M. Bik, C.N. Bernstein, E. Purdom, L. Dethlefsen, M. Sargent, S.R. Gill, K.E. Nelson, D.A. Relman, Science 308 (2005) 1635–1638.

[48] S. Langsrud, (2009). Biofilms in the Food and Beverage Industries (250-269). London: Woodhead Publishing.

[49] S.Y. Tong, J.S. Davis, E. Eichenberger, T.L. Holland, V.G. Fowler Jr, Clin. Microbiol. Rev. 28 (2015) 603–661.

[50] G.Y. Liu, A. Essex, J.T. Buchanan, V. Datta, H.M. Hoffman, J.F. Bastian, J. Fierer, V. Nizet, J. Exp. Med. 202 (2005) 209–215.

[51] M. Mandels, E.T. Reese, J. Bacteriol. 73 (1957) 269–278.

[52] B. Seiboth, S. Herold, C.P. Kubicek, Subcell. Biochem. 64 (2012) 367-390.

[53] J. Guarro, Eur. J. Clin. Microbiol. Infect. Dis. 32 (2013) 1491–1500.

[54] I. Doczi, T. Gyetvai, L. Kredics, E. Nagy, Clin. Microbiol. Infect. 10 (2004) 773-776.

[55] P. Godoy, E. Nunes, V. Silva, J. Tomimori-Yamashita, L. Zaror, O. Fischman, Mycopathologia 157 (2004) 287–290.

[56] C. Perez, M. Paul, P. Bazerque, Acta. Biol. Med. Exp. 15 (1990) 113-115.

[57] G.H.S. Bonjar, S. Aghighi, N.A. Karimi, J. Biol. Sci. 4 (2004) 405-412.

[58] M.Y. El-Naggar, S.A. El-Assar, S.M. Abdul-Gawad, J. Microbiol. Biotechnol. 19 (2009) 468–473.

[59] M.I. Hossain, M. El-Harbawi, Y.A. Noaman, M.A.B. Bustam, N.B.M. Alitheen, N. A. Affandi, G. Hefter, C.Y. Yin, Chemosphere 84 (2011) 101–104.

[60] J. N. Pendleton, B.F. Gilmore, Int. J. Antimicrob. Agents 46 (2015) 131-139.

[61] B.G.Tweedy, Phytopathology 25 (1964) 910-918.

[62] K. S. Prasad, L. S. Kumar, S. C. Shekar, M. Prasad, H. D.Revanasiddappa, Chemical Sciences Journal, 12 (2011) 1–10.

[63] T. D. Thangadurai, K. Natarajan, Transition Metal Chemistry, 26 (2001) 500–504.

[64] Z. H. Chohan, M. Arif, M. A. Akhtar, C. T. Supuran, Bioinorganic Chemistry and Applications, (2006) 1-13.

LIST OF RESEARCH PUBLICATION

1. **Tanuja Kumari**, Ram Gopal, Ankit Goyal and Jyoti Joshi, "Formation and optical properties of pure nano-sized anatase titania by low-temperature aqueous sol-gel route" , Journal of the Australian Ceramic Society Volume: 2 / 1-7 / 2018 DOI: 10.1007/s10904-018-1001-x

2. **Tanuja Kumari**, Ram Gopal, Ankit Goyal and Jyoti Joshi ,"Sol–Gel Synthesis of Pd@PdO Core–Shell Nanoparticles and Effect of Precursor Chemistry on Their Structural and Optical Properties", Journal of Inorganic and Organometallic Polymers and Materials Volume: 27 / 1-10 / 2018 DOI: 10.1007/s41779-018-0278-0

3. Jyoti Joshi, **Tanuja Kumari**, Yogesh Duchania ,"Aza-BODIPY: As an organic photovoltaic material", International Journal of Engineering Technology, Management and Applied Sciences Volume :3 / 200-211 / 2015

4. Jyoti Joshi, Bidya Sagar Joshi, Yogesh Duchania, **Tanuja Kumari** ,"Applications of Schiff's bases metallorganic derivatives- A review", International Journal of Engineering Science & Technology Volume :2 / 99-115 / 2015

5. Tanuja Kumari, Jyoti Joshi, Bidya Sagar Joshi, "Synthesis, structural characterization and biological studies of novel Co(II) complexes with N-O donor chelating ligands derived from 8-hydroxyquinoline" (Communicated)

6. Tanuja Kumari, Jyoti Joshi, Bidya Sagar Joshi, "Synthesis, characterization and antimicrobial activity of novel 8-hydroxyquinolenium based ionic compounds comprising of organic-inorganic framework " (Communicated)

LIST OF CONFERENCES/WORKSHOPS ATTENDED

1. Participated and presented paper entitled "**Synthesis and characterization of novel ionic compounds comprising of organic-inorganic framework**" in the International conference ISCB-2018 held at Manipal University Jaipur from 11-13 January, 2018.

2. Participated and presented paper entitled "**Synthesis and Characterization of novel lanthanum(III) complexes of Betti base**" in the International conference on frontiers at the chemistry- allied sciences interface (FCASI-16)" held at **University of Rajasthan** from 25th -26th April, 2016.

3. Participated and presented paper entitled "**Synthesis and Characterization of Schiffs bases derived from Betti base and their Aluminium complexes**" in International conference, "Current challenges in drug discovery research (CCDDR 2015)" held at **MNIT, Jaipur** from 23rd -25th November, 2015.

4. Participated and presented paper entitled "**Aza-BODIPY: As an Organic Photovoltaic Material**" in International Conference "Emerging Trends of Engineering, Science, Management and its applications (ICETESMA-15)" held at **JNU, Delhi** on March 01, 2015.

5. Participated and presented paper entitled "**Novel boron complexes derived from catechol and diazoaminobenzene**" in 102nd Indian Science Congress-2015 held at **University of Mumbai** from 3rd-7th January, 2015.

6. Participated in National Seminar on "**Chemistry for Economic Growth and Human Comforts**" on August 31, 2013 organized by Department of Chemistry, **University of Rajasthan**, Jaipur.

7. Participated and completed the workshop on "**Modern spectroscopic techniques**" organized by Sophisticated Instrumentation Centre (SIC), **IIT-Indore** on 22nd-23rd February, 2013.

BRIEF BIO-DATA

Ms. Tanuja Kumari has done her Graduation in Science from Maharani Rameshwari Mahila PG Mahavidyalaya, Darbhanga (Lalit Narayan Mithila University Darbhanga) in the year 2007. She is Post Graduate in Chemistry from Department of Chemistry, Lalit Narayan Mithila University, Darbhanga in the year 2009. She qualified GATE in 2012 and joined her Ph.D. in January, 2013 under the supervision of Dr. Jyoti Joshi, Professor, Department of Chemistry, Malaviya National Institute of Technology Jaipur. She has published four research papers in National and International journals of repute. She has participated and presented her research work in various National and International conferences and symposium. She has volunteered in community development programs viz. Cancer awareness program and HIV-AIDS awareness program held at MNIT in the year 2014.